New Technological Solutions to Improve the Aerodynamic Characteristics of an Aircraft Wing

PEEP LAUK

**TAL
TECH** PRESS

TALLINN UNIVERSITY OF TECHNOLOGY
School of Engineering
Department of Mechanical and Industrial Engineering
This dissertation was accepted for the defence of the degree of Doctor of Philosophy
In Mechanical and Industrial Engineering on: 23.04.2019

Supervisors:

PhD Toivo Tähemaa
Department of Mechanical and Industrial Engineering
Tallinn University of Technology
Tallinn, Estonia

PhD Aleksander Kartušinski
Department of Mechanical and Industrial Engineering
Tallinn University of Technology
Tallinn, Estonia

Oponents:

Assoc Prof. Eduardas Lasauskas
Department of Aeronautical Engineering
Vilnius Gediminas Technical University
Vilnius, Lithuania

PhD Mart Enneveer
Estonian Aviation Academy
Tartu, Estonia

Defence of the thesis: 17.06.2019, Tallinn

Declaration: Hereby I declare that this doctoral thesis, my original investigation and achievement, submitted for the doctoral degree at Tallinn University of Technology, have not been previously submitted for doctoral or equivalent academic degree.

Peep Lauk

_____
signature

Õhusõidukite tiiva aerodünaamiliste omaduste parandamine uute tehnoloogiliste lahenduste abil

PEEP LAUK

**TAL
TECH**
KIRJASTUS

Contents

List of publications

The list of publications by the author, on the basis of which the thesis has been prepared. The academic publications are referred to in the text as Paper I, Paper II, Paper III and Paper IV.

I   **Lauk, P.**; Unt, K-E. (2015). Influence of miniflaps on sailplane flight characteristics. Aviation, 19 (3), 105−111. 10.3846/16487788.2015.1104793. ETIS classification 1.1

II   **Lauk, P.**; Seegel, K.-E.; Tähemaa, T. (2017). Impact of variable geometry miniflaps on sailplane flight characteristics. Aviation, 21 (4), 119−125. 10.3846/16487788.2017.1415228. ETIS classification 1.1

III   **Lauk, P.**; Seegel, K.-E.; Tähemaa, T. (2018). The Influence of Variable Geometrical Modifications of the Trailing Edge of Supercritical Airfoil on the Characteristics of Aerodynamics. International Journal of Mechanical, Aerospace, Industrial, Mechatronic and Manufacturing Engineering, 12 (4), 261−266. ETIS classification 1.2

IV   **Lauk, P.**; Tähemaa, T.; Seegel, K-E. (2018) Advanced trailing edge flap design for commercial Aircraft. Toulouse, AEGATS´18 Conference, France / 23 − 25 October 2018. ETIS classification 3.2

Author's contribution to the publications

Contribution to the papers included in this thesis is following:

Paper	Original idea	Study design and methods	Data collection and handling	Contribution to result interpretation and manuscript preparation	Responsible for result interpretation and manuscript preparation
I	PL	PL	PL	PL, K-EU	PL
II	PL	PL	PL, KES	PL, KES, TT	PL
III	PL	PL	PL	PL, KES, TT	PL
IV	PL	PL	PL	PL, TT, KES	PL

PL - Peep Lauk
KES - Karl-Erik Seegel
TT - Toivo Tähemaa
KEU - Karl-Erik Unt

Introduction

The problem formulation. Carrying with commercial aircraft is the fastest type of transport but at the same time causing the biggest environmental pollution. As of October 2018, 37,400 commercial airplanes were used worldwide. The most common is the single aisle, medium range aircraft, accounting for 28,550 which is over 76% of the total number of commercial aircrafts. Extra large aircraft such as Boeing 777, Airbus 380, etc. only form 4.25% of the total numbers of commercial aircraft. (Flaig, 2018) The following example illustrates the environmental pollution caused by a commercial aircraft. In 5,000 flight hours per year, one modern, medium-range aircraft consumes around 12,900 t of aviation fuel and generates 40,663 t of CO_2. On flights across the Atlantic, burning fuel generates by more than three times more harmful waste than commercial cargo weight. It is widely known that the burning of fuel leads to global climate change and global average temperature increase. Thus, reducing the fuel consumption of a medium-sized aircraft by only 1% can reduce CO_2 emissions by 406.6 t in 5000 flight hours per year. Also, at 700 EUR/t fuel price, this would allow the aircraft operators to save a total of more than 2.5 billion Euros per year for all single aisle, medium range aircrafts. (Flaig, 2018) Another problem is related to the increased complexity of commercial aircraft systems. The development of new technologies that reduce fuel burning should be designed with low complexity devices. This is necessary in order to increase the reliability of the systems and to reduce the maintenance costs.

The object of research. The research object is an aircraft wing. The aerodynamic characteristics of the wing have an important role in the overall performance of the aircraft. Reducing the aerodynamic drag of a wing also reduces fuel consumption and the emission of harmful pollutants to the environment. The reduction in fuel consumption of aircraft will also reduce direct costs for aircraft operators. Reducing the weight of the aircraft structure allows to increase the weight of commercial cargo or the flight range. The aim of this doctoral thesis is to investigate and improve aircraft lift/drag ratio by using new technological solutions of the wing.

The hypothesis. Based on various articles and background studies, a hypothesis was made that using variable geometry modifications of the leading and trailing edge of the wing and using innovative technologies can reduce the aerodynamic drag and increase the lift. Initially, these assumptions had not been scientifically proven and needed a proof.

The tasks of the thesis. In order to achieve the research objective, the following tasks must be carried out.

- Apply computational and experimental methods to analyse the effect of the trailing edge modifications of the aerodynamic characteristics of the wing. Based on the results of the aerodynamic analysis, design the trailing edge devices for the glider. The next step is to analyse the variable geometry trailing edge modification of the wing and its kinematics design for the glider. Experimental tests are performed by gliders. If the results are promising, the next step is to investigate the impact of trailing edge modifications on the aerodynamic characteristics of commercial aircraft wing by using CFD software.
- Design a novel kinematic solution for actuating leading and trailing edge flap with less complexity, higher reliability and lower maintenance cost.
- Design new wing leading edge flap kinematic solution for use with natural laminar wing.

The methodology of research. The aerodynamic characteristics of the wing airfoil are initially theoretically analysed using different computational methods and free flight testing by using gliders. In experimental studies, tests are carried out on a glider in a free flight using special equipment and improved methodology. XFLR5 simulation software based on XFLR code was selected for computational modelling, however, mainly the solving method of the Navier-Stokes equation was used at the transonic speeds.

Moreover, novel type of miniflaps with variable geometry are introduced and analysed from flight optimization point of view. According to the forecast, the number of aircraft is expected to double over the next twenty years. To keep the pollution load under control, radical improvements should be undertaken in the aircraft design. The above reasons determined the choice of the subject for this thesis.

The aerodynamic characteristics of the aircraft wing mainly depend on airfoil characteristics. The aerodynamic characteristics of the aircraft and gliders are defined by lift-drag polar, an aerodynamic coefficient indicating the dependency between the airfoil drag coefficient and its lift coefficient. The main objective usually is to reduce the drag coefficient and, if necessary, to increase the lift coefficient. In doing so, the use of gliders in testing new technological solutions is very important. Typically, most of the aerodynamic innovations are first tested on gliders and only after that on aircraft. For example, gliders have been deployed to commercial aircraft in winglet, variable chamber (VC) trailing edge flaps, natural laminar flow (NLF) airfoils, but also CFRP composite structures. The development of both aircraft types also has a similar objective: increasing the lift/drag (L/D) ratio at different required airspeeds.

The study focuses mainly on two aspects. First, the airflow behaviour is analysed near to the trailing edge, depending of the profile, at higher Cl values. Sailplanes are particularly interested in the Cl range from 1.2 to 1.7, whereas for commercial aircraft, Cl values from 0.55 to 0.7 are of interest. For the small Re numbers (such as those of glider and UAV wings), XFLR5 software based on the XFOIL code is used to analyse the aerodynamic characteristics. The results of the analysis were also confirmed by the results of the test flights.

Commercial aircraft wing trailing edge airflow behaviour at high Re and Mach numbers is used in CFD simulation based on Reynolds-averaged Navier-Stokes equations (RANS). The main analysis is performed on supercritical airfoil, as well as on the effect of the various wing trailing edge modifications on aerodynamic parameters, using CFD software STAR-CCM+. Based on the aerodynamic efficiency of the modifications and the loads generated, technical solutions are designed. The strength analysis for the technical solutions is performed mainly using Solid Works and Solid Edge softwares. Several devices were built using selective laser sintering (3D printing) - a good example of this is the variable geometry miniflap mechanism for glider LAK-17B made of stainless steel and titanium alloys.

The second aspect of the study is developing a leading edge flap solution which is particularly suitable for use with the natural laminar flow (NLF) airfoil. The technology currently in use allows to maintain the laminar airflow only on the upper side of the wing. On the lower side of the wing, the laminar flow is disturbed by the retracted Krueger flap. According to the novel solution, the leading edge flap is located inside the wing during the flight. To extend the leading edge flap, the lower wing panel is first bent so that the flap can be actuated out of the leading edge of the wing. In the extended flap position, the lower wing panel is closed. Also, the leading edge flap protects the wing from the insect contamination and icing.

High lift system aerodynamic drag and weight can be reduced by using the new swivel beam system (SBS) kinematic solution for flap and slat movement. According to this solution, there is no need for the flap track beams, the laminar flow on the lower side of the wing is prolonged and its aerodynamic drag is reduced.

The novel aerodynamic and technological solutions developed for using commercial aircraft would allow to save more than 10% fuel consumption, but the choice of solutions depends on the size of the aircraft and the Re number of the wing. For example, the leading edge flap solution developed on the NLF wing is suitable for small and medium-sized regional aircraft with a Re number that does not exceed 30×10^6. On large airplanes, the use of NLF airfoil is complicated due to the very high smoothness requirements of the wing surface. At the same time, the trailing edge miniflap would be suitable for use especially on large commercial aircraft due to its size. However, a trailing edge flap movement SBS solution can be used from UAV-s to heavy transport aircraft.

The novel solutions shown in this thesis have been presented at various aviation conferences, including at the Airbus Headquarters in Toulouse, France. The greatest value of the new technological solutions presented in this thesis lies in their simple design. As a result, these solutions can be used to improve the performance of different types of aircraft.

Abbreviations

ADHF	Advanced dropped hinge flap
AR	Aspect ratio
AoA	Angle of attack
CAS	Calibrated airspeed (m/s)
Cd	Drag coefficient
Cdi	Induced drag coefficient
CFD	Computational fluid dynamics
Cl	Lift coefficient
Cl max	Maximum lift coefficient
Cm	Moment coefficient
CMF	Cruise Miniflap
CFRP	Carbon Fiber Reinforced Plastic
Cp	Pressure coefficient
DSF	Double slotted flap
FL	Flight level (ft)
FM	Fowler motion
ft	Foot
GF	Gurnay flap
IAS	Indicated airspeed (m/s)
kN	Kilonewton
L/D ratio	Lift/drag ratio
MiniTED	Mini trailing edge devices
M	Mach number
NLF	Natural laminar flow
NM	Nautical mile
RANS	Reynolds-averaged Navier-Stokes equations
Re	Reynolds number
SAR	Specific Air Range (km)
SBS	Swivel Beam System
SSF	Single Slotted Flap
TAS	True airspeed (m/s)
TE	Trailing edge
TOW	Takeoff weight (kg)
UAV	Unmanned aerial vehicle
Vcas	Calibrated airspeed (m/s)
VC flap	Variable Chamber flap
VGMF	Variable geometry miniflap
Vy	Sink speed (m/s)
λ; AR	Aspect ratio

1 Influence of trailing edge modifications on the aerodynamic performance of the wing at low speeds

To increase the L/D ratio at different Cl values, the simplest solution is deflecting the trailing edge flaps. Unfortunately, the deflecting of the trailing edge flaps is in the optimal range. It depends on the type of airfoil and the wing aspect ratio (AR). At the flap deflecting angle higher than optimal, the airflow separation will start from the trailing edge and the drag is increased. One of the most effective methods for increasing the L/D ratio at higher Cl values than possible with a traditional flap solution, is by using different trailing edge modifications, including the miniflaps, at the trailing edge of the wing.

These devices can be divided into fixed deflecting angle modifications and variable deflecting angle solutions. For an aircraft with a narrow optimal range of speeds, fixed modifications of trailing edge, such as the Gurnay flap, can be used. Many unmanned aerial vehicles (UAV) fly most of their flight time (in loiter mode) in a narrow Cl range. The fixed angle miniflaps were tested on a sailplane as described in the following chapter. The purpose was to improve the L/D ratio of gliders and UAV-s to Cl>1.0 values.

1.1 Impact of fixed angle miniflaps on sailplane flight performance

Miniflaps can be divided into two classes: fixed deflection angle devices and variable shape or angle devices. Fixed shaped devices can be fixed under the wing span, they are lightweight and rigid, but the optimum range of flight speeds is narrow. Variable shape devices are much more complicated, but the range of flight speeds used is much wider. Below, the different types of miniflaps, their structure and the results of flight tests are presented.

1.1.1 Types of miniflaps and their aerodynamic description

Miniflap (incl. mini TED, microflap) is a 0.5-4% at wing chord narrow flap of the trailing edge, which is meant for increasing the lift coefficient and decreasing the wing airfoil drag usually at higher lift coefficients. Miniflaps can be grouped into four types: Gurney Flap (GF), Mini split flap, Divergent trailing edge (Figure 1) and mini plain flap
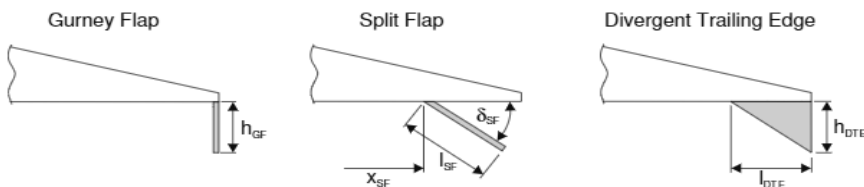
Figure 1. Miniature Trailing-Edge Devices (miniTEDs) (Richter et al., 2011).

(Figure 11). The first deflected angle is a 90° with the airflow. This device, increasing the lift coefficient, was first used by the Formula 1 racer Dan Gurney and was introduced in aviation after Prof. Robert Liebeck published his article in 1978 (Liebeck, 1978). Using a 1.25% high Gurney flap, the Newman airfoil maximum lift coefficient rose, but surprisingly, at the same time the drag coefficient reduced. Unfortunately, at the GF height over 2%, the lift coefficient increased but the drag began to grow faster.

Figure 2. Von Karman vortex street at the behind of the Gurney flap (Richter, 2010).

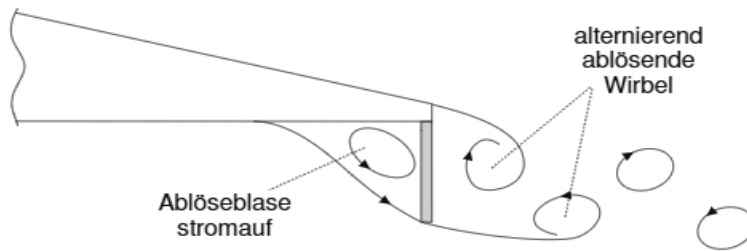In his search for a solution to this paradox, Liebeck created a hypothesis according to which the vortices behind the GF are accompanied by the diminishing of the thickness of the trailing edge boundary layer, thus decreasing the growth of the drag and increasing lift force (Figure 2). This hypothesis was corrected by Kai Richter in 2010 (Richter, 2010). According to this, instead of two stationary vortexes, a vortex row (von Karman vortex street) is formed behind the miniflap. Dimensions of the vortex depend on GF height, AoA and Re number. This hypothesis is confirmed by wind tunnel testing (Figure 3) which showed that the airfoil NACA 4412 boundary layer transition separation location expands at adding 1% GF, AoA 4°, from 92 to 98% (Jang et al., 1998). Also, the Cl increased from 0.818 to 1.167.

   Despite of its small size, the miniflap is a greatly effective mean for increasing the lift force. Using the same airfoil, it was found that 4% high GF increased the lift force more than at 25% chord length plain flap deflection angle +9° (Vlasov et al., 2007). At the same time, the hinge moments induced by the deflecting flaps were smaller. At smaller miniflap deflection angles the airfoil drag decreased significantly (Bloy et al., 1995).

   Using miniflaps with airfoil NACA 63 2-215, L/D max was maintained at 2% chord when a 45° miniflap was used at a higher lift coefficient. When the miniflap deflection angle was increased up to 90°, the lift coefficient increased, but L/D max ratio decreased. When the miniflap deflection angle is increased more than 45°, the lift coefficient growth intensity will reduce (Figure 4).
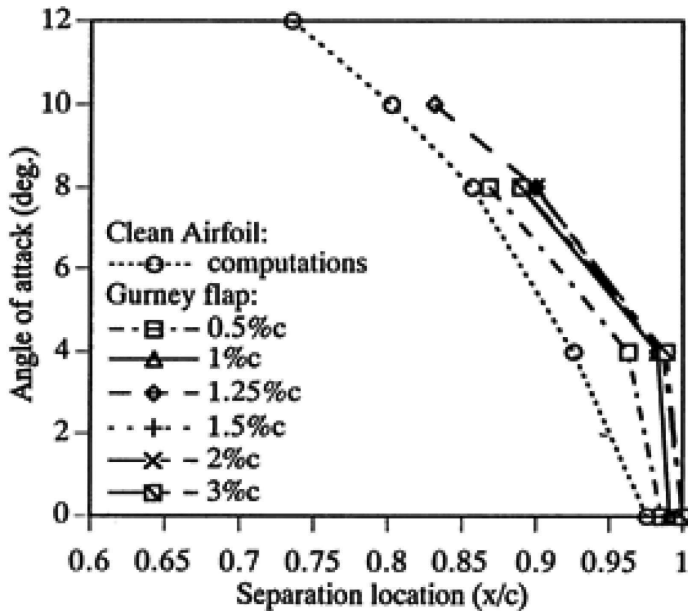
Figure 3. Influence of Gurney flap width on upper surface boundary layer separation location (Jang et al., 1998).

Therefore, with a symmetric airfoil NACA 0012, the Cl max increased 12.3% at a deflection angle of 45° of a 1.5% chord of the wing miniflap, 15.1% at 60° and 17.4% at 90° (Wang et al., 2008). The use of a miniflap increases the wing negative pitching moment depending on the miniflap width and deflection angle. By using airfoil NACA 5414 at Cl=1.0, the 2% miniflap deflecting from 0 $^{\circ}$ to 45° Cm increased from -0.122 to - 0.225 (Figure 5) (Bloy et al., 1997).

Figure 4. The impact of 1,5% chord length of the wing miniflap deflection angle on airfoil NACA 0012 lift coefficient (Wang et al., 2008).

Figure 5. Influence of pitching moment coefficient about quarter-chord line with lift coefficient (Bloy et al., 1997).
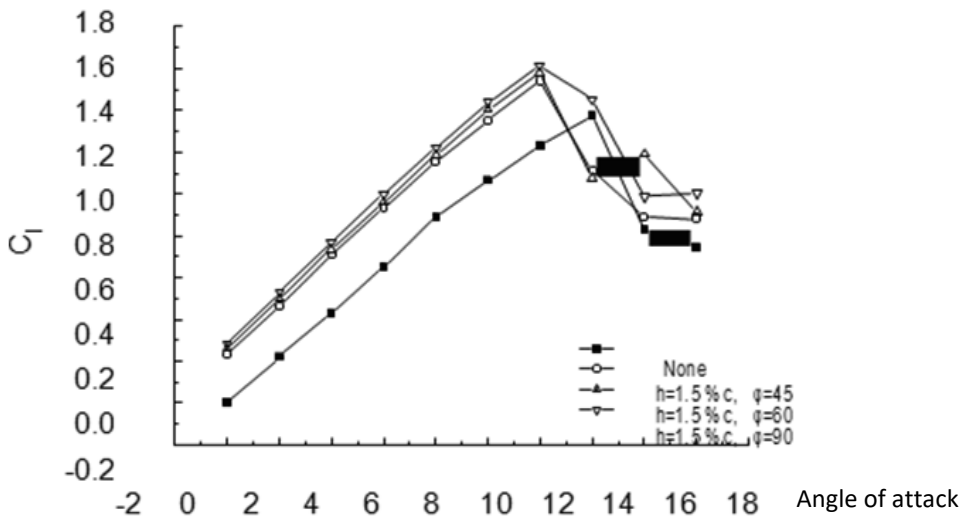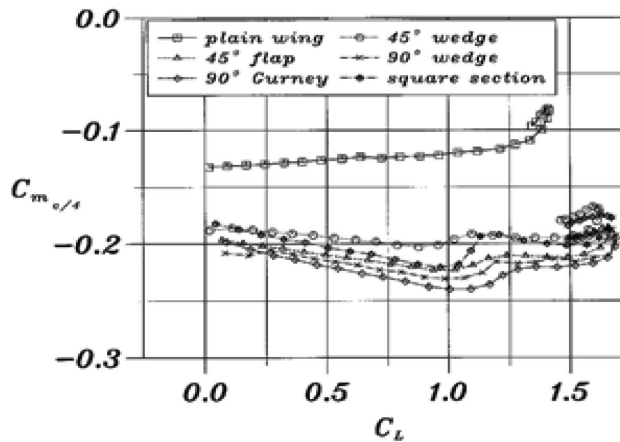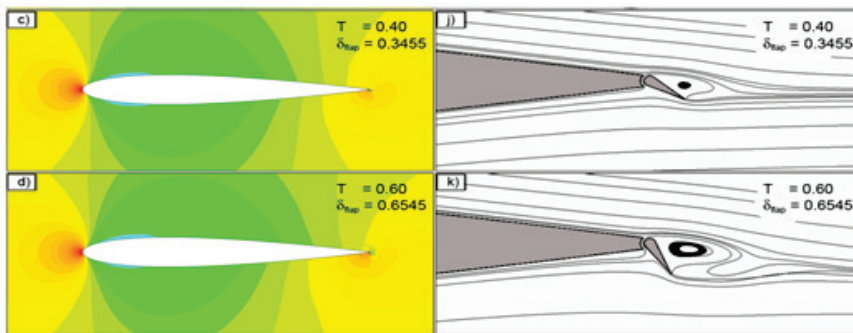

Figure 6. Influence of miniflap deflection angle on airfoil NACA 0012 pressure distribution and trailing edge vortices (van Damm et al., 2007).

In a similar approach to the use of the plain flap, the deflection of the miniflap increases to some extent the reach of the airfoil HQ-17, as the angle of attack is smaller at the same Cl (Bechert et al., 2001). This diminishes the role of the vortices behind the miniflap in the whole drag (Figure 6). The figure clearly shows that by increasing miniflap deflection angle, the lower pressure distribution on the upper side of the wing extends (compare c;j vs. d;k). Due to the increase in the pressure difference between the upper and lower side of airfoil, the lift coefficient increases. Behind the miniflap, depending on this relative length of the chord and angle of attack, a similar von Karman vortex street was formed (van Dam et al., 2007).

   An excellent result was achieved when a trailing edge wedge was used for airfoil S 904 (Bruscoli, 2011). At Re $1x10^6$, at 2% wing chord length and 0.8% high trailing edge wedge at Cl=0.52, the drag coefficient decreased from 0.0083 to 0.0049 and with Cl=0.8, from 0.0103 to 0.0068 (Figure 7). Unlike with other kinds of miniflaps, when trailing edge wedge was used, Cl max decreased compared to the standard airfoil. (Paper I) This supports the result of Jarzabek (Jarzabek, 2011).
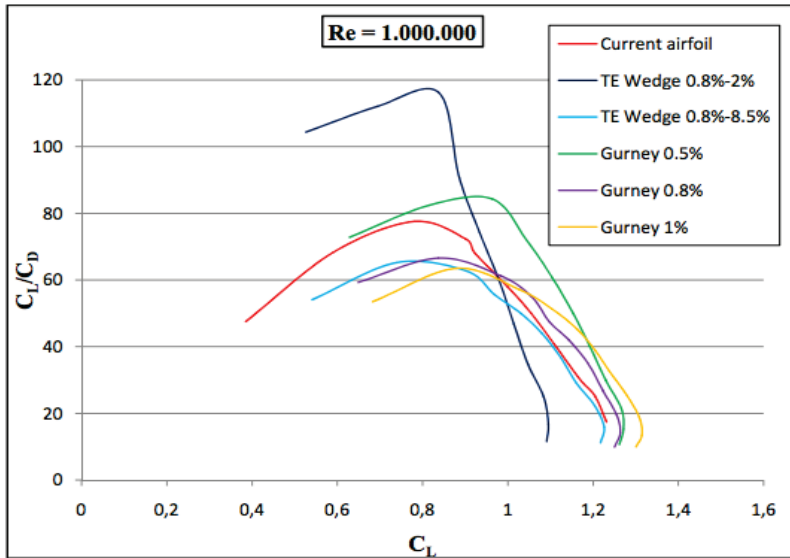
Figure 7. Influence of different types of miniflaps on airfoil S 904 L/D performance (Bruscoli, 2011)

1.1.2 Design of the miniflaps to improve glider climbing performance

Miniflap design was based on climbing performance polar for gliders (Figure 8).
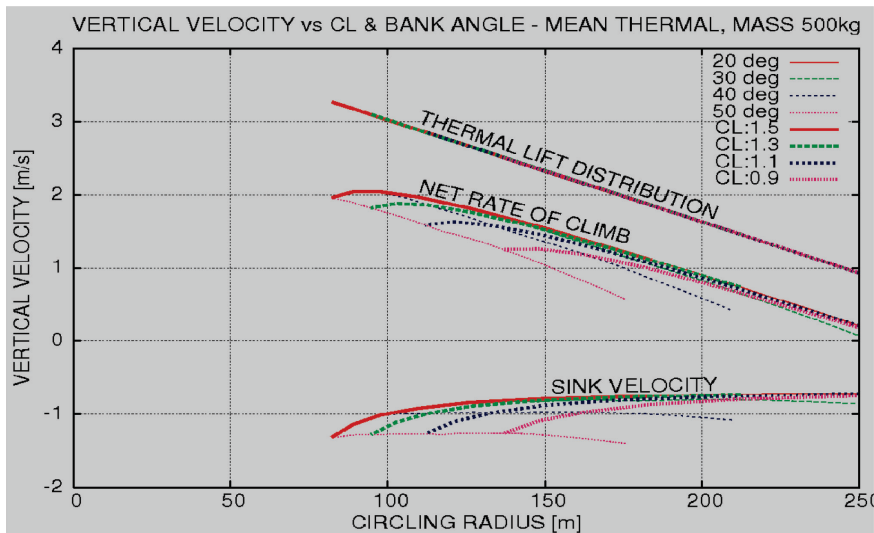
Figure 8. Influence of lift coefficient, circling radius and bank angles on climb performance of glider Diana 2 in a) narrow thermal, b) mean thermal (Kubrynsky, 2006).

As can be seen clearly from this figure, despite the increase in sink speed, at higher Cl values the glider's climbing speed still increases flying in narrow and mean thermals. The miniflaps are of interest for using when flying in thermals at Cl>1.0. Higher wing loading 50-60 kg/m² used with 15 m and 18 m class sailplanes preferably requires flap lift

coefficient at Cl=1.4 – 1.6 in thermals (Figure 8). Increasing the lift coefficient up to 1.3 – 1.5, the Diana 2 sailplane climbing speed increased by 0.2 m/s in mean and wide thermals and even by 0.4 m/s in narrow thermals (Kubrynsky, 2006). The used flap positions +14° – +28° enable to increase Cl max to 1.65 – 1.7, but starting from Cl 1.4 – 1.45 the profile drag begins to grow rather sharply as the boundary layer begins to separate from the upper surface of the flap and from Cl 1.5, also the roll control starts deteriorating.

Miniflap designing is based on previous research and modelling with the XFoil software. To analyse miniflaps' influence on glider's flight performance, test flights with DG-1000 were made on Prof. Joseph Mertens's (Akademische…, 2006) initiative in Aachen in 2006. For these tests, 20 mm wide miniflaps (2.2%) of the chord were used. 5 test flights were made at flap deflection angles +15°, +30°, +45°, +60° and +90°. When flying in thermals, the best results were achieved at flap deflection +30° and +45°. Due to greater drag at landing, the most favourable flap deflection was + 90°. It appeared that at flap deflection +60° and +90° the drag increased significantly. Unfortunately, due to the bad weather conditions it was not possible to continue these test flights.
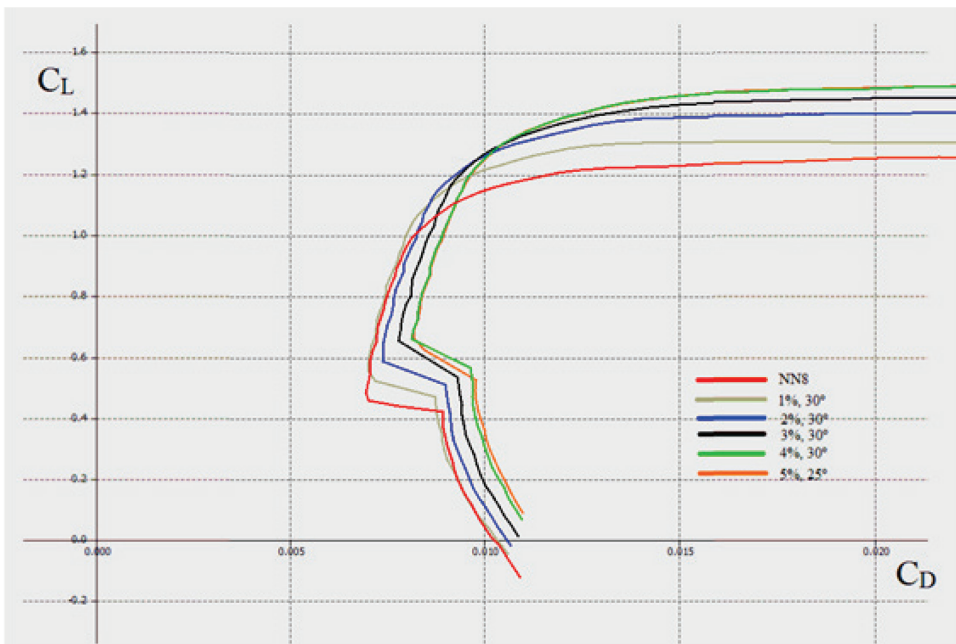
Figure 9. Influence of miniflap deflection angle on the airfoil NN-8 aerodynamic characteristics, based on modelling with XFLR 5 software at Re 1.1x10^6 (Balagura, 2013).

As the wing loading and wing aspect ratio of modern sailplanes will grow in future, Cl 1.5 – 1.7 needs to be used. To model the miniflap, the XFoil software (Drela, 1989) XFLR5 v. 696 was used. This modelling was also done based on the results of the wind tunnel tests of the wing airfoil NN-8 (Ostrowski, 1981). According to the calculations, for the SZD-48-3 Jantar-Standard 3 glider with airfoil NN-8 the optimum miniflap size was a 2% lenght of the chord at 30° deflection angle. Using the miniflap with airfoil NN-8, the drag

was less at Cl>1.02 compared to the standard wing, and also the Cl-max increased (Figure 9).

To test these calculated results, miniflap sections at fixed angle from a 1.5 mm thick CFRP with relative wing chord ratio 2%, incl. ailerons, were made at the Estonian Aviation Academy, Department of Aircraft Engineering. The miniflaps were attached using a double-sided adhesive tape. Figures 10 and 11 depict the fixed miniflaps on the lower side trailing edge of the sailplane wing.

Figure 10. Fixed angle miniflaps on sailplane Jantar-Standard 3 wing.
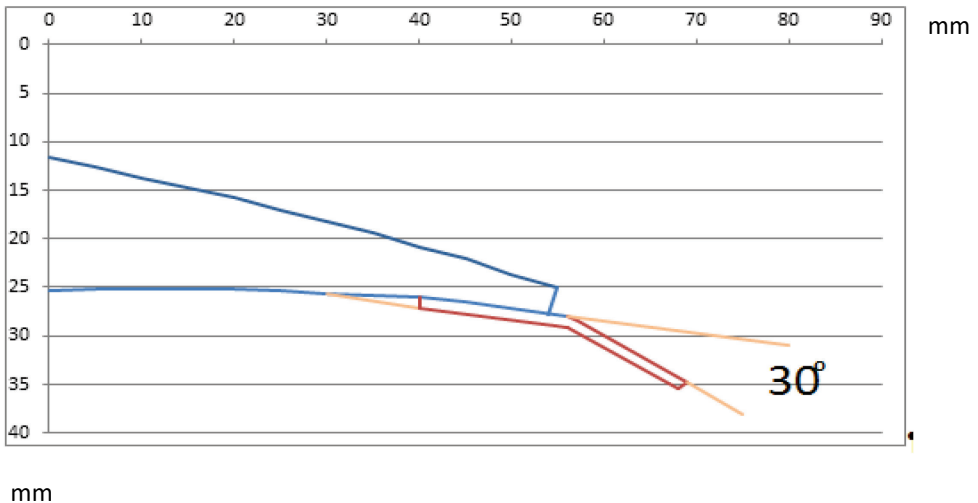
Figure 11. Fixed angle miniflap attached to the lower side of the Jantar-Standard 3 wing's trailing edge (Paper I).

1.1.3 Methodology and tests

To perform the flight tests, the methodology developed by Johnson (Johnson, 1989) was used. In addition to comparing the sink speed, the parallel flight method was used (Hendrix, 2011). This methodology was chosen because it has proven the most accurate in decades of use. Today, it is the most reliable glider flight test methodology. In addition, the importance of a parallel test flight should be highlighted. This method makes it

possible to eliminate the effects of vertical movement of the atmosphere and increase the accuracy of the measurements.

Test flights were performed in the airspace of Ridali Aerodrome in South Estonia in 2012-14. The gliders were operated by the pilots Matti Sillajõe, Alari Õun and Peep Lauk. In the early morning, the gliders were towed by planes simultaneously to 1,700 m from the ground. During the gliding the sailplanes flew parallel to each other at the distance of 30-50 m at equal speeds. To find out and compare the sink speed the flight was divided into separate sections. The same speed was maintained for 240 seconds and at the same time the altitude change was measured. The test flight was completed at the flight altitude of ca 600 m from the ground, which was higher than the inversion layer. To determine the angle of attack versus speed, separate test flights were performed, as at different angles of attack the flight speed had to be kept for 10 seconds each time. Each test variation was repeated two or three times. The collected results were adjusted based on the variance of air pressure and temperature. The most dangerous was the test flight with DFS-60, and it was carried out by the author of this thesis. This device filled most of the cockpit, worsened the view and disrupted the glider control. To get the most accurate results, most of the subsequent miniflap test flights were performed by the highly experienced Estonian glider pilot Matti Sillajõe. Before the flight tests the glider's altimeter and speed indicator were calibrated, the calibrating equipment used was the air data test set D. Marchiori MPS 43. To reduce the influence of the fuselage on the flight data, a Pitot' tube was additionally installed on the upper fuselage. The test flight program was prepared based on the modelling results of the XFLR5 software. The first test flight already showed that the miniflaps proved to be much more effective than the model had shown. Due to this, the flight plans had to be changed significantly and the air speed indicator was additionally calibrated before the next test flights. (Paper I) To calibrate the airspeed indicator, the static probe DFS-60 was used to perform the test flights. Most of test flights were made at IAS from 65 to 101 km/h.

A graph of calibrated speeds was completed on the basis of the collected results (Figure 12). The Dynon Avionics equipment D100 was used for accurate measuring and recording, and an additional Pitot' tube was attached to the sailplane for validation the flight parameters. To record the cockpit data and the position of the second glider and, in addition, to observe the airflow by tuft, GoPro cameras were used, attaching the first camera to the stabilizer and the other two in the cockpit. In the test flights, the parallel flight method with two gliders of the same type was applied. A miniflap was used with only one glider, the other one was used for comparison. Before the test flights, both gliders were weighed together with pilots and, where necessary, water ballast was added. Both gliders had the same centre of gravity and wing loading (G/S 35.78 kg/m²).
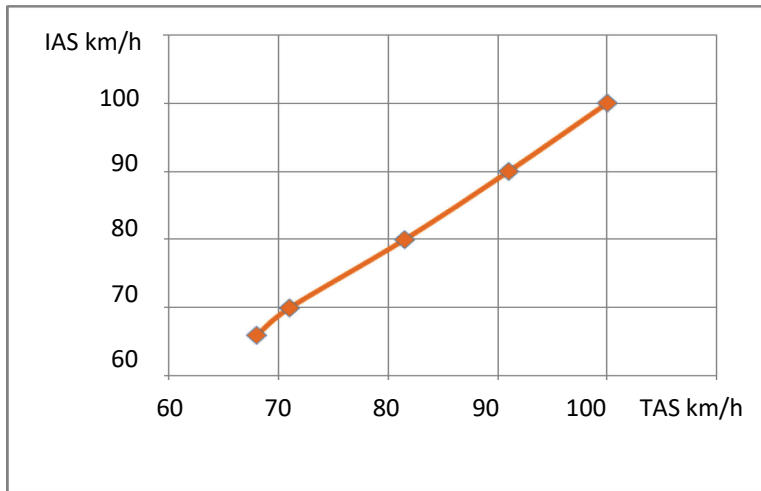
Figure 12. IAS and TAS values obtained from calibrating flights.
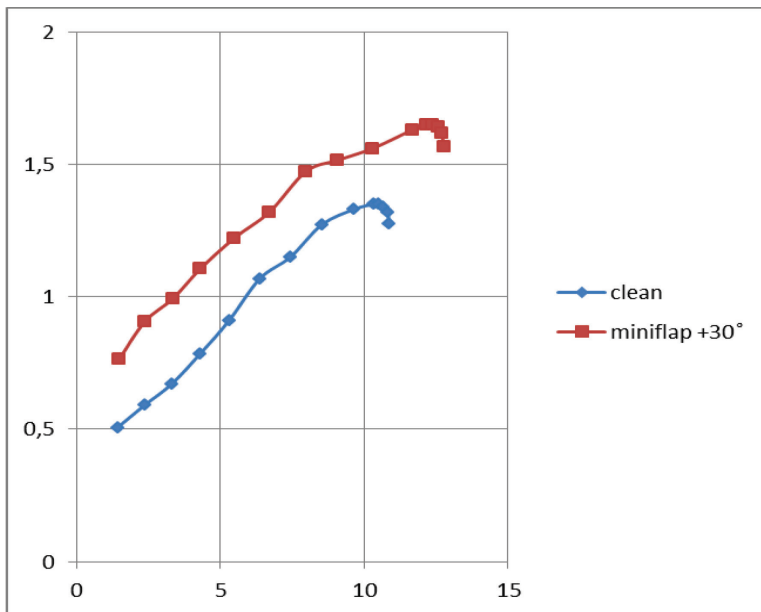
Figure 13. Glider SZD-48-3 Jantar-Standard 3 lift coefficient Cl versus angle of attack with a +30° deflected 2% chord length miniflap (Paper I).

1.1.4. Flight test results

With 2% of the wing chord miniflaps at a 30° deflection angle, the sailplane's stall speed reduced from 75 to 66 km/h and the Cl max increased from 1.35 to 1.66 (Figure 13), taking only a small growth of the wing area. In addition, the critical angle of attack of the wing increased by 1.6° from 9.6° to 11.2°.

The increasing of the critical angle of attack by using Gurney flap has been noted by the authors of several articles (Cavanaught et al., 2007). Usually, the increasing has not exceeded 1°, but according to one research the critical angle of attack increased by 2.1°

21

(Vlasov et al., 2007). The analysis of the obtained test flight results indicated that using miniflaps with lift coefficient Cl ranges from 0.99 to 1.21 and from 1.32 to 1.66, the drag of the glider decreased compared to the standard configuration and the L/D ratio of the glider improved Cl>1.0, especially in Cl range from 1.08 to 1.19 (Figure 14).

The drag decreasing may be caused not only by the reduce of the airfoil drag, but it may also be linked to the decrease of the fuselage drag and the interference drag, because the angle of attack decreased 2.5° at the same airspeed. At the airspeed of 81 km/h (Cl 1.13), a considerably anomalous decreasing in the sink speed up to 0.63 m/s and increase in the L/D ratio at the same airspeed can be noticed. Considering the dispersion of the instrument accuracy and the results obtained during the test flights, the value of the measurement uncertainty was 12.3%. This means +/- 0.25° in AoA and +/- 0.85 cm/s in sink speed. Therefore, the measurement uncertainty is approximately 8 times smaller than the difference in the test results and therefore, the final results are credibly correct. The most probable cause for the drag decreasing is the thinning boundary layer near to the trailing edge as a result of the vortex appearing behind the miniflap on the wing. At airspeeds under 70 km/h the sink speed grew, mainly due to the induced drag, which is generated due to the not high aspect ratio of the wing (20.2) for gliders. At the airspeeds over 86 km/h (Cl< 0.99), the miniflap increased the sailplane drag. Test pilots have confirmed that by using the miniflap the glider longitudinal stability increased and the roll control of low flight speed improved. At further growth of the airspeed up to 150 km/h, additionally to the drag also the loads on the ailerons increased significantly. (Paper I) The test pilot confirmed that the loads on the ailerons exceeded the normal forces for controls more than twice.
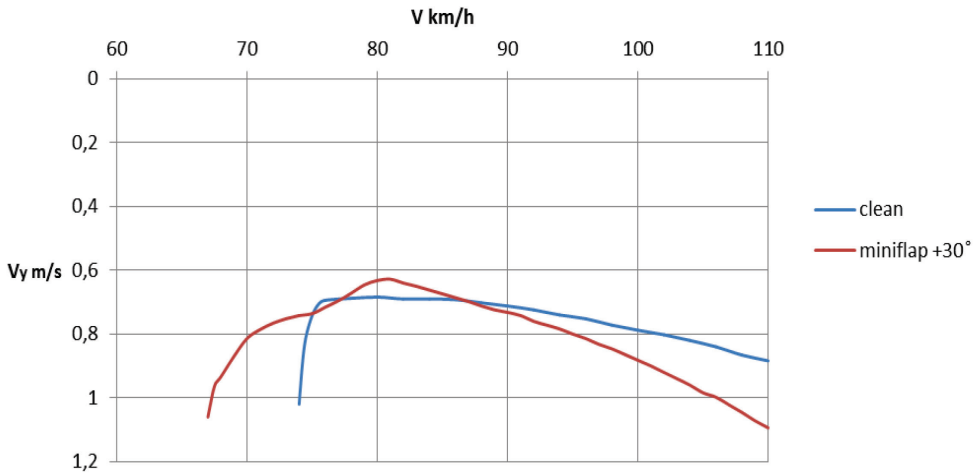
Figure 14. Miniflap 2% of the wing chord (deflection angle +30°) influence on glider Jantar-Standard 3 performance. G/S 35.78 kg/m² (Paper I).

The glider's required towing airspeed decreased typically for this type of glider from 125-130 km/h to 115-120 km/h. Near to the critical angles of attack, the sailplane roll stability and controllability were maintained. On one test flight, the pilot inadvertently exceeded the critical angle of attack and flew like that for ca 10 seconds. The controllability was maintained, but the vibration accompanying the stall increased, as also the T-stabilizer was located inside while in the vortices area. To observe the glider's actual behaviour in thermals, a separate flight was performed with the main

objective of identifying any changes in controllability and stability caused by the use of miniflaps. On the day of the test flight, the weather was windy and turbulent and the thermals were narrow and intermittent. Despite of the turbulence the glider's stability and controllability remained good and showed no significant variation from the normal configuration. In spiral flight in thermals, it was possible to turn to a back angle of 35°-40° while maintaining the airspeed of 76 km/h, which is significantly lower than the standard airspeed (85-90 km/h) of this type of glider at the given mode.

The most important aspect of this thesis is that for the first time the impact of the miniflap on the aircraft was systematically measured. Using the obtained data, it is possible to design a fixed deflection angle miniflaps for unmanned and conventional aircraft. The hypothesis of the efficacy of miniflap was confirmed during the test flights. Above expectations, the efficiency of the miniflap proved to be higher than the previous modelling had shown. Based on the collected data, it is also possible to design variable geometry miniflaps for aircraft, gliders and large UAV-s, which can extend the range of low drag flight speed.

1.2 Impact of variable geometry miniflaps on glider flight characteristics

The fixed deflection angle miniflaps significantly improved the glider's climbing performance, but at high speeds they decreased glider's flight performance (Paper I). To increase the range of optimal airspeeds the author of this thesis decided to design variable geometry miniflaps and test them on glider with trailing edge flaps.

1.2.1 Aerodynamic design of a variable geometry miniflap

Wing trailing edge flaps improve gliders' flight characteristics. When flying in thermals, the flaps are deflected downward, whereas in the straight and speed flight they stand in the neutral position or are even deflected upward (negative position) during the speed flight. To minimize the glider's drag, the flap position is changed according to the airspeed of flying. Today, the non-slotted plain flaps are most commonly used due to their simple design. Most of the modern gliders, having wing airfoils with relative thickness of 12.7-13.4% of the chord, enable thermal flying by applying the lift coefficients 1.4-1.5 without significantly increasing the drag. Although the Fowler flaps are more effective in generating lift, then due to the slot, they also generate relatively higher drag. The non-slot flaps (also referred to as Wortmann flaps, Figure 15) for glider SB-11 designed in Akaflieg Braunchweig proved suitably effective. In the extended position, these would contribute to the maximum lift coefficient increase up to 1.7. Additionally, the total area of the wing was also expanded by up to 25%.
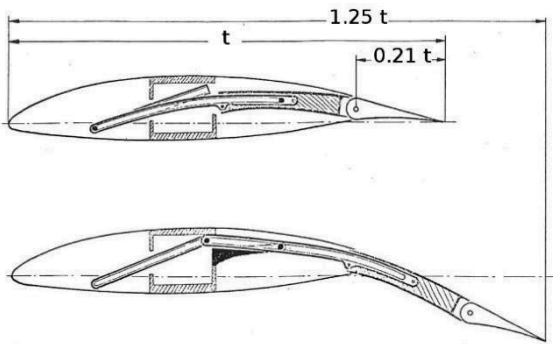
Figure 15. SB-11 glider using Wortmann flaps (Horstmann et al., 1979).

The flight performance of the SB-11 is better than that of other gliders of similar wingspan, but its main disadvantages include less wing torsional stiffness and complicated structure of flap controls. Today, relatively thin airfoils are used, with their laminar flow on the lower surface of the wing extending up to 92-95% of the wing chord, which do not enable using that kind of flaps because these would interrupt the laminar flow. The aspect ratio of the wing is also much higher and the use of the Wortmann flap increases the risk of the wing flutter. To calculate real aerodynamic characteristics for the variable geometry miniflaps (VGMF), the author of this thesis used the XFLR 5 software (XFLR5, 2017). The XFOIL code was developed by M. Drela from MIT (Drela, 1989). Using this software, the author designed optimal shape and deflection angle VGMF for the wing with airfoil LAP 7-131/17. The airfoil pressure diagram is described in Figure 16. In this Figure, presented by using VGMF, a laminar flow was maintained up to 68% of the chord on the upper side of the airfoil at Cl=1.75. While on the lower side of the airfoil, the laminar flow reaches up to 75% of the chord. Despite of the flow near to the VGMF trailing edge being separated, the drag remains relatively low. The lifting center is located 42.5% of the chord. Accordingly, the center of gravity should be 38-40% of the MAC. In Figure 17, airfoil polars without and with VGMF are compared. By using VGMF, airfoil max L/D ratio increased from 175 (Cl 1.3) to 201 (Cl at 1.7), i.e. nearly by 14.6%. (Paper II) This is a far better result than using a conventional type of flap. However, it can be clearly seen that at Cl values below 1.3 it is practical to retract the VGMF to decrease the drag. It should be noted that the above-mentioned perfect results are realistic when flying in non-turbulent atmosphere if the wing is clean. When contaminated with insects or water drops, the airfoil drag may increase more than twice.

Thickness	=	12.78%	Polar Type =	0
Max. Thick.pos.	=	39.80%	NCrit =	10.000
Max. Camber	=	11.20%	Forced Upper Trans. =	1.000
Max. Camber pos.	=	37.20%	Forced Lower Trans. =	1.000
Number of Panels	=	102	Alpha =	0.50 °
			Cl =	1.752
			Cm =	-0.307
			Cd =	0.009
			L/D =	194.832
			Upper Trans. =	0.679
			Lower Trans. =	0.749
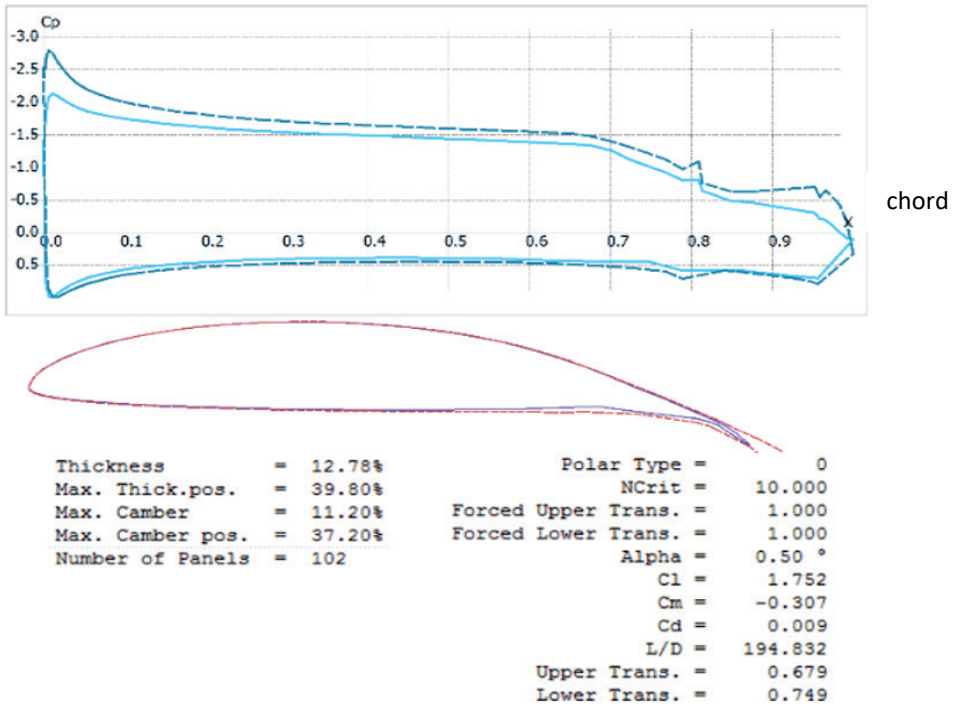
Figure 16. Pressure distribution on the LAP 7-131/17 airfoil, flaps +15º, with VGMF +16,7º (above) and airfoil aerodynamic characteristics (below), at the Re 1,1x10⁶ (Paper II).
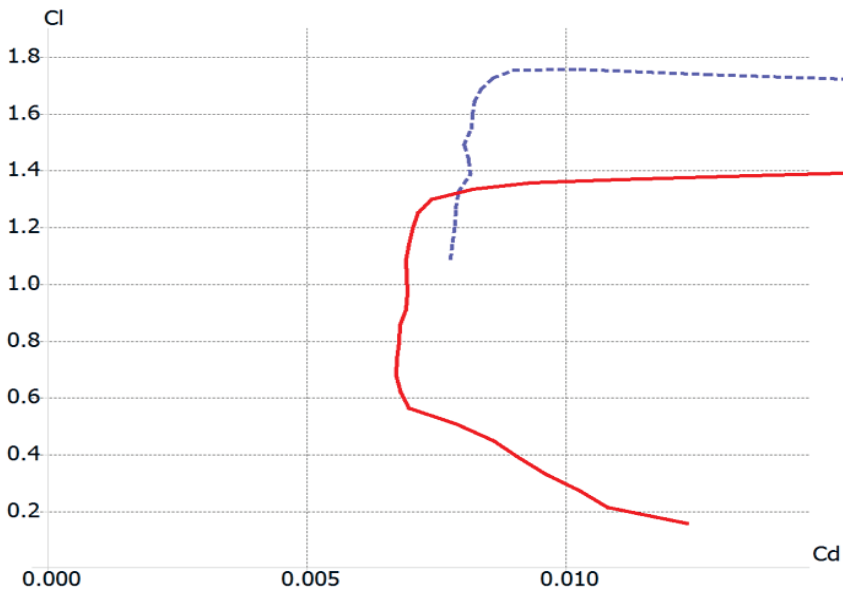
Figure 17. Airfoil LAP 7-131/17 polars, with flaps at +15º with and without the VGMF.

With flaps deflecting at +15º downward, the VGMF +16,7º at the airfoil angle of attack of 0º increased the lift coefficient by 0.669.
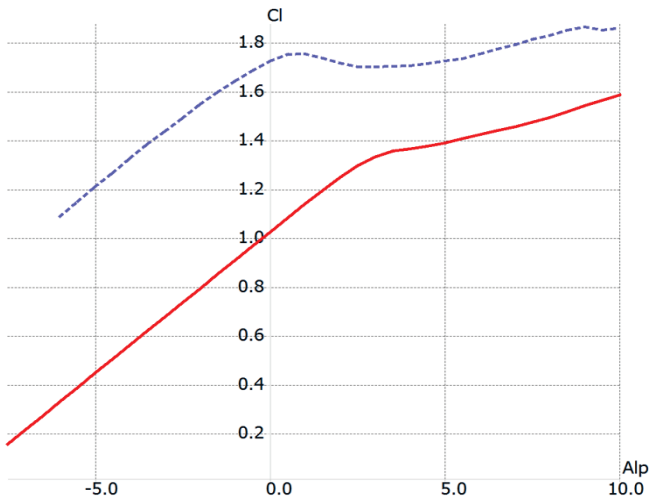
Figure 18. VGMF influence on airfoil LAP 7-131/17 lift coefficient (flap angle +15º) Cl versus AoA (Paper II).

Variable geometry miniflaps are accommodated inside the flaps. For the VGMF extending, the lower aft side of the flap is covered with flexible precurved mylar seal. Like Wortmann flaps, extending the VGMF increased the wing area by 6.5% and could be deflected by 16.7º (Figure 19). The picture shows a top view of the VGMF, made of carbon fiber behind the trailing edge of the flap.

Figure 19. VGMF in extended position.

To improve the roll control at the beginning of the test flights, miniflaps were also attached to the trailing edge of the ailerons. Their use was later abandoned because the roll controllability was good enough.
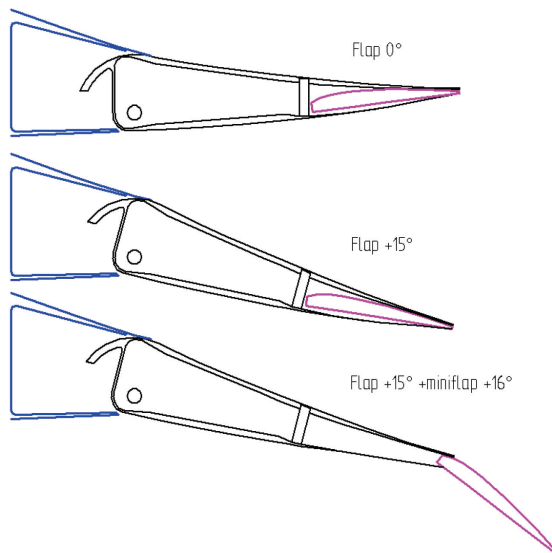
Figure 20. VGMF different positions with flap in glider LAK-17B wing.

Like the Wortmann flap, there are no slots between the flap and VGMF, but instead, to ensure smooth movement of the miniflap, the rear lower section of the flap is made flexible (Figure 20). Wider flap width (17% of the wing chord) is needed for completing the VGMF flap track and actuating mechanism inside the flap. By using VGMF together with the flap at deflection angle +15˚, the airfoil's maximum lift coefficient increased from 1.36 to 1.75, i.e. by 28.5% (Figure 18), on the other hand, the critical angle of attack decreased from 3.5° to 0.5°. To ensure the optimal lift distribution alongside the wing, for actuating the flaps and VGMF, it is also necessary to deflect the ailerons downward at an angle that exceeds the deflection angle of the flaps.

1.2.2 Technological design of a variable geometry miniflap

From an engineering perspective, designing a control mechanism for VGMF is a serious challenge because the wings of the glider flex during the flight. Normally, the wing tips of Lak-17B flex approximately 0.50 m upward above the neutral position during the flight. At maximum overloading, the wing tip reaches approximately 2.5 m upward or 1.5 m below the neutral position at 18-meter wingspan. Also, under these conditions, the VGMF control mechanism must work smoothly (Figure 21).

Figure 21. LAK-17B with VGMF to make a test flight.

The torsional stiffness of flaps is a very important indicator and its center of gravity should stay within the permitted limits. To increase the torsional rigidity, an extra spar and ribs were bonded inside the flap.

Figure 22. VGMF control mechanism inside the flaps.

To minimize the weight of the flap, 1.5 mm thick balsa wood sheets were used between the CFRP layers. The miniflaps were designed by the author of this thesis at the Department of Aircraft Engineering of the Estonian Aviation Academy (Figure 22). Many of miniflap control elements were milled from aluminium alloy mark 7075. Several complex elements were produced from stainless steel 316R, by using 3D laser sintering at the Powder Metal Laboratory at Tallinn University of Technology (Figure 23).
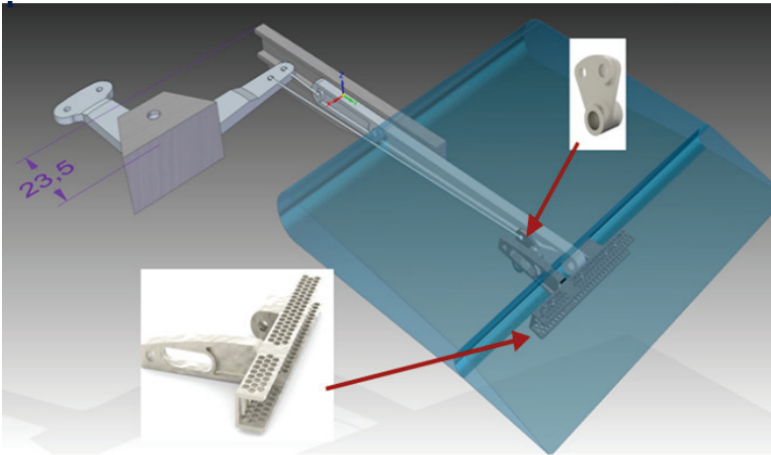
Figure 23. 3D laser printed control elements inside the flaps.

The actuating mechanisms inside the flap move simultaneously through the connected CFRP guide tube (Figure 24). The miniflap control mechanism consists of three devices: the actuating mechanism (blue), a miniflap track beam and guide rail (yellow and red), as well deflecting mechanism which is located inside the front side of the miniflap.
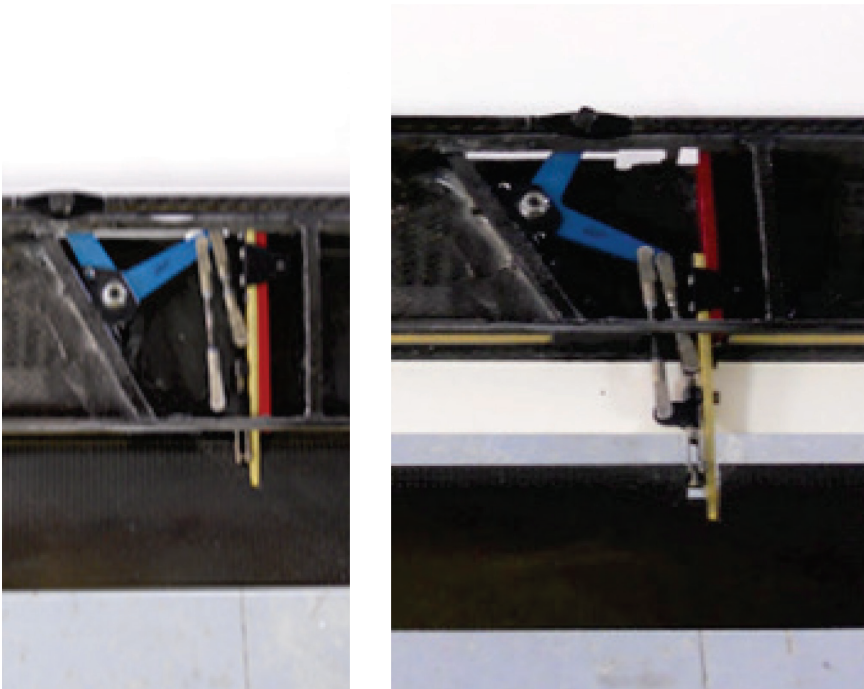
Figure 24. The novel control mechanism of miniflaps, created by the author of this thesis, in retracted and extended positions. (Paper II).

The flap's lower rear side is coated with elastic precurved mylar sealing (Figure 25).

Figure 25. The miniflaps in extended position. The precurved mylar seal coated at the lower side of the flap's trailing edge.

With the wings rigging (joining), the miniflap controls were joined automatically with the fuselage controls. The average weight of the new flaps designed with miniflaps is 142 g (7%) less, compared to that of the standard flaps. This actuating device designed by the author has been published in the journal "Aviation" No. 4, 2017 and international experts have acknowledged it as a highly promising technological solution. The center of gravity of the flaps was located near to the allowable rear position. With their flaps' torsional rigidity being lower than that of the standard flaps, the glider's maximum allowed airspeed was limited to 180 km/h. The fact that the new flaps were lighter in weight, enabled to increase the thickness of CFRP skin laminates and, thus, to achieve the relevant torsional rigidity. Miniflaps actuating is controlled in the cockpit by using a manually operated lever. Before the test flights, non-destructive tests were carried out. Finally, the miniflaps connected to the flaps were loaded to the 3G overload. Both the deflection angle and the twist angle of the flaps were measured. Similar test of the mechanical devices under overloads was performed. The positioning of the VGMF on the wings is shown in Figure 26.
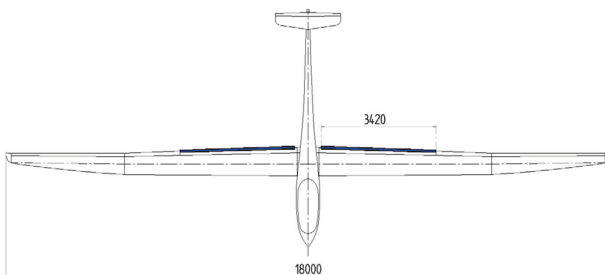
Figure 26. VGMF positioning on glider LAK-17B.

1.2.3 Flight test methodology

To perform the flight tests, the methodology developed by Richard Johnson was used (Johnson, 1989), together with the J. Hendrix flight data recorder (Hendrix, 2011). Before the flight tests, the airspeed indicator was calibrated, using the Air Data Test Set MPS 43. (Paper II) As is widely known, airflow over the glider affects the indicator readings during the flight. Due to this the DFS-60 static probe was used for calibrating airspeed indicator

additionally. The test flight results provided by calibrating airspeed indicator with different flap and airbrake positions have been presented in Figure 27.
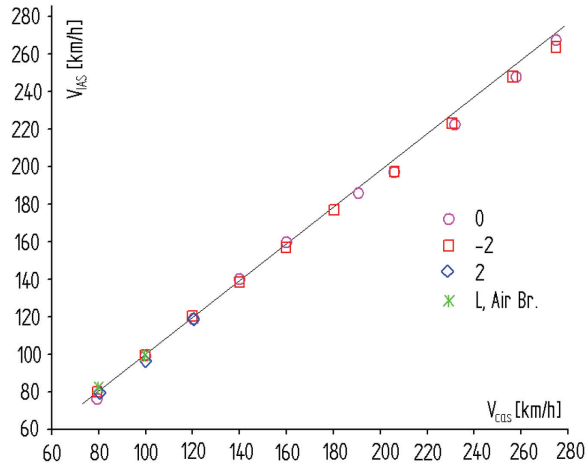
Figure 27. Test flights results provided by calibrating airspeed indicator in glider.

For data recording during the test flights, the LX Eos flight recorder was used. The flight test data obtained were processed and analysed, using the AJ1.IGC Software (IGC, 2017). The software enables to analyse and reproduce in 3D space the flight data received. Additionally, a GoPro camera was used in the cockpit to measure the glider's pitch angle, and to video record flying at different air speeds. For parallel flying, gliders with the same flight characteristics were used, but mostly the glider LAK-19T that had undergone a thorough pre-flight calibration. Before test flights, the take-off weight of the glider was determined and additional weight (water) was loaded to the tail ballast tank so as to shift the centre of gravity to the allowable rear position. During test flight, the wing loading of both gliders was 39.39 kg/m². The corrected results of the test flights are presented in Table 1.

Table 1. Corrected results of test flights. (Paper II)

LAK-19T	CAS km/h	76,4	78,3	80,4	84,6
	Vy m/s	0,940	0,744	0,643	0,577
LAK-17B flap+15°	CAS km/h	76,7	78,1	80,2	82,0
	Vy m/s	1,088	0,892	0,737	0,628
LAK-17B flap+9°+VGMF	CAS km/h	74,8	76,4	79,5	83,2
	Vy m/s	1,092	0,803	0,555	0,660
LAK-17B flap+15°+VGMF	CAS km/h	72,6	74,1	76,4	79,0
	Vy m/s	1,115	0,805	0,638	0,692

To perform the test flights, the gliders were towed to the altitude of 2,500 m above the ground. During the glide flight, the sink speed was measured at different airspeeds and also by using different positions of flaps and miniflaps. Each flight leg at a constant airspeed lasted for 180 seconds. In parallel flying, the gliders flew side by side at 30-50 meters from each other. The difference between the sink speeds was compared by using the video recording. Measurement was stopped above the inversion layer, and the measurement results were adjusted based on the variance of air pressure and temperature readings with those of the standard atmosphere. For calculations, the formulas presented by Pätzold were used (Pätzold, 2014).
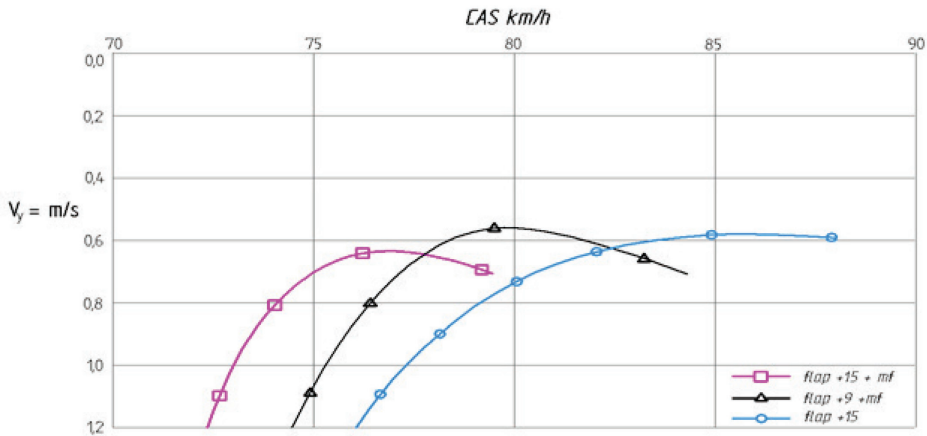

Figure 28. LAK-17B sink speed influence on VGMF in different flap positions.

1.2.4 Flight test results

As a result of the test flights at the airspeed of 72-82.5 km/h, the variable geometry miniflaps decreased the sink and stall speed of the LAK-17B glider (Figure 28). The flaps were deflected downward at +9˚ and +15˚; the ailerons were deflected same time at +14.4˚ and +21.2˚. With the flap deflection angle at +9° at the airspeed of 79.5 km/h, the sink speed was decreased when using the VGMF from 0.775 to 0.555 m/s, i.e. by 39.6%. With the flap deflection angle at +15°, the optimal flight speed decreased, but the sink speed increased. One of the main factors causing the aerodynamic drag to increase is the canal between the flap and the fuselage that is formed when the flap is deflected and that violates the elliptic lift distribution on the wing. Deflecting the flap also induces the growth of the interferent drag. Unlike the narrow (e.g. 2% length of the wing chord) miniflaps, those making up to 6.5% of the length did not increase the critical angle of attack but, rather, decreased that angle by 3° (Figure 18). The decreasing lift in overcritical angle of attack when using miniflaps was relatively slow, and the decrease in the critical angle of attack, likewise, was not significant. Also, the glider's lateral stability decreased, because during the stall, the lift coefficient decreases more near to the ailerons. Under the impact of miniflaps, the maximum increase in lift coefficient C_l obtained was from 1.41 to 1.58, i.e. by 12% and the stall speed decreased at the same time from 75.4 to 72 km/h, i.e. by 4.7%. The aerodynamic effectiveness of the miniflaps was reduced by their relatively small wing surface area. The miniflaps take over for 45% of the total wing area. If the miniflaps were located along the wing's trailing edge, from

root to tip, the lift coefficient could rise up to 32%, which allows to reduce the stall speed by 13.8%. At the airspeed in excess of 82.5 km/h, i.e. C_l<1.2 the miniflaps increased the drag, and due to this it is practical to retract the miniflaps into the flaps before increasing airspeed. Considering the dispersion of the instrument accuracy and the results obtained during the test flights, the value of the measurement uncertainty was 13.4%. This means +/-0.25° and +/-1.0 cm/s in sink speed. Therefore, the measurement uncertainty is approximately 7.5 times smaller than the difference in the test results and therefore, the final results are credibly correct. Several glider pilots tested the use of miniflaps in thermals. Dependent on each pilot's weight, a 35°-40° bank angle in spiral flight was performed at the airspeed range of 80-85 km/h (at wing loading 39 kg/m²), which is significantly lower than the designed airspeed (90-100 km/h) of this type of glider. The effect of using VGMF is particularly considerable when flying in narrow thermals. Before the test flights, additional weight was loaded to the tail ballast tank. By changing the centre of gravity from 26 to 35% of MAC, the glider's flying characteristics improved and at the same time, its stall speed decreased. However, additional change of the centre of gravity up to 39.9% of MAC did not lead to further improvement of the glider's flight characteristics. Instead, its stall characteristics degraded. The lateral stability could slightly be improved when reducing the ailerons' deflection angle by 1°-2°. (Paper II)

1.2.5 Conclusion

The defended statements

- With 2% of the wing chord, all wingspan fixed angle miniflaps at a 30° deflection angle, the sailplane's Jantar-Standard 3 stall speed reduced from 75 to 66 km/h and the Cl max increased from 1.35 to 1.66 (Paper I).
- The critical angle of attack of the wing increased by 1.6° from 9.6° to 11.2°. The analysis of the obtained test flight results indicated that using miniflaps with lift coefficient Cl ranges from 0.99 to 1.21 and from 1.32 to 1.66, the drag of the glider Jantar-Standard 3 decreased compared to the standard configuration.
- The L/D ratio of Jantar-standard 3 glider improved Cl>1.0, especially in Cl range from 1.08 to 1.19. (Paper I) As a result of free flight tests, the fixed miniflap effect significantly exceeded the calculated results for this type of glider.
- Using variable geometry miniflaps allows to improve the L/D ratio of LAK-17B glider within the range of Cl from 1.2 to 1.58 (Paper II). At the same time, the critical angle of attack decreased by 3°. The highest rise of L/D ratio was achieved when using the miniflaps (reaching up to 39.8% at Cl=1.29).
- Test pilots confirmed that by using miniflap, the glider's longitudinal stability increased and the roll control of low flight speed improved.

Effectiveness of miniflaps could still be higher if instead of covering 45% they would cover up to 65-75 % of total wing area. In this thesis, it was found that the miniflaps somewhat improved the stall characteristics. At the same time, this issue should be investigated systematically. The main importance of this thesis is that for the first time, the author designed and tested the miniflap, which simultaneously changes both the angle of deflection and the area of the wing. Its effect is significantly higher than that of the widely known plain flap. In addition to the aerodynamic effect, the device proved to be reliable, despite the large deformation of the wing during the flight. Thickness of the airfoil used previously was in between from 15% to 17% and had much higher drag. Also, the wing

flexed in flight much less due to smaller aspect ratio. For the first time, the variable area flap was successfully tested and used in such a thin (thickness 13.1%) low drag wing, despite the high elastic deformation during the flight. Actuating device proved that it is possible to design a light and reliable device and proved its usability in extreme conditions. The similar device can be used in the future inside the thin trailing edge flaps of commercial aircraft and large UAV-s.

2 Impact of trailing edge modifications on the aerodynamic performance of the wing at high speed

2.1 Influence of trailing edge modifications on the aerodynamic characteristics of a supercritical airfoil at transonic speeds

One of the most effective methods for increasing the L/D ratio on commercial aircraft at Cl values from 0.55 to 0.7 and at Mach=0.78-0.85, is to use various modifications to the trailing edge of the wing. These modifications are divided into two. The most known modifications include the diverged trailing edge (DTE). It is used by commercial aircraft in McDonnel Douglas MD-11 and also in Boeing B777X. DTE allows to avoid the wave drag growth that is associated with the increase in Cl value of over 0.55. Unfortunately, at Cl values less than 0.50, DTE-s increase drag. Airbus, a leading European aircraft manufacturer, has tested the mini split flap called miniTED with an adjustable angle of deflection. The results obtained and their use in miniflap design are discussed in the next chapter.

2.1.1 High speed flight test results with miniTED-s
Successful developments up to large scale demonstrations have taken place, e.g. such as in-flight testing of multifunctional mini Trailing Edge Devices (miniTED-s). The miniTED-s are a highly efficient concept where large effects can be obtained with a small chord device attached directly on the wing/flap trailing edge (Reckzeh, 2014).

Figure 29. MiniTED (in red colour) as multifunctional add-on device on the A340 Flaps in Flight Test. (Reckzeh, 2014).

The above-mentioned devices require a separate actuating system, which has to be embedded on the moveable trailing edge flap carrying the miniTED.

   Based on the test flight, the miniTED deflection in flight at subsonic speeds of 0.70-0.82 Mach enables to decrease the wing drag from above Cl 0.53 (Richter, 2010). The mini split flap is proved more effective than the plain miniflap type. Different researches have noted out that depending on the aircraft type, the optimum miniTED deflection angle is

7.5°-22.5° (Gardner et al., 2006). Some role in the reducing of the drag might be attributed also to the decreasing of 2-2.5° on the fuselage slope angle. In wind tunnel tests with the model of the Airbus A340-300 at Mach=0.82, the use of a 2% chord miniTED at 7.5° deflection angle increased the aircraft's L/D ratio by 4.4% at Cl=0.65 and by 6.07% at Cl=0.67 (Figure 30). (Paper I) This responds to A340-300 flight weight of accordingly 181,000 kg and 224,700 kg at flight level FL 390 and Mach=0.82. The fuel consumption decreases proportionately. The received results are comparable to the effect of using winglets. It should be accented that the use of miniflaps for aircraft gives significant results at wing loadings over 600-700 kg/m². The highest fuel economy is attained with the use of both the miniflaps and the winglets. In case of turbulence, with changing the miniflaps angle during the flight, the load distribution can be changed (Gardner et al., 2006), decreasing the wing bending moment that is induced by the turbulence in airspace.

Although miniTED had a relatively high aerodynamic efficiency, its technical solution was complicated. The thin miniTED was not rigid enough and required a simultaneous cooperation of many electric actuators. However, this solution is not sufficiently reliable for using on commercial aircraft.
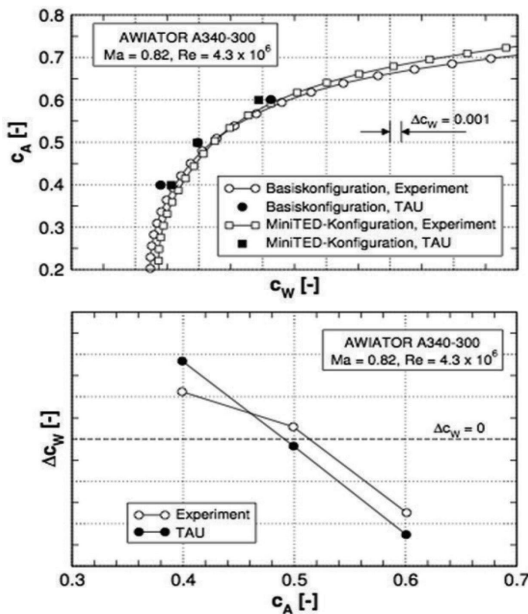
Figure 30. Impact of miniTED (+7.5°) on A340-300 drag at different Cl values. (Richter, 2010).

In the Boeing CLEEN framework (Wilsey, 2012), miniflaps were tested on an American Airlines Boeing 737-800 in September 2012. The 3% chord of the wing mini plain flaps at the angle of 30° were used. In addition to reducing the fuel consumption miniflaps enable to reduce the noise at takeoff and at landing as the required airspeed at takeoff is lower and the aircraft's angle of ascent is greater. (Paper I)

2.1.2 Aerodynamic performance of the supercritical wing

Airflow control near to the wing at transonic speed is complicated. From Mach=0.74 the Cl low drag region of supercritical airfoils becomes quite narrow. For example, at the airspeed of Mach=0.78, the low drag region of the airfoil SC(2)-0410 is between Cl=0.4 and Cl=0.5. The Cl range of the airfoil SC(2)-0710, due to the higher chamber at the same Mach, is within the range from 0.55 to 0.70. At the same time, at lower Cl values the drag of SC(2)-0710 is higher than that of the airfoil SC(2)-0410. Due to the air traffic and meteorological conditions there is often need for using the Cl range between 0.45 and 0.7 during the flight. A fixed shape airfoil of a commercial aircraft is usually designed for the optimal range of Cl=0.5–0.55, but at the values higher or lower than this, the drag and fuel consumption start to increase. The main reason for the drag increase is the arising shock wave on the upper side of the wing.

   Figure 31 presents the Mach field over the supercritical airfoil SC(2)-0410 and the pressure distribution on the surface of the airfoil at the angle of attack of +0.5^0 at Mach=0.78 (Paper III). While the airflow exceeds the supersonic airspeed on the upper side of the airfoil, the changes in the pressure and airspeed are relatively smooth.
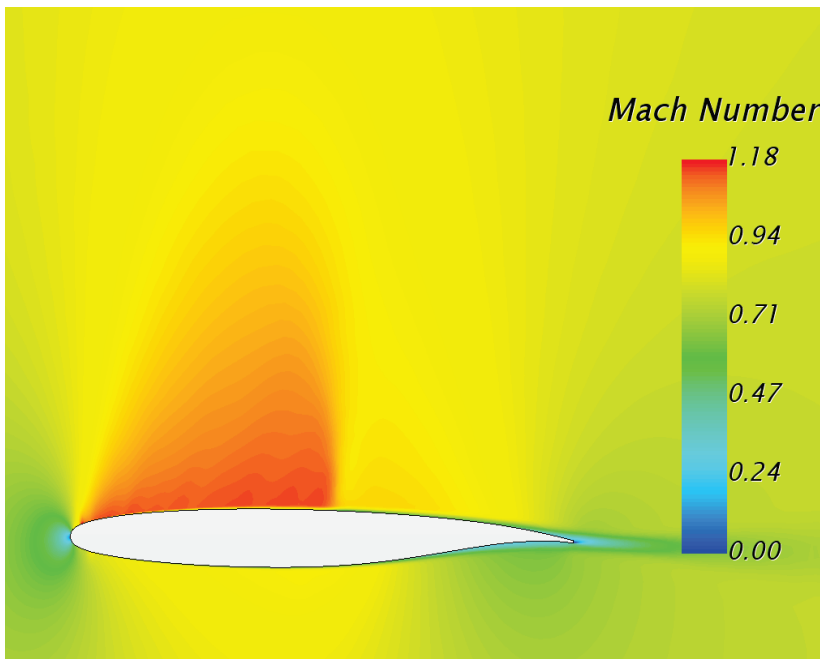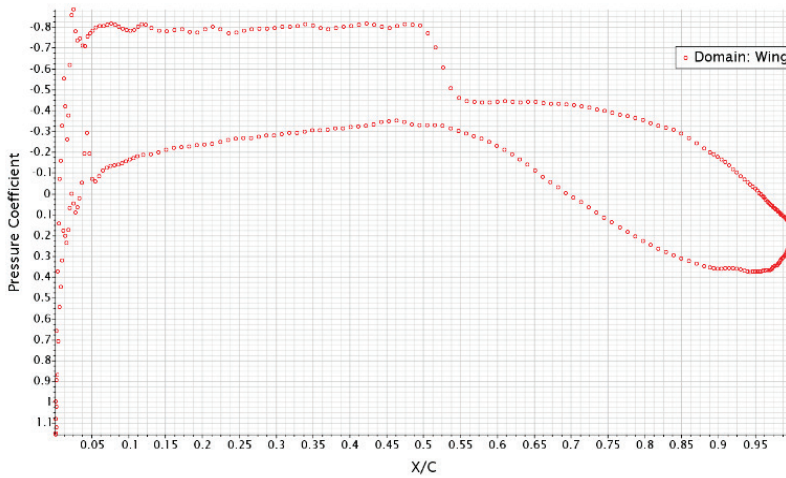
Figure 31. Supercritical airfoil SC(2)-0410, Mach field and pressure distribution at Mach=0.78, α =0.5º and Cl=0.476.

The Mach field situation is significantly changed when increasing the angle of attack of the same airfoil by up to +1.5⁰. As can be seen in Figure 32, a strong shock wave on 64% of the chord on the upper side of the airfoil causes a rapid decrease of air speed and with that, increase of the drag. Behind the shock wave the increase of the boundary layer thickness is clearly visible.
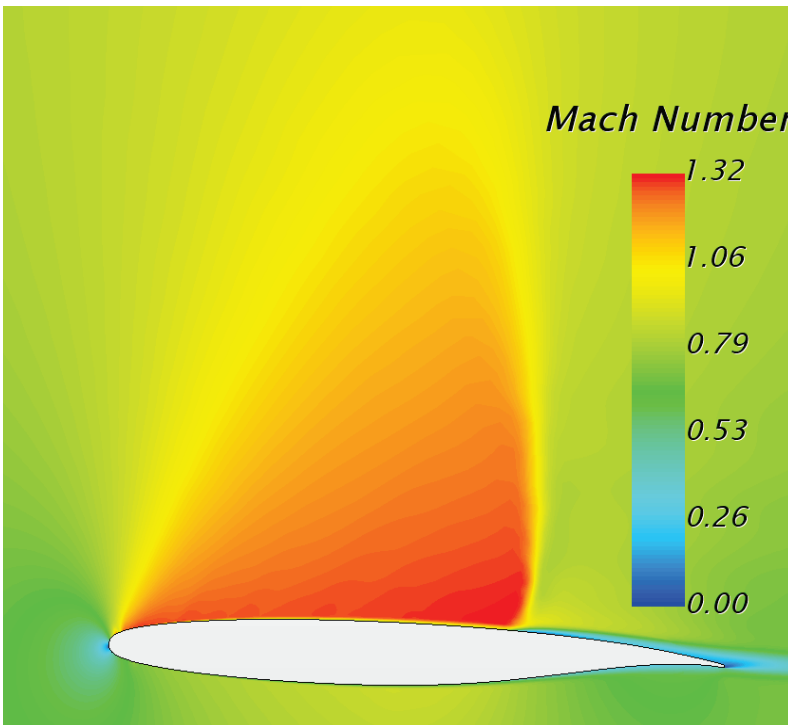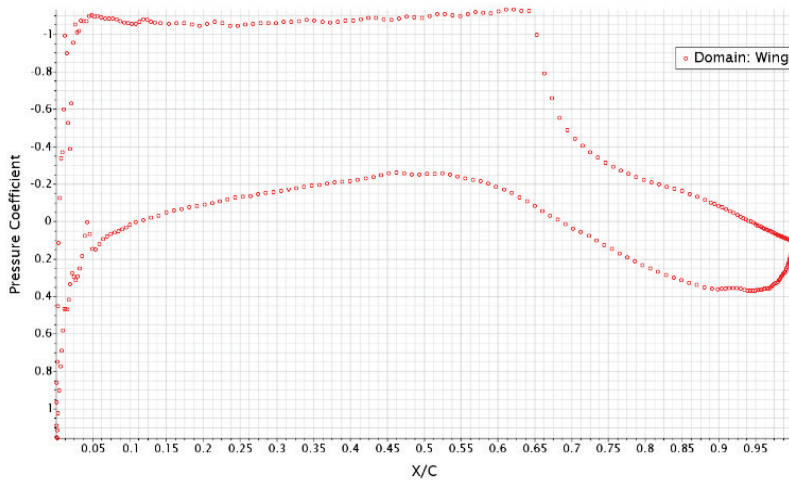
Figure 32. Supercritical airfoil SC(2)-0410, Mach field and pressure distribution at M=0.78, α =1.5º, Cl=0.7037.

2.1.3. The effect of the cruise miniflap profiles on the aerodynamic performance of the wing

To solve the problem discussed above, the author of this thesis designed the cruise miniflap (CMF) for the supercritical airfoil SC(2)-0410 with the width of CMF 4% of the chord, using CFD software STAR-CCM+. Like the Wortmann flap, it can be retracted at lower Cl=0.52 and extended at higher Cl values. The extended CMF also deflects downward by about 3.5º (STAR-CCM+, 2017).

   To make the calculations, the standard atmospheric conditions data were used. The Re number selected in the calculations was 7.7×10^6. By thoroughly examining earlier research work, in particular the studies by Harris and Henne, the author was inspired to compare different trailing edge profiles. Different shape profiles were calculated at the trailing edge of the CMF. It was also important to compare them with standard (sharp) trailing edge (CMF-A). Computational calculations were based on Reynolds-averaged Navier-Stokes (RANS) Solution (equations). Estimates for most of these modifications showed the maximum lift coefficient increasing and the wave drag relatively reducing. Figure 33 presents different CMF profile shapes that were used for calculations. At the angle of attack of 0º only 4% wide of the airfoil chord, the CMF-D increased the lift coefficient from 0.365 to 0.857, i.e by 0.492, that means more than twice (Figure 34). Using the CMF-D airfoil trailing edge profile, the angle of attack reduces by 2.41º to the same lift coefficient. (Paper III) The most important results that can be applied to the design of new commercial aircraft are mainly presented on pages 42-46 of this research.
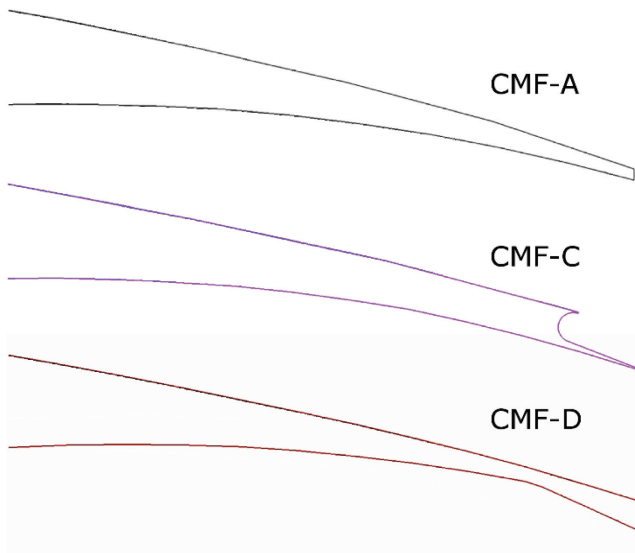
Figure 33. Different CMF trailing edge profiles that were used for calculations.
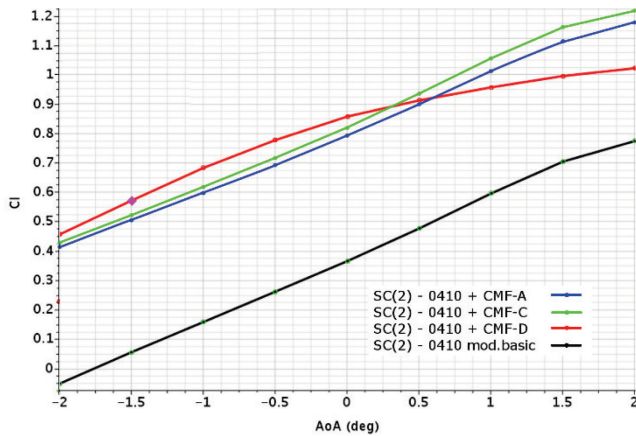
Figure 34. Influence of different CMF profiles on airfoil SC(2)-0410 lift coefficient.

The CMF-C with a cavity trailing edge increased the Cl coefficient at the same angle of attack up to 0.825, i.e. by 0.46. Both of the above-mentioned CMF profiles obtained are higher when compared to the standard sharp trailing edge of 0.2% thickness, i.e 0.41. Due to the high efficiency, the CMF-s are suitable for optimizing the lift distribution along the wing, which enables to reduce the induced drag (Gardner et al., 2006).

Comparing the pressure distribution of airfoil (Figure 35) with different trailing edge profiles it its clearly visible that the CMF significantly reduces the airfoil's upper side Cl level from 1.1 to 0.8, as an average, and expands the plateau of negative pressure from 64% to 81% of the chord. (Paper III)
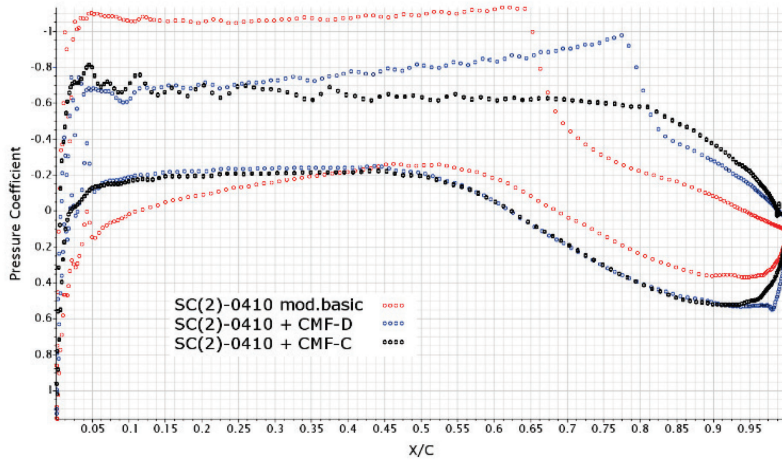
Figure 35. Influence of different CMF profiles on pressure distribution at M=0.78, Cl=0.70.

With the reduction of negative pressure, also the air flow speed is reduced, and with that, the wave drag on upper side of the airfoil. Comparing the Mach fields of different CMF-s, it appeared that the use of CMF changes the structure of the shock wave. The normal strong shock wave is characteristic of the basic airfoil. By using the CMF, the shock wave moves closer to the trailing edge, also the transition is wider and has a lambda-shaped pattern (Figure 36).
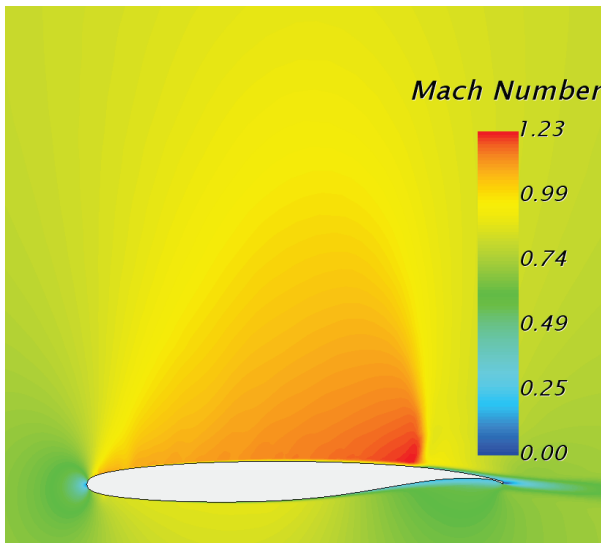
Figure 36. Supercritical airfoil SC(2)-0410 with CMF-D Mach field M=0.78, Cl=0.682.

An especially low shock wave was formed when using the CMF-C with cavity. Its trailing edge height is 0.7% of the airfoil chord. The shock wave reduced significantly and the transition of air pressure on the upper side of the wing is smoother when compared to other CMF profiles (Figure 37). With the use of the CMF, the lifting centre of the airfoil moves towards the trailing edge while increasing the nose down coefficient. The

comparison of calculated aerodynamic polars shows (Figure 38) that by using CMF-s, the decrease of the drag begins from Cl>0.50–0.52. CMF-D is more effective when compared to the other types of CMF-s. The use of CMF-D reduces the airfoil drag at lift coefficients of Cl=0.65 and Cl=0.70 by 20.34% and by 26.57%, respectively. (Paper III)
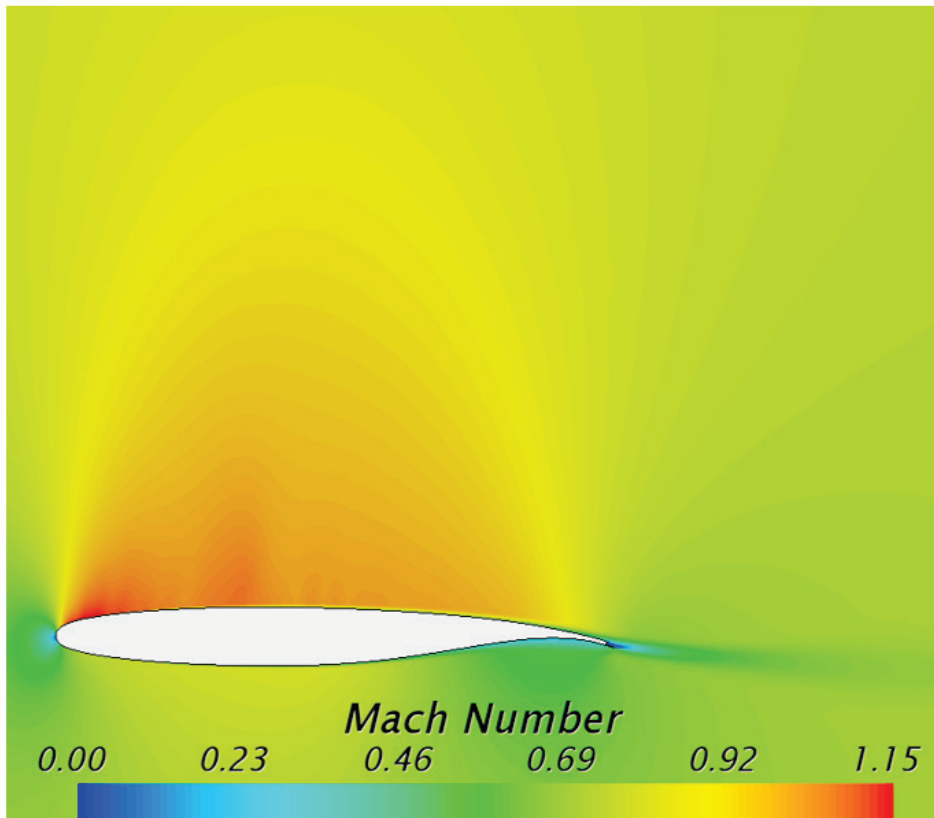
Figure 37. Airfoil SC(2)-0410 with CMF-C Mach field at M=0.78, Cl=0.70.

Despite the positive effect of the cavity trailing edge on pressure distribution, the CMF-C drag is a bit higher than that of the CMF-D. But the cavity height and deflection angle optimization can still be drag reducing. The optimal thickness of the trailing edge cavity remains within the range of 0.5–0.9% of the chord, and depends on the relative thickness of the airfoil, Mach number and the Cl value.
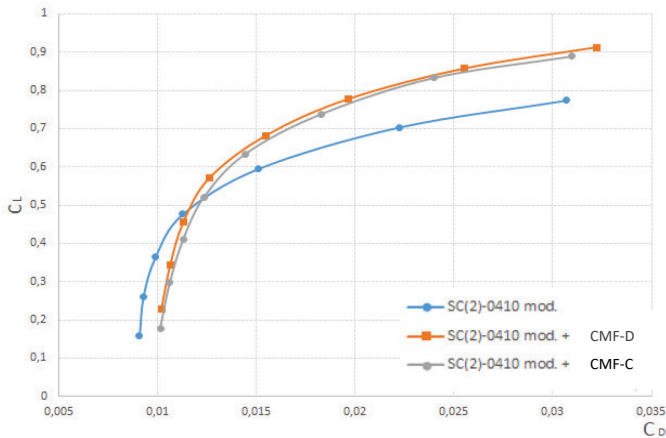
Figure 38. Calculated aerodynamic polars of SC(2)-0410 airfoil with different CMF profiles.

With the higher Cl value, the height of optimal cavity is higher. The same principle is used in other CMF design. The cavity trailing edge allows to control the size of the von Karman vortex and the separation from the trailing edge. By modelling the wing body configuration, the use of CMF-D may increase the L/D ratio of a medium-sized twin-engine commercial aircraft by up to 5 % (Figure 39). (Paper III)
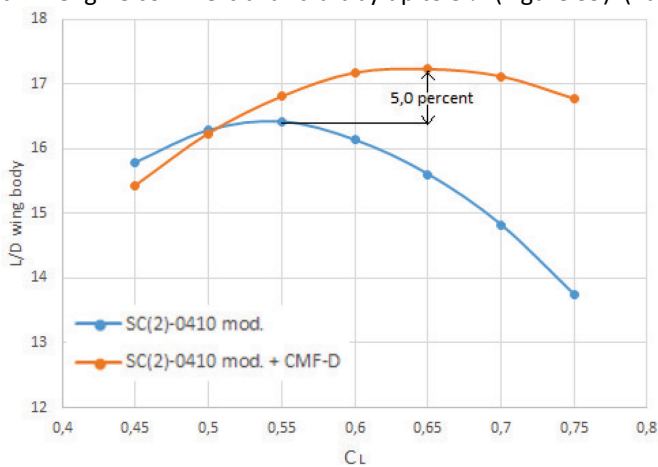
Figure 39. Comparison of calculated wing body L/D characteristics for a medium-sized twin-engine aircraft.

This graph shows that the use of CMF-D increases the max L/D ratio at Cl=0.65 and the wing effective aspect ratio (AR) remains within the range of 10.7–12.0. If the wing aspect ratio is lower than 10, the effectiveness of CMF decreases significantly, because the increasing in Cl creates the increase in the induced drag.

 Another important influence is that the extension of CMF brings the centre of lift to move rearwards the trailing edge of the wing. When the centre of gravity is fixed, the use of CMF increases the balanced drag because the stabilizer must produce higher negative lift. Increasing of the balanced drag can be up to 2% rise of the total drag of the aircraft. The similar result was reached also by P. A. Henne (Henne, 1990).
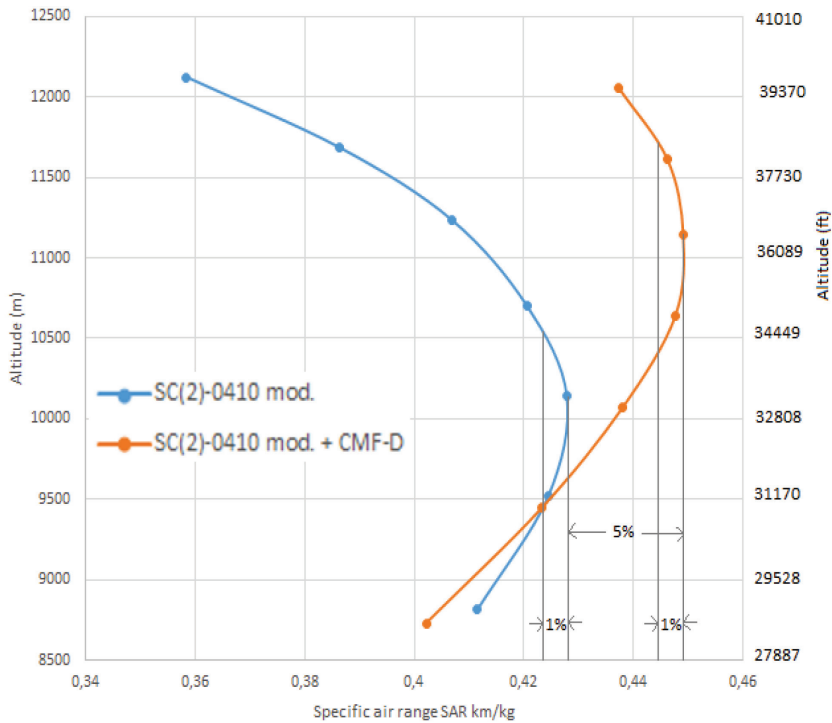
Figure 40. CMF-D influence on Specific Air Range (SAR) example for a typical medium-sized twin-engine aircraft.

Increase of the balanced drag can be prevented by using the trim tank in the tail of the aircraft. Usually this tank is designed as located inside the stabilizer. By using the CMF during the flight, the centre of gravity is moved behind along the chord by pumping the fuel from the central tank to the trim tank in the tail. Before the take-off and the landing, the fuel is pumped back into the central tank to increase the longitudinal stability.

2.1.4. The impact of cruise miniflap on the specific air range (SAR)

By using CMF, it is possible to increase the specific air range (SAR) (Figure 40). Specific air range is the ratio between true air speed and gross fuel consumption expressed as air nautical miles per gallon or kilometres per kilogram of fuel. It is a measure of the fuel efficiency of the aircraft. This figure shows the influence of optimal altitude with the CMF on SAR of a typical medium-sized twin-engine aircraft with the flight weight of 77,000 kg. As shown in this figure, the optimal altitude rises for about 900 m, and the low fuel consumption altitude range also increases.
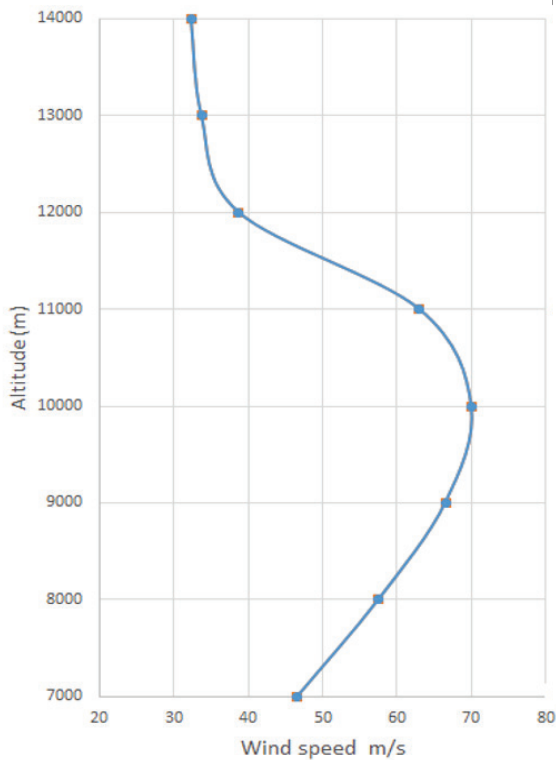
Figure 41. Wind speed inside a typical jet stream at different altitudes.

Strong winds inside the jet streams, appearing in various regions of the world, have a significant influence on the air traffic. The polar jet stream with the prevailing direction of the wind from the west to the east has a major impact on the air traffic in European airspace.

The typical jet stream wind speeds depend on altitudes and are shown in Figure 41. As it can be seen, the maximum wind speed remains within the range of altitude FL 300–340 on an average. The impact of the wind on an aircraft SAR decreases significantly with the rise of altitude from FL 340–400 upwards. Accordingly, flying in headwind is advisable within the range of altitude FL 380–400, and flying in tailwind within the range of altitude FL 310–330. In transatlantic flights from east to west, the use of CMF allows to increase altitude from FL 340 to FL 380, which enables to reduce the fuel consumption by about 5.7% in the conditions where an intensive jet stream is prevailing for about 25% of flight track. On the opposite flight, it is reasonable to use the altitude of FL 330. By this model, the optimization of flight levels would help to save all in all 3.1% of the fuel. (Paper III)

In the aircraft industry, the complex technical solutions have often been the cause why many great ideas have not been implemented. The main causes include the reduced operating reliability and the increased maintenance costs of the actuating systems. The technical solution patented by the author of this thesis is simple, reliable and requires low maintenance work (Figures 42).
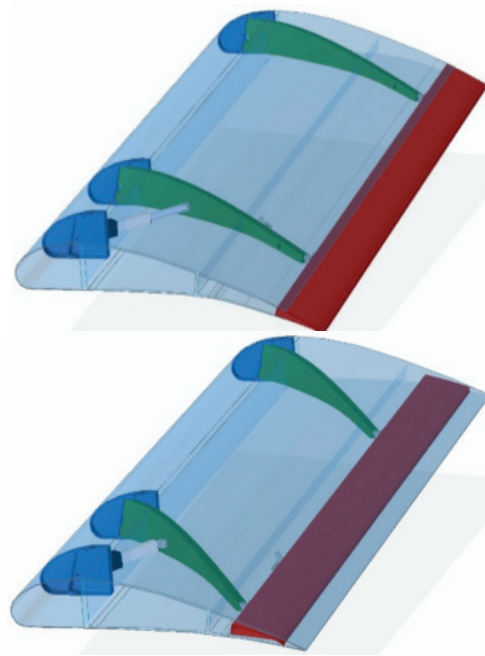
Figure 42. CMF actuating mechanism in extended and retracted positions (Patent application EP 17207454.4).

The most important units of this device are swivel beams that enable to retract and extend the CMF flap and concurrently change the deflecting angle. The motion of the CMF reasons the split flap deflecting, positioned under the CMF, and helps to reduce the friction drag by moving CMF. The centre of gravity of the actuating unit is located in the front side of the flaps. Due to this, the CMF can be used inside the ailerons because the mass balancing to prevent aileron flutter is not necessary. The main advantage of this solution compared to the VGMF presented in the previous chapter is that it contains approximately 3 times smaller number of moving parts. This makes the solution much simpler in terms of technology. Together with the reduction weight of CMF, it is possible to reduce the production cost of the entire aircraft, as well as to increase the aircraft reliability. (Paper III)

The most practical is to calculate the fuel consumption of the aircraft, using the Breguet Range Equation [1]. Knowing the specific fuel consumption of the propulsion system and other basic parameters of the aircraft, it is possible to calculate the range of the aircraft using the following formula (Young, 2018).

$$\text{Range} = \frac{V(L/D)}{g \cdot \text{SFC}} \ln\left(\frac{W_{\text{initial}}}{W_{\text{final}}}\right) \qquad [1]$$

where:
V - airspeed
L - lift coefficient
D - drag coefficient
SFC - specific fuel consumption
g - acceleration of gravity

$W_{initial}$ - aircraft take-off weight
W_{final} - aircraft landing weight

When the range is known, the following formula can be used to calculate the fuel consumption, also named as Fuel flow (mf) [2] (Young, 2018).

$$m_f = \frac{Winitial - Wfinal}{R/V}; \quad [2]$$

where:
mf - fuel flow, kg/h
R - range, km

From the above formulas shown, it can be seen that the drag reduction and the fuel consumption decrease proportionally. By increasing L/D ratio by 5%, the fuel consumption will also decrease by 5%. This assumption is true if the remaining parameters, except the weight, are constant.

2.1.5. Conclusion

The present study is focused on determining the effect of miniflaps on the aerodynamic characteristics of the wing on fully-turbulent flow conditions at Mach=0.78 and the Reynolds number 7.7×10^6. State-of-the-art computational fluid dynamic (CFD) methods were used.

The defended statements

- The CMF-D with the 4% of the airfoil chord with the deflecting angle of 3.5° increases the Cl by 0.492, that means more than twice in AoA 0°, therefore being much more efficient than the miniTED and other modifications tested earlier (Richter, 2010).
- The use of CMF-D caused the reduction of the airfoil drag at Cl=0.65 and Cl=0.70 by 20.34% and by 26.57%, respectively. It allows to increase the aircraft's maximal L/D ratio by 5% and considerably reduce the aircraft's fuel consumption. The main purpose of using the CMF is reducing the wave drag of the wing.
- Using the different deflection angles of CMF, it is possible to optimize the lift distribution along the wing and reduce the induced drag by 3-5%.
- By using the CMF, the centre of lift will move significantly backward of the wing chord. It is reasonable to change the position of CMF backward during the flight by pumping the fuel into the trim tank of the tail of aircraft.
- By using the CMF, it is possible to reduce the impact of meteorological conditions on the flight time and fuel consumption of the aircraft, mainly due to the impact of jet streams. Using the CMF allows to use the most optimal flight level during the flight and additionally reduce the fuel consumption by 3.1–5.7% and shorten the flight time.
- The simple CMF technical solution, developed by the author of this thesis (Patent applications EP17207454.4 and US 16/220,337), is more reliable and entails lower production and maintenance costs. If necessary, this device can be installed inside the aileron, because the centre of gravity of the device is in the front side of the aileron.

3 Advanced trailing and leading edge flap design for commercial aircraft

The high lift device performance of a commercial aircraft has a very important role in the flight efficiency and safety. At the same time, the construction of these devices is complex and requires a lot of maintenance work. Currently, the rack and pinion drive has become the most popular drive system for commercial aircraft slats (Figure 43).
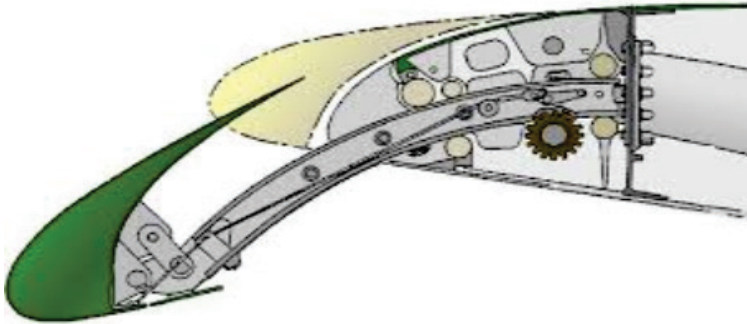
Figure 43. Rack and pinion drive system for slats. Used for the Boeing 757; Airbus 320 et al. (Niekerke, 2013).

In addition, the gear wheel and the torque tube drive system also include geared rotary gearboxes (GRA), offset gearboxes, torque limiter. Many of these units contain gears in different sizes which are usually highly loaded to increase the power to weight ratio. Due to its complex design, this system has several drawbacks. The high load is caused
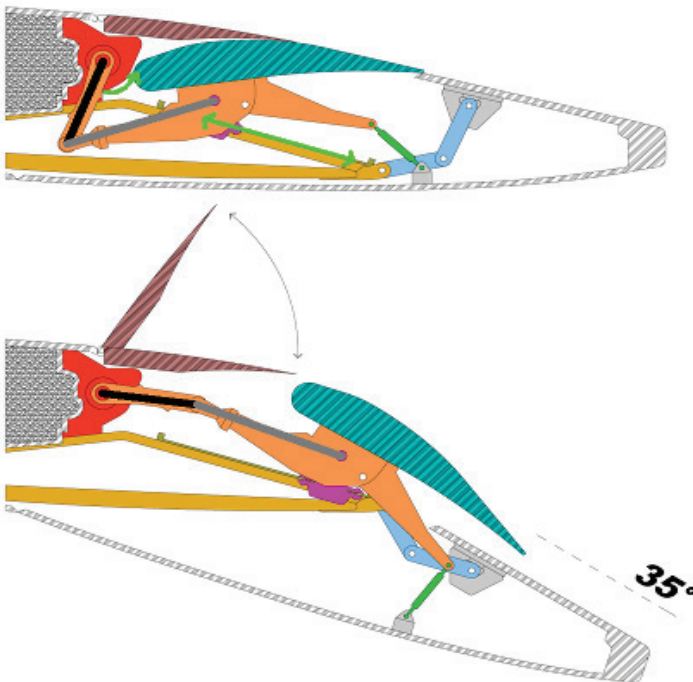
Figure 44. Link track trailing edge flap actuating system in Airbus A320 (Aircraft…, 2015).

by repeated faults in the gears. In addition to this, the fuel leakages occur in these systems at the junction between the fuel tank and track cans. A fuel leak can cause fire in the aircraft. Similar drive system components are also widely used to move the trailing edge flaps (Figure 44). Because the rotary gearbox loads are higher, incidents have occurred where gear failure has caused torque shaft breakage. Surprisingly, there have been even cases where a slat track beam has broken during the flight. In the next study, a new kinematic and less complex high lift actuating system was designed.

3.1 Development of the swivel beam system (SBS)

The swivel console equipped wing slats have been used for many years. The first patent on a similar device was taken already in the beginning of the last century by the British aeronautical engineer F.H. Handley Page (Page, 1921). By his invention, the axles of the system were positioned almost parallel and allowed to extend and retract the wing slats. This solution can be used also in automatically operated slats involvement system. In cruise flight, the air flow helps the retracting of wing slats. By increasing the angle of attack, the direction of the resultant force also changes, so that the slats are extended. As the slot has an optimum shape, then the velocity of the boundary layer air flow increases, and the lift coefficient increases considerably.

Today, similar system can be seen mostly in light aircraft. For example, it has been designed in Superstol (Cox, 2015) (Figure 45) and in Antonov An-2 aircrafts. This system stands out for its simple design, light weight and minimum maintenance costs. Its drawback, worth mentioning, is the constant angle of the slat which does not depend on the position of the slat. However, for wing flaps, such design has never been used. It is so because during the Fowler motion, the flap deflection angle should also be changed to increase the lift coefficient.

Figure 45. Just Superstol aircraft and its automatic slat mechanism (Cox, 2015).

Using the swivel beam system in the straight wing, the Fowler motion of the flaps is relatively not large (Figure 46).
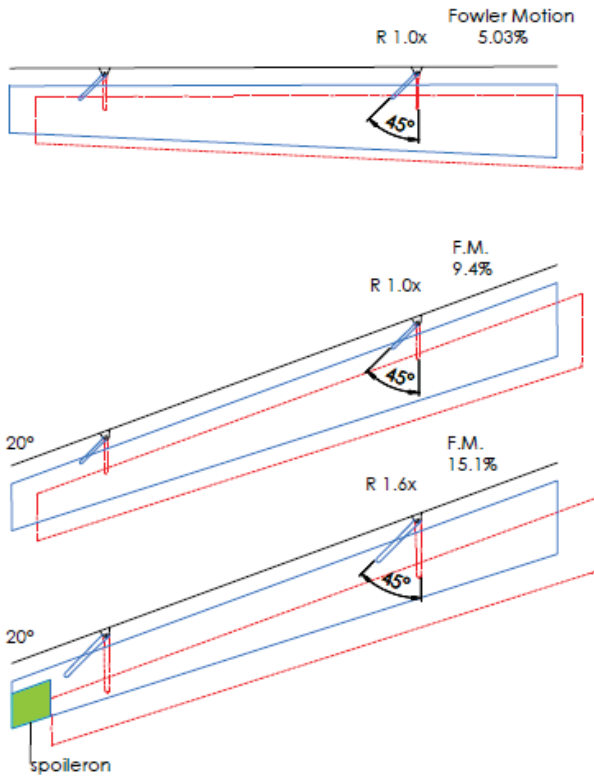
Figure 46. Influence of the wing sweep on flap Fowler motion, actuated by swivel beams.

Assuming that the swivel beam length equals to 17% of the wing chord and the flap chord equals to 29% of the wing chord, the Fowler motion of a straight wing can be about 5%. The Fowler motion of a sweep wing can be significantly higher. With the swivel beam of the same length and at the 45° angle of turn, the Fowler motion may increase in excess of 9% at the wing sweep angle of 20°. With the swivel beam length increasing by 27.3% at the wing chord and at the 45° angle of turn, the Fowler motion will increase in excess of 15% at the same sweep angle. (Paper IV) Spoilerons can be recommended to cover up the flaps' outboard edge. In the patented (Patent application EP 17207523.6) swivel beam system (SBS), the author of this thesis has added also a device, which can simultaneously deflect the flaps and the slats (Figure 47). The deflecting device at the front of the flap is operated on the cardan principle. Depending on the necessary deflection angle of the flaps, the swivel beam β-axis remains set toward the flap tilt rod at 43° to 72°. Y- and β-axis remain at 90° of each other. By turning the swivel beam, the mechanism rotates around β- and y-axis, thus changing the flap deflection angle simultaneously. Here, the rule is that when the flap tilt rod angle is smaller, the flap deflection angle is higher. (Paper IV)
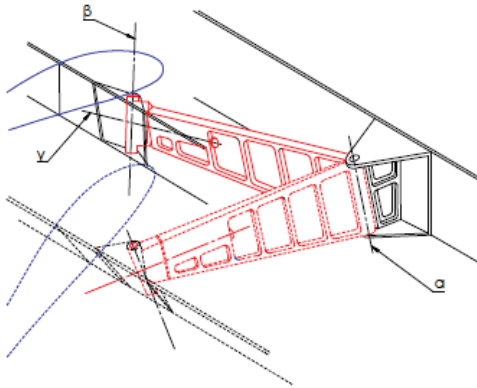
Figure 47. Swivel beam with the transmission mechanism to change the flap deflection angle (Patent application EP 17207523.6).

3.2 High lift system aerodynamic design by using SBS

For the cost-effective air transport, the aerodynamic performance of high lift system has a significant role. According to the source (Butter, 1984), the high lift performance affects the typical twin-engine jet commercial aircraft's total performance as follows:

5% increase in maximum lift coefficient allows to 12-15% increase of payload;

5% increase of take-off L/D ratio allows to 20% increase of payload;

5% increase of maximum lift coefficient in landing configuration allows to 25% increase of payload.

Such results are confirmed by Daniel Reckzeh in his work (Reckzeh, 2004). The above values often remain out of reach because of the existing limitations. In a typical medium range twin-engine aircraft, increasing the maximum lift coefficient by 2.0% can increase the flight weight from 75,000 kg to 76,495 kg, which means carrying 16 more passengers. Improving the L/D ratio of 2.0% during the take-off will facilitate an aircraft of the same class to increase its payload by transporting 10 more passengers. These examples show that relatively small changes in the aerodynamic performance of the high lift system can significantly affect the aircraft's payload and performance.

In medium- and long-range commercial aircrafts, the use of variable chamber (VC) flaps allows to increase the L/D ratio. Dependent on the aircraft's flight weight and also its cruise speed and altitude, it is possible to optimize its flap positions. Usually, the flap deflection range is between -1.7° and +3.5°. Yet, it will allow to minimize the aircraft's fuel consumption. (Paper IV) The variable chamber flaps have proven to be important in aircraft with NLF airfoil wing design, because their low drag region is relatively narrow. According to data (A350-900, 2018) published on the Airbus company website, the variable chamber type flap ADHF deflection angle optimization helps to save up to 2% of the Airbus A350 XWB's fuel.
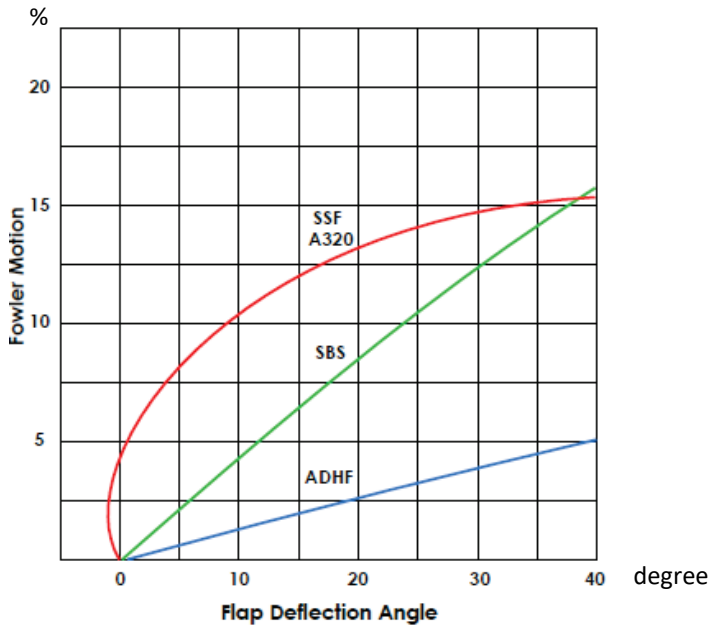
Figure 48. Influence of kinematic solution on the flap Fowler motion.

The flaps actuated by SBS are deflected proportionally according to the swivel beam rotation. Figure 48 describes the interdependence between the flaps' Fowler motion and the deflection angle in different flap kinematic solutions. In a typical medium-sized aircraft A320 with single slotted flap, the maximum Fowler motion is 15.4% that is near to the SBS flap's Fowler motion value of 15.82%. Well-known ADHF flap has a maximum Fowler motion value only slightly in excess of 5%. Despite of the Airbus A320 flap's relatively high Fowler motion in take-off position, its drag exceeds the SBS and ADHF solutions because the gap with 2.2% height of the chords leads to the increase of drag. The SBS flaps, however, do not have a slot in take-off position. Figure 49 compares the SSF and SBS flap solutions in the landing configuration.
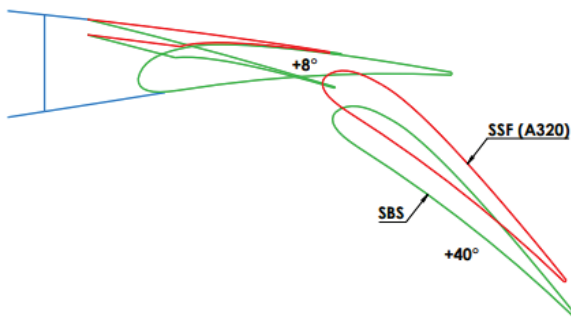
Figure 49. Link-track (A320) and SBS flaps compared in landing positions.

In the landing position, deflecting the SBS spoilers by +8° allows to increase the chamber of the high lift system and additionally the lift coefficient (Wang et al., 2017) (Figures 49 and 50).
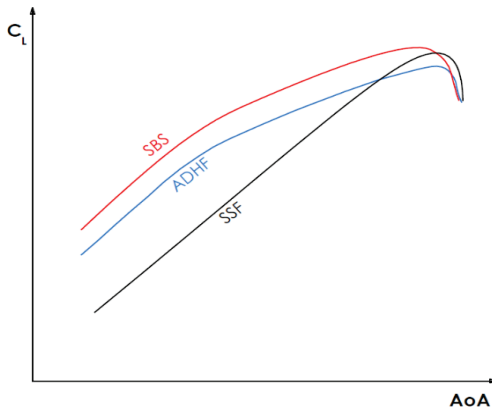
Figure 50. Estimated Cl/AoA for the pre-optimized flap configurations.

The SBS wide spoiler (25.7% of the chord) and flap (29.3%) enable to increase its Cl above those of the other types. At the same time, its critical angle of attack decreases somewhat. The main reason for lower Cl value at ADHF originates from the smaller flap chord (19% of the wing's chord). By using the SBS flaps with a variable chamber function, it is possible to reduce the fuel consumption in the cruise flight and, explicitly, the payload can be increased. Reducing critical angle of attack is especially important for stretched fuselage aircraft, as their AoA in approach is smaller due to the higher risk of tail strike.

3.3 Swivel beam systems kinematic solutions

The SBS kinematic solution can be designed for use with one or two slots trailing edge

Cruise

flap -1,7° - +3,5°

Take-off

flap +15 °

Landing

flap +40 °
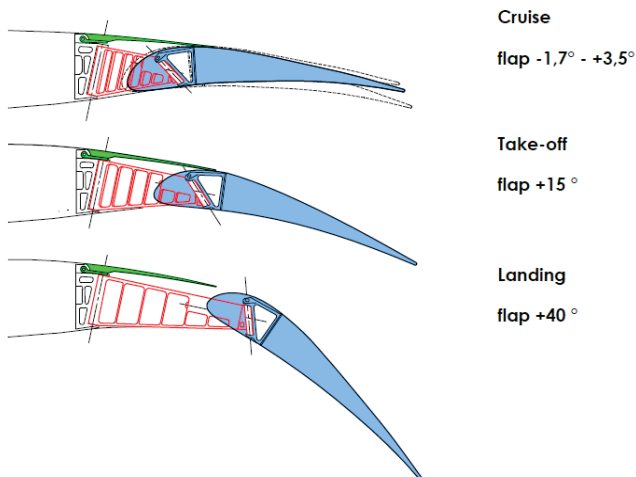
Figure 51. SBS single-slotted flap positions.

flaps. Figure 51 shows the flap positions in single slot flap solution.

During the cruise flight, the flap optimum deflection angle can be exactly adjusted by the swivel beam system, within the range from -1.7° to +3.5°, dependent on the airspeed, altitude and flight weight of the aircraft. By flap deflecting, the spoilers (coloured green)

are also deployed. In the take-off position, the flaps have no slot. With the slot perform, the boundary layer on the flap would be significantly disturbed as the swivel beam's turn angle to the air flow exceeds 30°. In the landing position, the swivel beam is practically located parallel to the air flow. By deflecting the spoiler, an optimum shape slot is formed. The spoilers could also be used to increase the effect of ailerons in the aircraft's roll. Already a few degrees negative angle contributes to airflow separation on the flap's upper surface, thus causing a considerable decrease in the lift. Compared to current flap solutions, the SBS has the following advantages:

- Higher lift during approach and landing. Deflected spoilers (+8°) allow to raise the Cl by 7-8%, compared to SSF, during approach and landing, and with this, it is possible increase the weight of the commercial cargo by 20-25%.
- Smaller drag, because the wing does not have flap track beams and fairings. For example, in B757, such drag makes up for 1.4-1.8% of the total drag of the aircraft (Thiede, 2000).
- By optimizing the flaps' deflection angle during the flight, it is possible to save 1.8-3.0% of the fuel (this, primarily, holds true especially for long-range aircraft).
- Lower gross weight. The flap functions as a push-rod. No actuators / servo motors are needed in the outboard wing section. The structure weighs less (for example A320; -300 kg) and the system is more reliable.
- Lower system complexity and lower manufacturing costs.
- Lower maintenance costs, due to the smaller number of bearings that need greasing.

The efficiency of flaps will, somewhat, be reduced by the flap track beams and fairings, that would reduce the airspeed behind the fairings, thus also the efficiency of the flaps.

Cruise
flap -1,7°-+3,5°

Take-off
flap +15 °

Landing
flap +40 °
aft flap +60 °
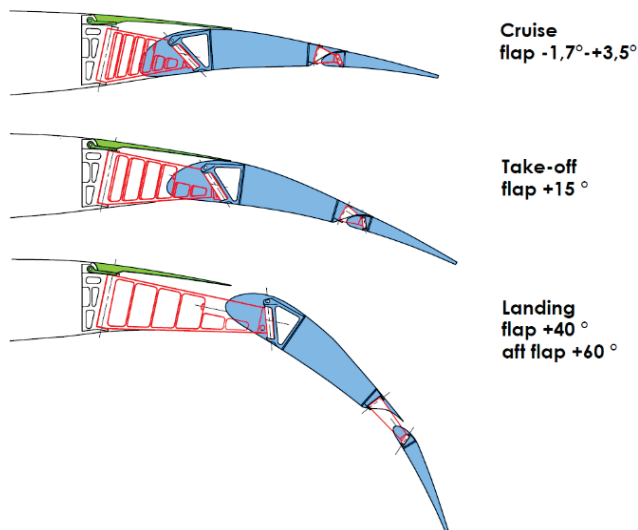
Figure 52. SBS double-slotted flap positions.

In a typical medium-sized commercial airplane, their width makes up for approximately 9% of the flap span. The width of the swivel beams, however, makes up for approximately 1.5% of the flaps' span. Should a higher CI maximum be required, it will be possible to use double-slotted flaps (Figure 52). Flaps are interconnected by using small swivel beams. In the take-off position, the flaps have no slots. In the landing position, both slots

will be open. The only drawback here is a small increase of the drag, due to more slits during the cruise flight. (Paper IV)

In a medium-sized twin-engine aircraft (A320) each flap track beam has the weight of approximately 45 kilograms. Altogether, there are 8 of those beams, 2 of which are accommodated inside the dry bay of the fuselage. Even more, these multiple bearings and trolleys have their weight to add. By using the SolidWork software, the SBS structural components were modelled, using the load range from 26.3 KN up to 89 KN.
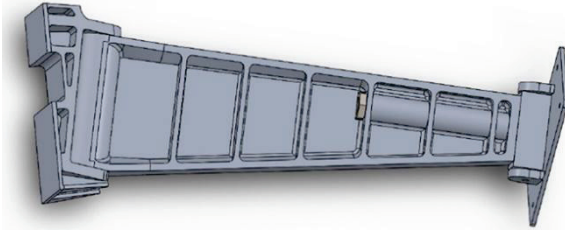
Figure 53. Completed SBS Unit.

The total weight of completed swivel beam unit, with 640 mm distance between the axes (Figure 53), dependent on the estimated load, is within the range of 9,476 g to 11,698 g. Using SBS in the medium-sized aircraft could possibly reduce the weight of the flap system roughly by 300 kilograms. With the smaller weight of high-lift system, the flutter risk of the wing will be decreased, and at the same time, the critical flutter speed will rise. Without significantly strengthening the wing, it will enable to extend the wing span and aspect ratio, and thus, decrease the induced drag of the aircraft. According to Rudolph (Rudolph, 1996), an aircraft's high lift systems production cost account for somewhere between 6% and 11% (potentially higher for more complex configurations) of the typical commercial aircraft. Using SBS, due to its lower complexity, would help to further reduce the manufacturing cost.

The problems with longitudinal movement of flaps can be solved as follows: onto the upper surface of outboard flap tip, spoilerons can be installed (Figure 54). In the cruise flight, spoilerons will adhere to the flap's upper surface, yet while during an intensive rolling of the aircraft, they will deflect upward similar to aileron movement. Only in the landing position, where the flap has moved sidewise, they get deflected up and down by up to 30°. To increase the rigidity, the spoilerons have been reinforced by attaching lateral ribs. (Paper IV)
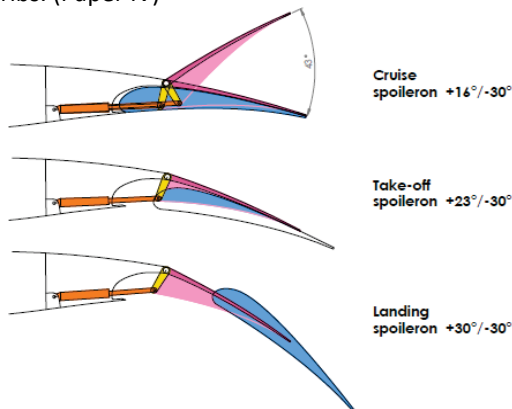
Figure 54. Settings of outboard flap spoilerons.

In cruise flight, the use of spoilerons helps to reduce significantly the wing torque moment. It is especially important for aircraft with high aspect ratio and sweep wing. By deploying the spoilerons upward, the aircraft can be put to positive yaw moment, by which the rudder deflection angle can be decreased.

   Based on wind tunnel tests, the use of outboard ailerons (as well as spoilerons) is a much more effective solution for lift increasing than using the inboard ailerons. In addition to the improvement in the roll control, the Cl reaches roughly 10% higher (by 0.16) than when using the inboard aileron (van Dam, 2002).
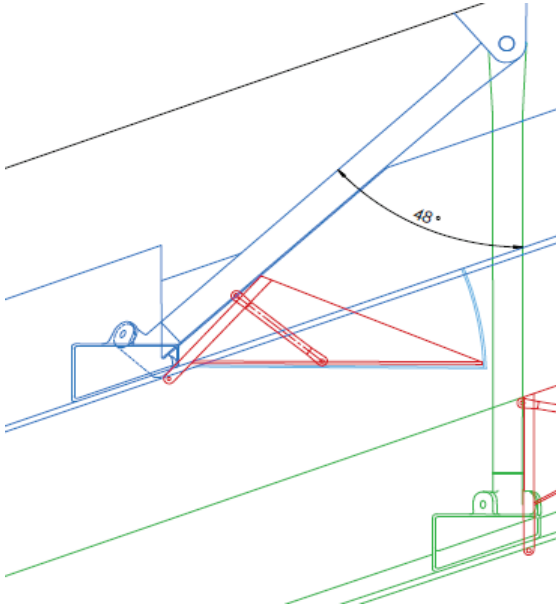
Figure 55. Nose door (coloured red) solution for SBS flaps.

For the flaps to perform with enough efficiency in the landing position, the forward nose door (colored red) are used in the flap's leading edge (Figure 55). By extending of the flaps, the forward nose doors are turned and will also completely cover the opening. In a medium-sized twin-engine aircraft, cylindrical motion can be implemented to deploy the trailing edge flaps in the wing. That being so, this system is less complex to design. Once the wing is with conical geometry, the use of full span flaps is necessary, for which the conical motion principle shall be applied and swivel beams of different length are used. On the underside, on their inboard side, the inboard flaps have a door that covers up the recess underside of the flap (Figure 56) (colored pink).
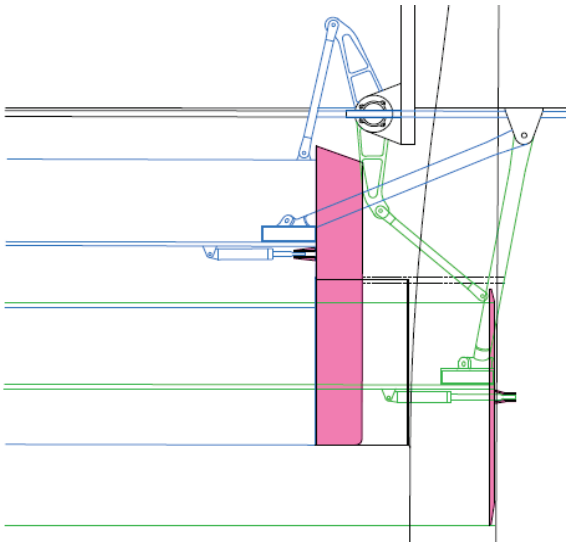
Figure 56. Inboard door positions beside the flap.

By changing the flap's deflection angle from -1.7° to +3.5°, the inboard door will be sliding along with the related flap. By increasing the flap deflection angle more than +5°, the inboard door will also be turned up to 90°. With the flap deflected, the tilted door increases the flap efficiency because the intensity of the flap tip vortexes will decrease. With the flap deflection angle reaching 15°, the square-shaped simple hinge flap, alongside the bell-shaped fairing, will also deflect. By deflecting the flap downward to landing position, the flap together with the door will be moved to reach the fuselage wall. Between the bell-shaped fairing and flap, a funnel-shaped space is formed. It does not significantly reduce the lift coefficient. At high angles of attack, in the areas close to the fuselage wall, separation of air flow takes place, which may somewhat disturb the engagement of flaps. The same split-flap space is formed also for Airbus A330neo, A350-900 and A350-1000 in the area where the fuselage wall and flap are alongside.

Once the wing is uniformly conical in shape, one rotary actuator in each wing will be sufficient for deflecting the flaps. In variable conical shape wing (with Yehudi flap), the flap's trailing edge angle changes considerably. Therefore, in the inboard section of the wing the two parallel motion rotary actuators shall be used (Figure 57).
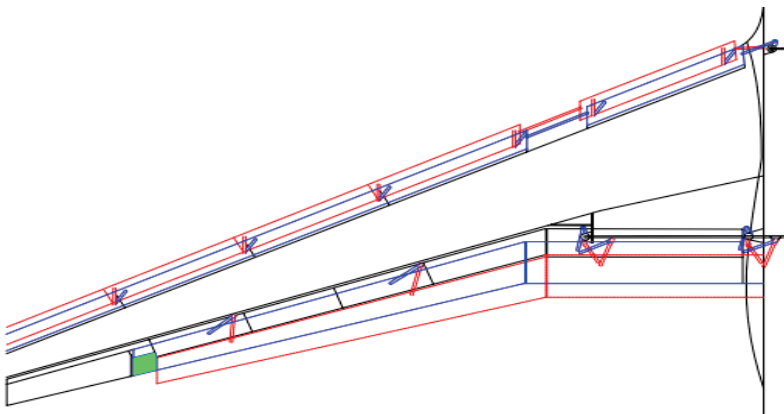
Figure 57. Swivel beam leading and trailing edge solutions with rotary actuators.

Due to the swivel beam's lateral motion, it will be reasonable to set the rotary actuators at a 90° angle, around longitudinal axis, unlike the conventional one. This kind of solution will simplify the connection needed between the torque tube and the geared rotary actuator's less offset gearboxes and torque limiters. The torque tube between the geared rotary actuators is relatively short and operates without additional transmission.

3.4 Low drag leading edge devices

The three-position slat is the most commonly used leading edge device on the commercial aircraft. Using the swivel beam system for actuating the leading edge slats, the turn axis of the swivel beam shall be set at 55°-60° from the vertical axis to achieve the necessary aerodynamic effect (Figure 58).
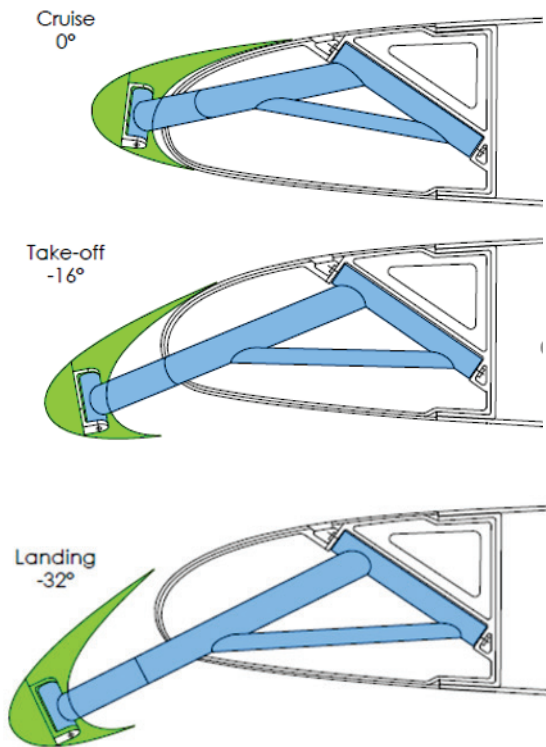
Figure 58. Outboard swivel beam slat positions.

On such occasions, a three-position slat solution can be implemented. In the take-off position, the slot between the main wing and the slat can be covered by the trailing edge of the slat. In the landing position, a slot of optimum shape will occur between the slat and the wing's leading edge. The slot inside the wing's leading edge (above the chord level) should be closed using a rotating door, to prevent a drop of the lift in the slat landing position. With a conventional high lift solution, the slat tracks with an airflow are usually at the angle of 25° to 35°, which increases the drag and decreases the lift. By using SBS, the drag and noise is smaller because the swivel beams are practically along the

airflow. At the same time, the slot below the chord level does not affect significantly the lift value. In the inboard wing section, it would be reasonable to use a slotless leading edge flap (Figure 59). (Paper IV)
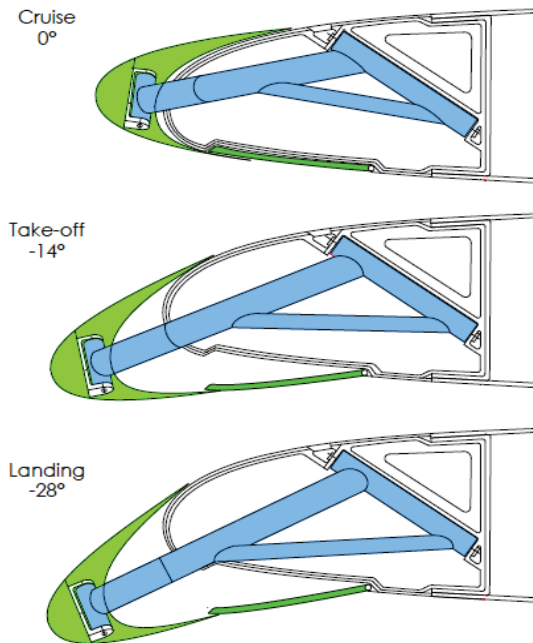
Figure 59. Slotless leading edge flap positions in the inboard section of the wing.

To minimize the aerodynamic drag and also the noise, the doors have been designed underneath to cover the opening between the flap's trailing and the wing's leading edge. The Figure 59 indicates that the deflection angles of leading edge flaps are smaller in the take-off and landing positions. Due to this, the lift coefficient and critical AoA are also smaller. By increasing the angle of attack, the airflow separation from the inboard section of the wing begins, helping to reduce the risk of stall. At the same time, it is a suitable technical solution to increase the L/D ratio in the aircraft during the take-off.

Slotless or drooped nose at Cl=2.6 has almost 24% smaller drag (Wang et al., 2016) when using a conventional slat system. At the same time, Cl maximum is significantly smaller and accounts for 82-88%, compared to the slotted solution. Also, with a slotless solution, a smaller critical AoA is between 14°-17°, while with the slotted solution it reaches up to 24°. Using the wing with positive sweep angle that is less than 20° allows to use a slotless solution along the whole wing span. To prevent the wingtip stall, in a wing with higher sweep angle, it is necessary to use a slotted solution in the outboard section of the wing.

The SBS has the following advantages compared to the conventional slat solutions:
•   Simple and reliable design and reasonable manufacturing cost
•   Lower weight
•   Lower maintenance costs
•   No need for the slat-track cones that have proven to be potentially fatigue cracking and cause fuel leaks.

An aircraft with a shorter wing span will need only one geared rotary actuator per wing. An aircraft with a longer wingspan should be equipped with an extra actuator in the outboard wing, and then they could also perform the autoslat function.

3.5 Conclusion

Using the SBS kinematic solution in a high lift system, it will be possible to increase the aircraft`s L/D ratio while decreasing its fuel consumption.

The defended statements

- Higher lift during approach and landing. Deflected spoilers (+8º) allow to raise the Cl by 7-8%, compared to SSF, during approach and landing, and with this, it is possible to increase the weight of the commercial cargo by 20-25%.
- Smaller drag, because the wing does not have flap track beams and fairings. For example, in B757, such drag makes up for 1.4-1.8% of the total drag of the aircraft (Thiede, 2000).
- By optimizing the flaps' deflection angle during the flight, it is possible to save 1.8-3.0% of the fuel (this, primarily, holds true especially for long-range aircraft).
- Lower empty weight of aircraft.
- Lower system complexity and lower manufacturing costs.
- Lower maintenance costs.
- No need for the slat-track cones that have proven to be potentially fatigue cracking and cause fuel leaks.

Due to the lack of flap track beams and using variable chamber function, it will be possible to save 3.7-3.9% of the fuel at the aircraft cruising distances of over 3,000 NM. Also, by decreasing the weight of fuel, the payload can be increased, thus making the air transport more cost-effective. Using the SBS would also enable to reduce the expenses made on the manufacturing and maintenance of the flaps and slats.

4 New leading edge flap solutions for use in natural laminar flow (NLF) wings

The application of natural laminar flow (NLF) on transport aircraft is a promising future technology offering significant potential for increasing the aircraft fuel efficiency (ICAO, 2010). As outlined in a number of studies, a fuel burn improvement in the order of 10-15% (Allison et al., 2010; Wicke et al., 2012) is possible by generating laminar flow on an aircraft wing. Despite that the higher drag reduction can be achieved with using hybrid laminar flow control (HLFC), tested in B757-200 (Young et al., 2000), the NLF wing design is attractive because, unlike active laminar flow control (LFC) and HLFC methods, it does not require additional systems to be integrated with the aircraft (Allison et al., 2010). Using the natural laminar airfoils allows to reduce the wing profile drag, but at the same time, achieve the required very smooth wing and tail surfaces.

4.1 The NLF wing and tail surface requirements

The design of a leading edge flap should take into account the requirements for natural laminar flow. This includes surface waviness, roughness, and maximum allowable heights and widths for steps and gaps, especially on the nose side of the wing. The NLF wing surface quality requirements, at the high Reynolds numbers, are shown in Figure 60 published in the article (Boeing…, 1999).
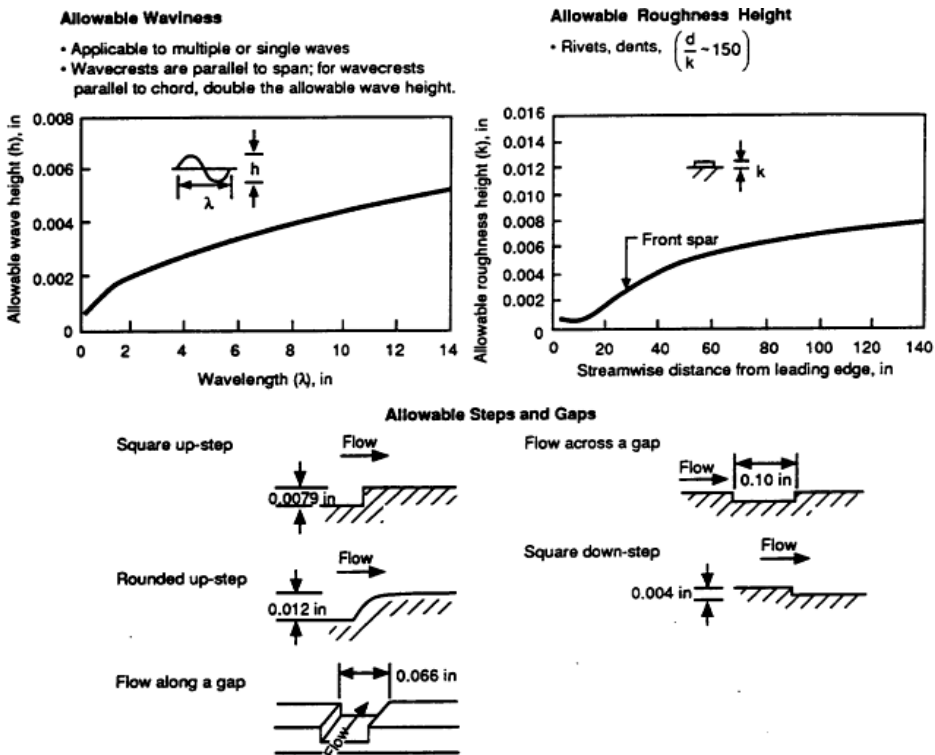
Figure 60. Surface quality requirements by using NLF airfoils at high Re numbers (Boeing…, 1999).

As can be seen in Figure 60, the wavelength of 10 inches (254 mm) per wing width shall not exceed 0.1 mm. Square down step must also not exceed 0.1 mm. Maximum width of gap is allowed up to 2.54 mm and rounded up-step up to 0.3 mm. Natural laminar flow is seriously affected by insect contamination. Previous figure shows that the roughness associated with the contamination must not exceed 0.05-0.1 mm. These requirements are not as stringent when flying at higher flight levels as FL 390, also on the outer wing part where the Re number is smaller. However, in most of the area of the wing, these requirements apply. Using standard slat technology, the step and gap dimensions significantly exceed the requirements set to ensure the NLF flow. Therefore, the standard leading edge flaps are not acceptable as these will have manufacturing irregularities (steps or gaps) at the junction with the main wing that will alter the laminar behaviour in cruise (Iannelli et al., 2013) Figure 61.
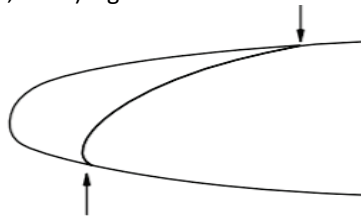
Figure 61 Incompatibility of standard leading edge slat with NLF technology (Iannelli et al., 2013).

4.2 Slat solutions currently tested

Currently, three leading edge solutions have been developed. Each of them has its advantages and disadvantages.
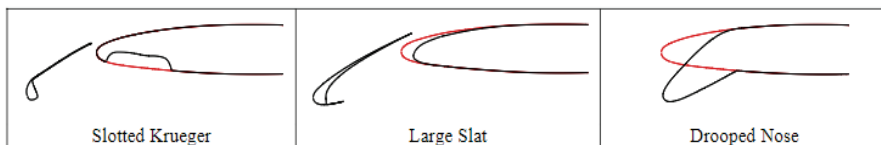
Figure 62. Leading edge device concepts evaluated (Iannelli et al., 2013).

- The Krueger device on compromise to ensure a good performance at low-speed conditions, a loss of laminar flow is only on the lower side at cruise conditions (Figure 63).
- Large Slat with very long chord (about 30%). The problem with this solution is the higher step on the trailing edge of the slats, which occurs with deformation of the wing during the flight. As a result, the thickness of the boundary layer and the drag are increased.
- Drooped nose is a concept applied to maintain the laminar flow on both surfaces of the wing at cruise conditions. The slotless design is not as effective in lift increasing as the previous solutions, also, there is a greater risk of insect contamination and partially lost laminar flow (Iannelli et al., 2013).
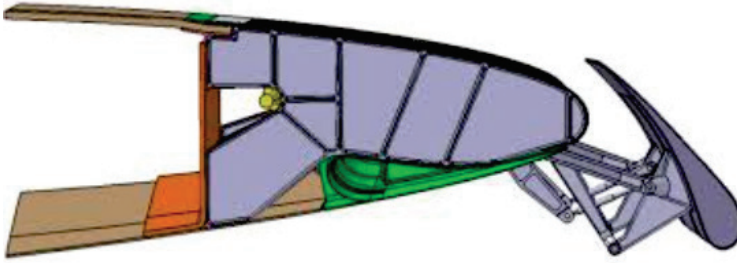
Figure 63. Krueger flap in extended position (Hansen, 2015).

This actuating system, shown in above figure, has based its folding bull nose on the Krueger design and it is modified B757 HLFC concept.

4.3 New leading edge flap design

Using the potential of the new technology, developed by the author of this thesis, it is possible to extend the laminar flow on the lower side of the wing from 5% to 67% of the chord. To achieve this, the lower panel has formed a partially flexible (Figure 65) and separate line in the airfoil's leading edge. If the height of the rounded step is less than 0.3 mm, natural laminar flow is maintained. However, if due to the deformation of the airfoil the step height increases by more than 0.3 mm, the passive suction is applied through the slot on the leading edge. By extending the laminar flow in the lower side of the wing in using the airfoil OA-JTI-1, it is possible to reduce the airfoil drag coefficient additionally by up to 23% (Cd from 0.00486 to 0.00326).
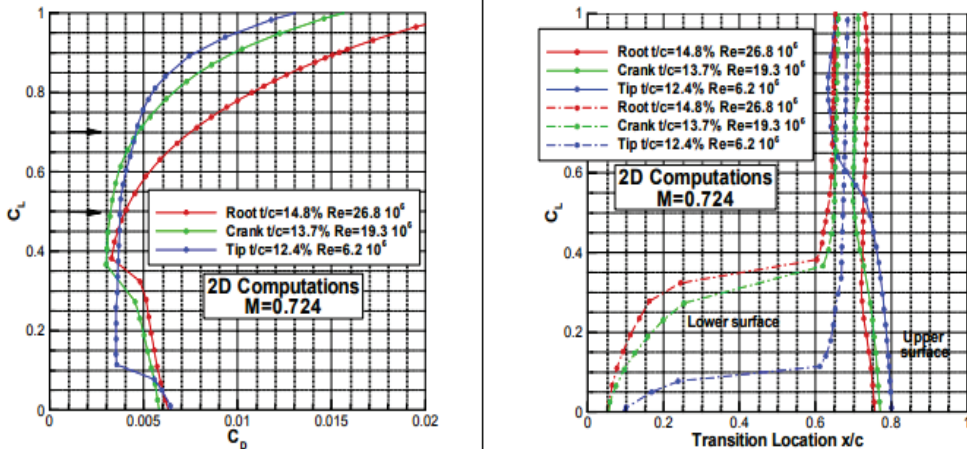
Figure 64. OA-JTI-1 supercritical NLF airfoil polar and laminar to turbulent transition influence on lift coefficient (Salah El Din et al., 2014).

The above-mentioned airfoil is designed to be applied in the future innovative Green Regional Aircraft. From reference, three airfoils have been developed that differ from each other basically for their thickness-to-chord ratios. In the root, the airfoil thickness is 14.8%, at the crank 13.7%, and at the tip 12.4%. (Salah El Din et al., 2014) According to

the new actuating solution, during the cruise flight, the leading edge flaps (coloured green in Figure 65) are located inside the wing. The actuating of the leading edge flap is based on the use of swivel beams (coloured blue). The upper wing panel is rigid and practically does not change its shape during the flight. The lower panel, however, is bendable. The panels are interconnected with ribs (coloured violet). The panel joint line is located below the chord line. This ensures that the upper panel maintains a natural laminar flow. If necessary, an interlocking mechanism can be added to the nose section of the wing. Swivel beams are actuated by using the screw actuators (coloured red in Figure 66). To deflect the lower panel, the torque tube and supports are used.
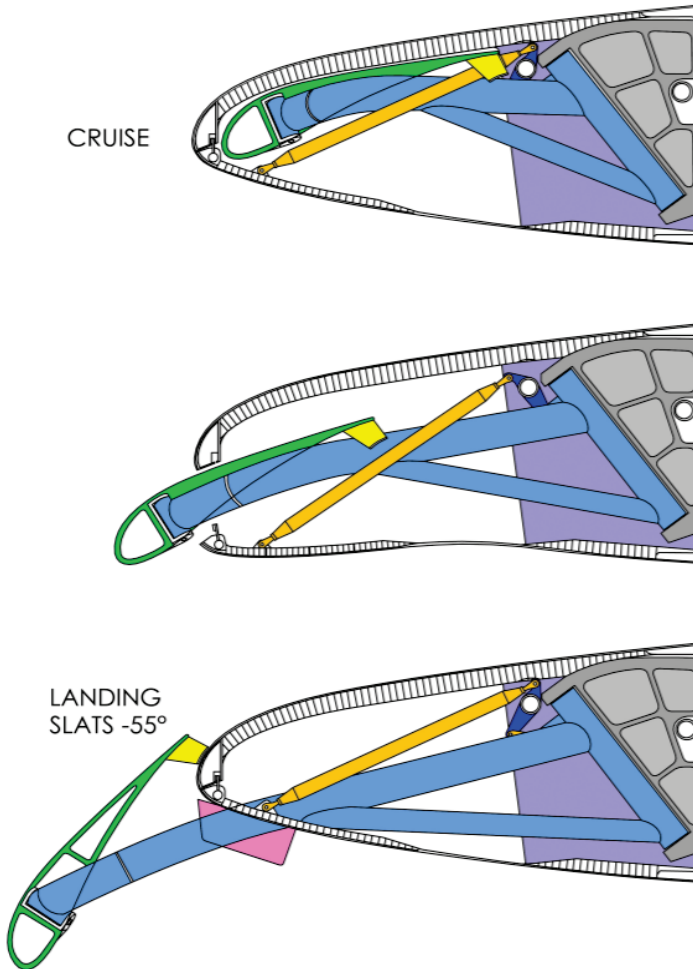
Figure 65.Basic positions of the novel leading edge flap solution for use with the NLF wing.

Before the flap extension, the lower wing panel bends by using supports downward and then the swivel beam turns together with the slats. After the slat extension, the lower wing panel is closed and locked. Unlike in previous slat solutions, the swivel beam is then rotated up to 88º. There are only small doors for swivel beam openings in the leading edge of the wing (coloured pink).
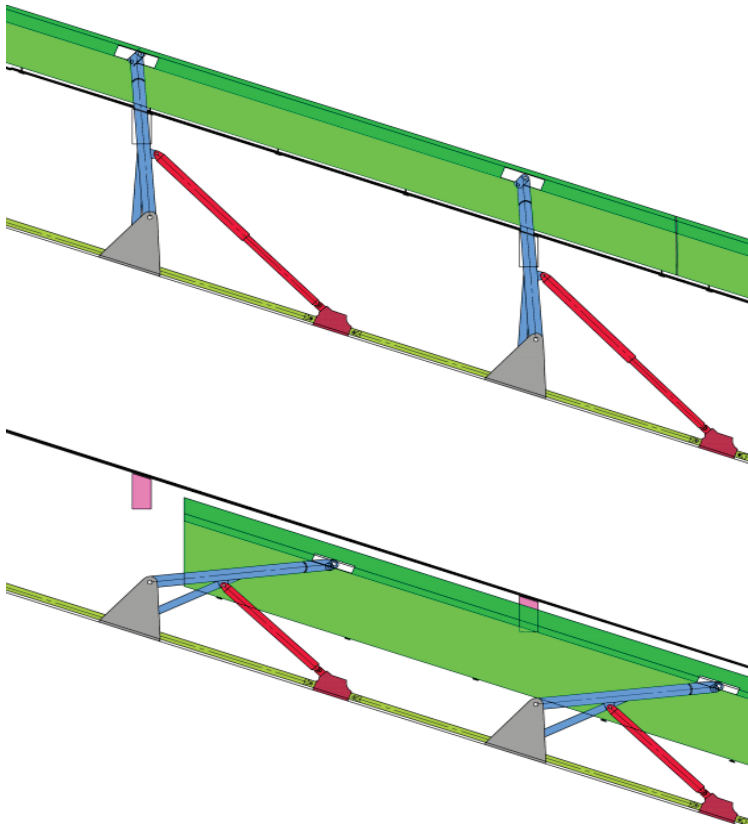
Figure 66. The novel leading edge flap positions. View from above.

To reinforce the flap against the bird strikes, supports are added (coloured yellow in Figure 65). Compared to the classic Krueger flap, the weight of the new leading edge flap system is smaller because its attachment device is on the front spar, whereas the Krueger flap attachment is located on the front of leading edge of the wing and requires reinforcement with many ribs. This solution has the following advantages:

 * Smaller drag during the cruise flight
 * It is possible to design slat in optimal shape
 * Less noise
 * Insect shielding effect, against insect contamination
 * Lower complexity and reliable structure
 * No need for the slat track cones, which can cause cracks and fuel leaks. Despite the fact that with the novel leading edge flap solution, natural laminar flow is possible on the lower side of the wing, it has been designed so that during operation, the steps and gaps are increased and may disturb the laminar flow. In this case, a passive suction can be used especially through the slots in the nose section of the wing. Figure 67 below depicts a basic scheme of functional operation of a passive suction. Such design was tested on the Boeing B757 HLFC. In commercialization, this design can be simplified by eliminating the ducting pipes.
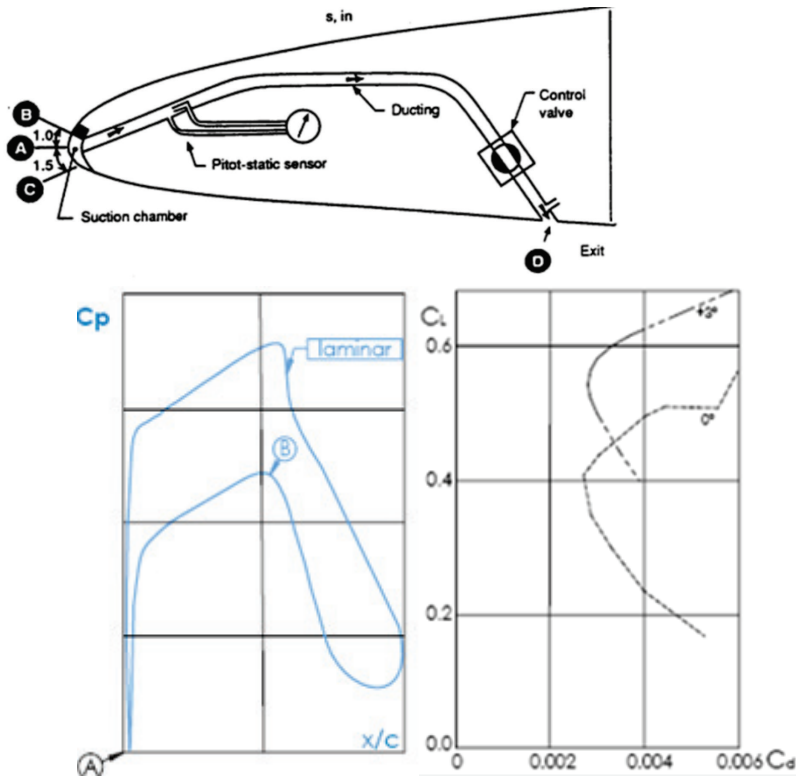
Figure 67. Pressure difference between leading edge A and center section B on the lower side of the wing. Right side: Influence of the flap deflecting angle on the NLF airfoil performance (Boeing… 1999).

Passive suction is based on a relatively high pressure difference between the front and center sections of the wing. The pressure difference exeeds 1,200 kg/m² at Mach=0.78 and FL 390. The position of the control valve depends mainly on the air speed. Passive suction has been successfully tested by NASA and is used to reduce the drag of the Boeing 787-9 fin and stabilizer (Figure 68). The low drag region in the NLF airfoils is relatively narrow and to ensure the low drag, the trailing edge flap and aileron deflection angle has to be changed. For example, a 3° change in the flap deflection angle results in a significant increase in the low drag region as shown on the right graph in Figure 67. For actuating the flaps, is also suitable to use the swivel beam system described in Chapter 3. Also, SBS does not include any flap track beams that can cause headlong transition from the laminar flow to turbulent flow.
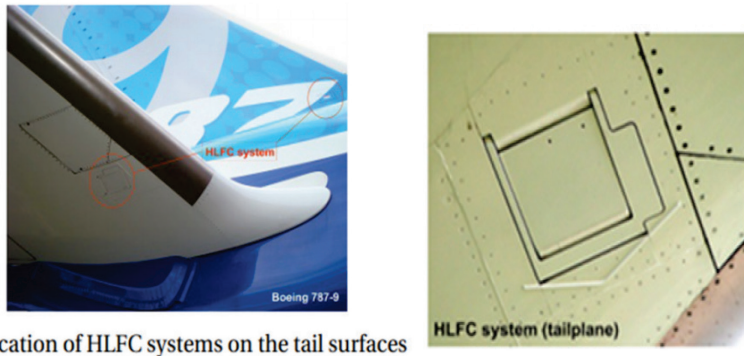
(a) Location of HLFC systems on the tail surfaces

HLFC system (tailplane)

Figure 68. Nose section of the Boeing 787-9 HLFC stabilizer and fin (Hemmen, 2018)*.*

4.4 Novel slotless rotable nose leading edge solution for inboard section of the NLF wing

The inboard section of the wing is frequently used as a slotless Krueger flap or drooped nose. Both options help to raise the lift coefficient, while their critical angle of attack is smaller than the outboard wing. They also help to prevent the deep stall of the wing, because their stall runs earlier than the outboard of the wing. Typical drooped nose section positions in Airbus A350 are shown in Figure 69.
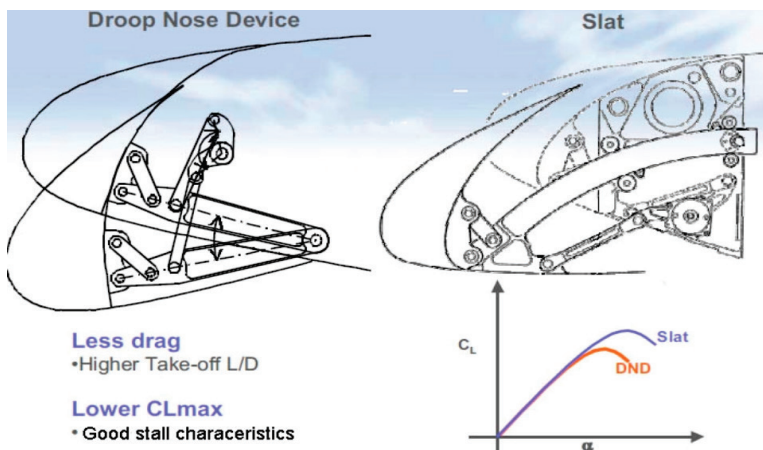
Figure 69. Droop nose device kinematics comparison with the slat device (A350…, 2013)*.*

The technical solution, developed by the author of this thesis, is for using especially on the NLF inboard section of the wing. This solution increases the airfoil chamber and nose radius, and along with that, also the lift coefficient. However, the critical angle of attack is smaller than the slotted leading edge flaps. The most important is the smaller drag during the take-off and the higher L/D ratio. Rotary actuator deflects simultaneously on the lower panel of the wing and rotates the nose door. This device is not complex in design and therefore, its maintenance costs are smaller than those of the commonly used leading edge devices.

CRUISE

TAKE-OFF
LANDING
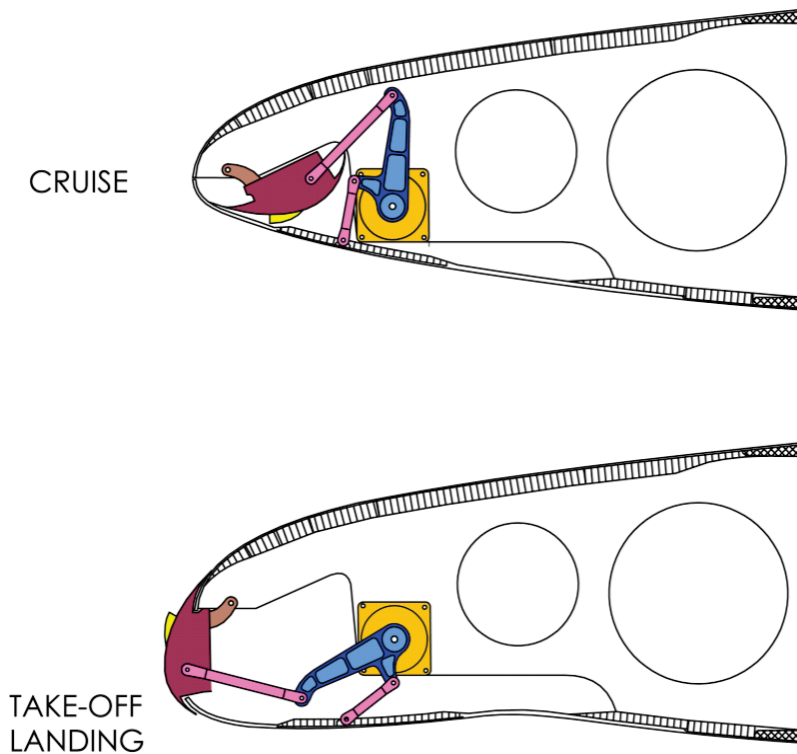
Figure 70. Rotable nose door to increase the lift coefficient on inboard section of the wing.

Rotable nose door works like the drooped nose, increasing the lift coefficient and protecting the wing against the deep stall. To increase the lift coefficient, the vortex generators can be added to the nose section (coloured yellow). The rotating nose section has an insect shielding effect because its wide edges cover the nose section of the laminar airfoil. In addition, compressed air can be blown through the slots under the wide edges of the nose door to prevent insect contamination during the take-off and landing. When using a straight wing in regional aircraft, a rotable nose door to increase the lift coefficient during the take-off and landing is sufficient and no separate slat solutions are required. The nose door can be used to attach the anti-icing protection equipment. Due to its lower weight and high L/D ratio in the take-off, this device could be used widely on regional aircraft with NLF wings.

4.5 Conclusion

The application of natural laminar flow (NLF) on transport aircraft is a promising future technology, offering significant potential for increasing the aircraft fuel efficiency (ICAO, 2010). According to several studies, the fuel burn improvement can be in the order of 10-15% (Allison et al., 2010; Wicke et al., 2012). Using a standard slat solution, it is not possible to maintain the laminar flow due to the steps between the slat and the wing. With the new technological solution, the leading edge flap is accommodated inside the wing during the flight. Using laminar flow on the upper side of the wing allows to reduce the fuel consumption by 5%, the technical solution developed by the author of this thesis also allows to extend the laminar flow on the lower side of the wing up to 67% at the

leading edge of the wing and additionally reduce the fuel consumption by 3.7-3.9%. The actuating of the leading edge flap is based on the use of swivel beams. The upper wing panel is rigid and practically does not change its shape during the flight. The lower panel, however, is bendable. Before the flap extension, the lower wing panel bends by using supports downward, and then the swivel beam turns together with the slats. After the slat extension, the lower wing panel is closed and locked. In addition to the smaller drag, this leading edge flap solution has an insect shielding effect. Another technical solution is based on the use of rotable nosedoor. This solution allows to save same amount of fuel like the previous one. Aerodynamically, this solution is similar to the drooped nose, the profile of the nose section of the wing is of variable shape. Due to the lack of slat, its L/D ratio is higher on the takeoff and landing, but Cl max is lower than that of the slotted solution. Therefore, this solution is suitable for use on the inboard side of the wing.

Despite the fact that with the novel leading edge flap solution, natural laminar flow is possible on the lower side of the wing, it has been designed in a way that during operation, the steps and gaps are increased and may disturb the laminar flow. In this case, a passive suction can be used especially through the slots in the nose section of the wing. Passive suction is based on a relatively high pressure difference between the front and center sections of the wing. The control valve is located under the center section of the wing. The position of the control valve depends mainly on the air speed.

The technological solutions developed by the author of this study make it possible to use the full potential of laminar flow and thereby, achieve the maximum fuel economy.

Using the above-described technical solutions together, we can reduce the fuel consumption even further. For example, using the SBS and NLF leading edge flap solutions together, it is possible to reduce the fuel consumption by 9.27% on a typical twin-engine medium range aircraft, provided that the weight of the structure is 300 kg lighter than that of a basic aircraft. Moreover, using all three above-described solutions together, it is possible to reduce the fuel consumption, according to the equation [1] and formula [2] described in Chapter 2, by 10.77% at the basic aircraft structure weight.

For an aircraft of the same class with a range of 4,400 NM and the fuel consumption of 2580 kg/h, a 10.77% reduction in the fuel burn would mean saving 277.87 kg fuel per hour. Provided that the total flight time is 5,000 flight hours per year, the total fuel savings amount to 1,389,330 kg, which at €700/t fuel cost means a reduction in the operating costs of an aircraft amounting to €972,523/yr. The amount of harmful CO_2 emissions also decreases in this case by 4,376,389 kg/year per aircraft. In addition, also the maintenance costs are reduced. According to the above estimate, commercial aircraft pollute the environment significantly more, compared to other means of transport. It holds particularly true about freighters, whereas the pollution generated by contemporary passenger aircraft does not exceed the pollution caused by family cars. Using the wing modifications developed in this study, it will be possible to reduce the fuel consumption of a typical twin-engine medium-range aircraft by 1.75 l/100 km/per passenger on a 4,000 NM flight.

5 Conclusion

Harmful pollution to the environment caused by aircraft has become a serious problem. According to the forecast, the number of commercial aircraft is expected to double by 2032 compared to 2017 (Flaig, 2018). In order to prevent further pollution increasing, the efficiency of aircraft should increase and the fuel consumption should be radically reduced. Aircraft operators are also interested in reducing fuel consumption, as fuel costs account for a large proportion of the aircraft's operating costs. One effective approach to reducing the fuel consumption and noise is to reduce the wing's aerodynamic drag. The purpose of this thesis is to provide, based on aerodynamic analyses, various technological solutions to reduce wing drag and increase the lift.

The defended statements

- According to the results of Jantar Standard 3 sailplane test flights, the most effective was fixed angle miniflap 2% wide (of the wing chord) and +30° deflected downward. Wing drag decreased, compared to the standard solution, with the lift coefficient Cl between 0.99 and 1.66. The largest drag reduction was reached at Cl=1.21. At the same time, critical angle of attack rose 1.6°. At less than Cl 0.99, miniflaps started to increase the drag. It follows from the above that the fixed angle miniflaps are suitable for gliders and unmanned aircraft with a relatively narrow range of flight speeds.

- Variable geometry miniflaps (VGMF) should be used to achieve a wider range of flight speeds and LAK-17B glider was selected for testing this. Miniflaps built inside this glider's trailing edge flaps were 6.5% wide (of the wing chord) and with a deflection downward up to +16.7°. The test flights revealed that VGMF miniflaps reduced the drag when Cl was above 1.2. Whereas, the best result was achieved at Cl=1.29 when the sink speed of the glider was reduced even by 39.6%. At the speeds below Cl=1.2, the miniflaps were retracted into the trailing edge flaps so as to avoid any additional drag. Many of the small details of the miniflap were produced by 3D selective laser melting from the stainless steel and titanium alloys. Thanks to thoughtful design, the miniflaps mechanism worked perfectly, despite the extreme deflecting of the wings during the flight.

- Using the experience of modelling and testing the miniflaps with gliders was applied to improve the aerodynamic performance of the commercial aircraft wings at higher Mach numbers. As is known, the wing drag of a commercial aircraft starts to grow intensively from M>0.74 onwards as a result of the increasing wave drag. To reduce the growth of drag, a supercritical airfoil SC (2)-0410 that is used on commercial aircraft was modelled with different shape cruise miniflaps (CMF) at M=0.78. CMF-D proved the most effective modification, with a 20.34% reduction of airfoil drag at Cl 0.65 and even 26.57% reduction of drag at Cl=0.70, compared to the standard airfoil. With this modification, the complete aircraft L/D ratio increases by 5%, whereas the width of the CMF is only 4% of the wing chord and deflection angle is +3.5°. Equally, it is possible to reduce fuel consumption. At lifting coefficient lower than Cl=0,5, CMF-s no longer reduce the drag and it is reasonable to retract them inside the trailing edge flaps. The use of CMF allows to increase the optimal flight altitude and thereby reduces jet stream influence on the aircraft fuel consumption and flight time. To actuating the CMF, a relatively simple and reliable solution was developed based on a swivel beam system. According to this method, the actuators located in the nose section of the

trailing edge flap rotate the swivel beams and along with them the CMF, and with a such design, there is no longer need for a complex flap track mechanism.

- The kinematic solution that is based on a swivel beam system can also be used for actuating the leading edge flaps and trailing edge flaps during the flight. This technical solution allows to decrease the drag giving up the flap track beams and increase the commercial aircraft L/D ratio on average by 3.4%-3.8%. This result is achievable with a variable chamber flaps. Furthermore, the trailing edge flap with adjustable deflection angle function also allows to reduce fuel consumption by 1.8%-3.0%. Spoiler deflecting allows to rise the Cl during approach and landing and with it increase the weight of the commercial cargo by 20-25%. Also, the swivel beam system is lighter in weight and entails lower production and maintenance costs.
- Special leading edge flaps actuated by swivel beams were designed for using with natural laminar flow (NLF) airfoil wings. Unlike Krueger flaps, these are located inside the wing in the flight. During the take-off and landing, the lower wing panel is first bent so that from this opening the slat can move out. In the extended slat position, the lower wing panel closes this opening. This solution will allow the laminar flow to be maintained also on the lower surface of the wing. As is known, with the solution currently in use, the laminar flow is only maintained on the upper side of the wing. On the lower side, the flow is disturbed by the retracted Krueger flap. Depending on the aircraft and laminar airfoil type, the solution described above would allow to save 3.6% to 3.8% of fuel. The extended leading edge flap protects the wing from contamination with insects, which also helps to maintain the laminar flow during the flight.
- Using the above-described technical solutions together, can reduce the fuel consumption even further. For example, using the SBS and NLF leading edge flap solutions together, it is possible to reduce the fuel consumption by 9.27% on a typical twin-engine medium range aircraft, provided that the weight of the structure is 300 kg lighter than that of a basic aircraft. Moreover, using all three above-described solutions together, it is possible to reduce the fuel consumption by 10.77% at the basic aircraft structure weight. For an aircraft of the same class with a range of 4,400 NM and the fuel consumption of 2580 kg/h, a 10.77% reduction in the fuel burn would mean saving 277.87 kg fuel per hour (Airbus 321 neo). Provided that the total flight time is 5,000 fh per year, the total fuel savings amount to 1,389,330 kg, which at €700/t fuel cost means a reduction in the operating costs of an aircraft amounting to €972,523/yr. The amount of harmful CO_2 emissions also decreases in this case by 4,376,389 kg/year per aircraft. In addition, also the maintenance costs are reduced.
- Using the technical solutions developed in this thesis will help to improve the aircraft efficiency and reduce harmful pollution to the environment caused by aircraft and save tens of billions of euros per year if applied wider.

  In doing so, all the tasks that were set up for this thesis, are fully completed.

For further studies, a ground-based wing demonstrator on a scale 1:1 would need to be built. Potential step and gap dimensions would then be measured while loading the demonstrator, to establish whether these remain within the limits of requirements set for NLF airfoil wings. The results obtained will serve as a basis for further developments of the technical solutions described above. In conclusion, the technical solutions developed in this thesis will help to improve the aircraft efficiency and reduce harmful pollution to the environment caused by aircraft. Karl Erik Seegel from the Estonian Aviation Academy will continue this research work in the future.

References

Aircraft Flap Track Amature - Animation and Rigging - Blender *...Blender Artists. (2015).* A320 Flap Track.png443×502 68.3 KB. Available from Internet: https://blenderartists.org/t/aircraft-flap-track-amature/658868

Akademische Fliegergruppe an der Universität Karlsruhe e.V. *Jahresberisht 2005 & 2006*. (2007). (in German), {cited 15 May 2014}. Available from Internet: http://www.akaflieg.uni-karlsruhe.de/vp-content/uploads/2015/03/2005-2006.pdf.

Allison, E, Kroo, I., Suziki, Y. and Martins-Ricas, H. (2010). Aircraft conceptual design with natural laminar flow. *27th International Congress of the Aeronautical Sciences (ICAS)*, Nice, France,2010.

A350-900 (2018). Shaping efficiency. *Airbus Website*. Available from internet: https://www.airbus.com/aircraft/passenger-aircraft/a350xwb-family/a350-900.html

A350 Flight Tests Official Thread Part 4 - Page 5 - *Airliners.net* (2013). Avaible from internet: https://www.airliners.net/forum/viewtopic.php?t=561287&start=200

Balagura, J. (2013). Miniklappide aerodünaamilise mõju modelleerimine õhusõidukile Jantar-Standard 3. Eesti Lennuakadeemia. *Lõputöö.*

Bechert, D. W., Meyer, R. and Hage, W. (2001). Drag reduction of Gurney flaps and divergent trailing edges. http://www.dlr.de/at/Portaldata/2/Resources/dokumente/at/*AIAA2000_*2315.pdf

Bloy, A. W., Tsioumanis, N., Mellor, N. T. (1997). Enhanced aerofoil performance using small trailing-edge flaps. *Journal of aircraft,* Vol 34 No .4, 1997.

Bloy, A. W. and Durrant, M. T. (1995). Aerodynamic Characteristics of an aerofoil with small Trailing edge flaps. *Wind Engineering*, Vol.19, No.3, 1995, pp.167-172.

Boeing Commercial Airplane Group (1999). High Reynolds Number Hybrid Laminar Flow Control (HLFC) Flight Experiment II. Aerodynamic Design. *NASA / CR-1999-209324*. Available from internet: https://ntrs.nasa.gov/archive/nasa/casi.ntrs.nasa.gov/19990052586.pdf

Bruscoli, S. (2011). Airfoil optimization for a solar powered aircraft. http://oatd.org/oatd/record?record=oai%5C%3Aetd.adm.unipi.it%5C%3Aetd-05212011-180923

Butter, D. J. (1984). Recent Progress on Development and Understanding of High-Lift-Systems*, AGARD*-CP 365.

Cavanaugh, M. A., Robertson, P., Mason, W. H. (2007). Wind tunnel test of Gurney Flaps and T-strips on an NACA 23012 Wing. http://www.dept.aoe.vt.edu/ ~mason/Mason_f/*AIAA2007*-4175.pdf

Cox, B. (2015). Just Aircraft's SuperSTOL Extreme: Economy Class, STOL Performance, *Plane&Pilot*. Published October 30, 2015. Available from internet: https://www.planeandpilotmag.com/article/just-aircrafts-superstol-extreme-economy- class-stol-performance/#.W5PqhiQzbIU

van Dam, C. P., Chow, R. (2007). Computational investigations of small deploying tabs and flaps for aerodynamic load control. *Journal of Physics*: Conference Series 75 (2007)

van Dam, C. P. (2002). The aerodynamic design of multi-element high-lift systems for transport airplanes. *Progress in Aerospace Sciences* 38, 101-144.

Drela, M. (1989). XFOIL : An analysis and design system for low Reynolds number airfoils. *Proceedings of the Conference Notre Dame Indiana*, June 5-7 1989 New York: Springer Verlag, 1989, p. 1-12.

Flaig, A.(2018). R&T for the Aircraft of the Future. SVP Airbus R&T. AEGATS 18, Toulouse, 23.10.2018.

Gardner, A. D., Nitzsche, J., Neumann, J., Richter, K. (2006). Adaptive load redistribution using mini-teds, *2006 Congress of the International Council of the Aeronautical Sciences (ICAS)*, 3-8 September 2006, Hamburg, Germany. (cited 2 Dec 2017), Available from internet http://www.icas.org/ICAS_ARCHIVE/ICAS2006/PAPERS/216.PDF

Hansen, H. (2015). Laminarität für zukünftige Verkehrsflugzeuge Überblick, Anforderungen und Status. *Wissenschaftstag Braunschweig 2015*. Ergebnisse des Airbus Technologieprogramms Low Drag Aircraft (TOP-LDA). Available from internet: https://www.dlr.de/Portaldata/17/Resources/dokumente/wissenschaftstag/2015/Laminaritaet_fuer_zukuenftige_Verkehrsflugzeuge_Ueberblick_Anforderungen_und_Status_Schlipf.pdf

Harris, Ch. D. (1990). NASA Supercritical Airfoils. *Nasa Technical Paper* 2969, 1990. (cited 16 Dec 2017) (online), Available from internet: http://www.soton.ac.uk/~jps7/Aircraft%20Design%20Resources/aerodynamics/supercritical%20aerofoils.pdf

Hemmen, J.P.P. (2018) Towards Practical Hybrid Laminar Flow Control. Technische Universiteit Delft. Master Thesis. Available from internet: http:// repository tudelft.nl/

Hendrix, J. (2011). Parallel-flight testing with your flight data recorder. http://www.oxaero.com/Parallel Flight Testing.pdf

Henne, P. A. (1990). Innovation with Computational Aerodynamics. The Divergent Trailing-Edge Airfoil"., *Progress in Astronautics and Aeronautics*, pp. 221-261 (cited 18 Dec 2017), Available from internet: https://books.google.ee/books?id=5Ov2tHj0wxoC&pg=PA221&lpg=PA221&dq=Innovation+with+Computational+Aerodynamics+The+Divergent+Trailing-Edge+Airfoil%E2%80%9D..&source=bl&ots=SpMjwbaDmd&sig=TTNn5MHTfPapIXITraA8yxeKcws&hl=et&sa=X&ved=0ahUKEwjekNXS26jZAhVPaFAKHbnPBPYQ6AEIKTAB#v=onepage&q=Innovation%20with%20Computational%20Aerodynamics%20The%20Divergent%20Trailing-Edge%20Airfoil%E2%80%9D..&f=false

Horstmann, K. H., Quast, A. (1979). Wing profile design of the world championship sailplane SB-11. *Nasa Technical Memorandum* NASA TM-75829 19800022879

Iannelli, P., Wild, J., Minervino, M., Strüber, H., Moens, H. F., Vervliet, A. (2013). Design of a High-Lift System for a Laminar Wing. *5th european conference for aeronautics and space sciences (eucass).* Available from internet: https://elib.dlr.de/87420/1/ EUCASS2013_T21.pdf

ICAO, ICAO Environmental Report (2010). *Aviation and climate change*, Montreal, Quebec, Canada, 2010.

IGC Software (2017). Available from Internet: http//www.igssoftware.com

Jang, S. C., Ross, J. C., Cummings, R. M. (1998). Numerical investigation of an airfoil with a gurney flap. http://digitalcommons.calpoly.edu/cgi/viewcontent. cgi?article= 1001&context=aero_fac

Jarzabek, A. (2011). Low speed wind tunnel testing of aerofoil family for solar powered aircrafts. http://oa.upm.es/7428/1/PFC_Artur_Jarzabek.pdf

Johnson, R. H. (1989). Sailplane Performance Flight Test Methods. *Soaring* Magazine, May, 1989 http://www.oxaero.com/SailplaneFlightTestMethods.pdf

Kubrynsky, K. (2006). Aerodynamic design and cross-country flight performance analysis of Diana-2 sailplane. http://www.dianasailplanes.com/Tech_Soar_KK.pdf

Liebeck, R. (1978). Design of subsonic airfoil for high lift. *Journal of Aircraft* 15 (9). 547-561. Available from Internet: http://dx.doi.org/10.2514/3.58406 Liebeck, R. 1978.

Niekerk, B. (2013). Aviation studies project groep 1K 0. *Amsterdam.* Available from internet: http://barryvanniekerk.nl/wp-content/uploads/2013/08/Project-Flight-Controls-Group-1K.pdf.

Ostrowski, J., Skrynski, S., Litwinczyk, M. (1981). Discussion of test results in the design of laminar airfoils for competition gliders. http://ntrs.nasa.gov/archive/nasa/casi.ntrs.nasa.gov/19810007469.pdf

Page, F. H. (1921). Wing and similar member of aircraft. Available from internet: https://patents.google.com/patent/US1394344

Pätzold, F. (2014). Vorläufige Ergebnisse der Flugleistungsvermessung der Lak-17a (S5-3117) im Vergleichflugverfahren in Aalen-Heidenheim-Elchingeni 20/21. August 2012. Techniche Univärsität Braunschweig, Institut für Flugfürung 21.02.2014.

Reckzeh, D. (2014). Multifunctional wing moveables: design of the a350xwb and the way to future concepts. *29th Congress of the International Council of the Aeronautical Sciences. St. Peterburg 7-12 September 2014.* Available from internet: https://www.icas.org/ICAS_ARCHIVE/ICAS2014/data/papers/ 2014_0133 _paper.pdf

Reckzeh, D. (2004). Aerodynamic design of airbus high-lift wings in a multidisciplinary environment. *European Congress on Computational Methods in Applied Sciences and Engineering ECCOMAS 2004. Jyväskylä, 24—28 July 2004.* Available from internet: https://www.researchgate.net/publication/242581172_AERODYNAMIC_DESIGN _OF_AIRBUS_HIGH-LIFT_WINGS_IN_A_MULTIDISCIPLINARY_ENVIRONMENT

Richter, K., Rosemann, H. (2011). Steady Aerodynamics of Miniature Trailing-EdgeDevices in Transonic Flows. Conference: *29th AIAA Applied Aerodynamics Conference,* June 2011. Available from internet: https://www.researchgate.net/publication/225020493_Steady_Aerodynamics_of_Miniature_Trailing-Edge_Devices_in_Transonic_Flows

Richter, K. (2010). Untersuchungen zur Aerodynamik von Miniature Trailing-Edge Devices in transsonischen Strömungen.*DLR Deutches Zentrum für Luft- und Raumfahrt e.V.-Forschungerichte* 09/2010 (cited 20 Jan 2018) (online), Available from internet: https://www.researchgate.net/profile/Kai_Richter3/publication/224991403_Untersuchungen_zur_Aerodynamik_von_Miniature_Trailing-Edge_Devices_in_transsonischen_Stromungen/links/0deec52739504df5e9000000/Untersuchungen-zur-Aerodynamik-von-Miniature-Trailing-Edge-Devices-in-transsonischen-Stroemungen.pdf

Rudolph, P. K. C. (1996). High-Lift Systems on Commercial Subsonic Airliners. *NASA Contractor Report* 4746.

Salah El Din, I., Godard, J.-L., Rodde, A.-M., Moens, F., Andreutti, G., de Rosa, D., Di Muzio, M., Gemma, R., Baldassin, E., Calvi, N., Averardo, M. A., (2014). Natural Laminar Flow Transonic Wing Design Applied to Future Innovative Green Regional Aircraft. Available from internet: https://hal.archives-ouvertes.fr/hal-01082913/document

STAR-CCM (2017). (online), Available from internet: https://mdx.plm. automation. siemens.com/sites/all/themes/basic/assets/downloads/STAR-CCM+%20v11%20 brochure%202016.pdf

Tamm, M. (2018). Strength Analysis of Swivel Beam Trailing Edge Flap System for Commercial Aircraft. Estonian Aviation Academy. *Diploma Paper*.

Thiede, P. (2000). Aerodynamic Drag Reduction Technologies: *Proceedings of the CEAS/DragNet,* 19- 21 June 2000, Potsdam, p. 102-104.

Vlasov, V., Kogan, M., Nalivaiko, A. (2007). Investigation of the control of the flow around a wing using mini-flaps. http://link.springer.com/article/10.1134%2FS0015462 808 060173# page-1

Wang, J. J., Li, Y. C., Choi, K.-S. (2008). Gurney flap lift enhancement, mechanisms and applications. http://www.sciencedirect.com/science/article/pii/S0376042107000 784

Wang, W., Liu, P. (2017). Numerical study of the influence of spoiler deflection on high-lift configuration. Theoretical and Applied Mechanics Letters. Volume 7, Issue 3, May 2017, Pages 159-163
Available from internet: https://doi.org/10.1016/j.taml.2017.04.001

Wang, W., Liu, P., Tian, Y., Qu, Q. (2016). Numerical study of the aerodynamic characteristics of high-lift droop nose with the deflection of fowler flap and spoiler. Aerospace Science and Technology Volume 48, January 2016, Pages 75-85. Available from internet: https://doi.org/10.1016/j.ast.2015.10.024

Wicke, K., Kruse, M., Linke, F. (2012). Mission and Economic analysis of aircraft with natural laminar flow. *28 th International Congress of the Aeronautical Sciences*. 23- 28 September 2012, Brisbane, Australia. Available from internet: http://www.icas.org/ICAS_ARCHIVE/ICAS2012/ABSTRACTS/029.HTM

Wilsey, C. (2012). Continuous Lower Energy, Emissions and Noise (CLEEN) *Technologies Development.* Boeing Program Update https://www.faa.gov/about/ office_org/ headquarters_offices/apl/research/aircraft_technology/cleen/2011_consortium /media/Boeing_CLEEN_Projects_Briefing.pdf

XFLR5 Software (2017). Available from Internet: http://www.xflr5.com/xflr5.htm

Young, T. M. (2018). Performance of the Jet Transport Airplane. Analysis Methods, Flight Operations and Regulations. John Wiley and Sons Ltd., USA.

Young, T. M., Fielding J. P. (2000). Flight Operational Assessment of Hybrid Laminar Flow Control (HLFC*) Aircraft. Aerodynamic Drag Reduction Technologies* (p.102). Potsdam.

Acknowledgements

Abstract

New Technological Solutions to Improve the Aerodynamic Characteristics of an Aircraft Wing

Harmful pollution to the environment caused by aircraft has become a serious problem faced by aircraft engineers around the world. According to the forecast, the number of commercial aircraft is expected to double by 2032 compared to 2017. In order to prevent further pollution, the efficiency of aircraft should increase and the fuel consumption should be radically reduced. Aircraft operators are also interested in reducing fuel consumption, as fuel costs account for a large proportion of the aircraft's operating costs. One effective approach to reducing the fuel consumption and noise is to reduce the wing's aerodynamic drag. The purpose of this thesis is to provide, based on aerodynamic analyses, various technological solutions to reduce wing drag and increase the lift. Due to the specific features of various aircraft, different software is used for aerodynamic analysis and modelling of various wing modifications. For gliders and unmanned aircraft, due to the low Re number, the XFLR5 software based on the XFLR code was used, whereas for the analysis of commercial aircraft, a CFD simulation software STAR-CCM+, based on Reynolds-averaged Navier-Stokes equations (RANS), was applied. Test flights were also carried out to examine the effect of the miniflaps developed for gliders. According to the results of Jantar Standard 3 sailplane test flights, the most effective wing trailing edge miniflap modification was 2% wide (of the wing chord) and +30° deflected. Wing drag decreased, compared to the standard solution, with the lift coefficient Cl between 0.99 and 1.66. The largest drag reduction was reached at Cl=1.21. At the same time, at Cl values less than 0.99, miniflaps started to increase the drag. It follows from the above that the fixed angle miniflaps are suitable for gliders and unmanned aircraft with a relatively narrow range of flight speeds. Variable geometry miniflaps (VGMF) should be used to achieve a wider range of flight speeds and LAK-17B glider was selected for testing this. Miniflaps built inside this glider's trailing edge flaps were 6.5% wide (of the wing chord) and with a deflection of up to +16.7°. The test flights revealed that VGMF miniflaps reduced the drag when Cl was above 1.2. Whereas, the best result was achieved at Cl=1.29 when the sink speed of the glider was reduced even by 39.6%. At speeds below Cl=1.2 the miniflaps were retracted into the trailing edge flaps so as to avoid any additional drag. Many of the small details of the miniflap were produced by 3D selective laser melting from the stainless steel and titanium alloys. Interestingly, the weight of the flap equipped with the miniflaps was lower than the weight of standard flaps, probably due to its optimal design.

   The following project was intended to improve the aerodynamic performance of the commercial aircraft wings at higher Mach numbers. As is known, the wing drag of a commercial aircraft starts to grow intensively from M>0.74 onwards as a result of the increasing wave drag. To reduce the growth of drag, a supercritical airfoil SC (2)-0410 that is used on commercial aircraft, was modelled with different cruise miniflap (CMF) modifications at M=0.78. CMF-D proved as the most effective modification, with a 20.34% reduction of airfoil drag at Cl 0.65 and even 26.57% reduction of drag at Cl=0.70, compared to the standard airfoil. With this modification, the complete aircraft L/D ratio increases by approximately 5%, whereas the width of the CMF is only 4% of the wing chord and the deflection angle is +3.5°. At lifting coefficient lower than Cl=0,5, CMF-s no longer reduce the drag and it is reasonable to retract them inside the trailing edge flaps.

The use of CMF allows to increase the optimal flight altitude and thereby reduces jet stream influence on the aircraft's fuel consumption and flight time. To move the CMF, a relatively simple and reliable solution was developed based on a swivel beam system. According to this method, the actuators located in the nose section of the trailing edge flap rotate the swivel beams and along with them the CMF, and with a such design, there is no longer need for a complex flap track mechanism.

The kinematic solution that is based on a swivel beam system can also be used for actuating the leading edge flaps and trailing edge flaps during the flight. This technical solution allows to decrease the drag and increase the commercial aircraft L/D ratio on average by 1.4%-1.8%. Furthermore, the trailing edge flap with adjustable deflection angle function also allows to reduce fuel consumption by 1.8%-3.0%. Spoiler deflecting allows to rise the Cl during approach and landing and with this, increase the weight of the commercial cargo by 20-25%. Also, the swivel beam system is lighter in weight and entails lower production and maintenance costs.

Special leading edge flaps actuated by swivel beams were designed for using with natural laminar flow (NLF) airfoil wings. Unlike Krueger flaps, these are located inside the wing during the flight. During the take-off and landing, the lower wing panel is first bent so that from this opening the slat can move out. In the extended slat position, the lower wing panel closes this opening. This solution will allow the laminar flow to be maintained also on the lower surface of the wing. As is known, with the solution currently in use, the laminar flow is only maintained on the upper side of the wing. On the lower side, the flow is disturbed by the retracted Krueger flap. Depending on the aircraft and laminar airfoil type, the solution described above would allow to save 3.6% to 3.8% of fuel. The extended slat of the leading edge flap protects the wing from contamination with insects, which also helps to maintain the laminar flow during the flight.

For further studies, a ground-based wing demonstrator on a scale 1:1 would need to be built. Potential step and gap dimensions would be measured while loading the demonstrator, to establish whether these remain within the limits of requirements set for NLF airfoil wings. The results obtained will serve as a basis for further developments of the technical solutions described above. In conclusion, the technical solutions developed in this thesis will help to improve the aircraft efficiency and reduce harmful pollution to the environment caused by aircraft.

Lühikokkuvõte

Õhusõidukite tiiva aerodünaamiliste omaduste parandamine uute tehnoloogiliste lahenduste abil

Õhusõidukite poolt põhjustatud keskkonnasaaste on muutunud tõsiseks probleemiks, millega lennukiinsenerid üle maailma silmitsi seisavad. Üle kogu maailma on hetkel käigus 37 400 kommertslennukit. Nendest suurim osa on nn keskmise tegevus-raadiusega kahemootorilised reisilennukid (Boeing 737, Airbus 320 jt). Neid on käigus 28 550 (2018. a oktoobri seisuga) ehk üle 76% kommertslennukite üldarvust (Flaig, 2018).   Moodne reisilennuk (Airbus 321 neo) kulutab aasta ehk 5000 lennutunni jooksul keskmiselt 12 900 t lennukikütust ja emiteerib seejuures 40 663 t CO_2. Prognoosi järgi kasvab 2032. aastaks kommertslennukite arv võrreldes 2017. aastaga kaks korda. Edasise saastamise pidurdamiseks tuleks radikaalselt tõsta õhusõidukite efektiivsust, sh vähendada kütusekulu reisijate ja kaubaveol. Isegi 1% kütusekulu vähendamine võimaldaks vähendada CO_2 saastet antud näite puhul 406,6 t võrra. Kütusekulu vähendamisest on huvitatud ka lennukioperaatorid, sest kulutused kütusele moodustavad suure osa õhusõiduki opereerimiskuludest. Kui õnnestuks vähendada kommertslennukite kütusekulu 1%, siis lennukikütuse hinna juures 700 EUR/t oleks kõikide keskmise tegevusraadiusega kommertslennukite pealt saavutatav kokkuhoid üle 2,5 miljardi euro aastas.

   Üheks küllalt efektiivseks viisiks kütusekulu ja müra vähendada on tiiva aerodünaamilise takistuse vähendamine. Käesoleva uurimuse ülesanne ongi aerodünaamiliste analüüside alusel pakkuda välja erinevaid tehnoloogilisi lahendusi tiiva takistuse vähendamiseks ja tõstejõu suurendamiseks. Tulenevalt õhusõidukite eripärast kasutatakse aerodünaamiliseks analüüsiks ja erinevate modifikatsioonide modelleerimiseks erinevaid arvutiprogramme. Purilennukite ja piloodita õhusõidukite puhul kasutati, tulenevalt väikesest Re arvust, XFLR koodil põhinevat arvutiprogrammi XFLR5. Kommertslennukite tiiva analüüsil aga kasutati CFD simulatsiooni tarkvara STAR-CCM+, mis omakorda põhineb Reynoldsi keskmistatud Navier-Stokesi võrrandil (RANS). Lisaks viidi purilennukitele väljatöötatud miniklappide mõju selgitamiseks läbi testlennud. Purilennuki Jantar Standard 3 testlendude tulemusel osutus efektiivseimaks tiiva tagaserva miniklapi variandiks 2% laiune (tiiva kõõlust) ja +30° kaldenurgaga miniklapp. Võrreldes standardlahendusega vähenes tiiva takistus tõstejõu koefitsiendi Cl vahemikus 0,99-1,66. Suurim takistuse vähenemine saavutati Cl väärtusel 1,21. Samas Cl väärtustel alla 0,99 miniklapid hoopis suurendasid takistust. Eeltoodust järeldub, et fikseeritud nurgaga miniklapid sobivad purilennukitele, aga samuti piloodita õhusõidukitele, mille lennukiiruste diapasoon on küllalt kitsas. Laiema lennukiiruste diapasooni saavutamiseks tuleb kasutada muudetava geomeetriaga miniklappe (VGMF), mille testimiseks valiti purilennuk LAK-17B. Selle tagatiibade sisse ehitati 6,5% laiused (tiiva kõõlust) miniklapid, mida oli võimalik kallutada kuni +16,7° nurga alla. Testlendude käigus selgus, et VGMF-d vähendasid õhutakistust Cl väärtustel üle 1,2. Seejuures suurim efekt saavutati Cl väärtusel 1,29, kui purilennuki vajumiskiirus vähenes lausa 39,6%. Lennukiirustel, millele vastavad Cl väärtused alla 1,2, tõmmati miniklapid tagatiibade sisse, nii et need ei põhjustaks lisatakistust. Paljud miniklapi väikesed liikuvad metallosad valmistati 3D laserprinteri abil roostevabast terasest ja titaansulamitest. Tänu läbimõeldud miniklappide konstruktsioonile töötas mehhanism kergelt ka tiibade ekstreemselt suure läbipainde juures.

Tuginedes purilennukitel edukalt läbi viidud testide tulemustele oli järgnev projekt suunatud kommertslennukite tiiva aerodünaamiliste omaduste parandamisele kõrgematel Machi arvudel. Teatavasti hakkab kommertslennukite tiiva takistus alates M>0,74 lainetakistuse lisandudes kiirelt kasvama. Takistuse kasvu vähendamiseks testiti kommertslennukitel kasutatavat superkriitilist tiivaprofiili SC(2)-0410 koos erinevate miniklapi (CMF) variantidega M=0,78 juures. Efektiivseimaks osutus variant CMF-D, mille kasutamisel Cl=0,65 juures vähenes tiivaprofiili takistus 20,34% ning Cl=0,70 juures isegi 26,57% võrreldes standardse tiivaprofiiliga. Terve lennuki aerodünaamiline väärtus suureneb sellega ligikaudu 5%. Seejuures moodustab CMF-i laius ainult 4% tiiva kõõlust ning kaldenurk on +3,5°. Väiksemal tõstejõu koefitsiendil kui 0,5 CMF-d takistust enam ei vähenda ning need on otstarbekas tõmmata tagatiiva sisse. CMF-i kasutamine võimaldab suurendada optimaalset lennukõrgust ning vähendada sellega stratosfääri piiril kulgeva jugavoolude mõju lennukite kütusekulule ja lennukestvusele. CMF-i liigutamiseks töötati välja suhteliselt lihtne ja töökindel meetod, mille aluseks on pöördkonsoolid. Selle meetodi järgi pöörovad tagatiiva ninaosas paiknevad aktuaatorid pöördkonsoole ning nendega koos CMF-e ning sellise ehituse juures puudub vajadus keerulise „flap track" mehhanismi järele.

Pöördkonsoolidel põhinevat kinemaatilist skeemi saab kasutada ka esi- ja tagatiibade liigutamiseks lennu ajal. Selline tehniline lahendus võimaldab vähendada takistust ja tõsta kommertslennuki aerodünaamilist väärtust keskmiselt 3,4%-3,8%. Tagatiibade muudetava nurga funktsioon võimaldab seejuures vähendada kütusekulu 1,8%-3,0%. Spoilerite kallutamine 7-8° võimaldab tõsta tõstejõu koefitsienti ja koos sellega kasuliku koorma kaalu 20-25%. Pöördkonsool-mehhanism on ka kaalult kergem, vajab vähem hooldust ning selle tootmine on vähem kulukas.

Tiibadele, millel kasutatakse laminaarseid tiivaprofiile, projekteeriti pöördkonsoolidel põhinevad esitiivad. Erinevalt Krueger tüüpi esitiibadest paiknevad eelnimetatud seadmed lennu ajal tiiva sees. Stardil või maandumisel painutatakse esmalt alumist paneeli, nii et tekib tiiva esiserva avaus, millest mahub esitiib välja liikuma. Väljalastud asendis alumine tiivapaneel suleb avause. See lahendus võimaldab säilitada laminaarse voolu ka tiiva alumisel pinnal. Teatavasti säilitatakse praegu kasutusel oleva lahenduse puhul laminaarne vool ainult tiiva pealmisel küljel. Alumisel küljel rikub voolu sissetõmmatud Krueger tüüpi esitiib. Olenevalt lennukist ja laminaarsest tiivaprofiilist võimaldaks eeltoodud lahendus kokku hoida 3,6%-3,8% kütust. Esitiib kaitseb väljalastud asendis tiiba putukajäänustega saastumise eest ning ka see aitab säilitada lennu ajal laminaarset voolu.

Kasutades SBS ja NLF esitiibade lahendusi koos on võimalik saavutada kütuse 9,27% kokkuhoid, arvestades lennuki struktuuri kergenemist 300 kg võrra. Samas, kolme eeltoodud lahenduse kasutamisel oleks võimalik lausa 10,77% kütusesääst, mis omakorda tähendaks Airbus 321 neo puhul 277,87 kg kütuse kokkuhoidu tunnis. Eeldades, et antud lennuki üldlennuaeg aastas on 5000 lennutundi, siis oleks kütuse hinna juures 700 EUR/t aastane kütusesääst 972 523 eurot lennuki kohta aastas. Lisaks vähenevad ka tootmis- ja hoolduskulud. Uute tehnoloogiate laiemal kasutamisel on tulevikus võimalik vähendada saastekoormust ja hoida kokku kümneid miljardeid eurosid aastas. Töö autor usub, et sellega on ta püstitatud ülesanded lahendanud. Edaspidi jätkab antud uuringusuunda Karl-Erik Seegel.

Edasisteks uuringuteks oleks vajalik ehitada 1:1 mõõtkavas tiiva demonstraator (osa tiivast). Demonstraatori koormamisel mõõdetakse võimalike astmete ja pilude mõõtmed ning sellega selgitatakse välja, kas need jäävad NLF tiivaprofiilidele kehtestatud nõuete piiridesse. Saadud tulemused on aga aluseks eeltoodud tehniliste lahenduste edasiarendamisel.

Appendix

Patent I CRUISE MINIFLAPS FOR AIRCRAFT
Application number: EP17207454.4
Date of receipt: 14 December 2017

Acknowledgement of receipt

We hereby acknowledge receipt of your request for grant of a European patent as follows:

Submission number	5877795

Application number	EP17207454.4

File No. to be used for priority declarations	EP17207454

Date of receipt	14 December 2017

Your reference	529P1 EP

Applicant	Eesti Lennuakadeemia

Country	EE

Title	CRUISE MINIFLAPS FOR AIRCRAFT

Documents submitted	package-data.xml	ep-request.xml
	application-body.xml	ep-request.pdf (4 p.)
	DRAWNONEPO.pdf\529P1 EP drawings for filing final.pdf (7 p.)	SPECNONEPO.pdf\529P1 EP specification for filing final.pdf (10 p.)
	OTHER-1.pdf\Declaration University.pdf (1 p.)	f1002-1.pdf (1 p.)
	feesheetint.pdf (1 p.)	

Submitted by	CN=Margus Sarap 17390

Method of submission	Online

Date and time receipt generated	14 December 2017, 16:16 (CET)

Message Digest	B5:A7:BC:67:42:A6:4E:6E:DE:6A:D5:56:F5:89:35:A2:AB:6F:54:22

Correction by the EPO of errors in debit instructions filed by eOLF
Errors in debit instructions filed by eOLF that are caused by the editing of Form 1038E entries or the continued use of outdated software (all forms) may be corrected automatically by the EPO, leaving the payment date unchanged (see decision T 152/82, OJ EPO 1984, 301 and point 6.3 ff ADA, Supplement to OJ EPO 10/2007).

/European Patent Office/

Request for grant of a European patent

For official use only		
1 Application number:	MKEY	
2 Date of receipt (Rule 35(2) EPC):	DREC	
3 Date of receipt at EPO (Rule 35(4) EPC):	RENA	
4 Date of filing:		

5   Grant of European patent, and examination of the application under Article 94, are hereby requested.   ☒

Request for examination in an admissible non-EPO language:

> Taotlusele palutakse teha artikli 94 kohane ekspertiis

5.1   The applicant waives his right to be asked whether he wishes to proceed further with the application (Rule 70(2))   ☐

Procedural language: en

Description and/or claims filed in: et

6   Applicant's or representative's reference

> 529P1 EP

Filing Office: EP

Applicant 1

7-1   Name:

> Eesti Lennuakadeemia

8-1   Address:

> Lennu 40
> Kambja municipality
> 61707 Reola Village
> Estonia

10-1   State of residence or of principal place of business:

> Estonia

14.1 The/Each applicant hereby declares that he is an entity or a natural person under Rule 6(4) EPC.   ☒

15-1   Name: SARAP, Mr. Margus

   Company: Sarap and Putk Patent Agency

16-1   Address of place of business: Kompanii 1C

   51004 Tartu

   Estonia

17-1   Telephone: +3727477058

17-1   Fax: +3727477059

17-1   E-mail: patent@patent.ee

Inventor(s)

23   Inventor details filed separately   ☒

24   Title of invention

   Title of invention: CRUISE MINIFLAPS FOR AIRCRAFT

25   Declaration of priority (Rule 52)

   A declaration of priority is hereby made for the following applications

25.2   This application is a complete translation of the previous application   ☐

25.3   It is not intended to file a (further) declaration of priority   ☐

26   Reference to a previously filed application

27   Divisional application   ☐

28   Article 61(1)(b) application   ☐

29   Claims

   Number of claims: 7

29.1   ☒ as attached

29.2   ☐ as in the previously filed application (see Section 26.2)

29.3   ☐ The claims will be filed later

30   Figures

   It is proposed that the abstract be published together with figure No.   1

31   Designation of contracting states

All the contracting states party to the EPC at the time of filing of the European patent application are deemed to be designated (see Article 79(1)).

32   Different applicants for different contracting states

33   Extension/Validation

This application is deemed to be a request to extend the effects of the European patent application and the European patent granted in respect of it to all non-contracting states to the EPC with which extension or validation agreements are in force on the date on which the application is filed. However, the request is deemed withdrawn if the extension fee or the validation fee, whichever is applicable, is not paid within the prescribed time limit.

33.1 It is intended to pay the extension fee(s) for the following state(s):

33.2 It is intended to pay the validation fee(s) for the following state(s):

34   Biological material

38   Nucleotide and amino acid sequences

The European patent application contains a sequence listing as part of the description ☐

The sequence listing is attached in computer-readable format in accordance with WIPO Standard ST.25 ☐

The sequence listing is attached in PDF format ☐

Further indications

39   Additional copies of the documents cited in the European search report are requested

Number of additional sets of copies:

40   Refund of the search fee under to Article 9 of the Rules relating to Fees is requested ☐

Application or publication number of earlier search report:

42   Payment

Method of payment   Not specified

44-A Forms   Details: System file name:

| A-1 | Request | | as ep-request.pdf |
| A-2 | 1. Designation of inventor | 1. Inventor | as f1002-1.pdf |

44-B Technical documents

Original file name: System file name:

B-1	Specification in admissible non-EPO language	529P1 EP specification for filing final.pdf 7 claims 7 figure(s)	SPECNONEPO.pdf

B-2	Drawings / Translation of text in drawings	529P1 EP drawings for filing final.pdf 7 figure(s)	DRAWNONEPO.pdf

44-C Other documents

Original file name: System file name:

C-1	<other_document>	Declaration University.pdf	OTHER-1.pdf

45

General authorisation:

46 Signature(s)

Place: **Tartu**

Date: **14 December 2017**

Signed by: **Margus Sarap 17390**

Representative name: **Margus SARAP**

Capacity: **(Representative)**

Form 1002 - 1: Public inventor(s)

Designation of inventor

User reference: 529P1 EP
Application No:

Public

Inventor	
Name:	LAUK, Mr. Peep
Company:	Eesti Lennuakadeemia
Address:	Lennu 40
	Kambja municipality
	61707 Reola village
	Estonia
The applicant has acquired the right to the European patent:	As employer

Signature(s)

Place: **Tartu**

Date: **14 December 2017**

Signed by: **Margus Sarap 17390**

Representative name: **Margus SARAP**

Capacity: **(Representative)**

Internal fee calculation sheet

This sheet has been produced using data entered in Form EP1001E.

Applicant's or representative's reference

529P1 EP

Applicant 1

Eesti Lennuakadeemia

Representative 1

SARAP, Mr. Margus

Title of invention:

CRUISE MINIFLAPS FOR AIRCRAFT

Fees	Factor applied	Fee schedule	Amount to be paid
001 Filing fee - EP direct - online	0.7	120.00	84.00
002 Fee for a European search - Applications filed on/after 01.07.2005	1	1 300.00	1 300.00
015 Claims fee - For the 16th to the 50th claim	0	235.00	0.00
015e Claims fee - For the 51st and each subsequent claim	0	585.00	0.00
Total:		**EUR**	**1 384.00**

Erklärung von KMU, natürlichen Personen, Organisationen ohne Gewinn-erzielungsabsicht, Hochschulen oder öffentlichen Forschungseinrichtungen für die Zwecke von Gebührenermäßigungen gemäß Regel 6 EPÜ

Declaration for SMEs, natural persons, non-profit organisations, universities and public research organisations for the purpose of fee reductions under Rule 6 EPC

Déclaration à fournir par les PME, les personnes physiques, les organisations sans but lucratif, les universités et les organismes de recherche publics, en vue de l'obtention des réductions de taxe prévues à la règle 6 CBE

Zeichen des Anmelders / Applicant's reference /
Référence du(des) demandeur(s)
(max. 15 Zeichen / max. 15 characters / 15 caractères au maximum)

529P1 EP

Anmeldenummer oder, falls noch nicht bekannt, Bezeichnung der Erfindung: /
Application No. or, if not yet known, title of the invention: /
N° de la demande ou, à défaut, titre de l'invention :

CRUISE MINIFLAPS FOR AIRCRAFT

Für die Zwecke der Regel 6 EPÜ /
For the purposes of application of Rule 6 EPC, the undersigned/each of the undersigned[1] /
Aux fins de l'application de la règle 6 CBE, le (les) soussigné(s)[1],

EESTI LENNUAKADEEMIA
Lennu 40
Reola village
Kambja municipality, 61707 ESTONIA

erklärt der Unterzeichnete (erklären die Unterzeichneten)[1]: / declares that he is: / déclare(nt) être :

☒ ein kleines oder mittleres Unternehmen[2] / a small or medium-sized enterprise[2] / une petite ou moyenne entreprise[2],

☐ eine natürliche Person / a natural person / une personne physique,

☐ eine Organisation ohne Gewinnerzielungsabsicht, eine Hochschule oder eine öffentliche Forschungseinrichtung[3] / a non-profit organisation, a university or a public research organisation[3] / une organisation sans but lucratif, une université ou un organisme de recherche public[3]

nach Regel 6 (4) EPÜ zu sein. / as indicated under Rule 6(4) EPC. / au sens de la règle 6(4) CBE.

Im Falle mehrerer Anmelder wird die Gebührenermäßigung nur gewährt, wenn jeder Anmelder eine natürliche oder juristische Person im Sinne der Regel 6 (4) EPÜ ist.[4] / In the case of multiple applicants, each one must be an entity or a natural person under Rule 6(4) EPC for the fee reduction to apply.[4] / En cas de pluralité de demandeurs, la réduction de la taxe n'est accordée que si chaque demandeur est une entité ou une personne physique au sens de la règle 6(4) CBE.[4]

Bestehen begründete Zweifel an der Richtigkeit dieser Erklärung, kann das EPA im Erteilungsverfahren entsprechende Nachweise verlangen. / In the case of reasonable doubt as to the veracity of the present declaration, the EPO may, during the course of the grant procedure, require appropriate evidence. / Si l'Office a des raisons de douter de la véracité de la présente déclaration, il peut, au cours de la procédure de délivrance, inviter le(s) demandeur(s) à produire des preuves.

Sollte sich herausstellen, dass die Erklärung falsche Angaben enthält, so gilt die betreffende zu Unrecht ermäßigte Gebühr als nicht entrichtet, und die Anmeldung gilt gemäß Artikel 78 (2) bzw. Artikel 94 (2) EPÜ als zurückgenommen. / Should it become apparent that an incorrect declaration has been filed, the relevant fee, reduced without good reason, will be deemed not to have been paid and the application will be deemed to be withdrawn according to Article 78(2) or Article 94(2) EPC, as applicable. / S'il s'avère qu'une déclaration incorrecte a été produite, la taxe concernée, dont le montant a été indûment réduit, sera réputée ne pas avoir été acquittée et la demande sera réputée retirée conformément à l'article 78(2) ou, le cas échéant, à l'article 94(2) CBE.

Ort / Place / Lieu

Tartu

Datum / Date

14.12.2017

Unterschrift(en) des (der) Anmelder(s) oder Vertreter(s): / Signature(s) of applicant(s) or representative(s): / Signature(s) du (des) demandeur(s) ou mandataire(s) :

Margus Sarap, European Patent Attorney

Name des (der) Unterzeichneten bitte in Druckschrift wiederholen. Bei juristischen Personen bitte außerdem die Stellung des (der) Unterzeichneten innerhalb der Gesellschaft in Druckschrift angeben. / Please print name(s) under signature(s). In the case of legal persons, the position of the signatory within the company should also be printed / La (Les) signature(s) doi(ven)t être suivie(s) du (des) nom(s) en caractères d'imprimerie. S'il s'agit d'une personne morale, la fonction du signataire dans la société doit également être indiquée en caractères d'imprimerie.

bitte wenden / P.T.O. / T.S.V.P.

Cruise miniflaps for aircraft

Käesolev leiutis on mõeldud lennukite tiibade tõstejõu suurendamiseks ja takistuse vähendamiseks lennu ajal. Leiutisele vastav lennukitiiva miniklapp (cruise miniflap,

5   edaspidi CMF) moodustab osa lennukitiivast või tagatiivast ning temaga saab muuta lennu ajal lennukitiiva kumerust, pindala ja tekitada (cavity) õõnsuse lennukitiiva tagaserva.

TEHNIKA TASE

Tänapäeva pika lennuulatusega (long range) kommertslennukite kõrge pinnakoormus

10   ei võimalda neil stardijärgselt tõusta optimaalsele lennukõrgusele ilma, et tõuseks järsult aerodünaamiline takistus, sest kasutatavad tiivaprofiilid (wing profile) on disainitud väikese aerodünaamilise takistusega, tõstejõu koefitsiendiga (lift coefficient – C_L) vahemikus 0,45-0,6. Madalam lennukõrgus aga tingib väiksema lennukiiruse maa suhtes ning sellest tuleneva suhteliselt suurema kütusekulu. Tiheda

15   lennuliiklusega piirkonnas ei võimalda väiksem lennukõrgus tihti valida kõige otsemat teekonda sihtlennuväljani. Seega on raskete lennukite kütusekulu lennu esimeses osas suur. Käesolevas patenditaotluses kirjeldatav leiutis võimaldab suurendada tiiva tõstejõukoefitsienti 0,7-0,8-ni ilma, et takistuskoefitsient (drag coefficient) oluliselt tõuseks. See võimaldab kommertslennukitel tõusta stardijärgselt kõrgemale ja

20   parandada lennukite aerodünaamilist väärtust (L/D ratio), mille tulemusena väheneb oluliselt lennukite kütusekulu ja suureneb lennukaugus.

Lennuki tiiva muudetava kujuga tagaserva erinevaid variante on patenteeritud ka varem. Alljärgnevalt on olulisemad nendest välja toodud:

Dokumendis GB 2174341A, 5.11.1986, The Secretary of State for Defence (United

25   Kingdom) (1) on kirjeldatud superkriitilist tiivasektsiooni, millel on liigendiga tiiva külge kinnitatud klapp.

Dokumendis US6565045 B1, 20.05.2003, Onera on kirjeldatud aerodünaamilist pinda, näiteks tiib, millel on alarõhuga pind ja ülerõhuga pind, mis on ühendatud tiiva esiosas.

Dokumendis US 2007/0221789 A1, 27.09.2007, Hak-Tae Lee et al. on kirjeldatud tiiva

30   tagaserva täiustatud täiturmehhanismi.

Dokumendis US 2013/0214092 A1, 22.08.2013, Airbus Operations GmbH on kirjeldatud aerodünaamilist tiivaosa, mida on võimalik liigutada ajami ja täituriga, et käivitada täiendavad tagatiivad.

Dokument GB 2174341A kirjeldab superkriitilise tiivaprofiili tagaserva kinnitatud
5   seadet, millega saab muuta nii tiiva tagaserva kumerust kui ka paksust. Võrreldes eeltooduga on käesoleval leiutisel aerodünaamiline takistus väiksem, sest cavity (õõnsusega) tagaservaga superkriitilise tiivaprofiili aerodünaamiline takistus on väiksem kui paksema (blunt) tagaserva puhul, samuti kaasneb käesoleva seadme kasutamisega ka tiivapindala muutumine, millega saab veel täiendavalt vähendada
10   aerodünaamilist takistust. Erinevalt eelnevalt tehnika tasemest tuntud seadmetes nagu dokumentides US 6565045 B1 ja US 20070221789 A1 on antud käesolevale leiutisele vastava seadme kasutamisel tiiva tagaserva paksus, sissetõmmatud asendis, väiksem ning seetõttu on ka takistus C_L vahemikus 0,4-0,6 oluliselt väiksem. Eeltoodud järeldust ilmestab US 6565045 B1 toodud graafik millest selgub, et nende
15   väljatöötatud aerodünaamiline pind vähendab takistust tõstejõukoefitsiendist suurustel C_L >0,7. Käesolev leiutis aga C_L >0,63. Samuti on nende graafikul toodud takistuskoefitsient C_d oluliselt suurem ,kui käesoleval leiutisel. Leiutis US 2007/0221789 eeldab paljude effektorite üheaegset kasutamist ,sest ühe elemendi laius on suhteliselt väike. Käesolev leiutis on lihtsama konstruktsiooniga, jäigem ning
20   kokkuvõttes töökindlam. C_L vahemikus 0,4-0,75 on ta samuti väiksema aerodünaamilise takistusega Mach 0,75-0,8 juures. Võrreldes aga patendis US 2013/0214092 kirjeldatud seadmega on käesolevas leiutises kirjeldatud miniklapp (CMF) oluliselt väiksema aerodünaamilise takistusega, jäigem ning deformeerub õhuvoolu toimel vähem ja seega palju töökindlam viis parandada õhusõidukite
25   lennuomadusi.

Leiutise olemus

Käesolevalt välja pakutud leiutis lennukitiiva tagaserva miniklapp (CMF – Cruise miniflap) on täiendav aerodünaamiline pind, mis võib olla tiiva tagaserva, tagatiiva või kaldtüüride sees. Vastavalt vajadusele saab miniklappi (CMF-i) mehaaniliselt
30   aktuaatorite abil liigutada ning muuta sellega tiiva kumerust, pindala ja tagaserva kuju. Üleminek tiiva ja miniklapi (CMF-i) vahel on suhteliselt sujuv ning teravaid üleminekuid, mis on iseloomulikud tavalistele tagatiibadele, ei teki. Miniklapi (CMF) sektsioone võib olla ühel tiival üks kuni mitu. Mitme miniklapi sektsiooni kasutamisel on võimalik

optimeerida tõstejõu jagunemist tiivaulatuses ning sellega täiendavalt vähendada induktiivtakistust. (Cavity) õõnsusega tagaserv võimaldab vähendada takistust (tõstejõu koefitsient C_L>0,6) ning lennukiirustel Mach>0,65. Tagaserva optimaalne kõrgus oleneb kasutatavast tiivaprofiilist, tõstejõu koefitsiendist ning lennukiirusest.

5 Näiteks on superkriitilise tiivaprofiilil lennukiirusel Mach 0,78 ning tõstejõukoefitsiendil C_L 0,7 optimaalne õõnsusega (cavity) tagaserva kõrgus 0,7% tiiva laiusest (chord). Veelgi suurema tõstejõukoefitsiendi juures peaks optimaalne õõnsusega (cavity) tagaserva kõrgus olema suurem. Väiksema tõstejõukoefitsiendi juures kui C_L <0,6 õõnsusega (cavity) tagaserv takistust ei vähenda ning see on suletud asendis. (Cavity)

10 Õõnsusega tagaserv võib olla fikseeritud või muudetava kõrguse ja kujuga. Õõnsuse profiil võib olla nii kaarekujuline või kandiline. Kõrguse muutmiseks saab kasutada nii (CMF) miniklapi ülemist või alumist serva.

(CMF) CMF miniklapi kasutamisel vähenevad kulutused mootorite hooldusele ja remondile, sest lennu ajal vajalik võimsus on väiksem ning mootorid kuluvad selletõttu

15 vähem. Lisaks lennukite kütusekulu vähenemisele võimaldab leiutis vähendada loodusele kahjulike saasteainete ja müra emissiooni.

JOONISTE LOETELU

Käesolevast leiutisest parema ja detailsema ülevaate saamiseks kirjeldatakse seda alljärgnevates teostusnäidetes viidetega joonistele, kus :

20 Joonisel Fig.1 on näidatud (CMF) leiutisele vastava miniklapi asetsemist tiiva (tagatiiva) sees a) ja selle põhiliseid asendeid, kus tõusu ja kruiisilennu esimeses etapis kasutatakse asendit, mis on kujutatud joonisel kõige all c), kütuse kuludes ning lennumassi vähenedes lennu ajal, joonise keskel b) ja lennu lõpuosas üleval a) kujutatud asendeid;

25 joonisel Fig 2 on toodud kommertslennuki tiivaprofiili tõstejõukoefitsiendi ja takistuskoefitsiendi suhe lennukiirusel Mach 0.78. Jooniselt on näha, et alates tõstejõukoefitsiendist C_L 0.63 hakkab aerodünaamiline takistus kiiresti kasvama. CMF kasutamisel on aga võimalik vahemikus tõstejõukoefitsiendil C_L >0.62 aerodünaamilist takistust oluliselt vähendada. Lennumassi vähenedes (kütuse kulumisel) on aga

30 otstarbekas (CMF) miniklappi järk-järgult, lennu ajal, sisse tõmmata, sest tõstejõukoefitsiendi vahemikus C_L 0.4-0.6 on siis aerodünaamiline takistus väiksem;

joonisel Fig. 3 on näidatud erinevate tiiva tagaserva kujude mõju takistuskoefitsiendile tõstejõukoefitsiendil C_L 0.7 erinevatel lennukiirustel, joonisel oleval graafikul on

näidatud, et väikseima takistusega on kiirusel M 0.78 0.7% kõrgusega õõnsuse (cavity) tagaserv;

joonisel Fig. 4A on kujutatud lennukitiival erinevad (CMF) miniklapi sektsioonid erinevates asendites. Sellega on võimalik, vastavalt vajadusele, reguleerida tõstejõu

5   jagunemist kogu tiiva ulatuses. Suurim tõstejõu suurenemine saadakse (CMF) miniklappide kasutamisel koos kaldtüüride nurga suurendamise ja tiivaotsa winglettidega;

joonisel Fig. 4B on näidatud graafikul tõstejõu (koormuse) jagunemist tiival. Tavaliselt erineb tõstejõu jagunemine tiiva ulatuses ehitustehnilistel põhjustel ideaalsest

10   (elliptilisest). (CMF) miniklappide sektsioonide erinevate asenditega on võimalik tõstejõu jagunemine muuta väga lähedaseks elliptilisele ning vähendada sellega induktiivtakistust. Osaliselt võiks (CMF) miniklapp olla ka kaldtüüride sees.

Joonisel Fig. 5 on joonised erinevatest (CMF) miniklapi variantidest, kus joonisel Fig. 5A on kujutatud fikseeritud kõrgusega (CMF) miniklapi profiil, kusjuures sisse

15   tõmmatuna muudab profiili kuju tagatiiva ülemine ja alumine serv; Joonisel Fig. 5B on kujutatud (CMF-i) miniklapi ülemine paneel on muudetava nurga ja kõrgusega, kusjuures miniklapi sissetõmmatud asendis (cavity) õõnsus praktiliselt puudub; joonisel Fig. 5C on kujutatud miniklapi variant kandilise (cavity) õõnsuse profiili ja ülemise reguleeritava paneeliga; joonisel Fig. 5D on kujutatud miniklapi variant samuti

20   kandilise (cavity) õõnsa profiili ja alumise reguleeritava paneeliga; joonisel Fig. 5E on kujutatud miniklapi variant allapoole kumera alumise serva ja fikseeritud kõrgusega cavity tagaservaga, kusjuures sisse tõmmatuna muudab profiili kuju tagatiiva ülemine ja alumine serv.

Joonisel Fig. 6 on kujutatud tagatiiva tagaosa ristlõiget, kusjuures joonisel Fig. 6A on

25   kujutatud miniklappi täiesti sissetõmmatud asendis ning joonisel Fig. 6B on miniklapp täiesti väljalastud asendis. Joonisel Fig. 6C on kujutatud alumise kallutatava paneeli liigutusmehhanismi;

Joonisel Fig. 7A ja 7B on kujutatud miniklapi (cruise miniflap) liigutamise mehhanism, mis asub osaliselt väljaspool tagatiiba lennukitiiva voolundaja sees.

30   TEOSTUSNÄIDE

Joonisel Fig.6 on näidatud tagatiiva ristlõiget, milles on kasutatud miniklappi. Joonisel Fig.6A on kujutatud miniklapp (CMF) täiesti sissetõmmatud asendis. Joonisel Fig.6B

on kujutatud miniklapp aga täiesti väljalastud asendis. Joonisel Fig. 6C on kujutatud alumise kallutatava paneeli 5 liigutusmehhanismi, kus kallutatava alumise paneeli kronstein (horn) 15 on ühendatud läbi tagumise pöörleva liigendi 14 ajamiga 6, mis on ühendatud läbi esimese pöörleva liigendi 18 lennukitiiva tagatiiva

5   põhikonstruktsiooniga.

Lennukitiiva 1 tagumises osas või tagatiiva (flap) tagaservas 2 asub miniklapp 4 (cruise miniflap). Joonisel Fig 6A on miniklapp 4 sissetõmmatud (retracted state) asendis. Miniklapp on kinnitatud juhtkonsooli 7 tagumise otsa külge, juhtkonsooli 7 külge on kinnitatud tagumine rullik 8 ja esimene rullik 9, mis liiguvad tagatiiva

10   põhikonstruktsiooni küljes olevas juhttees 10. Rõhu erinevustest tingitud koormused jagunevad tagatiiva (flap) pinnalt tagatiiva esimese tala 16 ja tagumise tala 17 (spar) vahel. Tagatiiva põhikonstruktsiooni või juhttee 10 külge on kinnitatud elektrimootor 11 mis paneb läbi reduktori 13 pöörlema aktuaatori kruvimehhanismi 12, mille ots on kinnitatud tagumisse rullikusse 8 nii, et rulliku 8 küljes olev kruvimehhanismi mutter

15   liigub lineaarselt mööda kruvimehhanismi 12 kruvi, sellega koos liigub juhtkonsool 7 koos miniklapiga (cruise miniflap) kuni maksimaalse väljalastud asendini, mida on kujutatud joonisel Fig. 6B. Seejuures liiguvad tagumine rullik 8 ja esimene rullik 9 mööda juhtteed 10. Rullikute õlesandeks on stabiliseerida juhtkonsooli liikumist juhtees. Juhtee 10 on kinnitatud tiiva (tagatiiva) esimese tala 16 ja tagumise tala 17

20   külge. Cruise miniflap-i liikumisel väljalastud asendisse kaldub viimane samuti allapoole (extension angle) väljalaske nurga β võrra (vaata joonis 6B, nurk β jääb horisontaali ja minikapi alumise tasapinna vahele). Koos cruise miniflap-i liikumisega kallutatakse tiiva (tagatiiva) alumist paneeli 5 aktuaatori 6 abil. Aktuaator 6 on kinnitatud eesmise pöörleva liigendi 18 abil tiiva (tagatiiva) põhikonstruktsiooni külge

25   ning teise pöörleva liigendi 14 abil on aktuaator 6 kinnitatud alumist paneeli 5 liigutava kronsteini (horn) 15 külge. CMF (Cruise miniflap) sissetõmbamisel liiguvad kõik osad samal trajektooril aga vastupidises suunas kuni sissetõmmatud asendini.

Miniklappide liigutamiseks ettenähtud mehhanism (ajam (elektrimootor) 11, reduktor 13, kruvimehhanism 12 – kruvipaariks on keermestatud varb ja sellel liikuv

30   keermestatud mutter) koos juhtkonsooli 7, juhttee 10, esimese ja tagumise rulliku ning tagatiiva alumise paneeli liigutusmehhanismiga võib alternatiivses teostuses, eriti kui on tegemist suuremate lennukite tiiva tagatiibadega, paikneda lennuki tiiva voolundaja 19 sees (vaata joonis fig 7B). Seejuures võib kruvimehhanismi kruvi olla kinnitatud juhtkonsoolil selleks ettenähtud kronsteini külge, mis ei ole seotud tagumise rullikuga.

Cruise miniflap saab liikuda tiivast väljapoole kuni 7% arvestatuna tiiva laiusest (vaata Fig. 1C). Seejuures moodustub tiiva tagaserva õõnsus, mille suurim kõrgus H (vaata joonis Fig. 1C) võib ulatuda 1% tiiva laiusest. Seda miniklapi asendit kasutatakse lennuki maksimaalse stardimassi korral lennu algfaasis. Fig 1B toodud asendeid kasutatakse reisilennul, kui kütuse kuludes on ka lennumass vähenenud. Seejuures on cruise miniflap tiivast väljapoole 2-6% tiiva laiusest ning õõnsuse kõrgus harilikult 0,5-0,7% tiiva laiusest. Lennu lõppfaasis võib olla väikseima aerodünaamilise takistusega miniklapi asendiks Fig 1A näidatud sissetõmmatud asend. Miniklapp asub seejuures täielikult tiivakontuuri sees ja tagaserva kõrgus on 0,1-0,3% tiiva laiusest. Kasutades fikseeritud kõrgusega miniklappi Fig 5A siis tema kõrgus asendites Fig 1C ja Fig 1B ei muutu ning on harilikult 0,5-0,7% tiiva laiusest. Sissetõmmatud asendis aga õõnsus praktiliselt kaob, sest miniklapid on sügaval tiiva sees ja tagaserva kõrgus jääb vahemikku 0,1-0,3% tiiva laiusest.

Lennuki tavapärasel lennul on cruise miniflap tiivast väljapoole ulatuv 2-6% tiiva laiusest ning miniklapi tagumises servas oleva õõnsuse kõrgus on vahemikus 0,5-0,7% tiiva laiusest, aga lennu lõppfaasis on miniklapp täielikult tagatiiva kontuuri sees ja tagaserva kõrgus on vahemikus 0,1-0,3% tiiva laiusest. Miniflapi tagaservas oleva õõnsuse profiil on miniflapi tagumise serva pinnast sissepoole kumer, kusjuures miniklapi alumise poole serv on ulatuv ülemisest servast kaugemale 0,4-1,0 % tiiva laiusest. Alternatiivselt võib miniflapi tagaservas oleva õõnsuse profiil olla miniflapi pinnast sissepoole kandiline, seejuures miniklapi alumise poole serv on ulatuv ülemisest servast kaugemale 0,5-2,0% tiiva laiusest. Samuti võib erinevate konstruktsiooniliste lahenduste korral olla miniklapi ülemine pind allapoole liikuv või miniklapi alumine pind võib olla ülespoole liikuv.

Alternatiivsetes teostuste on (CMF) miniklapil erinevad tagumiste osade profiilid. Joonisel Fig.5A on kujutatud fikseeritud kõrgusega (CMF) miniklapi profiil, kusjuures sisse tõmmatuna muudab profiili kuju tagatiiva ülemine serv; joonisel Fig.5B on kujutatud (CMF-i) miniklapp, mille ülemine paneel on muudetava nurga ja kõrgusega, kusjuures miniklapi sissetõmmatud asendis miniklapi tagaserva õõnsus (cavity) praktiliselt puudub; joonisel Fig.5C on kujutatud miniklapi variant kandilise (cavity) õõnsuse profiili ja miniklapi ülemise reguleeritava paneeliga; joonisel Fig.5D on kujutatud miniklapi variant samuti kandilise (cavity) õõnsa profiili ja miniklapi alumise reguleeritava paneeliga; joonisel fig 5E on kujutatud lühema profiiliga (profiili alumine väljaulatuv osa on lühem) miniklapi varianti, kusjuures miniflapi alumisele pinnale on

antud allapoole kumerduv profiil ning miniklapi alumine tagumine serv on lühem võrreldes joonistel fig 5A kuni 5D kujutatud miniklappidega.

Reference symbol list:

5 1 - Wing

2 – Trailing edge flap

3 - Trailing edge

4 - Cruise miniflap

5 – Under panel

10 6 – Actuator for the under panel

7 - Juhtkonsool

8 - Tagumine rullik

9 - Esimene rullik

10 - Juhttee

15 11 - Elektrimootor

12 – Aktuaatori kruvimehhanism

13 - Reduktor

14 - Rear pivotal articulation

15 – Actuating horn

20 16 - First spar

17 - Rear spar

18 – Forward pivotal articulation

19 – Voolundaja

Patendinõudlus

1. Lennukitiiva tagatiiva miniklapp (cruise miniflap), mis on ette nähtud lennuki aerodünaamiliste omaduste parendamiseks, kus lennukitiiva (1) tagumises servas paikneva tagatiiva (2) põhikonstruktsioon hõlmab tiiva tagaserva (3), tagatiiva esimest ja tagumist tala (16, 17), tagatiiva ülemise paneeli ja kallutatava alumise paneeli vahel olevat miniklappi (4), mis on kinnitatud juhtkonsooli (7) külge, kusjuures juhtkonsool on liikuv tagumise ja esimese rulliku (8, 9) abil tagatiiva põhikonstruktsiooni külge kinnitatud juhttees (10) ning juhtkonsool on ühendatud tagumise rulliku abil aktuaatori kruvimehhanismiga (12), mis on ühendatud läbi reduktori (13) ajamiga (11), mis on ette nähtud miniklapi liigutamiseks tagatiivast välja ja sisse, kusjuures miniklapi tagumises servas on moodustatud õõnsus, mille kõrgus on kuni 1% miniklapi laiusest.

2. Lennukitiiva tagatiiva miniklapp (cruise miniflap), mis on ette nähtud lennuki aerodünaamiliste omaduste parendamiseks vastavalt punktile 1, kusjuures lennuki tavapärasel lennul on cruise miniflap tiivast väljapoole ulatuv 2-6% tiiva laiusest ning miniklapi tagumises servas oleva õõnsuse kõrgus on vahemikus 0,5-0,7% tiiva laiusest, ja et lennu lõppfaasis on miniklapp täielikult tagatiiva kontuuri sees ja tagaserva kõrgus on vahemikus 0,1-0,3% tiiva laiusest.

3. Lennukitiiva tagatiiva miniklapp (cruise miniflap), mis on ette nähtud lennuki aerodünaamiliste omaduste parendamiseks vastavalt punktile 1, kusjuures miniflapi tagaservas oleva õõnsuse profiil on miniflapi tagumise serva pinnast sissepoole kumer, kusjuures miniklapi alumise poole serv on ulatuv ülemisest servast kaugemale 0,4-1,0 % tiiva laiusest.

4. Lennukitiiva tagatiiva miniklapp (cruise miniflap), mis on ette nähtud lennuki aerodünaamiliste omaduste parendamiseks vastavalt punktile 1, kusjuures miniflapi tagaservas oleva õõnsuse profiil on miniflapi pinnast sissepoole kandiline, seejuures miniklapi alumise poole serv on ulatuv ülemisest servast kaugemale 0,5-2,0% tiiva laiusest.

5. Lennukitiiva tagatiiva miniklapp (cruise miniflap), mis on ette nähtud lennuki aerodünaamiliste omaduste parendamiseks vastavalt punktidele 1-4, kusjuures miniklapi ülemine pind on allapoole liikuv.

6. Lennukitiiva tagatiiva miniklapp (cruise miniflap), mis on ette nähtud lennuki aerodünaamiliste omaduste parendamiseks vastavalt punktidele 1-4, kusjuures miniklapi alumine pind on ülespoole liikuv.

7. Lennukitiiva tagatiiva miniklapp (cruise miniflap), mis on ette nähtud lennuki aerodünaamiliste omaduste parendamiseks vastavalt mistahes eelnevale punktile 1-6, kusjuures miniklapi liigutamiseks ettenähtud mehhanism, mis hõlmab juhtkonsooli, mille külge on kinnitatud miniklapp, juhtkonsooli esimest ja tagumist rullikut, mis on liikuvad tagatiiva põhiraami külge kinnitatud juhttees, juhtkonsooli kronsteini, mille külge on kinnitatud aktuaatori kruvimehhanismi, mille üks ots on läbi liigendite ühendatud reduktoriga, ning lennuki tagatiiva miniklapi liigutamiseks ette nähtud ajamit, mis on ühendatud reduktoriga ja on kinnitatud tagatiiva põhikonstruktsiooni külge, on paigutatud väljapoole lennuki tagatiiba tagatiiva voolundaja sisse.

Lühikokkuvõte

Käesolev leiutis pakub välja lennukitiiva tagatiivale lisatava miniklapi (cruise miniflap) erinevad konstruktsioonivariandid, millega on võimalik lennuki aerodünaamilisi omadusi parendada. Tagatiivale lisatud miniklapi tagumises servas on moodustatud 5 õõnsus, mille kõrgus on kuni 1% tiiva laiusest.
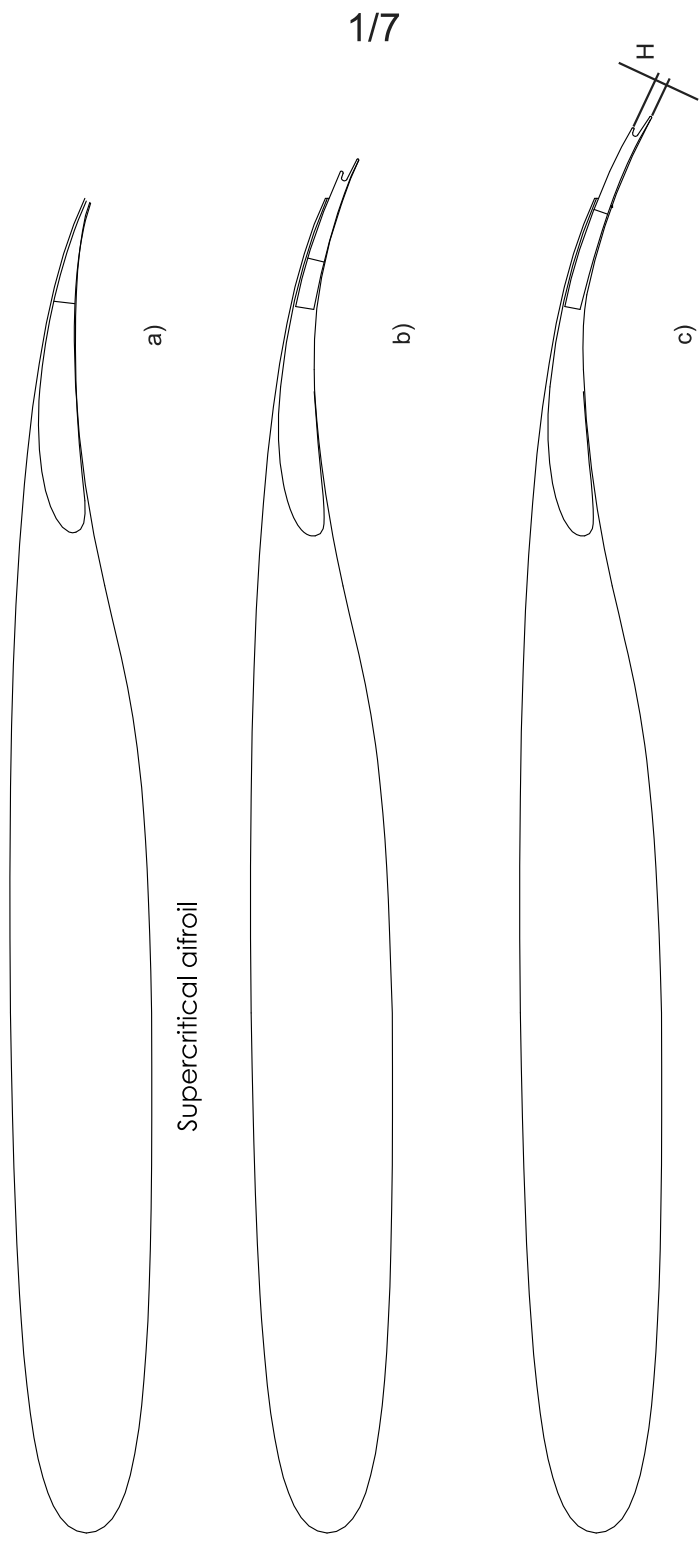
a)

b)

c)

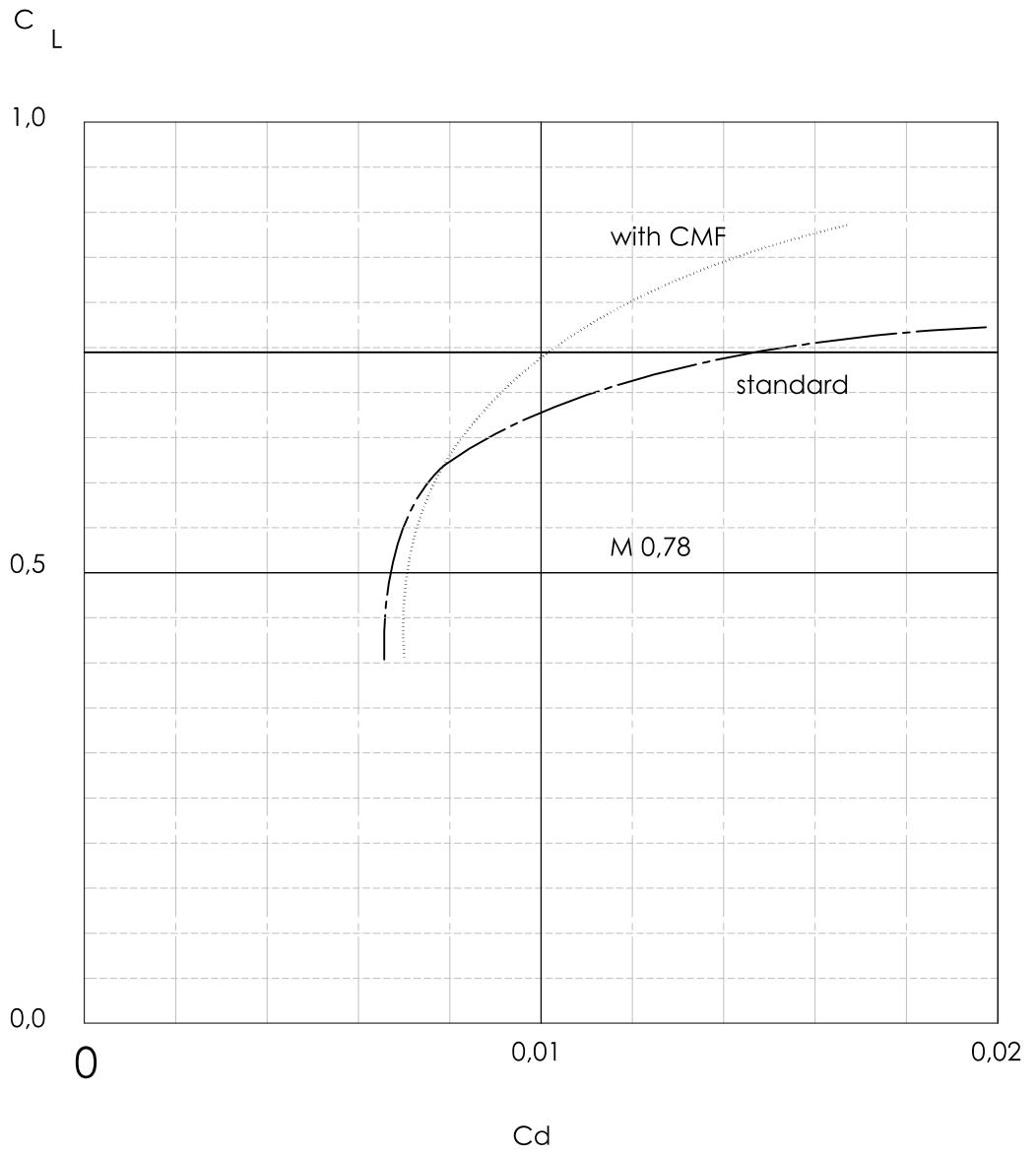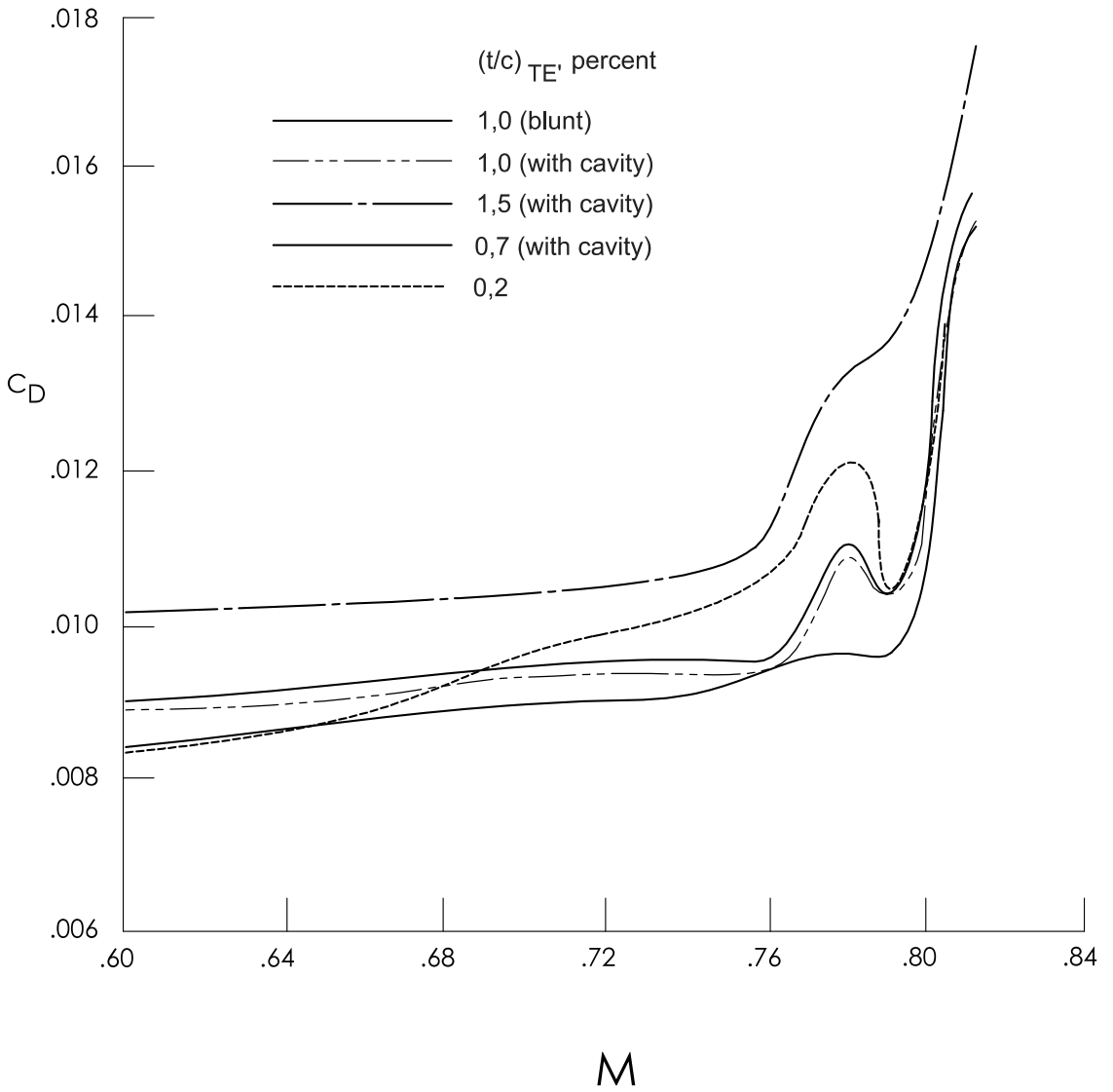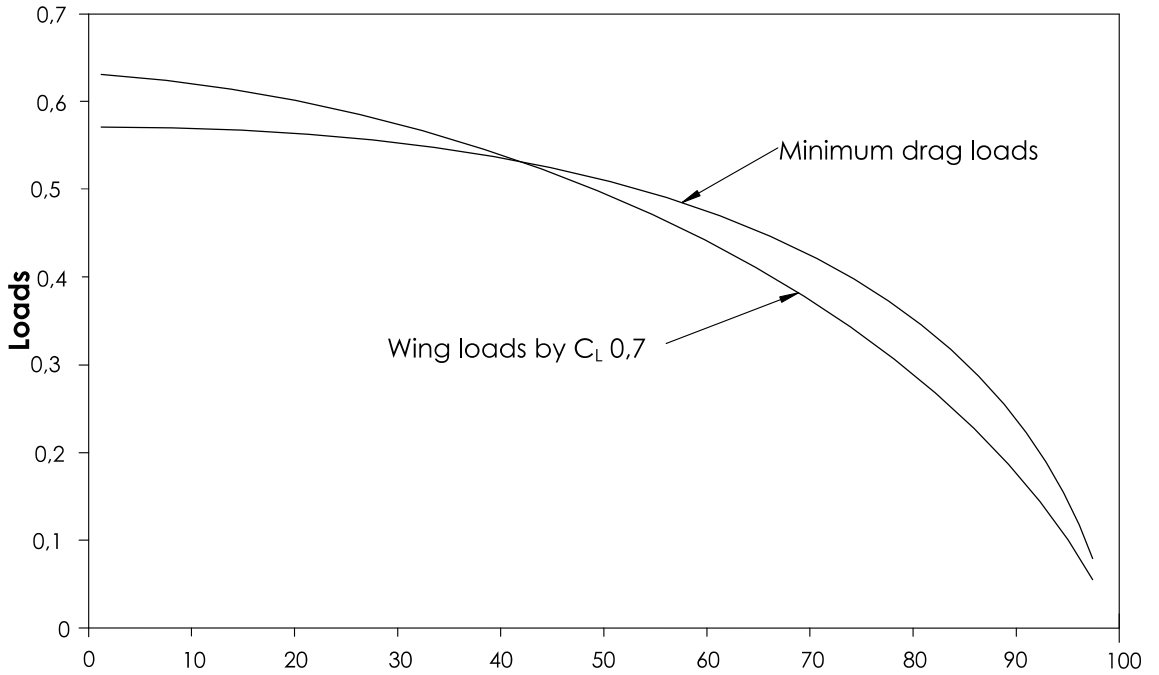Supercritical airfoil

Cruise miniflap settings

H

Fig. 1

Fig. 2

Fig. 3

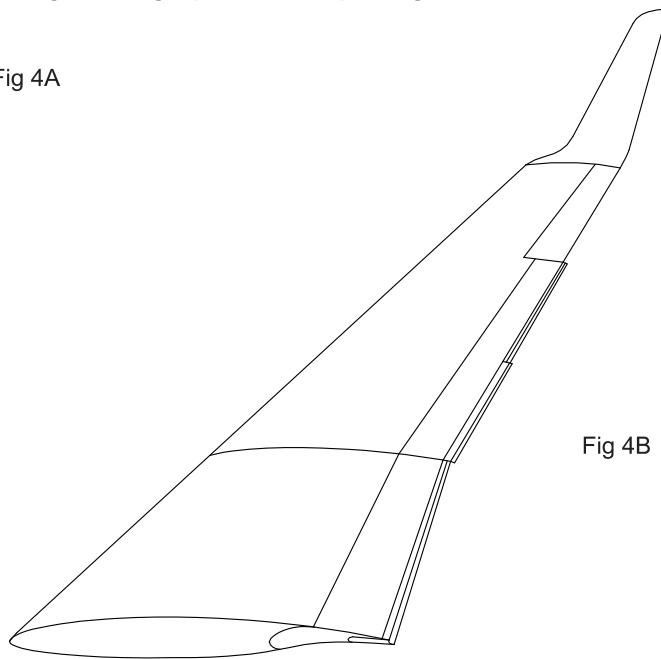**Wing loading optimiztion by using CMF C$_L$ 0,7**
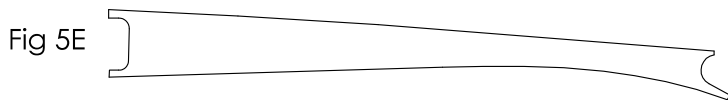
Fig 4A

Fig 4B
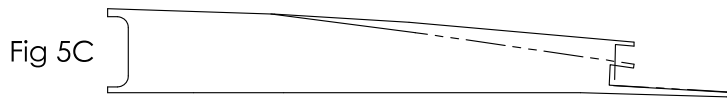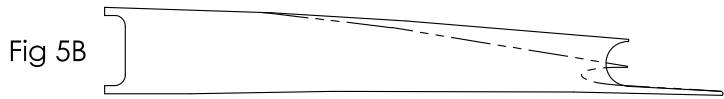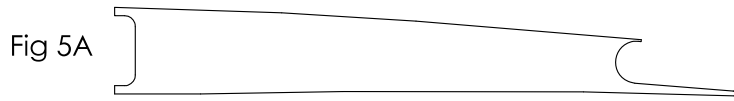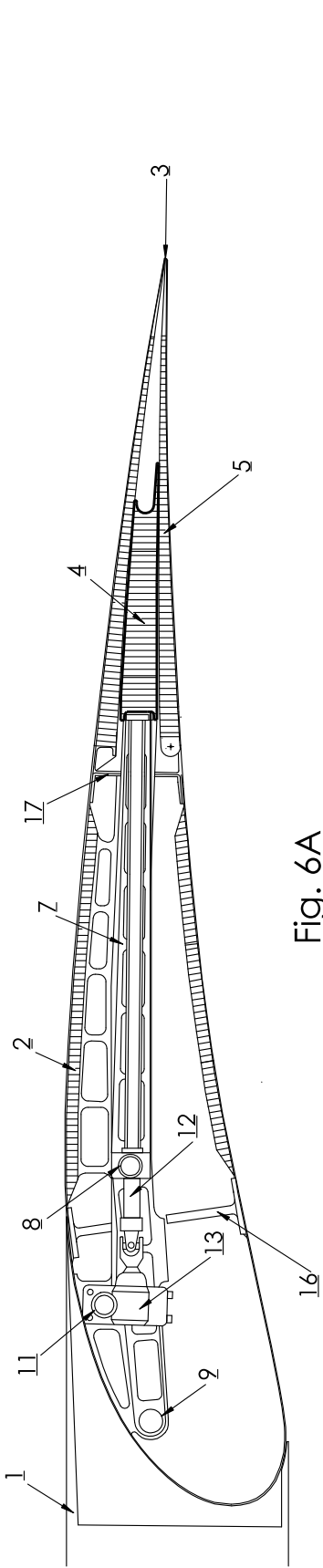
Fig. 4

Fig 5A

Fig 5B

Fig 5C

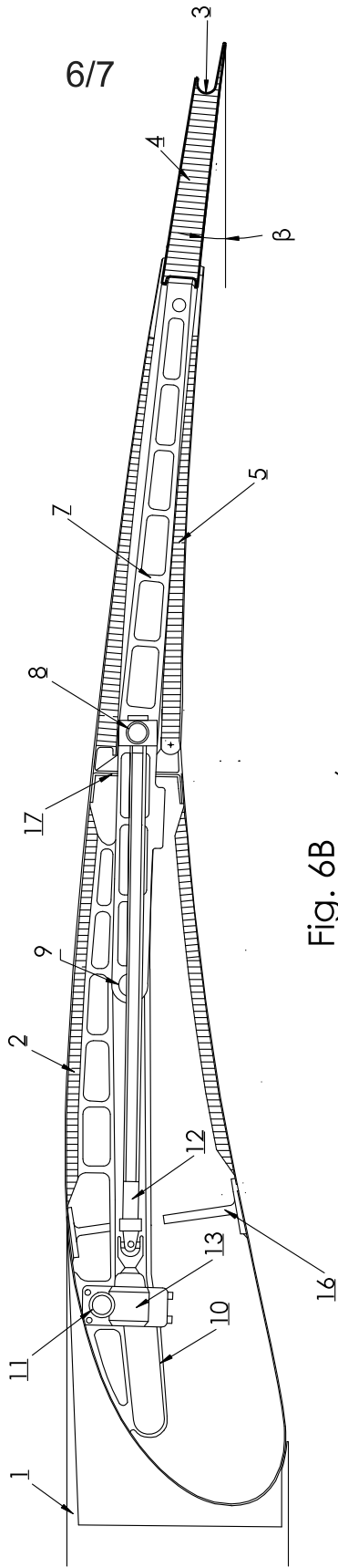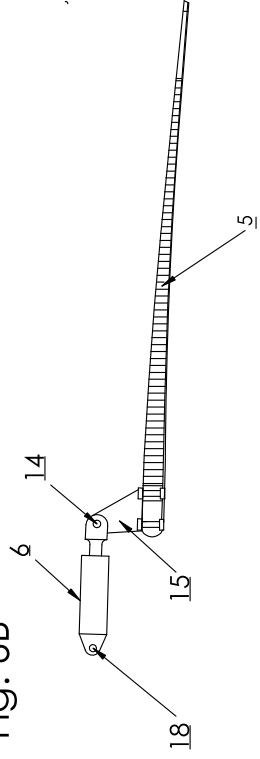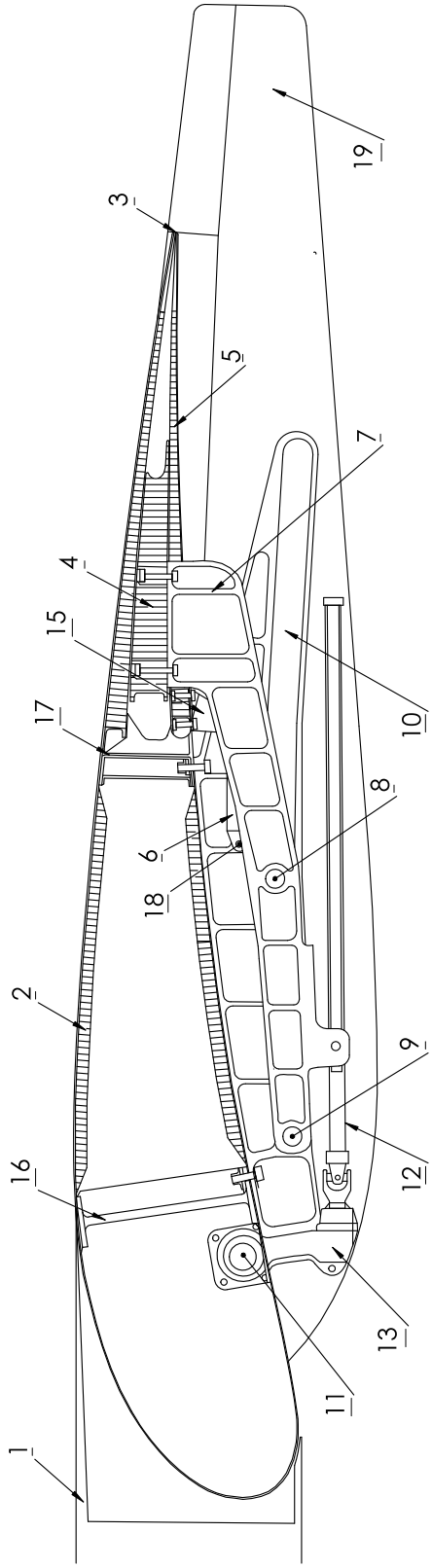Fig 5D

Fig 5E

Fig. 5

Fig. 6A
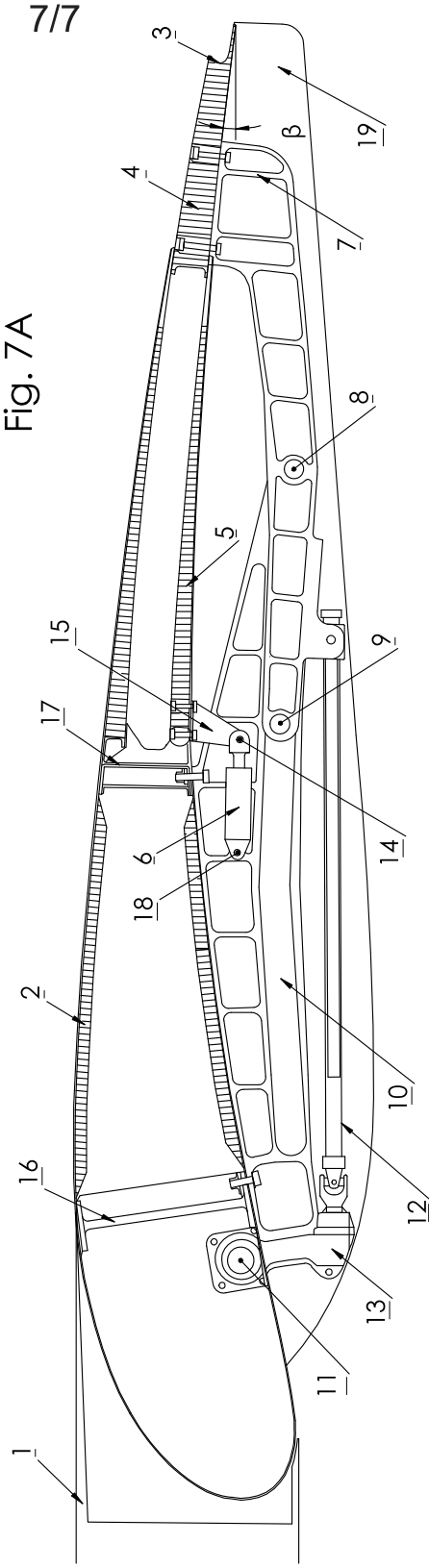
Fig. 6B

Fig. 6C

Fig. 7A

Fig. 7B

Cruise miniflaps for aircraft

TECHNICAL FIELD

This invention relates to increasing the aircraft wing lift and to decreasing the aerodynamic drag during flight. The cruise miniflap (hereinafter CMF) according to the invention is part of the aircraft wing or the trailing edge flap and it can be used to modify the camber and the area of the aircraft wing and to create a cavity within the wing trailing edge.

BACKGROUND ART

The high wing loading of modern long range commercial airplanes does not allow them to achieve the optimal cruise altitude after take-off without a sharp increase of the aerodynamic drag because the used wing profile has been designed for low aerodynamic drag, with the lift coefficient C_L within the range of 0.45–0.6. Lower cruise altitude, however, results in a slower ground speed, which in turn increases fuel consumption. In the areas of heavy air traffic, lower cruise altitude often prevents from selecting the direct route to the destination airport. Therefore, heavier aircraft have high fuel consumption in the first stage of the flight. The invention described herein provides means for increasing the wing lift coefficient to the level of 0.7–0.8 so that the drag coefficient does not grow substantially. It allows the commercial transport airliners to reach higher altitudes after take-off and to improve the aerodynamic value (lift to drag or L/D ratio), which substantially reduces fuel consumption and also lengthens the flight distance.

Various modified aircraft wing trailing edges have previously been patented. The most relevant of these are the following:

Document GB 2174341A, 5 November 1986, The Secretary of State for Defence (United Kingdom) (1), describes a supercritical wing section provided with a hinged flap attached to the wing.

Document US6565045 B1, 20 May 2003, Onera, describes an aerodynamic surface, such as a wing, comprising a reduced-pressure face and a pressure face which are connected at the rear section of the wing.

In document US 2007/0221789 A1, 27 September 2007, Hak-Tae Lee et al. describe an improved trailing edge aerodynamic control effector.

In document US 2013/0214092 A1, 22 August 2013, Airbus Operations GmbH, an aerodynamic wing section with ancillary flaps has been described which can be moved with a guide mechanism and a drive device for actuating the ancillary flaps.

Document GB 2174341A describes a device arranged to the trailing edge of a
5   supercritical wing profile, which can be used to modify the camber as well as the thickness of the wing trailing edge. Compared to the above solutions, the device according to this invention ensures lower aerodynamic drag because a supercritical wing profile with a cavity in the trailing edge has lower aerodynamic drag than a blunt trailing edge, and in addition, the device provided in this invention alters the area of
10   the wing, which also makes it possible to reduce the aerodynamic drag. Differently from the devices known in the prior art, such as the devices described in documents US 6565045 B1 and US 20070221789 A1, the device according to this invention, when in retracted position, provides a thinner trailing edge and consequently, also a substantially lower C_L value (0.4–0.6). The above-said implication can be illustrated
15   by the graph from US 6565045 B1 which reveals that the aerodynamic surface developed by the applicants reduces drag when $C_L > 0.7$. With the device according to this invention, the value of $C_L > 0.63$ is achieved. The graph cited above also shows that the drag coefficient C_d is substantially higher than the value achieved with the device provided in this invention. Document US 2007/0221789 anticipates the
20   simultaneous use of several effectors because the width of the element is relatively small. The device according to this invention has a simpler construction, it is more rigid and, all in all, more reliable. With C_L in the range of 0.4–0.75, the device provided in this invention also has lower aerodynamic drag at Mach 0.75–0.8. When compared with the device described in US 2013/0214092, the cruise miniflap
25   according to this invention (CMF) has lower aerodynamic drag, it is more rigid and becomes less deformed under the air flow, therefore, it provides for a more reliable way to improve the performance of aircraft.

SUMMARY OF INVENTION

The cruise miniflap (CMF) according to this invention is an ancillary aerodynamic
30   surface which can be provided at the trailing edge, in the trailing edge flap or the ailerons. If necessary, the cruise miniflap can be moved mechanically by means of actuators and this way it is possible to modify the camber, area and shape of the trailing edge. The transition between the wing and the CMF is relatively smooth and

there are no sharp transitions characteristics to conventional trailing edge flaps. One wing can be provided with one or more cruise miniflap sections. With the use of more than one cruise miniflap it is possible to optimise the distribution of lift along the span of the wing and additionally reduce induced drag. The trailing edge with a cavity

5   permits to reduce drag ($C_L > 0.6$) and at Mach > 0.65. The optimal height of the trailing edge depends on the used wing profile, the lift coefficient and the object's air speed. For example, when the Mach number of the supercritical wing profile at the cruise speed is 0.78 and the lift coefficient C_L is 0.7, the optimal height of the trailing edge with a cavity is 0.7% of the chord length. In the case of the higher lift coefficient

10   value, the optimal height of the trailing edge with a cavity is also higher. If the value of C_L is less than 0.6, the trailing edge with a cavity does not reduce drag and it is in the retracted position. The trailing edge with a cavity may be fixed or with a modifiable height and shape. The profile of the cavity may be arched or angular. To modify the height, the upper or lower edge of the CMF may be used.

15   The use of the CMF makes it possible to reduce the cost of maintenance and repair of the engines because the power required during the flight is reduced and therefore the engines do not wear so much. In addition to lower fuel consumption, the invention helps to reduce emission of pollutants and noise.

BRIEF DESCRIPTION OF DRAWINGS

20   In order to give a better and more detailed overview of the invention, the following embodiments with reference to the drawings will be described, of which:

Figure 1 depicts the position of the CMF according to the invention within the wing (trailing edge flap) (a) and its basic position, from which the one used in the initial position of take-off and cruise is depicted at the bottom of the figure (c), the position

25   employed during the flight when the amount of fuel and the in-flight weight are decreasing is in the middle (b), and the position used in the final stage is at the top of the figure (a);

Figure 2 depicts the lift coefficient and drag coefficient ratio of the wing profile for a commercial transport aircraft at the speed corresponding to Mach 0.78. As seen in

30   the figure, aerodynamic drag starts to grow rapidly at the C_L value of 0.63. With the use of the cruise miniflap of the invention, however, it is possible to reduce the aerodynamic drag substantially at the level of $C_L > 0.62$. When the in-flight weight decreases (because the fuel is being consumed), it is beneficial to retract the CMF

gradually during the flight because the aerodynamic drag is smaller if the value of C_L is within the range 0.4–0.6;

Figure 3 depicts the effect of various shapes of the wing trailing edge on the drag coefficient at the C_L value of 0.7 at different cruise speeds and the graph in the figure shows that the lowest drag at M 0.78 is achieved when the height of the cavity in the trailing edge is 0.7%;

Figure 4A depicts a wing with various CMF sections in different positions. It gives the possibility to control the distribution of the lift over the span of the wing as necessary. The greatest increase in lift is achieved when the cruise miniflaps (CMFs) are used with the increasing of the deflection angle of ailerons and with the winglets at the wing tip;

Figure 4B is a graph showing the distribution of the lift (load) over the length of the wing. Distribution of lift over the wing length usually differs from the ideal (elliptic) due to engineering reasons. By using different positions of the cruise miniflap (CMF) sections, distribution of lift can be approximated to the elliptical, which in turn reduces the induced drag. The cruise miniflap (CMF) may partially also be located within the ailerons.

Figure 5 depicts possible variants of the cruise miniflap (CMF); Fig. 5A shows a fixed-height miniflap (CMF) profile, the shape of which, when retracted, is modified by the upper and lower edge of the trailing edge flap; the miniflap in Fig. 5B has an upper panel with a changeable angle and height, whereas the cavity is almost non-existent when the miniflap is retracted; Fig. 5C shows a cruise miniflap with a rectangular cavity and an upper controllable panel; Fig. 5D shows a cruise miniflap with a rectangular cavity and a lower controllable panel; Fig. 5E shows a cruise miniflap with a lower edge which is curved downward and a trailing edge cavity of a fixed height, whereas the shape of the profile, when retracted, is modified by the upper and lower edge of the trailing flap;

Figure 6 depicts a cross-sectional view of the rear part of the trailing edge flap; Fig. 6A shows the cruise miniflap in its completely retracted position and Fig. 6B the cruise miniflap in the completely extended position. Fig. 6C shows the actuating mechanism for moving the deflectable under panel;

Figures 7A and 7B depict a mechanism for moving the cruise miniflap which is located partially outside the trailing edge flap within the wing fairing.

DESCRIPTION OF EMBODIMENTS

Fig. 6 is a cross-sectional view of the trailing edge flap in which the cruise miniflap is used. Fig. 6A depicts a cruise miniflap (CMF) in its completely retracted position. Fig. 6B depicts a cruise miniflap in its completely extended position. Fig. 6C depicts the
5   mechanism for moving the deflectable under panel 5 where the horn 15 of the deflectable under panel is coupled, through the rear pivotal articulation 14, with the actuator 6, which through the forward pivotal articulation 18 is connected to the main construction of the trailing edge flap.

The cruise miniflap 4 is located in the rear part of the wing 1 or the trailing edge
10 flap 2. In Fig. 6A, the cruise miniflap 4 is in the retracted position. The miniflap is attached to the rear end of the control unit 7, also the rear roller 8 and the first roller 9 are attached to the control unit 7, which move along the flap track 10 fastened to the main construction of the trailing flap. The load occurring due to the pressure difference is distributed from the trailing flap surface between the first spar 16 and the
15 rear spar 17. To the main construction of the trailing edge flap or the flap track 10, an electrical motor 11 is fixed that rotates, through the reduction gear 13, the screw mechanism 12 with its end fixed to the rear roller 8 in a way that the nut attached to the roller 8 moves in a linear manner along the screw of the screw mechanism 12 and together with this, the control unit 7 with the cruise miniflap moves until it is in the
20 entirely extended position, as shown in Fig. 6B. At the same time, the rear roller 8 and the first roller 9 are moving along the flap track 10. The function of the rollers is to stabilise the movement of the control unit along the flap track. The flap track 10 is fixed to the first spar 16 and the rear spar 17 of the wing (trailing edge flap). When the cruise miniflap moves to the extended position, it also slopes downward by the
25 extension angle β (see Fig. 6B, the angle β is between the horizontal plane and the lower plane of the cruise miniflap). With the movement of the cruise miniflap, the under panel 5 of the wing (trailing edge flap) is sloped by means of the actuator 6. Through the forward pivotal articulation 18, the actuator 6 is fixed to the main construction of the wing (trailing edge flap) and by means of the rear pivotal
30 articulation 14, it is fixed to the actuating horn 15 which moves the under panel 5. When the cruise miniflap (CMF) is being retracted, all parts move along the same trajectory, but in the opposite direction until the miniflap is in the retracted position.

In an alternative embodiment, especially in the case of the trailing edge flaps of a large aircraft, the mechanism for moving cruise miniflaps (drive (electrical motor) 11, reduction gear 13, screw mechanism 12 with the screw pair comprising of a threaded rod and a threaded nut moving along it) with the control unit 7, flap track 10, first and
5   rear roller and the mechanism for moving the under panel of the trailing edge flap may be located within the wing fairing 19 (see Fig. 7B). In this case, the screw of the screw mechanism may be fixed to the horn, provided for this purpose in the control unit, which is not coupled with the rear roller.

The cruise miniflap can be extended outwards up to 7% of the wing chord (see
10   Fig. 1C). By that, a cavity is formed in the trailing edge with the greatest possible height H (see Fig. 1C) of 1% of the chord. This position of the cruise miniflap is used at the maximum take-off weight of the aircraft in the initial stage of the flight. The arrangements shown in Fig. 1B are used at the cruise stage when the weight of the aircraft has decreased as the fuel has been consumed. In this case, the cruise
15   miniflap has extended outwards from the wing by 2–6% of the chord and the height of the cavity is usually 0.5–0.7% of the chord. In the final stage of the flight, the cruise miniflap may be in the retracted position with the lowest aerodynamic drag, which is shown in Fig. 1A. At that, the cruise miniflap is entirely within the wing configuration and the height of the trailing edge is 0.1–0.3% of the wing chord. When the fixed-
20   height cruise miniflap shown in Fig. 5A is used, its height in the arrangements depicted in Figs. 1C and 1B does not change and is usually 0.4–0.7% of the wing chord. In the retracted state, the cavity is virtually non-existent because the miniflaps are deep within the wing and the height of the trailing edge is in the range of 0.1–0.3% of the wing chord.

25   During the cruise, the cruise miniflap extends outwards from the wing by 2–6% of the wing chord and the height of the cavity in the rear end of the cruise miniflap is within the range of 0.4–0.7% of the wing chord, but in the final stage of the flight it is entirely within the trailing edge flap configuration and the height of the edge is in the range of 0.1–0.3% of the wing chord. The profile of the cavity in the miniflap rear edge is
30   curved inwards, whereas the edge of the lower side of the miniflap extends by 0.4–1.0% of the wing chord over the edge of the upper side. Alternatively, the profile of the cavity in the rear edge of the cruise miniflap may be rectangular and the edge of the lower side of the miniflap extends by 0.5–2.0% of the wing chord over the edge of

the upper side. In various embodiments, the upper surface of the cruise miniflap may be movable downwards or its lower surface may be movable upwards.

In alternative embodiments, the cruise miniflap may have rear sections with different profiles. In Fig. 5A, the profile of a fixed-height cruise miniflap (CMF) is shown, the shape of which in the retracted state is modified by the upper side of the trailing edge; Fig. 5B shows a cruise miniflap with an upper panel of a changeable angle and height, which has practically no cavity in the trailing edge when in retracted position; Fig. 5C shows a variant of the cruise miniflap with a rectangular cavity and an upper controllable upper panel; Fig. 5D shows another variant of the cruise miniflap with a rectangular cavity and a controllable under panel; Fig. 5E shows a variant of the cruise miniflap of a shorter profile (the lower section projecting outward is shorter) where the lower surface of the miniflap has a downward curving surface and the lower rear edge of the miniflap is shorter than that of the cruise miniflaps provided in Figs. 5A–5D.

REFERENCE SIGNS LIST

1 – Wing

2 – Trailing edge flap

3 – Trailing edge

4 – Cruise miniflap

5 – Under panel

6 – Actuator for the under panel

7 – Control unit

8 – Rear roller

9 – First roller

10 – Flap track

11 – Electrical motor

12 – Screw mechanism of the actuator

13 – Reduction gear

14 – Rear pivotal articulation

15 – Actuating horn

16 – First spar

17 – Rear spar

18 – Forward pivotal articulation

19 – Fairing

Claims

1. A cruise miniflap of the trailing edge flap for improving the aerodynamic properties of an aircraft, wherein the main construction of the trailing edge flap (2) of the wing (1) comprises the trailing edge (3), the first spar and the rear spar (16, 17), the cruise miniflap (4) located between the upper panel of the trailing edge and the deflectable under panel and fixed to the control unit (7), wherein the control unit can be moved by means of the rear roller and the first roller (8, 9) along the flap track (10) attached to the main construction of the trailing edge flap, and the control unit (7) is through the rear roller coupled with the screw mechanism (12) which by means of the reduction gear (13) is coupled with the drive (11) intended for moving the cruise miniflap out of and in the trailing edge flap, and wherein the cruise miniflap has a cavity in its rear edge, the height of which is up to 1% of the width of the miniflap.

2. The cruise miniflap of the trailing edge flap according to claim 1 for improving the aerodynamic properties of an aircraft, wherein during the cruise, the cruise miniflap extends outwards from the wing by 2–6% of the wing chord and the height of the cavity in the rear edge of the miniflap is in the range of 0.4–0.7% of the wing chord, and in the final stage of the flight the cruise miniflap is entirely within the trailing edge flap configuration and the height of the trailing edge is in the range of 0.1–0.3% of the chord.

3. The cruise miniflap of the trailing edge flap according to claim 1 for improving the aerodynamic properties of an aircraft, wherein the profile of the cavity in the rear edge of the cruise miniflap is curved inward and the edge of the lower side of the cruise miniflap extends over the upper edge by 0.4–1.0% of the wing chord.

4. The cruise miniflap of the trailing edge flap according to claim 1 for improving the aerodynamic properties of an aircraft, wherein the profile of the inward cavity in the rear edge of the cruise miniflap is rectangular and the edge of the lower side of the cruise miniflap extends over the upper edge by 0.4-1.0% of the wing chord.

5. The cruise miniflap of the trailing edge flap according to any of claims 1 to 4 for improving the aerodynamic properties of an aircraft, wherein the upper surface of the cruise miniflap can be moved downwards.

6. The cruise miniflap of the trailing edge flap according to any of claims 1 to 4 for improving the aerodynamic properties of an aircraft, wherein the lower surface of the cruise miniflap can be moved upwards.

7. The cruise miniflap of the trailing edge flap according to any of claims 1 to 6 for improving the aerodynamic properties of an aircraft, wherein the mechanism intended for moving the cruise miniflap comprising of a control unit to which the cruise miniflap is fixed, the first roller and the rear roller movable along the flap track that is attached to the main frame of the trailing edge flap, the actuating horn of the control unit to which the actuator screw mechanism is fixed and one end of which is, by means of articulations, connected with a reducing gear, and a drive for moving the cruise miniflap, which is connected with the reducing gear and fixed to the main construction of the trailing edge flap, is mounted within a trailing edge flap fairing located outside the trailing edge flap.

Abstract

This invention provides construction variants of a cruise miniflap that is added to the trailing edge flap of an aircraft wing and can be used for improving the aerodynamic properties of an aircraft. In the rear edge of the cruise miniflap, it has a cavity with a height of up to 1% of the wing chord.

a)

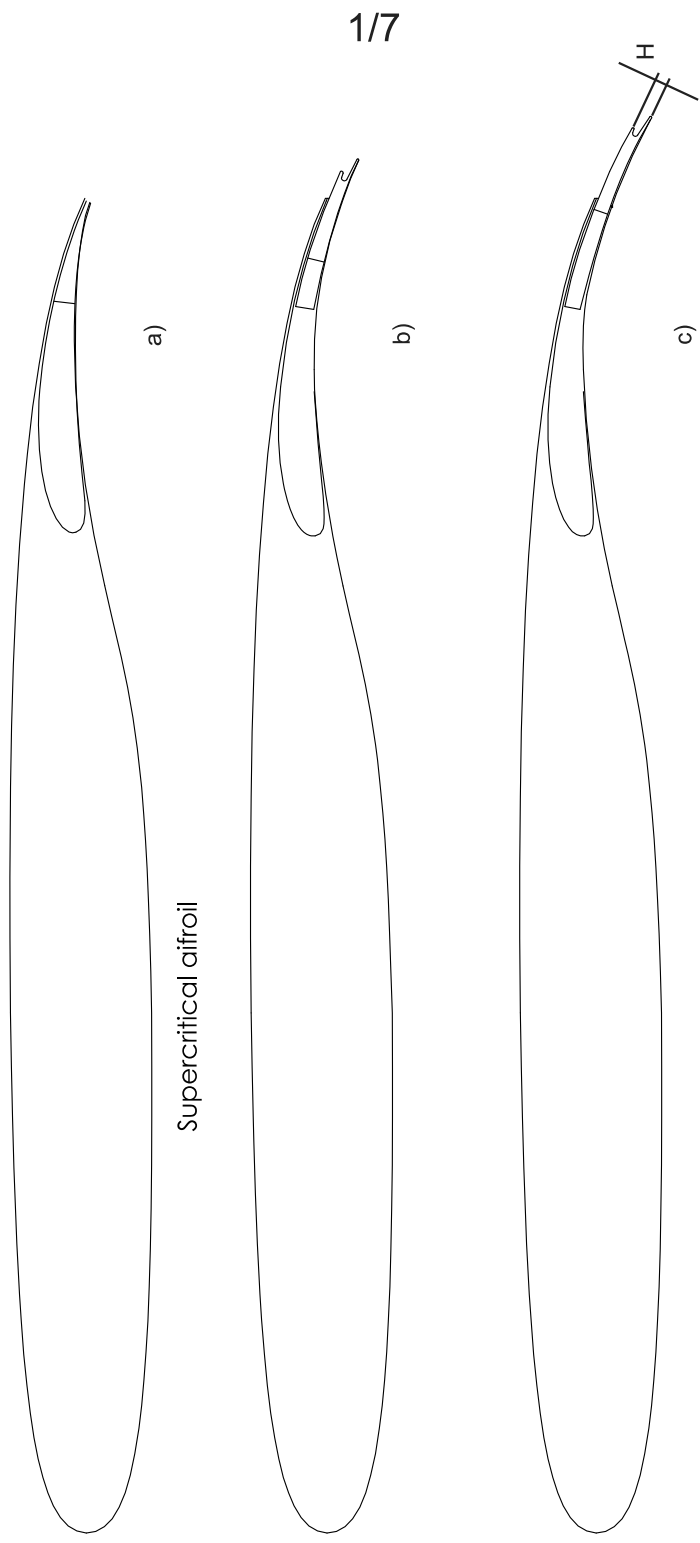Supercritical airfoil
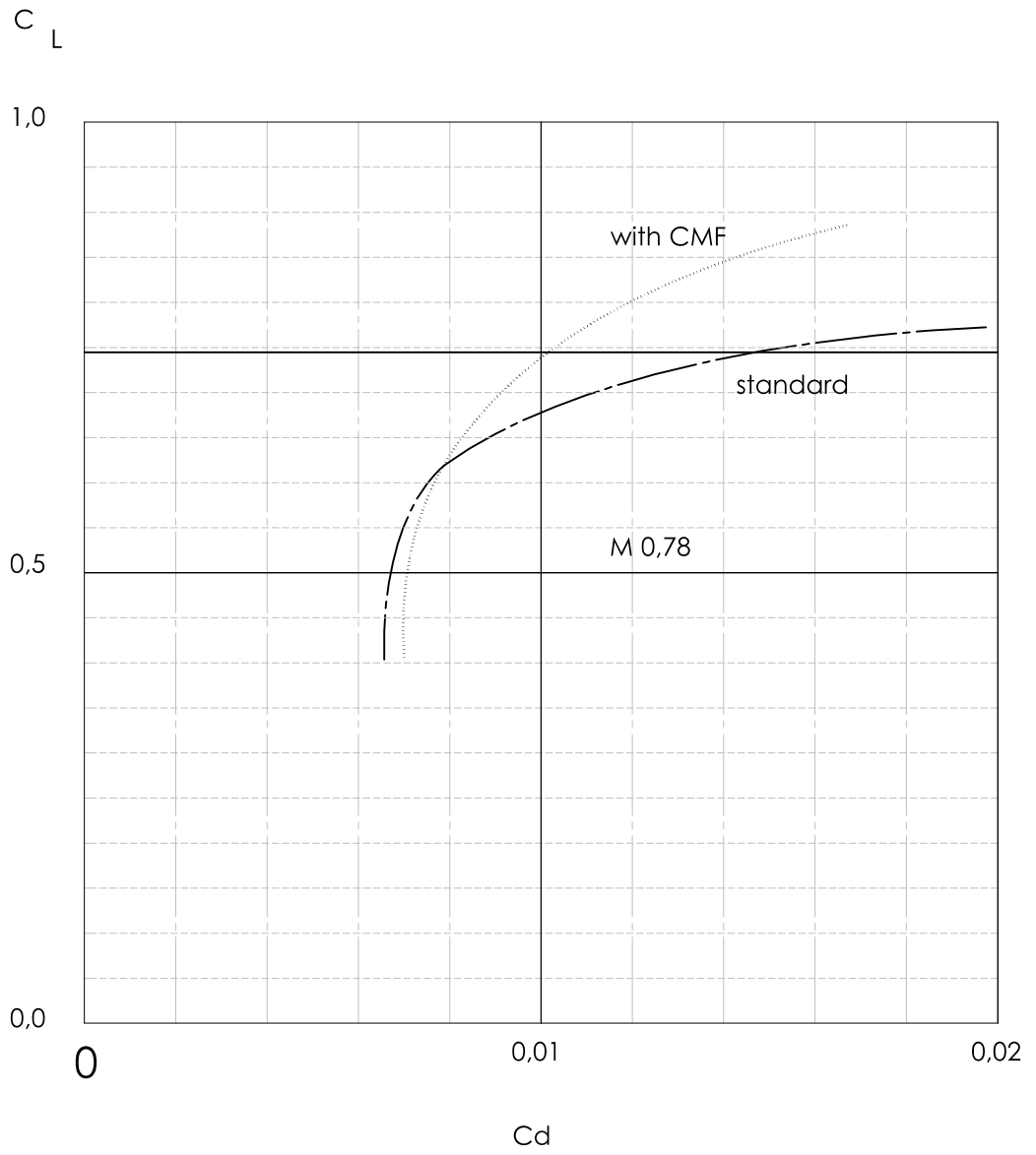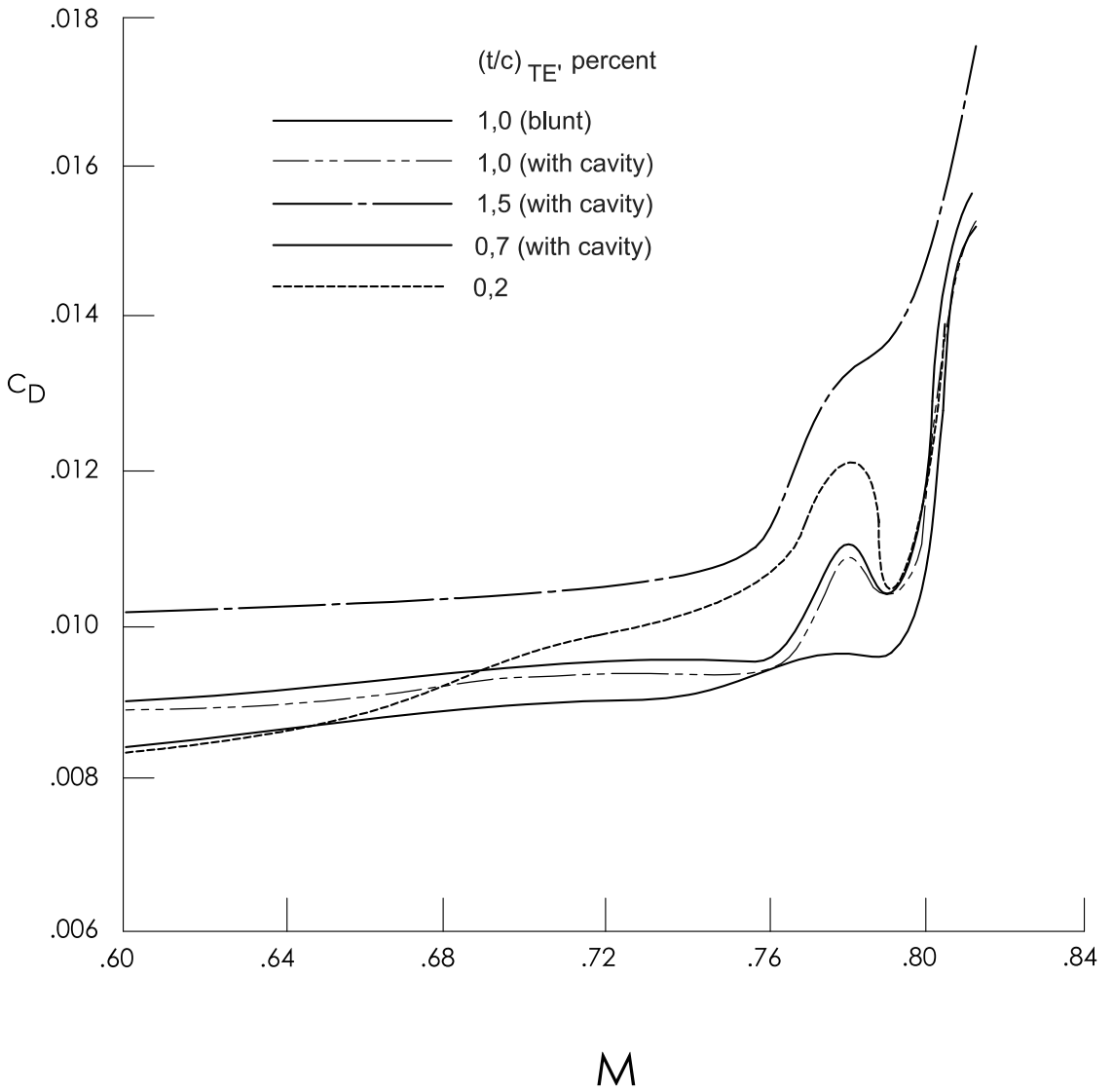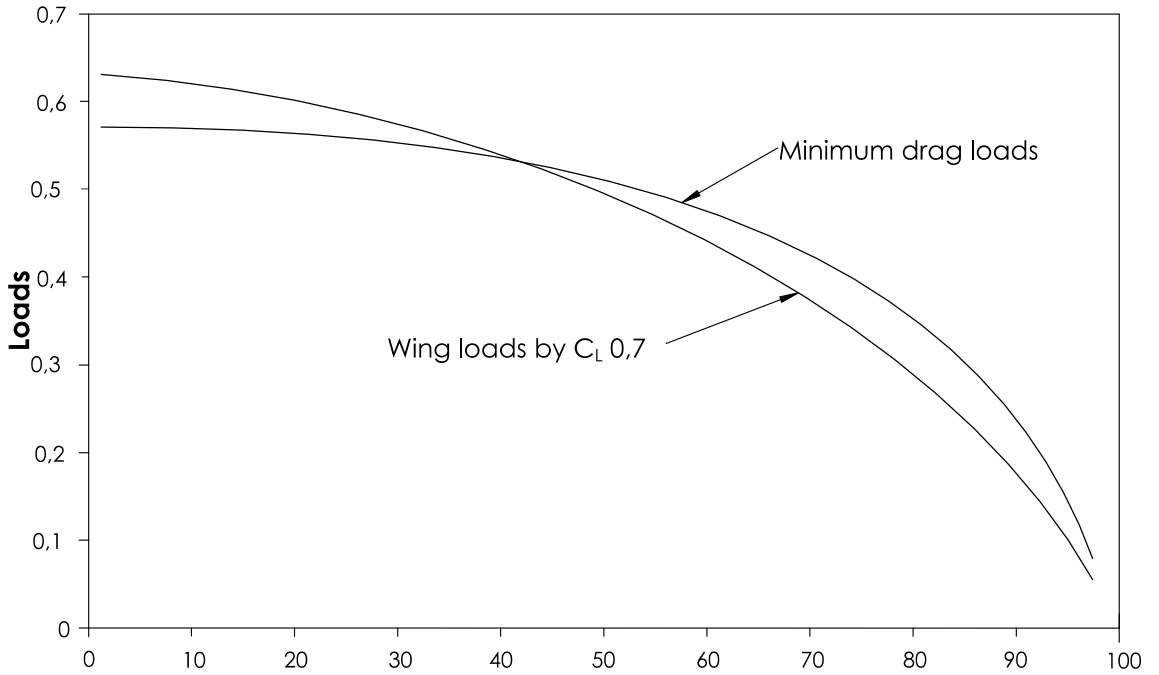
b)

c)

H

Cruise miniflap settings

Fig. 1

Fig. 2

Fig. 3
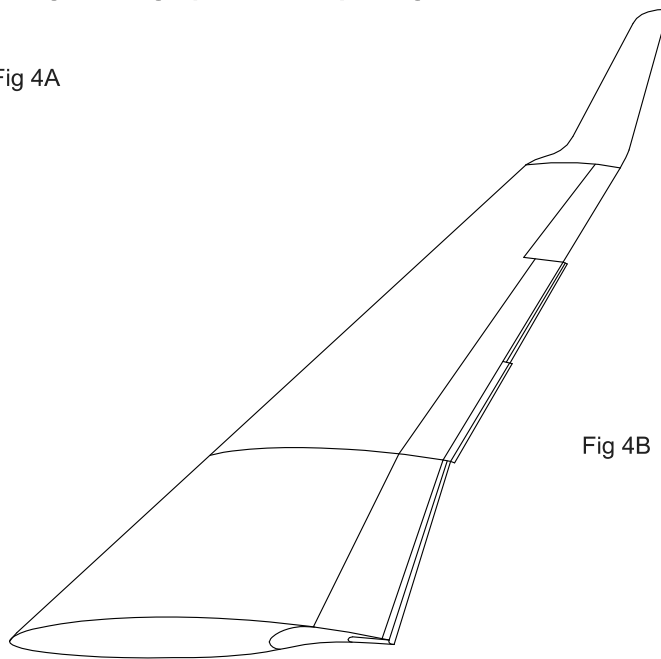
Wing loading optimiztion by using CMF C$_L$ 0,7
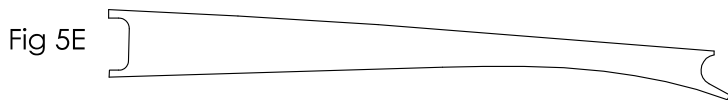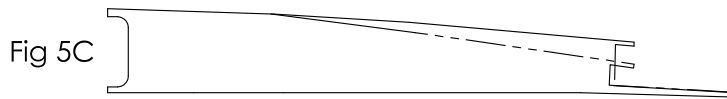
Fig 4A

Fig 4B

Fig. 4

Fig 5A

Fig 5B

Fig 5C

Fig 5D

Fig 5E
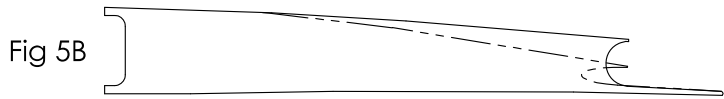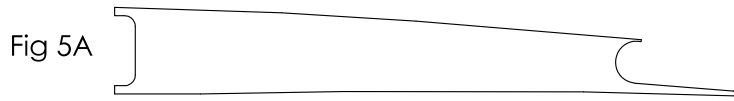
Fig. 5
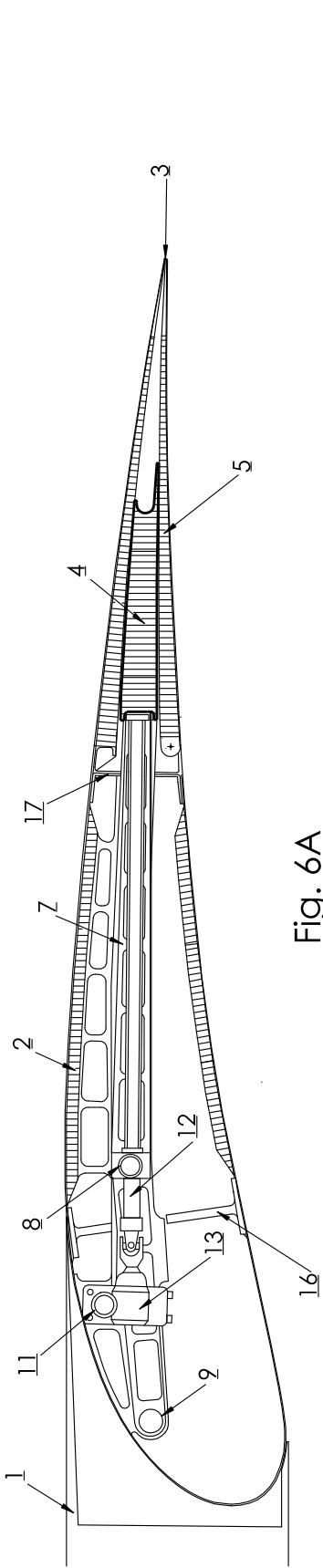
Fig. 6A
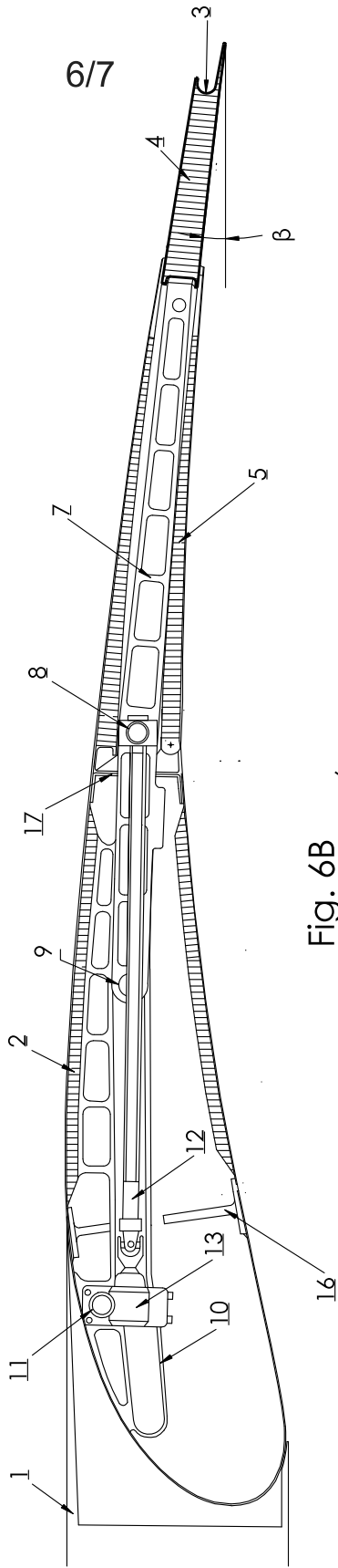
Fig. 6B
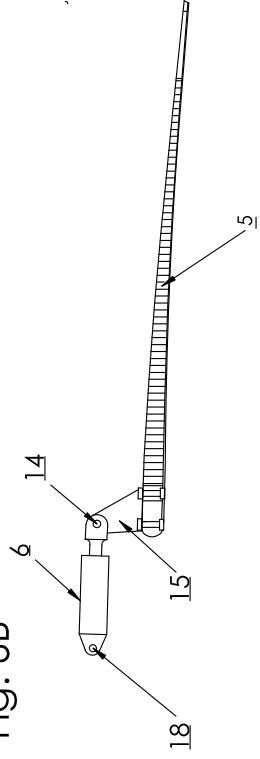
Fig. 6C
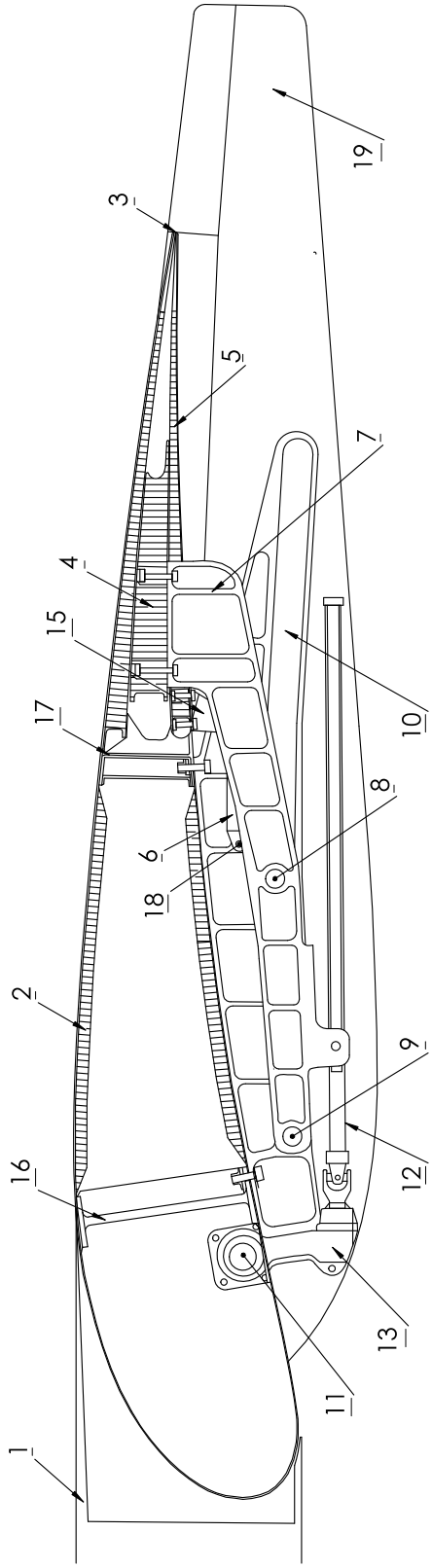
Fig. 7A
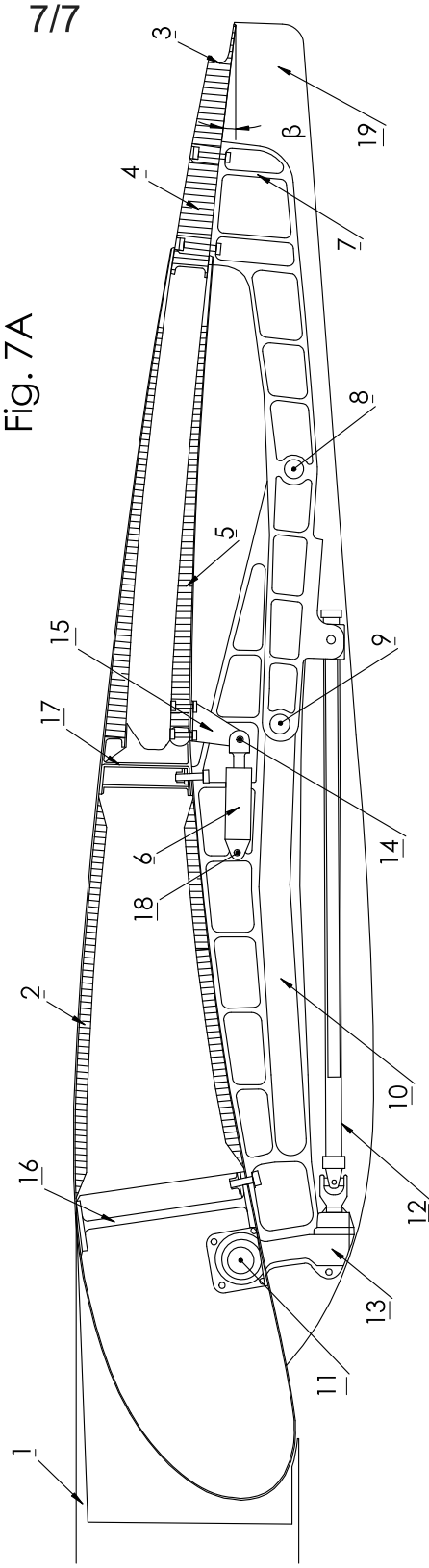
Fig. 7B

Patent II ACTUATING MECHANISM FOR TRAILING EDGE FLAPS AND LEADING EDGE SLATS
Application number: EP17207523.6
Date of receipt: 14 December 2017

Acknowledgement of receipt

We hereby acknowledge receipt of your request for grant of a European patent as follows:

Submission number	5878601

Application number	EP17207523.6

File No. to be used for priority declarations	EP17207523

Date of receipt	14 December 2017

Your reference	529P2 EP

Applicant	TALLINN UNIVERSITY OF TECHNOLOGY

Country	EE

Title	ACTUATING MECHANISM FOR TRAILING EDGE FLAPS AND LEADING EDGE SLATS

Documents submitted	package-data.xml	ep-request.xml
	application-body.xml	ep-request.pdf (4 p.)
	DRAWNONEPO.pdf\529P2 EP drawings final.pdf (10 p.)	SPECNONEPO.pdf\529P2 EP specification final.pdf (12 p.)
	OTHER-1.pdf\Declaration University.pdf (1 p.)	f1002-1.pdf (1 p.)
	feesheetint.pdf (1 p.)	

Submitted by	CN=Margus Sarap 17390

Method of submission	Online

Date and time receipt generated	14 December 2017, 18:33 (CET)

Message Digest   DE:DB:85:AA:E5:D2:A5:8B:FD:1D:D3:B8:9E:0C:CD:4C:BB:CC:CB:47

Correction by the EPO of errors in debit instructions filed by eOLF
Errors in debit instructions filed by eOLF that are caused by the editing of Form 1038E entries or the continued use of outdated software (all forms) may be corrected automatically by the EPO, leaving the payment date unchanged (see decision T 152/82, OJ EPO 1984, 301 and point 6.3 ff ADA, Supplement to OJ EPO 10/2007).

/European Patent Office/

Request for grant of a European patent

For official use only			
1 Application number:		MKEY	
2 Date of receipt (Rule 35(2) EPC):		DREC	
3 Date of receipt at EPO (Rule 35(4) EPC):		RENA	
4 Date of filing:			

5 Grant of European patent, and examination of the application under Article 94, are hereby requested. ☒

Request for examination in an admissible non-EPO language:

Taotlusele palutakse teha artikli 94 kohane ekspertiis

5.1 The applicant waives his right to be asked whether he wishes to proceed further with the application (Rule 70(2)) ☐

Procedural language: en

Description and/or claims filed in: et

6 Applicant's or representative's reference

529P2 EP

Filing Office: EP

Applicant 1

7-1 Name: TALLINN UNIVERSITY OF TECHNOLOGY

8-1 Address: Ehitajate tee 5
19086 Tallinn
Estonia

10-1 State of residence or of principal place of business: Estonia

14.1 The/Each applicant hereby declares that he is an entity or a natural person under Rule 6(4) EPC. ☒

Representative 1

15-1 Name: SARAP, Mr. Margus

Company: Sarap and Putk Patent Agency

16-1 Address of place of business: Kompanii 1C
51004 Tartu
Estonia

17-1

Telephone: | +3727477058

17-1

Fax: | +3727477059

17-1

E-mail: | patent@patent.ee

Inventor(s)

23   Inventor details filed separately   ☒

24   **Title of invention**

Title of invention: | ACTUATING MECHANISM FOR TRAILING EDGE FLAPS AND LEADING EDGE SLATS

25   **Declaration of priority (Rule 52)**

A declaration of priority is hereby made for the following applications

25.2   This application is a complete translation of the previous application   ☐

25.3   It is not intended to file a (further) declaration of priority   ☐

26   **Reference to a previously filed application**

27   **Divisional application**   ☐

28   **Article 61(1)(b) application**   ☐

29   **Claims**

Number of claims: | 8

29.1   ☒   as attached

29.2   ☐   as in the previously filed application (see Section 26.2)

29.3   ☐   The claims will be filed later

30   **Figures**

It is proposed that the abstract be published together with figure No. | 3

31   **Designation of contracting states**

All the contracting states party to the EPC at the time of filing of the European patent application are deemed to be designated (see Article 79(1)).

32   **Different applicants for different contracting states**

33 Extension/Validation

This application is deemed to be a request to extend the effects of the European patent application and the European patent granted in respect of it to all non-contracting states to the EPC with which extension or validation agreements are in force on the date on which the application is filed. However, the request is deemed withdrawn if the extension fee or the validation fee, whichever is applicable, is not paid within the prescribed time limit.

33.1 It is intended to pay the extension fee(s) for the following state(s):

33.2 It is intended to pay the validation fee(s) for the following state(s):

34 Biological material

38 Nucleotide and amino acid sequences

The European patent application contains a sequence listing as part of the description ☐

The sequence listing is attached in computer-readable format in accordance with WIPO Standard ST.25 ☐

The sequence listing is attached in PDF format ☐

Further indications

39 Additional copies of the documents cited in the European search report are requested

Number of additional sets of copies:

40 Refund of the search fee under to Article 9 of the Rules relating to Fees is requested ☐

Application or publication number of earlier search report:

42 Payment

Method of payment

Not specified

44-A Forms | Details: | System file name:

| A-1 | Request | | as ep-request.pdf |
| A-2 | 1. Designation of inventor | 1. Inventor | as f1002-1.pdf |

44-B Technical documents | Original file name: | System file name:

| B-1 | Specification in admissible non-EPO language | 529P2 EP specification final.pdf 8 claims 10 figure(s) | SPECNONEPO.pdf |
| B-2 | Drawings / Translation of text in drawings | 529P2 EP drawings final.pdf 10 figure(s) | DRAWNONEPO.pdf |

44-C Other documents

Original file name:

System file name:

| C-1 | <other_document> | Declaration University.pdf | OTHER-1.pdf |

45

General authorisation:

46 Signature(s)

Place: **Tartu**

Date: **14 December 2017**

Signed by: **Margus Sarap 17390**

Representative name: **Margus SARAP**

Capacity: **(Representative)**

Form 1002 - 1: Public inventor(s)

Designation of inventor

User reference: 529P2 EP
Application No:

Public

Inventor	
Name:	LAUK, Mr. Peep
Company:	Tallinn University of Technology
Address:	Ehitajate tee 5
	19086 Tallinn
	Estonia
The applicant has acquired the right to the European patent:	As employer

Signature(s)

Place: **Tartu**

Date: **14 December 2017**

Signed by: **Margus Sarap 17390**

Representative name: **Margus SARAP**

Capacity: **(Representative)**

Erklärung von KMU, natürlichen Personen, Organisationen ohne Gewinn-erzielungsabsicht, Hochschulen oder öffentlichen Forschungseinrichtungen für die Zwecke von Gebührenermäßigungen gemäß Regel 6 EPÜ

Declaration for SMEs, natural persons, non-profit organisations, universities and public research organisations for the purpose of fee reductions under Rule 6 EPC

Déclaration à fournir par les PME, les personnes physiques, les organisations sans but lucratif, les universités et les organismes de recherche publics, en vue de l'obtention des réductions de taxe prévues à la règle 6 CBE

Zeichen des Anmelders / Applicant's reference / Référence du(des) demandeur(s)
(max. 15 Zeichen / max. 15 characters / 15 caractères au maximum)

529P2 EP

Anmeldenummer oder, falls noch nicht bekannt, Bezeichnung der Erfindung: / Application No. or, if not yet known, title of the invention: / N° de la demande ou, à défaut, titre de l'invention :

ACTUATING MECHANISM FOR TRAILING EDGE FLAPS AND LEADING EDGE SLATS

Für die Zwecke der Regel 6 EPÜ /
For the purposes of application of Rule 6 EPC, the undersigned/each of the undersigned[1] /
Aux fins de l'application de la règle 6 CBE, le (les) soussigné(s)[1],

TALLINN UNIVERSITY OF TECHNOLOGY
Ehitajate tee 5
Tallinn 19086
ESTONIA

erklärt der Unterzeichnete (erklären die Unterzeichneten)[1]: / declares that he is: / déclare(nt) être :

☒ ein kleines oder mittleres Unternehmen[2] / a small or medium-sized enterprise[2] / une petite ou moyenne entreprise[2],

☐ eine natürliche Person / a natural person / une personne physique,

☐ eine Organisation ohne Gewinnerzielungsabsicht, eine Hochschule oder eine öffentliche Forschungseinrichtung[3] / a non-profit organisation, a university or a public research organisation[3] / une organisation sans but lucratif, une université ou un organisme de recherche public[3]

nach Regel 6 (4) EPÜ zu sein. / as indicated under Rule 6(4) EPC. / au sens de la règle 6(4) CBE.

Im Falle mehrerer Anmelder wird die Gebührenermäßigung nur gewährt, wenn jeder Anmelder eine natürliche oder juristische Person im Sinne der Regel 6 (4) EPÜ ist.[4] / In the case of multiple applicants, each one must be an entity or a natural person under Rule 6(4) EPC for the fee reduction to apply.[4] / En cas de pluralité de demandeurs, la réduction de la taxe n'est accordée que si chaque demandeur est une entité ou une personne physique au sens de la règle 6(4) CBE.[4]

Bestehen begründete Zweifel an der Richtigkeit dieser Erklärung, kann das EPA im Erteilungsverfahren entsprechende Nachweise verlangen. / In the case of reasonable doubt as to the veracity of the present declaration, the EPO may, during the course of the grant procedure, require appropriate evidence. / Si l'Office a des raisons de douter de la véracité de la présente déclaration, il peut, au cours de la procédure de délivrance, inviter le(s) demandeur(s) à produire des preuves.

Sollte sich herausstellen, dass die Erklärung falsche Angaben enthält, so gilt die betreffende zu Unrecht ermäßigte Gebühr als nicht entrichtet, und die Anmeldung gilt gemäß Artikel 78 (2) bzw. Artikel 94 (2) EPÜ als zurückgenommen. / Should it become apparent that an incorrect declaration has been filed, the relevant fee, reduced without good reason, will be deemed not to have been paid and the application will be deemed to be withdrawn according to Article 78(2) or Article 94(2) EPC, as applicable. / S'il s'avère qu'une déclaration incorrecte a été produite, la taxe concernée, dont le montant a été indûment réduit, sera réputée ne pas avoir été acquittée et la demande sera réputée retirée conformément à l'article 78(2) ou, le cas échéant, à l'article 94(2) CBE.

Ort / Place / Lieu

Tartu

Datum / Date

14.12.2017

Unterschrift(en) des (der) Anmelder(s) oder Vertreter(s): / Signature(s) of applicant(s) or representative(s): / Signature(s) du (des) demandeur(s) ou mandataire(s) :

Margus Sarap, European Patent Attorney

Name des (der) Unterzeichneten bitte in Druckschrift wiederholen. Bei juristischen Personen bitte außerdem die Stellung des (der) Unterzeichneten innerhalb der Gesellschaft in Druckschrift angeben. / Please print name(s) under signature(s). In the case of legal persons, the position of the signatory within the company should also be printed / La (Les) signature(s) doi(ven)t être suivie(s) du (des) nom(s) en caractères d'imprimerie. S'il s'agit d'une personne morale, la fonction du signataire dans la société doit également être indiquée en caractères d'imprimerie.

bitte wenden / P.T.O. / T.S.V.P.

Internal fee calculation sheet

This sheet has been produced using data entered in Form EP1001E.

Applicant's or representative's reference

529P2 EP

Applicant 1

TALLINN UNIVERSITY OF TECHNOLOGY

Representative 1

SARAP, Mr. Margus

Title of invention:

ACTUATING MECHANISM FOR TRAILING
EDGE FLAPS AND LEADING EDGE SLATS

Fees	Factor applied	Fee schedule	Amount to be paid
001 Filing fee - EP direct - online	0.7	120.00	84.00
002 Fee for a European search - Applications filed on/after 01.07.2005	1	1 300.00	1 300.00
015 Claims fee - For the 16th to the 50th claim	0	235.00	0.00
015e Claims fee - For the 51st and each subsequent claim	0	585.00	0.00
501 Additional filing fee for the 36th and each subsequent page	0	15.00	0.00
Total:		**EUR**	**1 384.00**

Lennukitiiva tagatiibade (trailing edge flaps) ja/või esitiibade (leading edge slats) liigutamise mehhanism

TEHNIKA VALDKOND

Käesolev leiutis on mõeldud lennuki tiibade aerodünaamilise takistuse ja kaalu
5   vähendamiseks. Lisaks võimaldab leiutis lihtsustada esitiibade ja tagatiibade liigutamise mehhanismi ja vähendada õhusõidukite tootmis- ja hoolduskulusid.

TEHNIKATASE

Tänapäeva lennukitel laialt kasutatavad Handly Page ja Krueger tüüpi esitiivad ning Fowler tüüpi tagatiivad on efektiivsed stardi-ja maandumiskiiruse vähendamiseks, kuid
10   on oma ehituselt keerulised ja hooldusmahukad. Lisaks on nimetatud seadmed ka raskemad kui teised esi-ja tagatiiva liigid.

Ameerika patendis number US 1,394,344, Handley Page Ltd, 18.10.1924 on kirjeldatud lennukitiiba ja selle esiservaga parallelselt konsooli külge kinnitatud esitiiba, mis liigub põhitiivast eemale konsooli pööramisel ümber põhitiivas oleva veritkaaltelje.
15   Patendis US 6,015,117, Broadbent, Michael C, 18.01.2000 on kirjeldatud analoogset lennukitiiva esitiiva liigutamise mehhanismi. Patendis number US 5,836,550, Boeing Co, 17.11.1998 on kujutatud lennukitiiva tagatiiva liigutamise mehhanismi, millega tagatiib kinnitatakse lennukitiiva külge.

Patenditaotluses number US2006/0202089, Airbus GmbH, 14.09.2006 on kirjeldatud
20   lennukitiib, mis koosneb põhitiivast ja tagatiivast ning selle liigutamiseks ette nähtud mehhanismist.

LEIUTISE OLEMUS

Käeoleva leiutise eesmärgiks on välja pakkuda selline lennukitiiva tagatiiva ja esitiiva kinnitus ning liigutus mehhanism, mille konstruktsioon oleks lihtsam ning töökindlam,
25   kui senised tuntud tehnilised lahendused. Samuti on eesmärgiks välja pakkuda tagatiiva ning esiserva pöördmehhanism, milles on vähem konstruktsiooni elemente ning mille töötamine oleks sujuvam ning mille kasutamisel paraneks lennuki tiiva aerodünaamika nii tavapärasel lennul, õhkutõusmisel kui ka maandumisel, mis võimaldaks kokku hoida lennukikütust, eriti pikkadel lendudel. Eesmärgid
30   saavutatakse sellise pöördkonsoolide abil lennuki esitiibade ja tagatiibade liigutamise mehhanismiga, mis koosneb pöördkonsoolidest, liugklappidest ning kallutatavatest tiiva esi- ja tagatiibadest, millega on võimalik vähendada tiibade aerodünaamilist

takistust nii õhkutõusul kui ka lennu ajal. Erinevalt US 1,394,344 patendis ja US 6,015,117 toodud esitiibade liigutamise seadmetest on leiutisele vastava pöördkonsooli liigutamise telg mitte vertikaalses asendis vaid kallutatud suure nurga all 50-60 kraadi (vaata Fig.7 ja Fig.8). See võimaldab muuta esitiivad

5 kolmepositsioonilisteks ja suurendada oluliselt nende efektiivsust. Stardiasendis on Handley Page tüüpi esitiivad (vaata Fig.7) kallutatud -12 kuni -20 kraadise nurga alla ja ilma piluta, seetõttu on aerodünaamiline takistus palju väiksem. Lennu ajal on esitiivad sissetõmmatud asendis. Maandumisel on aga esitiivad kallutatud -28kuni -32 kraadise nurga all ning tekkiv pilu suurendab nii tõstejõudu kui ka takistust. Tiiva

10 esiservas kere lähedal saab kasutada pöördkonsoolide liikumisel põhinevaid Kruegeri esitiibu. Erinevalt eeltoodutest ei teki nende kallutamisega märkimisväärseid pilusid esitiiva ja tiiva vahele. Õhutakistuse ja müra vähendamiseks kallutatakse esitiiva all olevat paneeli . Seejuures saab kasutada tiiva esiserva pöördkonsoolide vahele jäävat piirkonda täiendava kütusepaagina kuna puudub vajadus tiivasiseste aktuaatorite

15 järele. Sarnaselt patendis US 5,836,550 toodud seadmele saab antud leiutises toodud pöördkonsoolidega muuta samuti tagatiibade asendit. Erinevalt aga eeltoodud patendis kirjeldatud seadmest , mille tagatiiva liigutamine toimub kahe agregaadi (swivel link ja slaving mechanism) kaudu on antud leiutisel (vaata Fig. 1) üheks põhiosaks integreeritud pöördkonsoolid, mille pöördumisega kaasneb samaaegselt

20 tagatiibade kallutamine. Toimimisprintsiibilt erineb see seade US patendis toodust, sest on lihtsama ehitusega, kergem ning ka töökindlam. US 5,836,550 patendis pole arvestatud tagatiibade külgmise liikumisega kaasnevate pragude/vahede tekkimisega. Vahed tagatiiva ja kaldtüüri vahel vähendavad tõstejõudu ja suurendavad takistust. Antud leiutises sulgeb tagatiibade liikumise käigus tekkiva avause, liugpaneel ning

25 kokkuvõttes tagatiibade pindala, kallutatud asendis, suureneb. US 5,836,550 patendil on probleemiks suur õhutakistus stardil. Õhuvool ,suundudes lennu algfaasis läbi tiiva ja tagatiiva vahelise kanali (Fig.3c), milles asub palju õhutakistust suurendavaid agregaate (Fig. 2), pidurdub ning õhutakistus suureneb. Antud leiutises on antud probleem lahendatud alljärgnevalt. Õhkutõusul (Fig. 3) kui tagatiivad on kallutatud,

30 pöördkonsoolide poolt , +12-+20 kraadise nurga all, kallutatakse samal ajal tiiva tagaserva osa (spoilerid) allapoole, et vältida pilu tekkimist tagatiiva ja spoileri vahele. Nii on võimalik õhkutõusul suurendada lennuki aerodünaamilist väärtust ja vähendada kütusekulu. US 5,836,550 patendis toodud seadmest eristub antud leiutis selgelt üheks terviklikuks seadmeks integreeritud pöördkonsoolide, kallutatava tiiva esi-ja

tagaserva ja liugpaneelide kasutamise poolest. Pöördkonsoolide ehitus ja paigutus võimaldavad loobuda tiiva välimises osas aktuaatorite kasutamisest, sest tagatiibade liigutamiseks vajalik jõud kantakse üle tiiva keskosas olevalt tagatiivalt sarniiri kaudu (Fig. 2). Tulenevalt eeltoodust on antud leiutise aerodünaamiline takistus (drag)
5   väiksem ja aerodünaamiline väärtus (L/D ratio) kõrgem kui eeltoodud US patendil. Erinevalt US 2006/0202089 toodud patendist asuvad antud leiutise liigutusmehhanismid tiiva sees ning ei põhjusta lennu ajal lisatakistust. Olenevalt lennuki lennumassist ja lennukiirusest on pöördkonsoolide abil võimalik muuta tagatiibade asendit, lennu ajal, ka väikeses vahemikus, -2 kuni +4 kraadi.
10   Samaaegselt tagatiibade liigutamisega kaldub ka tiiva tagaserv (spoiler) vastavalt kas üles või allapoole nii, et ei tekiks pilusid. Maandumisel kallutatakse tagatiivad suure nurga +30 kuni +45 kraadise nurga alla. Seejuures tiibade tõstejõu ja takistuse suurendamiseks kallutatakse tiiva tagaserva nii, et tekiks optimaalse kõrgusega pilu tiiva tagaserva ja tagatiiva vahele. Koos tagatiibade liikumisega liigub tagatiiva suhtes
15   teleskooptüüpi liugpaneel (vaata Fig. 6). Tagatiibade kõverjoonelisel liikumisel, liigub liugpaneel vastavalt relsi suunale, juhituna torutala külge kinnitatud kronsteini rullikutest väljalastud asendisse. Pöördkonsoolide abil saab käitada ka kahe või mitmeastmelisi tagatiibasid (Fig. 4). Selleks kasutatakse tagatiiva külge kinnitatud väikest pöördkonsooli , mis omakorda liigutab aft flap-i tahapoole ja kallutab allapoole.
20   Pöördkonsool pöördub võrreldes pöördkonsoolile vastupidises suunas. Kui tagatiibade kasutamise põhiliseks eesmärgiks on tõstejõu/takistuse suhte tõstmine nagu näiteks pika lennukestvusega piloodita õhusõidukitel ja purilennukitel siis saaks kasutada Fig.9 ja Fig.10 toodud ilma piluta tagatiibasid. Selle tagatiivaliigi põhiline aerodünaamiline efekt seisneb tiivapindala suurendamises lennu ajal vahemikus 10-
25   20% ning kallutamises 12 kuni 18 kraadise nurga alla. Tiiva ja tagatiiva vaheline osa on kaetud painduvate paneelidega.

JOONISTE LOETELU

Käesolevat leiutist kirjeldatakse detailsemalt teostusnäitena viidetega joonistele, kus

Joonisel fig 1 on kujutatud lennukitiib ning sellele leiutisele vastava tagatiiva
30   liikumismehhanismi pöördkonsoolid;

Joonisel fig 2 on kujutatud lennuki tiib pealvaates, millel on kujutatud lennukitiiva tagatiiva ja lennukitiiva esitiiva liigutamise mehhanism vastavalt käeolevale leiutisele;

Joonisel fig 3 on kujutatud lennukitiiva tagatiiva erinevad asendid: a) lennuki tavapärasel lennul (cruise), kus tagatiiva kallutusnurk on null kraadi, b) lennuki startimisel (take-off), kus tagatiiva kallutusnurk on kuni 15 kraadi ja c) lennuki maandumisel (landing), kus tagatiiva kallutusnurk on kuni 40 kraadi;

5 Joonisel fig 4 on kujutatud lennuki tagatiiva (flap) ja selle külge pöördkonsoolmehhanismiga kinnitatud lisatagatiiva (aft flap) erinevad asendid: a) lennuki tavapärasel lennul (cruise), kus tagatiiva ja lisatagatiiva kallutusnurk on null kraadi, b) lennuki startimisel (take-off), kus tagatiiva ja lisatagatiiva kallutusnurk on kuni 15 kraadi ning c) lennuki maandumisel (landing), kus tagatiiva kallutusnurk on

10 kuni 40 kraadi ja lisatagatiiva kallutusnurk kuni 60 kraadi;

Joonisel fig 5 on kujutatud lennukitiiva tagatiiva ning lisatagatiiva liigutamise pöördkonsoolmehhanism;

Joonisel fig 6 on kujutatud lennukitiiva tagatiiva 9 suhtes liikuvat teleskooptüüpi liugpaneeli;

15 Joonisel fig 7 on kujutatud Handley Page tüüpi lennukitiiva esitiib erinevates asendites: a) lennuki tavapärasel lennul (cruise), kus esitiiva kaldenurk on null kraadi, b) lennuki startimisel (take-off), kus esitiiva kallutusnurk on kuni 16 kraadi, c) lennuki maandumisel (landing), kus esitiiva kallutusnurk on kuni 32 kraadi;

Joonisel fig 8 on kujutatud lennuki tiiva külge kinnitatud Kruegeri tüüpi esitiib, kus

20 õhutakistuse ja müra vähendamiseks on esitiib altpoolt suletud paneeliga, erinevad asendid: a) lennuki tavapärasel lennul (cruise), kus esitiiva kaldenurk on null kraadi, b) lennuki startimisel (take-off), kus esitiiva kallutusnurk on kuni -14 kraadi, c) lennuki maandumisel (landing), kus esitiiva kallutusnurk on kuni- 28 kraadi;

Joonisel fig 9 on kujutatud lennukitiib ilma piluta tagatiivaga, mida saab kasutada (ka

25 piloodita) õhusõidukitel ja purilennukitel, milles kasutatud pöördkonsoolid on omavahel ühendatud torutõukuritega ja liugpaneel asub tagatiiva kerepoolses otsas;

Joonisel fig 10 on kujutatud eeltoodud joonise külgvaate, erinevad asendid, kus a) tagatiib on sissetõmmatud asendis, kus kallutusnurk on null kraadi, b) tagatiib on väljalastud asendis, kus kallutusnurk on kuni 15 kraadi.

30 TEOSTUSNÄIDE

Lennuki tiib koosneb tavapäraselt lennukitiiva põhikonstruktsioonist ning selle küljes olevatest tagatiibadest. Suurematele lennukitel on lisatud lennukitiiva

põhikonstruktsioonile lennukitiiva liikuv esitiib, et tagada sujuvamat lennukitiiva aerodünaamikat lennuki õhkutõusmisel, lendamisel ning maandumisel. Joonisel fig 2 on kujutatud lennukitiiba, millele on olemas nii tagatiivad 9, kui liigutatav lennukitiiva esitiib 21, 23. Tagatiibade 9 liigutamine toimub tagatiibade liigutamise mootori 1 abil, millega pannakse pöörlema kruvimehhanism 2, mille abil pööratakse kronsteini 3 kaudu lennukitiiva tagatiiva liigutamise mehhanismi pöördkonsooli 4 (vaata joonis fig 2). Pöördkonsool omakorda liigutab šarniiri 5 kaudu tiiva konsoolile kinnitatud tagatiiba 9 vastavalt lennu suunas tahapoole või ettepoole. Tagatiibade sümmeetrilise liikumise tagab kruvimehhanismi 2 pöörav toru, mis ulatub läbi lennuki kere teise lennuki tagatiivani, millele on omakorda kinnitatud vastupidise keermega kruvimehhanism. Pöördkonsool on tagatiiva külge kinnitatud kardaanmehhanismiga, mis vastavalt pöördkonsooli pööramisega kallutab tagatiiba (vaata Fig. 3 ja Fig. 4).

Pöördkonsooli telg α on kallutatud vertikaalsuunast tahapoole kuni 12° kraadi (vaata joonis Fig. 3, tahapoole kallutamine tähendab siinkohal telje α kallet lennuki tiiva tagaserva poole või üldisemalt kallet lennuki saba poole). Pöördkonsooli 4 pööramisel kuni 39,7 kraadi (vaata joonised Fig. 2 ja Fig. 3) pöörab samal ajal tagatiib telje y ümber kuni 30 kraadi tagatiiva kaldenurgani kuni + 40 kraadi .

β ja y telg on omavahel 90 kraadise nurga all (vaata joonis Fig 5). Tagatiibade liikumisega kaasneb liugpaneeli 8 liikumine tagatiiva suhtes külje peale. Liugpaneeli profiil sarnaneb tagatiiva 9 profiiliga (Fig.6). Tema liikumine on juhitud torutala 12 poolt, mis asub rullikute 13 vahel. Liugpaneeli juhtimine toimub tõukuri 15 kaudu, mis omakorda on ühendatud torutalaga kronsteini 14 ja tiivaga läbi pöördliigendite 16 ja 17 (vaata joonis fig 9). Stardiasendis on tagatiiva kaldenurk aerodünaamilise takistuse vähendamiseks väiksem (+15kraadi) ja ilma piluta lennukitiiva põhikonstruktsiooni ja tagatiiva vahel. Selleks kallutatakse tagatiiva peal olevat spoilerit 6 allapoole (Fig. 2) vastu tagatiiva pealmist pinda. Lisaks joonisel toodud kolmele asendile reguleeritakse tagatiibade asendit lennu ajal vastavalt lennumassile ja lennukiirusele vahemikus — 2 kraadi kuni + 4 kraadi. Samaaegselt kalduvad tiiva peal olevad spoilerid vastavalt kas üles- või allapoole. Pöördkonsoole on võimalik kasutada kahe või rohkema astmeliste tagatiibade liigutamiseks. Lisaks peamisele tagatiivale on joonisel Fig.4 näha viimase külge kinnitatud pöördkonsoolidega liigutatav aft flap 10. Selle liigutamine toimub väikese pöördkonsooli 11 abil vastassuunas pöördkonsoolile 4. Aft flapi maksimaalne kaldenurk on +15 kuni +25 kraadi.

Pöördkonsoolide abil toimub samuti lennukitiiva esitiibade juhtimine (vaata joonised Fig 7 ja 8). Esitiibade liigutamise mootoriga 18, mis paneb pöörlema kruvimehhanismi 19, liigutatakse omakorda pöördkonsoole 20 (vaata joonis Fig 2). Kruvimehhanism ulatub läbi kere teise tiivakonsoolini, mille kruvimehhanism on vastupidise keermega.

5   Sellega tagatakse lennukitiiva esitiibade sümmeetriline liikumine. Lennukitiiva esitiibade pöördkonsoolide pöördetelg a on kallutatud vertikaalsuunast 50 kuni 60 kraadi ettepoole (lennuki esiotsa poole) ning see võimaldab kasutada kolmepositsioonilisi lennukitiiva esitiibasid. Fig.8 on kujutatud ilma piluta Krueger tüüpi lennukitiiva esitiivad 23, mis asuvad tiiva kerepoolses osas. Pöördkonsooli 20, mis

10   asub kronsteini 22 vahel, pööramisel ümber pöördtelje a, liigub esitiib 23 ettepoole-alla ja pöörab samal ajal kardaanmehhanismi 25 kaudu, tervet lennukitiiva esitiiba 21 ja 23. Õhutakistuse ja müra vähendamiseks on Kruegeri esitiib altpoolt suletud paneeliga 26. Ülejäänud esitiivad 21 on stardiasendis (joonis Fig.7) ilma piluta lennukitiiva esitiiva (joonis Fig 7 b)) ja lennukitiiva põhikonstruktsiooni vahel, maandumisasendis aga

15   piluga (joonis Fig 7 c)) ning ilma alumise kattepaneelita. Lennukitiiva esitiibade pööramine toimub samal põhimõttel nagu eelnevalt kirjeldatud tagatiiva liigutamise mehhanismil aga suurema nurga võrra.

Fig 9 ja 10 kujutatud tagatiibade juhtimine toimub alljärgnevalt. Pöördtoru 28 poolt liigutatakse tiiva 16 sees oleva tõukuri 29 poolt pöördkonsooli 4. Sarnaselt eeltoodutele

20   kaldub tagatiib pöörkonsoolide liikumise ajal. Erinevalt Fig. 2 toodud ehitusskeemist on Fig.9 esitatud pöördkonsoolid 4 omavahel ühendatud torutõukuritega 15 ja liugpaneel 8 asub tagatiiva kerepoolses otsas. Vastavalt tagatiiva liigutamisele painduvad tiiva küljes olevad painduvad paneelid 27, mis aitavad ära hoida pilude tekke. Koos tagatiibade liikumisega liigub ka liugpaneel 8 pikisuunaliselt tagatiiva

25   suhtes. Liugpaneeli tala 12 saab liikuda rullikute 13 vahel. Liugpaneeli juhitakse relsi 14 poolt, mille üks pool on võlli kaudu ühendatud liugpaneeli talaga 12 ja teine pool saab vabalt liikuda juhtrullikute 17 vahel.

Vaadeldav leiutis, mis koosneb pöördkonsoolidest, liugklappidest ning kallutatavast lennukitiiva tagatiivast ja/või esitiivast, võimaldab vähendada tiibade aerodünaamilist

30   takistust nii õhkutõusul kui ka lennu ajal. Leiutisele vastava pöördkonsooli liigutamise telg ei ole mitte vertikaalses asendis nagu senituntud konstruktsioonides, vaid kallutatud suure nurga all 50-60 kraadi (Fig.7 ja Fig.8). See võimaldab muuta lennukitiiva esitiivad kolmepositsioonilisteks ja suurendada oluliselt nende efektiivsust. Stardiasendis on Handley Page tüüpi lennukitiiva esitiivad (Fig.7) kallutatud -12 kuni -

20 kraadise nurga alla ja ilma piluta seetõttu on ka aerodünaamiline takistus väiksem. Lennu ajal on esitiivad sissetõmmatud asendis. Maandumisel on aga lennukitiiva esitiivad kallutatud -28 kuni -32 kraadise nurga all ning tekkiv pilu suurendab nii tõstejõudu kui ka takistust. Lennukitiiva esiservas kere lähedal saab kasutada

5 pöördkonsoolide liikumisel põhinevaid Kruegeri lennukitiiva esitiibasid. Erinevalt eeltoodutest ei teki nende kallutamisega märkimisväärseid pilusid lennukitiiva esitiiva ja lennukitiiva põhikonstruktsiooni vahele. Õhutakistuse ja müra vähendamiseks kallutatakse lennukitiiva esitiiva all olevat paneeli 26. Seejuures saab kasutada lennukitiiva esitiiva pöördkonsoolide vahele jäävat piirkonda täiendava kütusepaagina,

10 kuna puudub vajadus tiivasiseste aktuaatorite järele. Käesolevas leiutises kirjeldatud pöördkonsoolidega saab muuta ka tagatiibade asendit. Erinevalt aga varasemalt kirjeldatud lahendustest, kus tagatiiva liigutamine toimub kahe agregaadi (swivel link 50 ja slaving mechanism 35) kaudu on käesolevale leiutisele vastaval tehnilisel lahendusel (Fig. 1) üheks põhiosaks integreeritud pöördkonsoolid 4, mille

15 pöördumisega kaasneb samuti tagatiibade 9 kallutamine. Toimimisprintsiibilt on see võrreldes varasemate lahendustega lihtsama ehitusega, kergem ning ka töökindlam. Lahendatud on tagatiibade külgmise liikumisega kaasnevate pragude/vahede tekkimisega kaasnevad konstruktsiooni erinevused. Vahed tagatiiva ja kaldtüüri vahel vähendavad tõstejõudu ja suurendavad takistust. Antud leiutises sulgeb tagatiibade

20 liikumise käigus tekkiva avause, liugpaneeli 8 ning kokkuvõttes tagatiibade pindala suureneb, kallutatud asendis. Õhuvool, suundudes lennu algfaasis läbi lennukitiiva põhikonstruktsiooni ja tagatiiva vahelise kanali (Fig.1c-3), milles asub palju õhutakistust suurendavaid agregaate (Fig. 2 60, 63, 35, 50), pidurdub ning õhutakistus suureneb. Käesolevas leiutises on see probleem lahendatud alljärgnevalt. Õhkutõusul

25 (Fig. 3) kui tagatiivad 9 on kallutatud, pöördkonsoolide poolt 4 , +12 kuni+20 kraadise nurga all, kallutatakse samal ajal tiiva tagaserva osa 6 (spoilerid) allapoole, et vältida pilu tekkimist tagatiiva ja spoileri vahele. Nii on võimalik õhkutõusul suurendada lennuki aerodünaamilist väärtust ja vähendada kütusekulu. Leiutis eristub tehnika tasemest selgelt üheks terviklikuks seadmeks integreeritud pöördkonsoolide,

30 lennukitiiva kallutatava tagatiiva ja/või lennukitiiva esitiiva ning liugpaneelide kasutamise poolest. Pöördkonsoolide ehitus ja paigutus võimaldavad loobuda lennukitiiva välimises osas aktuaatorite kasutamisest, sest tagatiibade liigutamiseks vajalik jõud kantakse üle lennukitiiva keskosas olevalt tagatiivalt sarniiri 5 kaudu (Fig. 2). Tulenevalt eeltoodust on antud leiutise aerodünaamiline takistus väiksem ja

aerodünaamiline väärtus kõrgem. Liigutusmehhanismid asuvad lennukitiiva sees ning ei põhjusta lennu ajal lisatakistust. Olenevalt lennuki lennumassist ja lennukiirusest on pöördkonsoolide abil võimalik muuta tagatiibade asendit, lennu ajal, ka väikeses vahemikus, -2 kuni+4 kraadi. Samaaegselt tagatiibade liigutamisega kaldub lennukitiiva tagaserv (spoiler) vastavalt kas üles või allapoole nii, et ei tekiks pilusid. Maandumisel kallutatakse tagatiivad suure nurga +30 kuni+45 kraadise nurga alla. Seejuures lennukitiibade tõstejõu ja takistuse suurendamiseks kallutatakse lennukitiiva tagaserva nii, et tekiks optimaalse kõrgusega pilu lennukitiiva põhikonstruktsiooni tagaserva ja tagatiiva vahele. Koos tagatiibade liikumisega liigub tagatiiva 9 suhtes teleskooptüüpi liugpaneel 8 (Fig. 6). Tagatiibade kõverjoonelisel liikumisel, liigub liugpaneel vastavalt relsi 14 suunale, juhituna torutala 12 külge kinnitatud kronsteini rullikutest 17 väljalastud asendisse. Pöördkonsoolide abil saab käitada ka kahe või mitmeastmelisi tagatiibasid (Fig. 4). Selleks kasutatakse tagatiiva 9 külge kinnitatud väikest pöördkonsooli 11, mis omakorda liigutab aft flap-i tahapoole ja kallutab allapoole. Pöördkonsool 11 pöördub võrreldes pöördkonsoolile 4 vastupidises suunas. Kui tagatiibade kasutamise põhiliseks eesmärgiks on tõstejõu/takistuse suhte tõstmine nagu näiteks pika lennukestvusega (piloodita) õhusõidukitel ja purilennukitel siis saaks kasutada Fig.9 ja Fig.10 toodud ilma piluta tagatiibasid. Selle tagatiivaliigi põhiline aerodünaamiline efekt seisneb tiivapindala suurendamises lennu ajal vahemikus 10-20% ning kallutamises 12-18 kraadise nurga alla. Tiiva ja tagatiiva vaheline osa on kaetud painduvate paneelidega 27.

Lihtsama ehituse tõttu on vaadeldavad seadmed kasutatavad alates suurtest UAV-dest ja purilennukitest kuni suurimate kommertslennukiteni. Antud seadmete tootmiskulud võivad olla kuni kaks korda väiksemad ning hoolduskulud kaks kuni neli korda väiksemad kui hetkel kasutatavatel seadmetel. Nende seadmete kasutamine võimaldab säästa lennukikütust, ning hoida sellega oluliselt kokku õhusõiduki opereerimiskulusid. Samuti on lennukitiiva esiservade ja tagatiibade mass oluliselt väiksem kui hetkel kasutusel olevatel seadmetel.

Reference symbols:

1.) Tagatiibade liigutamise mootor

2.) Tagatiibade liigutamise kruvimehhanism

3.) Pöördkonsooli kronstein

4.) Tagatiibade liigutamise pöördkonsool

5.) Tagatiibadevaheline šarniir

6.) Spoilerid

7.) Kaldtüür

8.) Lennukitiiva liugpaneel

5   9.) Tagatiivad

10.)   Aft flap

11.)   Aft flap-i pöördkonsool

12.)   Liugpaneeli tala

13.)   Liugpaneeli tala juhtrullikud

10   14.)   Liugpaneeli juhtkonsool

15.)   Pöörkonsoolidevaheline tõukur

16.)   Lennukitiib

17.)   Juhtkonsooli rullikud

18.)   Esiservade liigutamise mootor

15   19.)   Esiservade liigutamise kruvimehhanism

20.)   Esiservade liigutamise pöördkonsoolid

21.)   Handley Page tüüpi esitiib

22.)   Esitiibade pöörkonsoolide kinnituskronsteinid

23.)   Krueger tüüpi esitiib

20   24.)   Pöördkonsooli esitiiva kinnituskronstein

25.)   Pöördkonsooli y-telje ümber pöörduv osa

26.)   Esitiiva all olev kallutatav paneel

27.)   Lennukitiiva tagaserva painduv paneel

28.)   Pöördtoru tagatiiva liigutamiseks

25   29.)   Pöördkonsooli tõukur

30.)   Lennukitiiva esimene tala

31.)   Lennukitiiva tagumine tala

Patendinõudlus

1. Lennukitiiva tagatiiva ja/või esitiiva liigutamise mehhanism, mis sisaldab lennukitiiva tagatiiva ja/või esitiiva liigutamise pöördkonsoole (4, 20), mille külge on kinnitatud vastavalt kallutatav lennukitiiva taga- või esitiib, lennukitiiva liugpaneel, lisaks hõlmab

5   lennukitiiva tagatiiva ja/või esitiiva liigutamise mehhanism tagatiibade ja/või esitiibade liigutamise mootorit ning lennukitiiva tagatiibade ja/või esitiibade liigutamise kruvimehhanismi, mis **erineb** selle poolest, et tagatiiva pöördkonsooli telg α on kallutatud vertikaalsuunast tahapoole kuni 12 kraadi, kusjuures pöördkonsooli pööramisel kuni 39,7 kraadi on tagatiib pöörduv telje y ümber kuni 30 kraadi tagatiiva

10   kaldenurgani kuni + 40 kraadi, kusjuures β ja y telg on omavahel 90 kraadise nurga all.

2. Lennukitiiva tagatiiva ja/või esitiiva liigutamise mehhanism vastavalt punktile 1, kusjuures esitiiva pöördkonsooli liigutamise telg on kallutatud vertikaalsest asendist välja ettepoole nurga all 50 kuni 60 kraadi, kusjuures esitiib on kallutatud lennuki

15   õhkutõusmisel -12 kuni -20 kraadise nurga alla, ning lennuki maandumisel on esitiib kallutatud -28 kuni -32 kraadise nurga all..

3. Lennukitiiva tagatiiva ja/või esitiiva liigutamise mehhanism vastavalt punktile 1, kusjuures tiiva esiservas kere lähedal on kasutatud pöördkonsoolide liikumisel põhinevaid Kruegeri esitiibasid.

20   4. Lennukitiiva tagatiiva ja/või esitiiva liigutamise mehhanism vastavalt punktile 3, kusjuures koos tagatiibade liikumisega on kaasnev liugpaneeli (8) liikumine tagatiiva suhtes külje peale, kusjuures liugpaneeli profiil on sarnane tagatiiva profiiliga.

5. Lennukitiiva tagatiiva ja/või esitiiva liigutamise mehhanism vastavalt punktile 4, kusjuures liugpaneeli liikumine on juhitud torutalaga (12), mis on paiknev rullikute (13)

25   vahel, tõukuri (15) kaudu, mis omakorda on ühendatud torutalaga kronsteini (14) ja tiivaga läbi pöördliigendite (16, 17).

6. Lennukitiiva tagatiiva ja/või esitiiva liigutamise mehhanism vastavalt punktile 5, kusjuures stardiasendis on tagatiiva kaldenurk aerodünaamilise takistuse vähendamiseks väiksem kuni +15kraadi ja ilma piluta lennukitiiva põhikonstruktsiooni

30   ja tagatiiva vahel.

7. Lennukitiiva tagatiiva ja/või esitiiva liigutamise mehhanism vastavalt punktile 5, kusjuures tagatiibade asend on reguleeritav lennu ajal vastavalt lennumassile ja lennukiirusele vahemikus — 2 kraadi kuni + 4 kraadi.

8. Lennukitiiva tagatiiva ja/või esitiiva liigutamise mehhanism vastavalt punktile 5, kusjuures peamisele tagatiivale on külge kinnitatud pöördkonsoolidega liigutatav aft flap (10), kusjuures aft flap on liigutatav väikese pöördkonsooli (11) abil vastassuunas tagatiiva pöördkonsoolile (4).

Lühikokkuvõte

Lihtsama ehituse tõttu on vaadeldavad seadmed töökindlamad ning kasutatavad alates suurtest UAV-dest ja purilennukitest kuni suurimate kommertslennukiteni. Antud seadmete tootmiskulud võivad olla kuni kaks korda väiksemad ning hoolduskulud kaks kuni neli korda väiksemad kui hetkel kasutatavatel seadmetel. Nende seadmete kasutamisel on võimalik säästa lennukikütust, ning hoida sellega oluliselt kokku õhusõiduki opereerimiskulusid. Samuti on esi-ja tagatiibade mass oluliselt väiksem kui hetkel kasutusel olevatel seadmetel.

FIG 1

FIG 2
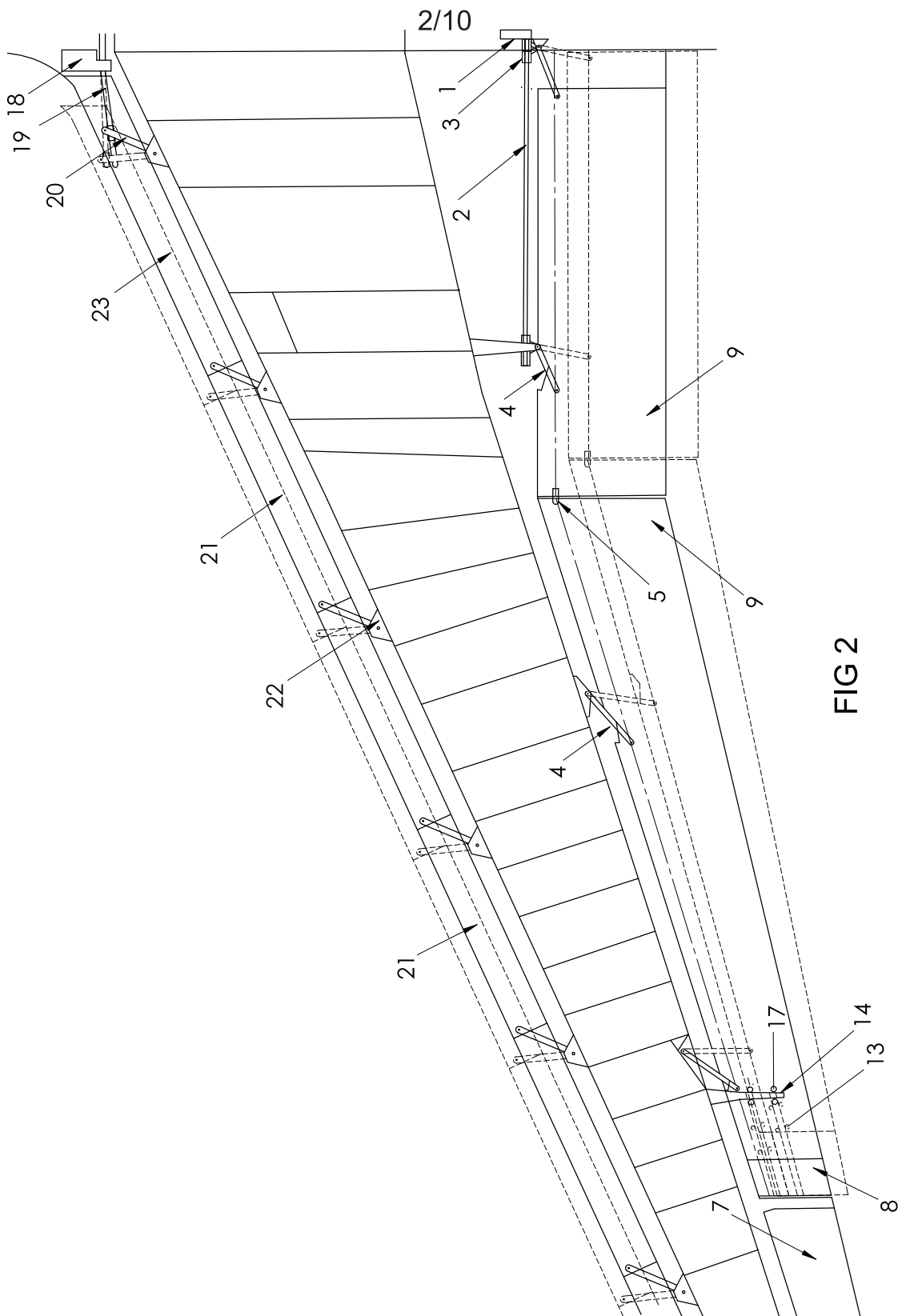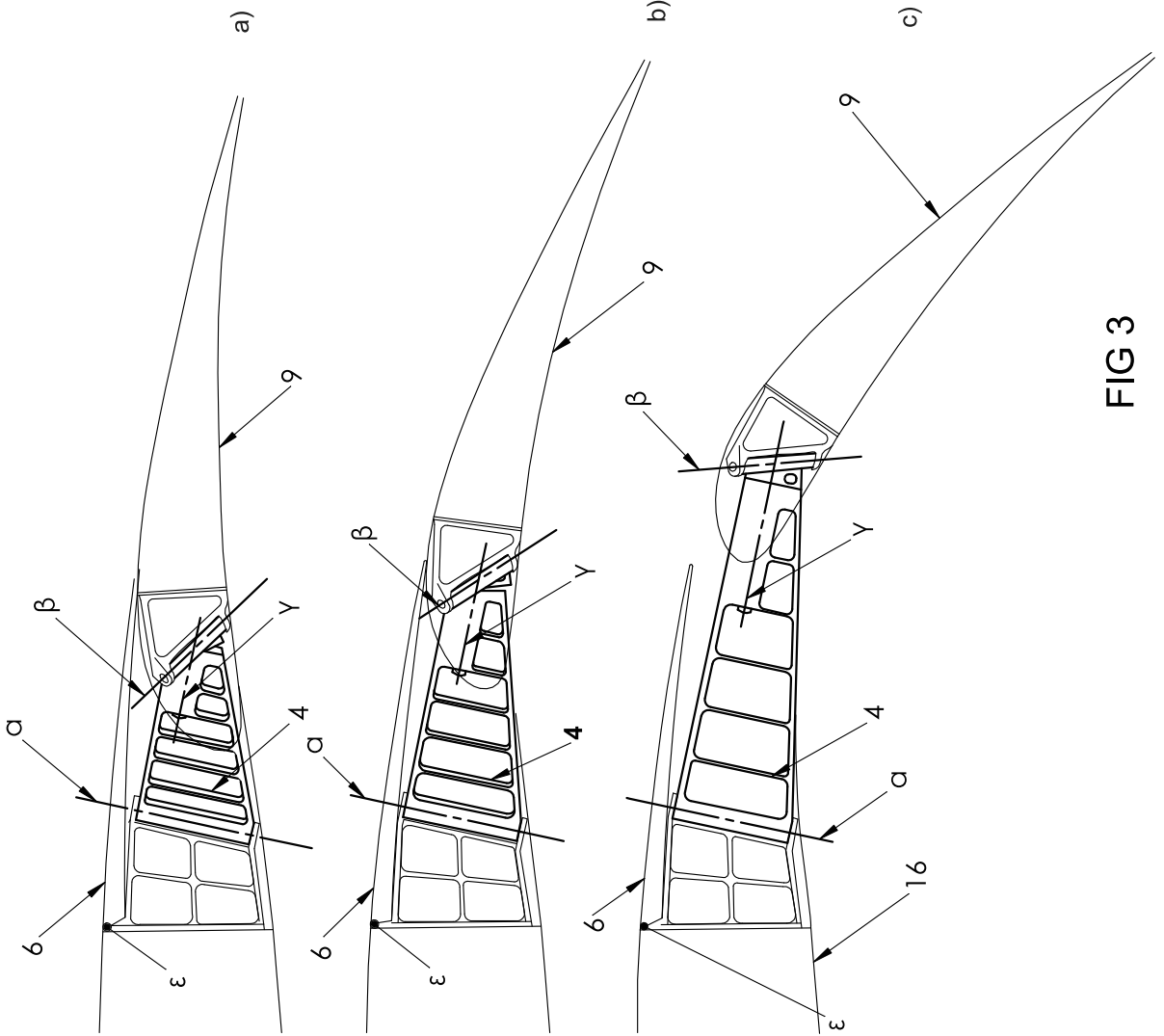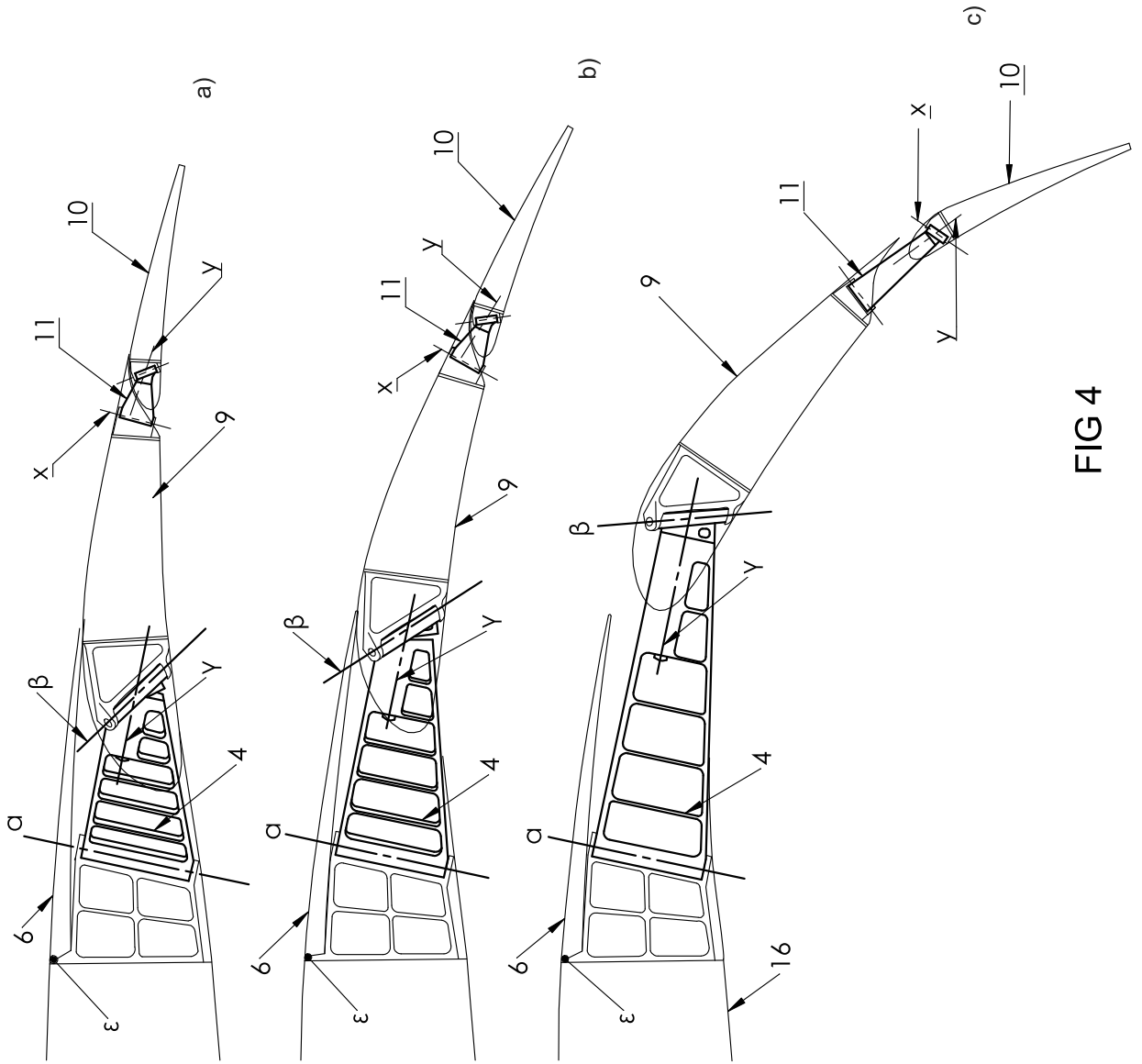
FIG 3

FIG 4

α

4

6

β

γ

FIG 5

14

17

13

12

9

8

FIG 6

a)

b)

c)

FIG 7

a)

β

Y

23

α

22

20

25

24

26

x

b)

α

22

23

20

β

Y

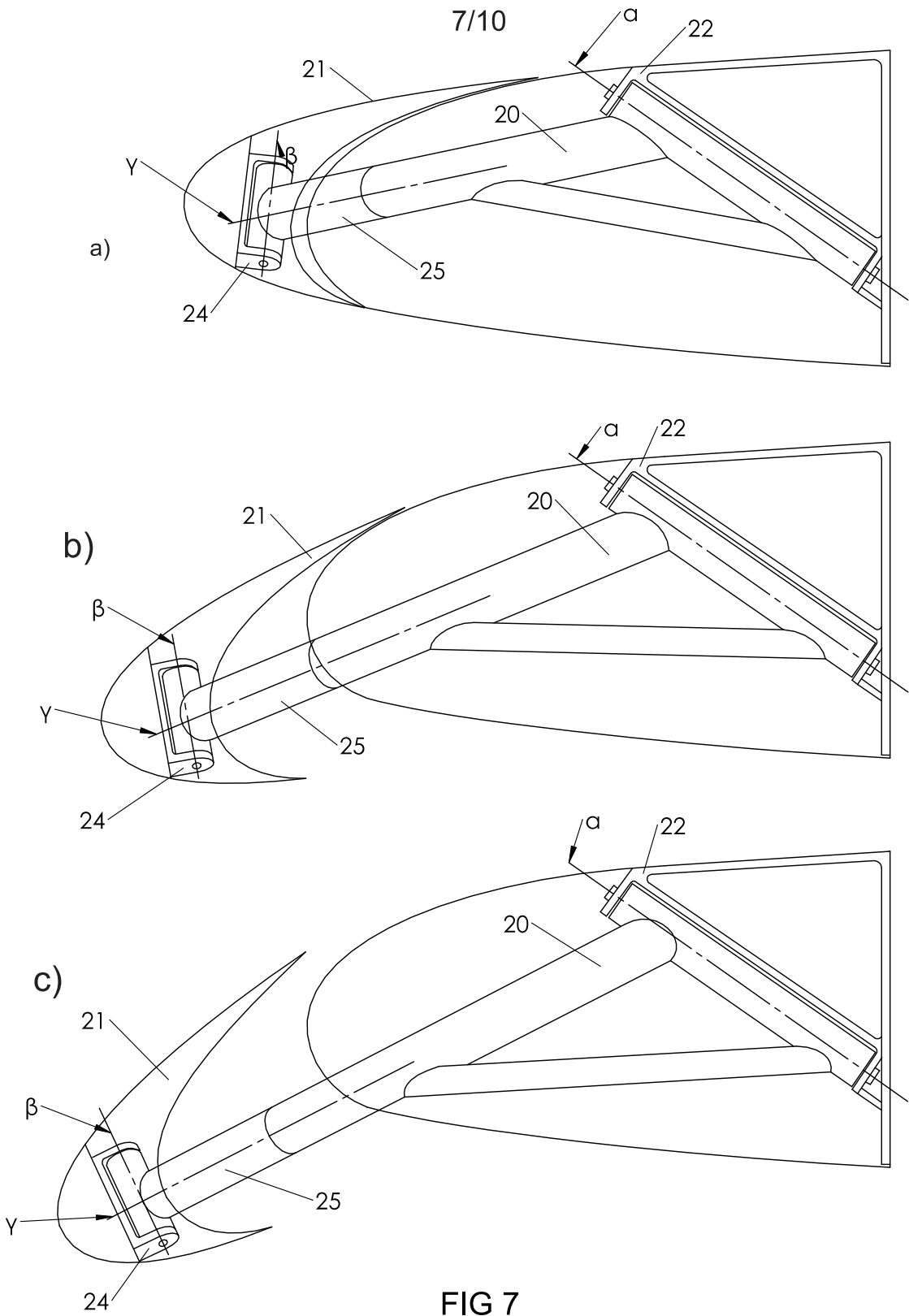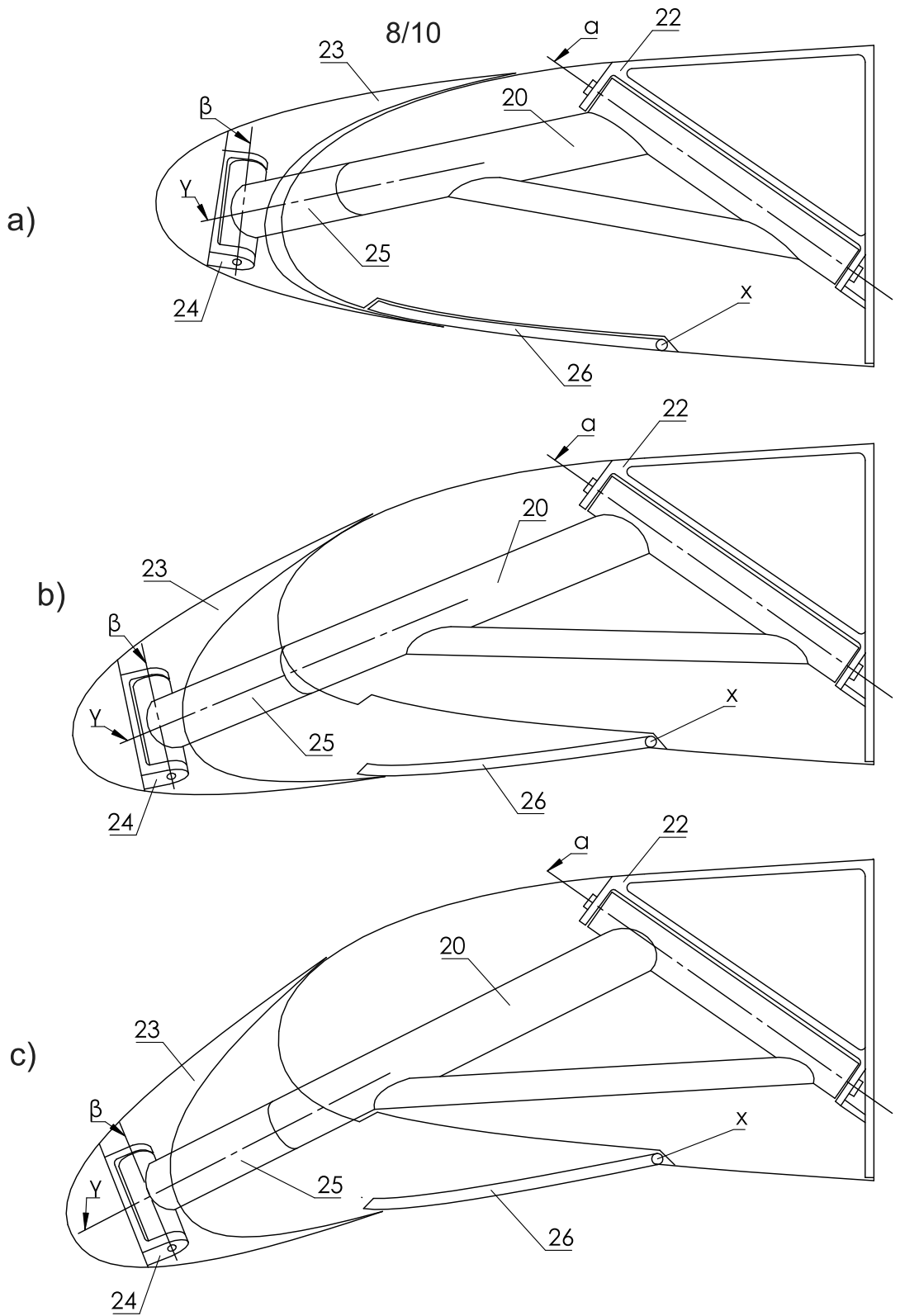25

24

26

x

c)

α

22

23

20

β

Y

25

24

26

x
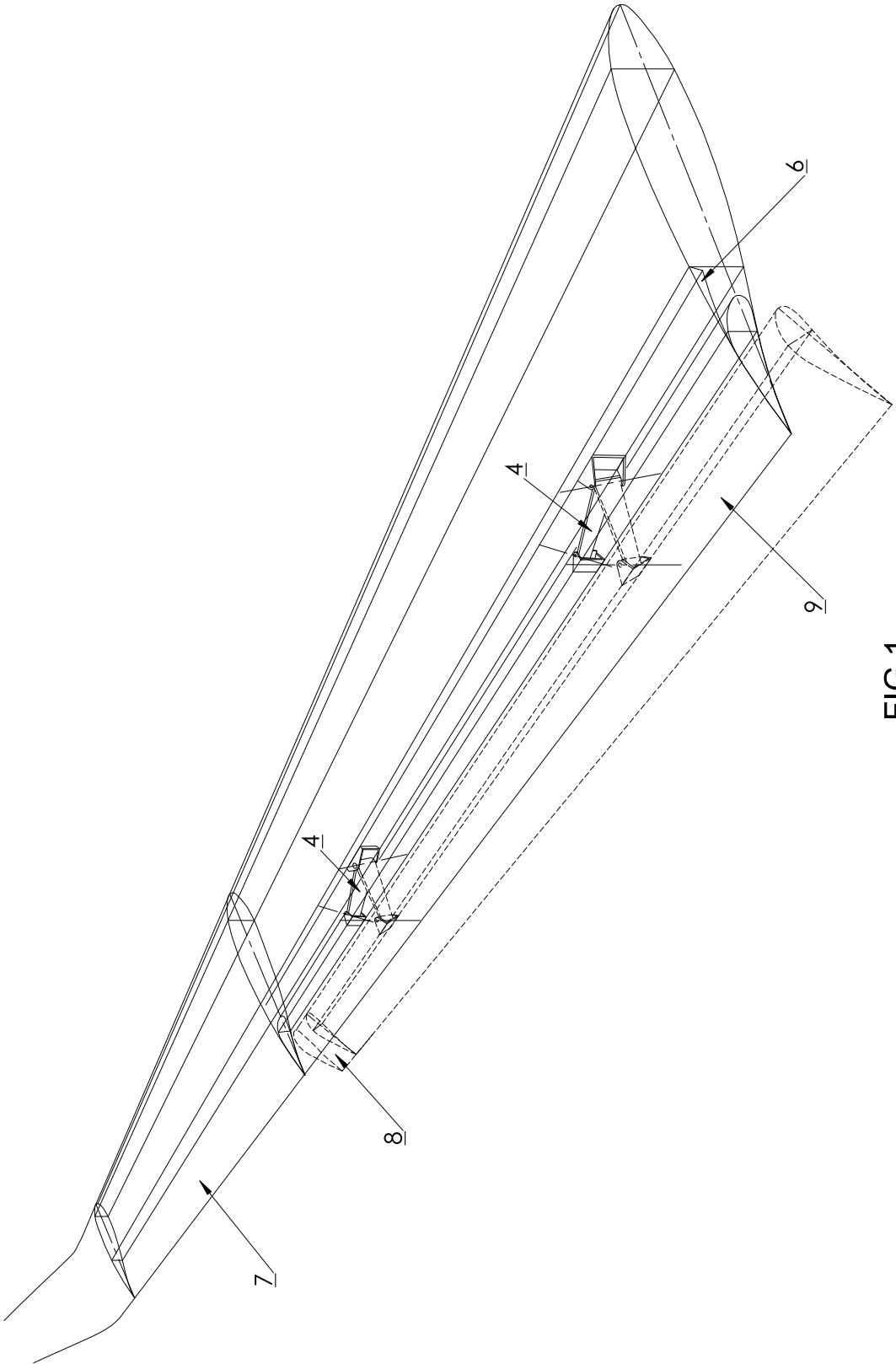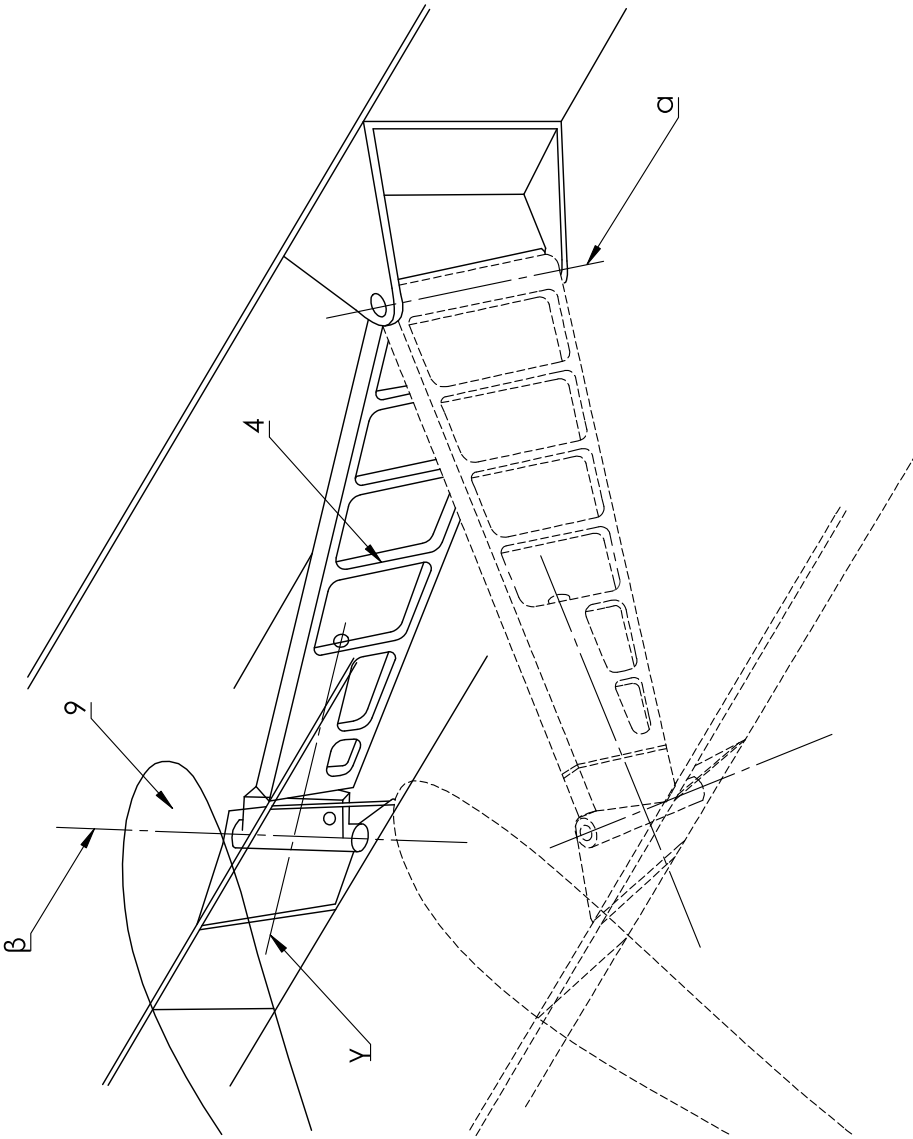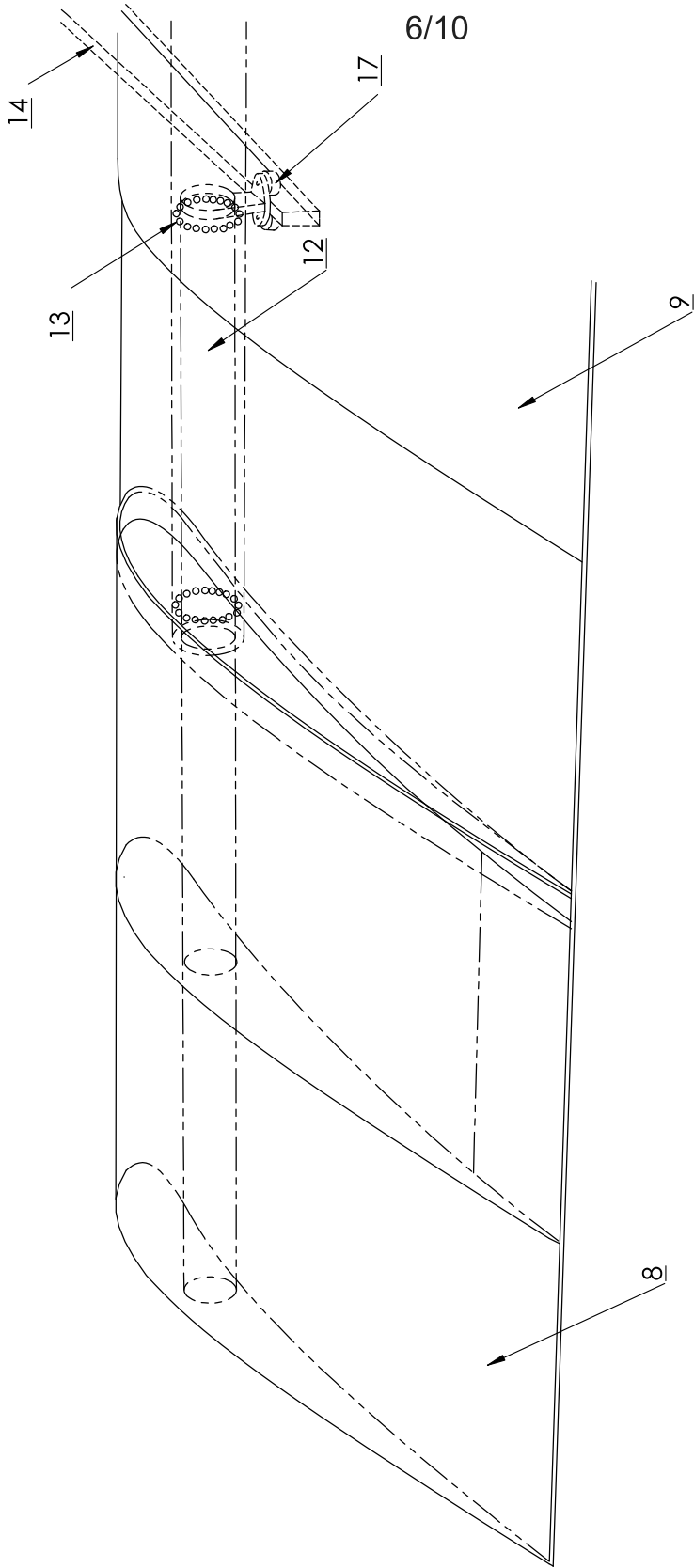
FIG 8
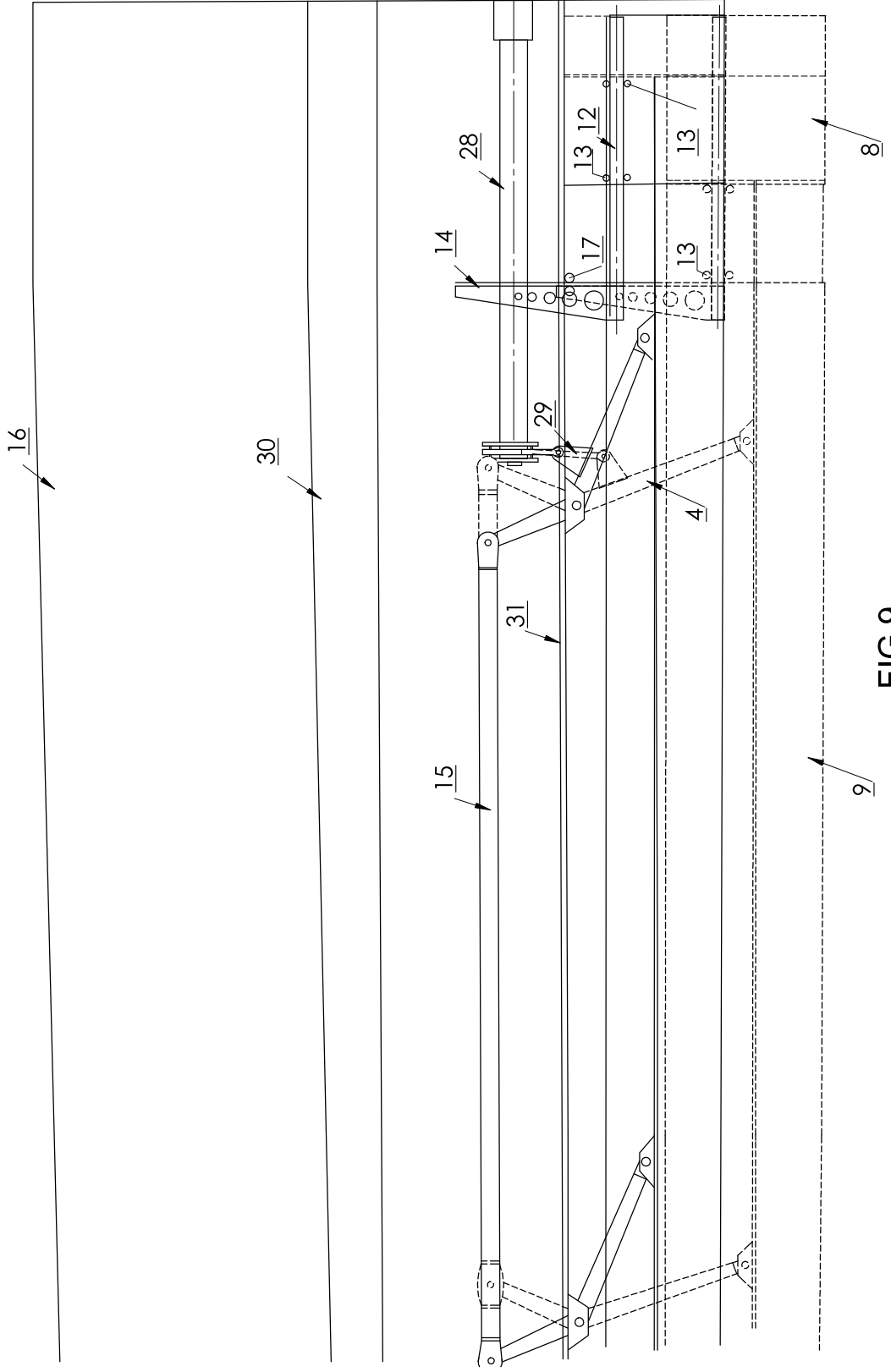
FIG 9
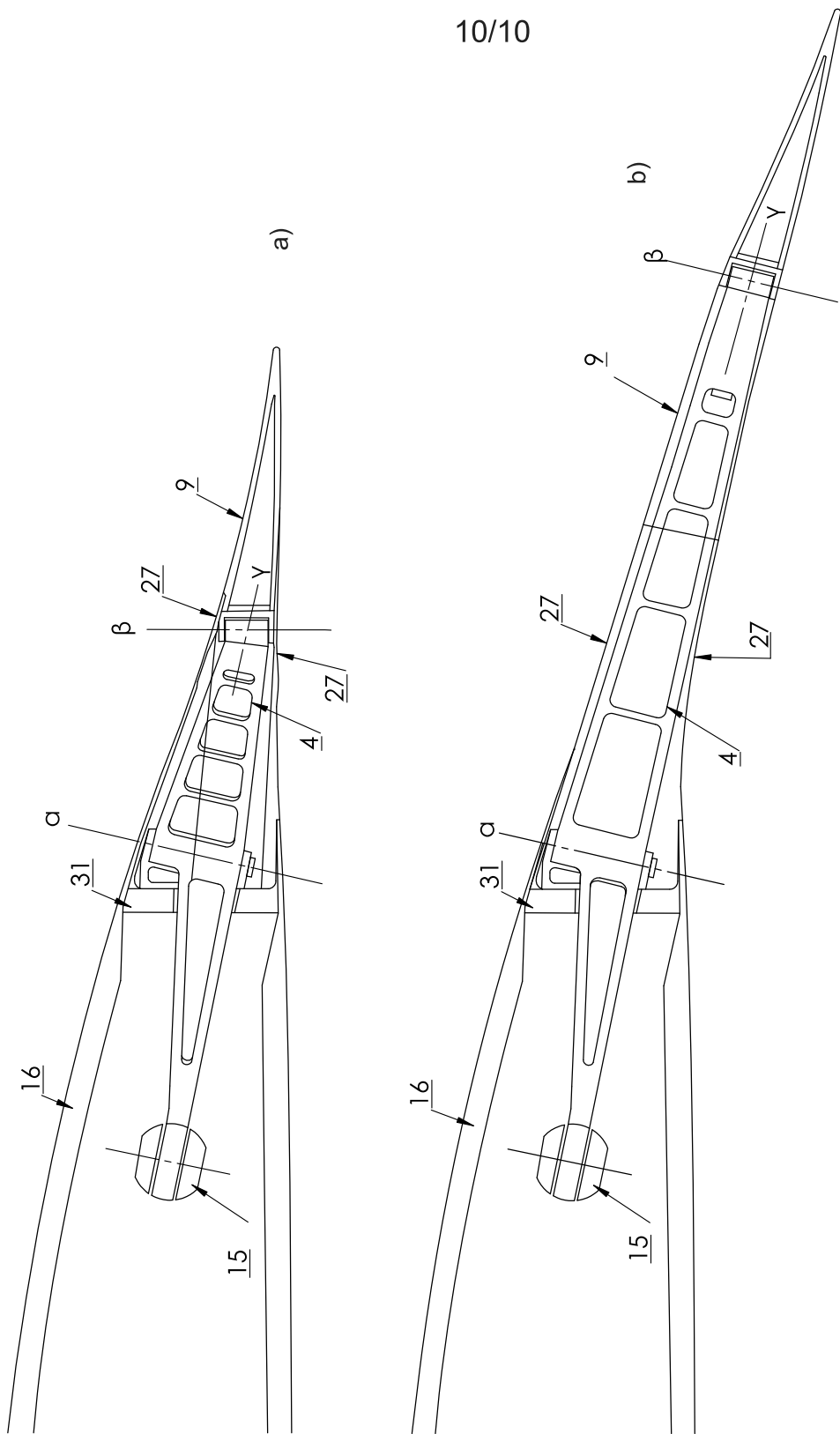
FIG 10

Actuating mechanism for trailing edge flaps and/or leading edge slats

This invention is intended for reducing the aerodynamic drag and weight of aircraft wings. In addition, the invention provides a way to improve the actuating mechanism for leading edge slats and trailing edge flaps and to reduce the production and maintenance costs of aircraft.

BACKGROUND ART

The Handley-Page and Krueger type leading edge slats and Fowler type trailing edge flaps often used on modern airliners are effective in reducing the take-off and landing speed, but their construction is complex and they need intensive maintenance. Also, the said devices are heavier than other types of leading edge slats and trailing edge flaps.

US Patent No. 1,394,344, Handley Page Ltd, 18 Oct 1924, describes an aircraft wing and a leading edge slat, which in parallel with the leading edge of the main wing is connected with the latter and moves away from the main wing when the arm is pivoted around the vertical pivot of the main wing. In US Patent No. 6,015,117, Broadbent, Michael C, 18 January 2000, an analogous actuating mechanism for moving a leading edge slat is described. In US Patent No. 5,836,550, Boeing Co, 17 November 1998, an actuating mechanism for moving a trailing edge flap is described which connects the trailing edge flap with the main wing.

In patent application US2006/0202089, Airbus GmbH, 14 September 2006, an aircraft wing comprising of a main wing and a trailing edge flap and an actuating mechanism for moving the flap are described.

SUMMARY OF INVENTION

The objective of this invention is to provide a fastening and an actuating mechanism for the trailing edge flap and the leading edge slat, which would have a simpler construction and would be more reliable than the technical solutions known in the prior art. Also, the objective of the invention is to provide a pivoting mechanism for the trailing edge flap and leading edge slat with fewer construction elements and smoother operation, which would improve the aerodynamic performance of the aircraft during the cruise, take-off and landing and would reduce fuel consumption, especially during longer flights. The purpose of the invention is achieved by means of

an actuating mechanism for pivoting leading edge slats and trailing edge flaps of the aircraft comprising pivot arms, slide panels and inclinable leading edge slats and trailing edge flaps, which can be used to increasing lift and reduce aerodynamic drag during the take-off and flight of an aircraft. Unlike the devices provided in documents

5   US 1,394,344 and US 6,015,117, the movement axis of the pivot arm according to this invention is not vertical but inclined by a substantial angle of 50–60 degrees (see Fig. 7 and Fig. 8). By this, the leading edge slats can be adjusted between three positions and are made much more effective. In the take-off position, the Handley-Page type slats (see Fig. 7) are inclined by an angle of –12 to –20 degrees and there

10   is no slot, which is why the aerodynamic drag is much lower. During the flight, the leading edge slats are in the retracted position. At landing, the slats are inclined by an angle of –28 to –32 degrees and the slot formed by this increases the lift as well as drag. Near the fuselage, Krueger type leading edge slats may be used at the leading edge, which are operated by means of pivot arms. Differently from the

15   above-mentioned devices, no substantial slots are formed when the flaps are drooped. In order to reduce drag and noise, the panel below the leading edge slat is sloped. The area between the pivot arms of the leading edge of the wing can be used as an additional fuel tank because there is no need for any actuators within the wing. As the device provided in US Patent No. 5,836,550, the device according to

20   this invention provides a way for adjusting the position of trailing edge flaps with pivot arms. Differently from the above-cited device, which is moved by a swivel link and a slaving mechanism, the main components of the device provided in this invention (see Fig. 1) are integrated pivot arms which during their pivotal movement also incline trailing edge flaps. The operation of the device provided in this invention

25   differs in principle from the device of the referred US patent because its construction is simpler, it weighs less and is more reliable. In US Patent No. 5,836,550, the formation of slots/gaps during the lateral movement of trailing edge flaps has not been taken into consideration. The slots between the trailing edge flap and the ailerons reduce lift and increase drag. According to this invention, the slot that forms

30   due to the motion of trailing edge flaps is closed by a slide panel and as a result, the area of trailing edge flaps increases when they are drooped. The drawback of US Patent No. 5,836,550 is high drag at start-off. The air flow directed at the initial position of the flight through the channel between the wing and the trailing edge flap (Fig. 3c) is inhibited because of the number of assembly units (Fig. 2) and the drag

increases. In the device of this invention, the problem is avoided in the following manner. At take-off (Fig. 3), when the trailing edge flaps are inclined by means of the pivot arms at an angle of +12 to +20 degrees, the spoilers at the rear part of the trailing edge are, at the same time, moved downwards to avoid the formation of a slot between the trailing edge flap and the spoiler. This way, aerodynamic performance of an aircraft can be increased during take-off and fuel consumption can be reduced. Differently from the device provided in US Patent No. 5,836,550, the device of this invention is an integrated unit comprising of pivot arms, a movable leading edge and rear edge, and slide panels. Due to the configuration and location of pivot arms, there is no need to use actuators in the outside section of the wing because the force required for moving trailing edge flaps is transferred from the flap in the centre of the wing by means of the articulation (Fig. 2). As a result, the device provided in this invention has lower drag and a higher lift/drag ratio (L/D) than the device according to the above-cited US patent. Differently from the device provided in US 2006/0202089, the actuating mechanisms provided here are located within the wing and do not produce any additional drag during the flight. Depending on the cruise weight and speed of the aircraft, the pivot arms can be used to modify the position of the trailing edge flaps during the flight even by a smaller degree, by –2 to +4 degrees. While the trailing edge flaps are moving, the spoiler is also moved accordingly, i.e. upward or downward, without any slots formed. At landing, the trailing edge flaps are positioned at a large angle, up to +30 to +45 degrees. In order to increase the lift and drag of the wings, the spoiler is inclined so that a slot of an optimal height forms between the spoiler and the trailing edge flap. While the trailing edge flaps are moving, the telescopic slide panel is also moving in relation to the trailing edge flap (see Fig. 6). During the curvilinear movement of the trailing edge flaps the slide panel moves along the track to the extended position, controlled by the rollers of the holder fitted to the tube spar. By means of the pivot arms, two- or multi-phase trailing edge flaps may be operated (Fig. 4). For this purpose, a small pivot arm attached to the trailing edge flap is used, which in turn moves the aft flap backward and sways it downwards. The rotation of this pivot arm is reversal in relation to the other. When the trailing edge flaps are mainly employed for increasing the lift/drag ratio, e.g., in the case of long-term pilotless aircrafts and sailplanes, the trailing edge flaps without slots depicted in Fig. 9 and 10 can be used. The basic aerodynamic effect of this type of trailing edge flaps is the increase of the wing area

during the flight by 10 to 20% and deflected it at the angle of 12 of 18 degrees. The area between the wing and the trailing edge flap is covered with flexible panels.

BRIEF DESCRIPTION OF DRAWINGS

The invention will now be described in more detail with reference to the figures, of

5   which:

Figure 1 depicts an aircraft wing and the pivot arms of the actuating mechanism for a trailing edge flap according to this invention;

Figure 2 is the top view of the aircraft wing which illustrates the actuating mechanism for a trailing edge flap and a leading edge slat according to this invention;

10   Figure 3 depicts various positions of the trailing edge flap: a) the cruise position where the deflection angle of the trailing edge flap is zero degrees, b) the take-off position where the deflection angle of the trailing edge flap is up to 15 degrees, and c) the landing position where the deflection angle of the trailing edge flap is up to 40 degrees;

15   Figure 4 depicts various positions of the trailing edge flap and an additional aft flap attached to it by means of the pivot arm mechanism: a) the cruise position where the deflection angle of the trailing edge flap and the aft flap is zero degrees, b) the take-off position where the deflection angle of the trailing edge flap and the aft flap is up to 15 degrees, and c) the landing position where the deflection angle of the trailing

20   edge flap is up to 40 degrees and that of the aft flap is up to 60 degrees;

Figure 5 depicts the pivot arm mechanism for moving the trailing edge flap and the aft flap;

Figure 6 depicts a telescopic slide panel moving in relation to the trailing edge flap 9;

Figure 7 depicts various positions of the Handley-Page type leading edge slat: a) the

25   cruise position where the deflection angle of the leading edge slat is zero degrees, b) the take-off position where the deflection angle of the leading edge slat is up to 16 degrees, and c) the landing position where the deflection angle of the leading edge slat is up to 32 degrees;

Figure 8 depicts various positions of the Krueger type leading edge slat attached to

30   the aircraft wing, wherein the leading edge slat is closed from the underside with a panel for reducing drag and noise: a) the cruise position where the deflection angle

of the leading edge slat is zero degrees, b) the take-off position where the deflection angle of the leading edge slat is up to –14 degrees, and c) the landing position where the deflection angle of the leading edge slat is up to –28 degrees;

Figure 9 depicts a wing with a trailing edge flap without a slot, which can be used on
5   aircraft and sailplanes (also unmanned) and where the pivot arms are connected by means of pushrods and the slide panel is located at the inboard tip of the trailing edge flap;

Figure 10 is a side view of the previous figure showing various positions in which a) the trailing edge flap is in the retracted position with the deflection angle of zero
10   degrees, b) the trailing edge flap is in the extended position where the deflection angle is up to 15 degrees.

DESCRIPTION OF EMBODIMENTS

The aircraft wing usually comprises of a regular main construction and trailing edge flaps mounted on the fixed wing. Larger aircraft also have a movable leading edge
15   slat mounted on the main construction to ensure a smoother aerodynamic performance at the take-off, cruise and landing of the aircraft. Figure 2 shows an aircraft wing with both trailing edge flaps 9 and movable leading edge slats 21, 23. The motion of the trailing edge flaps is actuated with a motor 1, which rotates the screw mechanism 2, which in turn rotates, through the holder 2, the pivot arm 4 that
20   functions as the actuating mechanism for trailing edge flaps (see Fig. 2). The pivot arm moves, by means of the articulation 5, the trailing edge flap 9 mounted on the wing arm either backward or forward relative to the flight direction. The symmetrical motion of trailing edge flaps is ensured with the tube which rotates the screw mechanism 2 and extends through the fuselage to the other trailing edge flap to
25   which a screw mechanism with a reverse thread is fitted. The pivot arm is fixed to the trailing edge flap with a mechanism which moves the trailing edge flap accordingly when the pivot arm is turned (see Fig. 3 and Fig. 4).

The pivot arm axis α is sloped backward from the vertical direction by up to 12 degrees (see Fig. 3, backward slope means the slope of the axis α towards the rear
30   edge of the wing or, more generally, towards the empennage). When the pivot arm 4 is turned up to 39.7 degrees (see Fig. 2 and Fig. 3), the trailing edge flap rotates at the same time around the axis y by up to 30 degrees to the deflection angle of the trailing edge flap up to +40 degrees.

The angle between the axes β and y is 90 degrees (see Fig. 5). With the motion of the trailing edge flaps, the slide panel 8 moves laterally relative to the trailing edge flap. The profile of the slide panel resembles the profile of the trailing edge flap 9 (Fig. 6). Its movement is controlled with the tube spar 12, which is placed between the rollers 13. The slide panel is controlled with the pusher 15, which in turn is connected to the tube spar through the holder 14 and to the wing through the pivotal articulations 16, 17 (see Fig. 9). In order to reduce aerodynamic drag, the deflection angle of the trailing edge flap in the take-off position is smaller (+15 degrees) and without a slot between the main construction of the wing and the trailing edge flap. To achieve that, the spoiler 6 on the trailing edge flap is turned downward (Fig. 2) against the upper surface of the trailing edge flap. In addition to the three positions shown in the figure, the trailing edge flaps are adjusted during the flight, depending on the cruise weight and speed of the aircraft, within the range of –2 to +4 degrees. At the same time, the spoilers on the wing move upwards or downwards, respectively. The pivot arms can be used for moving two- or multi-phase trailing edge flaps. In addition to the main trailing edge flap, Figure 4 shows a movable aft flap 10 attached to it, which can be moved with pivot arms. The aft flap 10 is moved with a small pivot arm 11 in the reverse direction relative to the pivot arm 4. The maximum deflection angle of the aft flap is +15 to +25 degrees.

The pivot arms are also used to control the movement of leading edge slats (see Figs. 7 and 8). The motor 18 for moving the leading edge slats also rotates the screw mechanism 19, which in turn moves the pivot arms 20 (see Fig. 2). The screw mechanism extends through the fuselage to the other wing, in which the screw mechanism has a reverse thread. This ensures the symmetrical movement of the leading edge slats. The pivot a of the leading edge slat pivot arms is inclined by 50 to 60 degrees forward from the vertical direction (towards the front end of the aircraft), which makes it possible to use leading edge slats having three possible positions. Fig. 8 shows the Krueger type leading edge slats 23 without a slot, which are located in the inboard section of the wing. When the pivot arm 20, mounted to the holder 22, rotates around the pivot a, the leading edge slat 23 moves forward and down and at the same time, rotates through the mechanism 25 the entire leading edge slat 21 and 23. In order to reduce drag and noise, the Krueger type leading edge slat is closed from below with a panel 26. The rest of the leading edge slats 21 are in the take-off position (Fig. 7) between the leading edge slat without a slot (Fig. 7b) and the

main construction of the wing, whereas the landing position is with a slot (Fig. 7c) and without the lower cover panel. The movement of the leading edge slats is based on the same principle as the actuating mechanism of trailing edge flaps, only a larger angle is used.

5   Figures 9 and 10 illustrate the operation of trailing edge flaps as follows. The torque tube 28 moves the pivot arm 4 through the pusher 29 located in the wing 16. Similarly to the above-described, the trailing edge flap is sloped when the pivot arms move. Differently from the arrangement depicted in Fig. 2, pivot arms 4 in Fig. 9 are connected to pushrods 15 and the slide panel 8 is located in the inboard section of

10   the trailing edge flap. With the movement of the trailing edge flap, also the flexible panels 27 fitted to the wing move, which prevents the formation of slots. With the motion of the trailing edge flaps, the slide panel 8 moves longitudinally in relation to the trailing edge flap. The slide panel spar 12 is movable between the rollers 13. The slide panel is controlled by the track 14, one end of which is connected to the slide

15   panel spar 12 through a shaft and the other end is freely movable between the guide rollers 17.

The arrangement of the invention comprising of pivot arms, slide valves and deflectable trailing edge flaps and/or leading edge slats helps to reduce aerodynamic drag at the take-off as well as during the flight. The axis of the movement of the pivot

20   arm according to the invention is not vertical, as in the constructions known in the art, but at an angle of 50 to 60 degrees (Fig. 7 and Fig. 8). By this, leading edge slats can be adjusted between three positions, which substantially increase their effectiveness. In the take-off position, the Handley-Page type leading edge slats (see Fig. 7) are inclined at an angle of −12 to −20 degrees and they are without a slot,

25   which is why the aerodynamic drag is much lower. During the flight, the leading edge slats are in the retracted position. At landing, the slats are inclined at an angle of −28 to −32 degrees and the slot formed as a result of this increases the lift as well as drag. Near the fuselage, Krueger type leading edge slats may be used which are operated by means of pivot arms. Differently from the previously mentioned

30   arrangements, no substantial slots are formed between the leading edge slats and the main construction of the wing when the leading edge slats are drooped. In order to reduce drag and noise, panel 26 below the leading edge slat is sloped. The area between the pivot arms of the leading edge of the wing can then be used as an additional fuel tank because the actuators within the wing are not needed. The pivot

arms described herein can also be used for adjusting the position of the trailing edge flaps. Differently from the solutions described in the prior art, where the trailing edge flaps are moved by two components (swivel link 50 and slaving mechanism 35), the main components of the arrangement according to this invention (Fig. 1) are

5   integrated pivot arms 4 which during their pivotal movement also move trailing edge flaps 9. Compared to earlier solutions, the operating principle of the construction according to this invention is simpler and more reliable. Solutions are also given for the construction differences resulting from the formation of slots/gaps as a result of the lateral movement of the trailing edge flaps. The slots between the trailing edge

10   flap and ailerons reduce lift and increase drag. According to this invention, the slot formed with the motion of trailing edge flaps is closed by the slide panel 8 and, all in all, the area of trailing edge flaps increases when they are in a drooped position. The air flow directed at the initial stage of the flight through the channel between the main construction of the wing and the trailing edge flap (Fig. 1c–3) is inhibited because of

15   the number of components (Fig. 2 60, 63, 35, 50), and the drag increases. This problem is avoided in the device of this invention in the following manner. At take-off (Fig. 3), when the trailing edge flaps 9 are positioned by means of the pivot arms 4 at an angle of +12 to +20 degrees, the spoilers 6 at the rear part of the trailing edge are moved downwards so as to avoid the formation of a slot between the trailing edge

20   flap and the spoiler. This way, the aerodynamic performance of an aircraft during take-off can be increased and fuel consumption reduced. The device according to this invention is an integrated unit comprising of pivot arms, a movable trailing edge flap and/or leading edge slat, and slide panels and it clearly differs from the devices known in the prior art. Due to the configuration and location of pivot arms, there is no

25   need for actuators in the outside sections of the wing because the force required for moving the trailing edge flaps is transferred from the flap in the centre of the wing by means of the articulation 5 (Fig. 2). As a result, the arrangement according to this invention reduces aerodynamic drag and increases aerodynamic performance. The actuating mechanisms are placed inside the wing and they do not cause any

30   additional drag. Depending on the flight weight and speed of the aircraft, the pivot arms can be used to adjust the position of the trailing edge flaps during flight even by a small degree, by –2 to +4 degrees. While the trailing edge flaps are moving, the spoiler is moved accordingly, i.e. upward or downward, without forming any slots. At landing, the trailing edge flaps are positioned at a large angle, up to +30 to +45

degrees. In order to increase the lift and drag of the wings, the spoiler is inclined so that a slot of optimal height forms between the spoiler and the trailing edge flap. While the trailing edge flaps are moving, the telescopic slide panel 8 is also moving in relation to the trailing edge flap 9 (Fig. 6). During the curvilinear movement of the trailing edge flaps, the slide panel moves along the track 14 to the extended position, controlled by the rollers 17 of the holder fitted to the tube spar 12. The two- or multi-positions trailing edge flaps may also be operated by means of the pivot arms (Fig. 4). For that, a small pivot arm 11 attached to the trailing edge flap 9 is used, which in turn moves the aft flap backward and sways it downwards. The rotation of the pivot arm 11 is reversal relative to the pivot arm 4. When the trailing edge flaps are mainly employed to increase the lift/drag ratio, e.g., in the case of long endurance (unmanned) aircraft and sailplanes, the trailing edge flaps without slots depicted in Fig. 9 and 10 can be used. The basic aerodynamic effect of this type of trailing edge flaps is the increase of the wing area during the flight by 10 to 20% and the deflection angle of 12 to 18 degrees. The area between the wing and the trailing edge flap is covered with flexible panels 27.

Due to the simpler construction of the devices described herein, they can be used on various aircraft, from large UAVs and sailplanes to commercial airliners. The production costs of the described devices may be two times smaller compared with the known devices and their maintenance costs up to four times smaller than those of the devices used at present. By employing the devices provided in this invention, fuel consumption is reduced, which also significantly reduces the operating costs of an aircraft. In addition, the weight of leading edge slats and trailing edge flaps is reduced substantially compared to the use of devices known in the art.

REFERENCE SIGN LIST

1. Engine for moving trailing edge flaps
2. Screw mechanism for moving trailing edge flaps
3. Holder of pivot arm
4. Pivot arm for moving trailing edge flaps
5. Articulation between the trailing edge flaps
6. Spoilers
7. Aileron
8. Slide panel of the wing

9.   Trailing edge flaps

10.   Aft flap

11.   Aft flap pivot arm

12.   Slide panel spar

5   13.   Rollers of the slide panel spar

14.   Control track of the slide panel

15.   Pusher between the pivot arms

16.   Wing

17.   Rollers of the control track

10   18.   Engine for moving leading edge slats

19.   Screw mechanism for moving leading edge slats

20.   Pivot arms for moving leading edge slats

21.   Handley-Page type leading edge slat

22.   Holders of the leading edge slat pivot arms

15   23.   Krueger type leading edge slat

24.   Leading edge slat pivot arm holder

25.   Section of the pivot arm revolving around axis y

26.   Inclinable panel under leading edge slat

27.   Flexible panel of the trailing edge

20   28.   Torque tube for moving the trailing edge flap

29.   Pivot arm pusher

30.   First spar of the wing

31.   Rear spar of the wing

Claims

1. An actuating mechanism for the trailing edge flap and/or the leading edge slat, comprising of pivot arms (4, 20) for moving the trailing edge flap and/or the leading edge slat to which, respectively, the inclinable trailing edge flap or leading edge slat is connected, a slide panel, an engine actuating the movement of the trailing edge flap or the leading edge slat, and a screw mechanism for moving the trailing edge flap or the leading edge slat, **characterised in that** the axis α of the pivot arm of the trailing edge flap is inclined downwards by up to 12 degrees in relation to the vertical direction, wherein with the rotation of the pivot arm by up to 39.7 degrees, the trailing edge flap may be turned around the axis y by up to 30 degrees to the deflection angle of +40 degrees, whereas the angle between the axes β and y is 90 degrees.

2. The actuating mechanism for the trailing edge flap and/or the leading edge slat according to claim 1, wherein the axis of movement of the pivot arm is inclined forward in relation to the vertical direction at an angle of 50 to 60 degrees, and wherein at the take-off of an aircraft, the leading edge slat is at an angle of –12 to –20 degrees, and at landing, the leading edge slat is at an angle of –28 to –32 degrees.

3. The actuating mechanism for the trailing edge flap and/or the leading edge slat according to claim 1, wherein the Krueger type leading edge slats operating on the motion of the pivot arms are used in the wing section near the fuselage.

4. The actuating mechanism for the trailing edge flap and/or the leading edge slat according to claim 3, wherein the motion of the trailing edge flaps also causes lateral movement of a slide panel (8) in relation to the trailing edge flap and the profile of the slide panel resembles the profile of the trailing edge flap.

5. The actuating mechanism for the trailing edge flap and/or the leading edge slat according to claim 4, wherein the movement of the slide panel is controlled by the tube spar (12) placed between the rollers (13) through the pusher (15) which in turn is connected to the tube spar by the holder (14) and to the wing through articulations (16, 17).

6. The actuating mechanism for the trailing edge flap and/or the leading edge slat according to claim 5, wherein for increasing lift and reducing aerodynamic drag, the deflection angle of the trailing edge flap in the take-off state is less than +15 degrees

and there is no slot between the main construction of the wing and the trailing edge flap.

7. The actuating mechanism for the trailing edge flap and/or the leading edge slat according to claim 5, wherein the position of the trailing edge flaps may be adjusted during the flight in the range of –2 to +4 degrees depending on the cruise weight and speed.

8. The actuating mechanism for the trailing edge flap and/or the leading edge slat according to claim 5, wherein an aft flap (10) movable by the pivot arms is attached to the main trailing edge flap and the aft flap can be moved by a small pivot arm (11) in the reverse direction in relation to the movement of the pivot arm (4) of the trailing edge flap.

Abstract

Due to a simpler construction, the devices described in this specification are more reliable and can be used on various aircraft from large UAVs and sailplanes to commercial airliners. The production costs of the described devices may be two

5   times smaller and maintenance costs two to four times smaller than those of the devices used at present. By employing the devices provided in this invention, fuel consumption may be reduced, which also significantly reduces the operating costs of an aircraft. In addition, the weight of the leading edge slats and trailing edge flaps is reduced substantially compared to the devices known in the art.

6

4

9

4

8

7
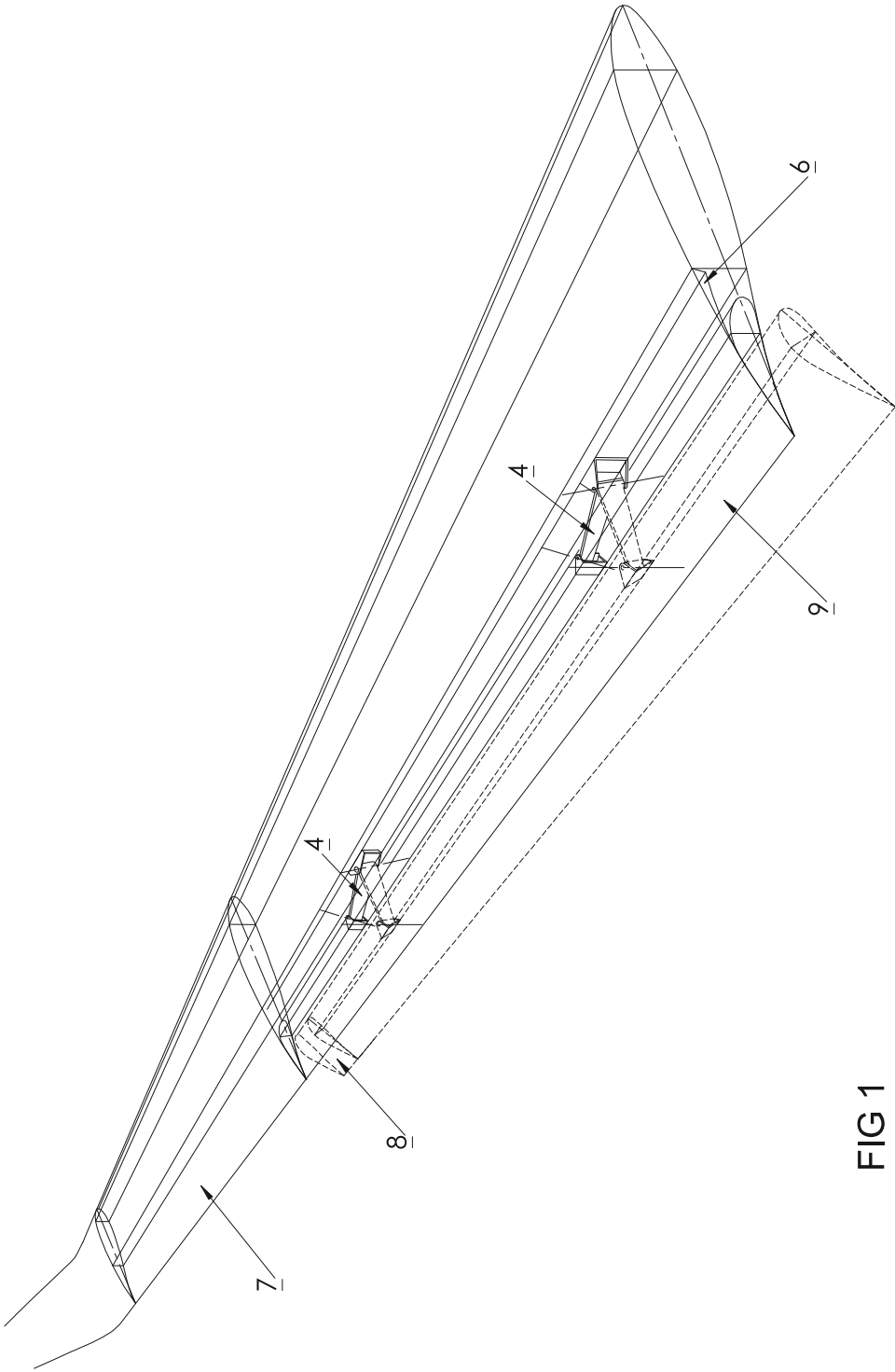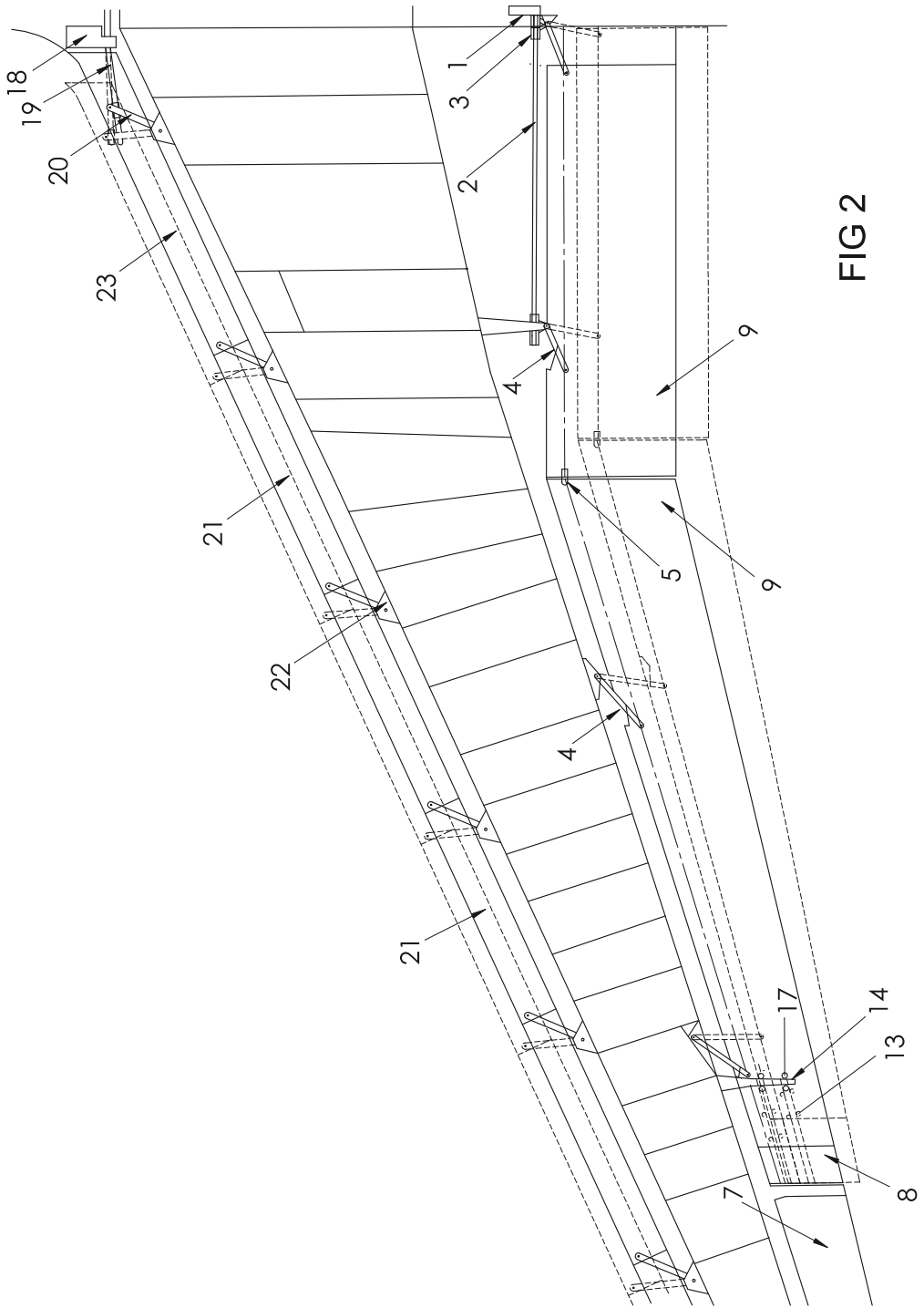
FIG 1

FIG 2

FIG 3

FIG 4

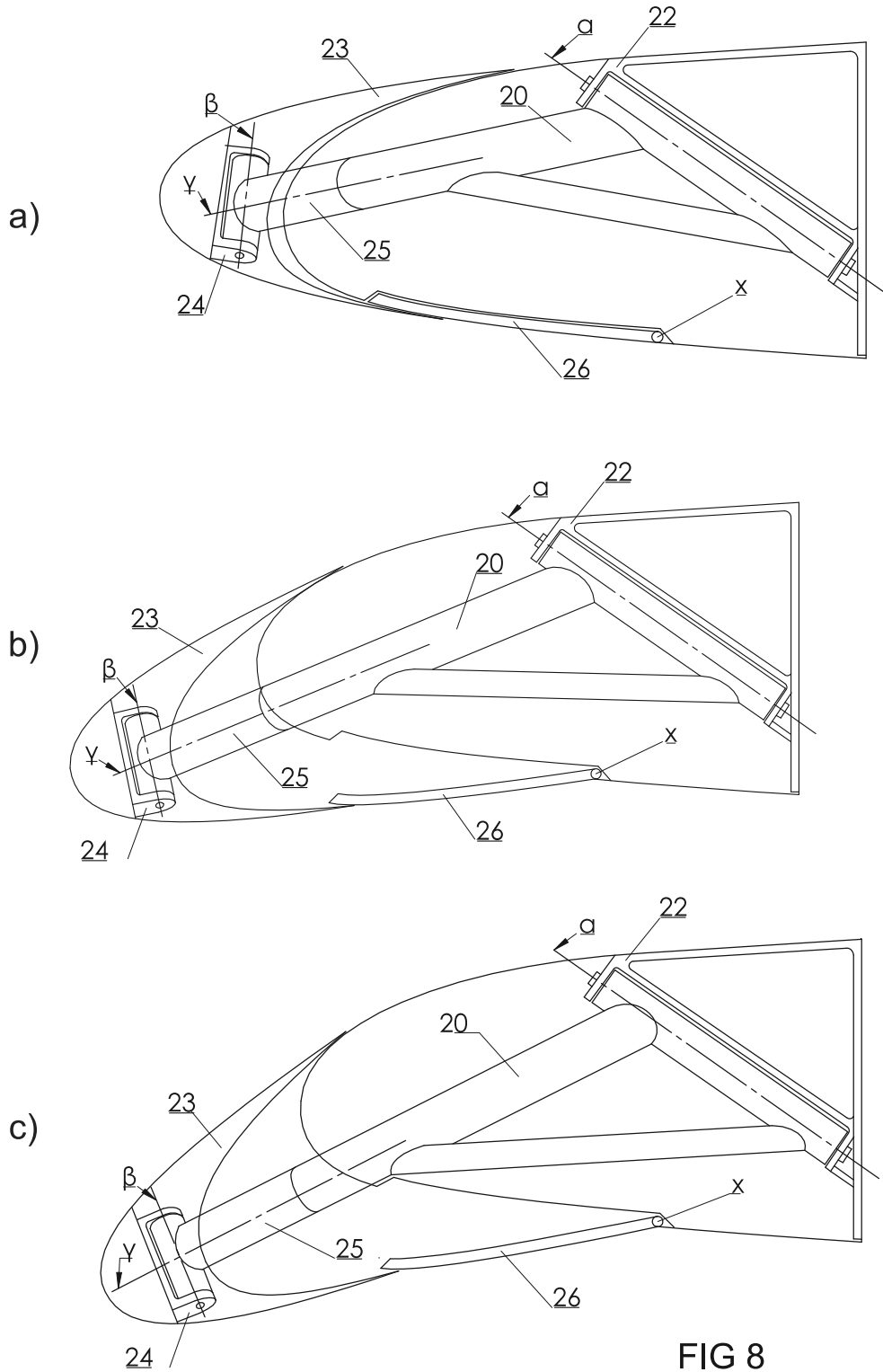FIG 5

14

17

13

12

9

8
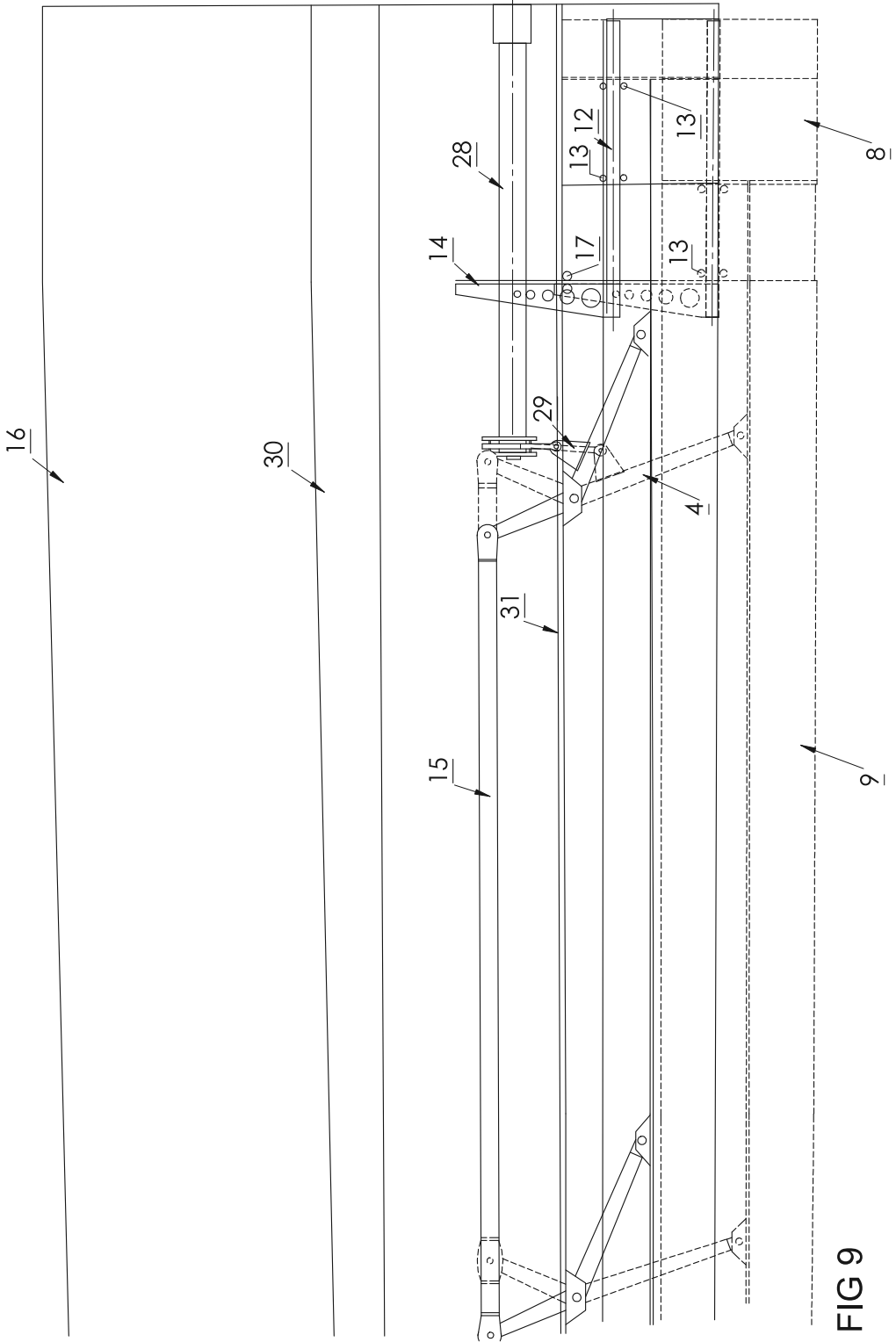
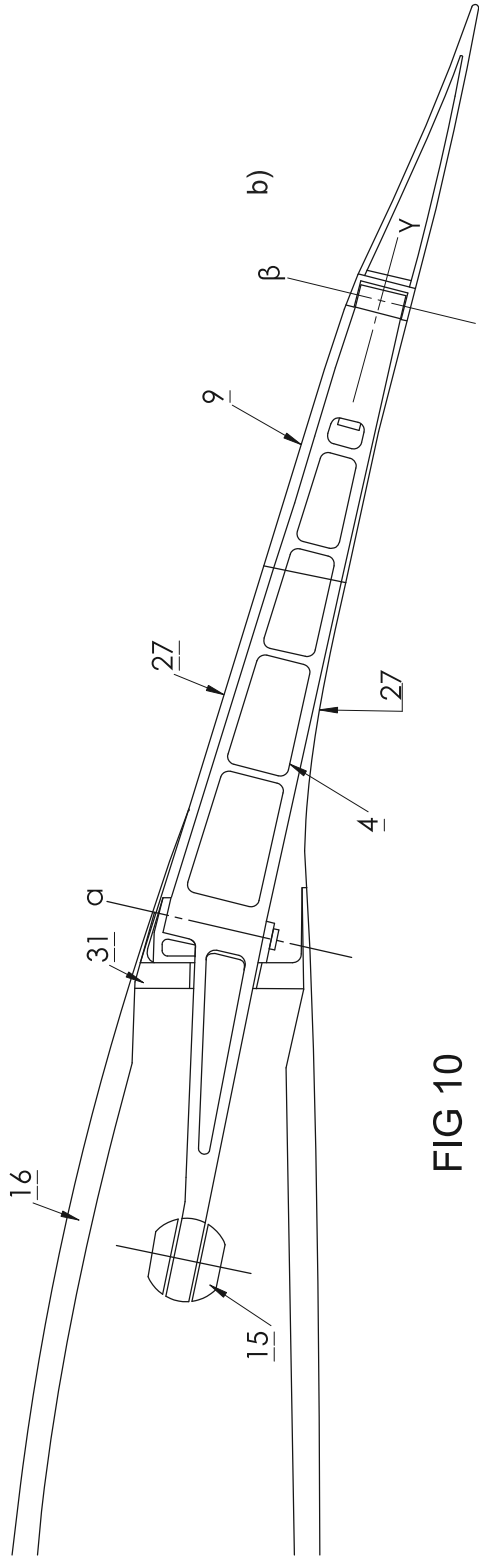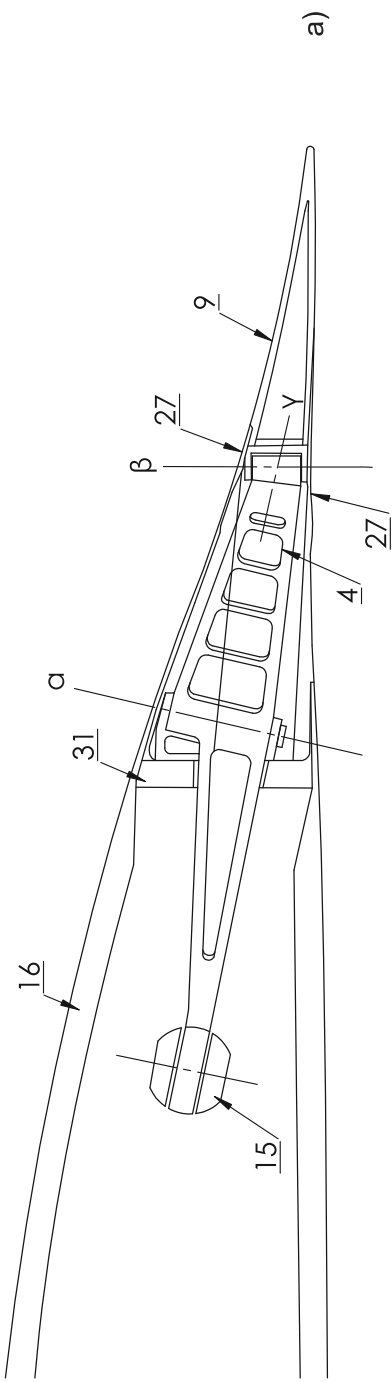FIG 6

FIG 7

a)

FIG 8
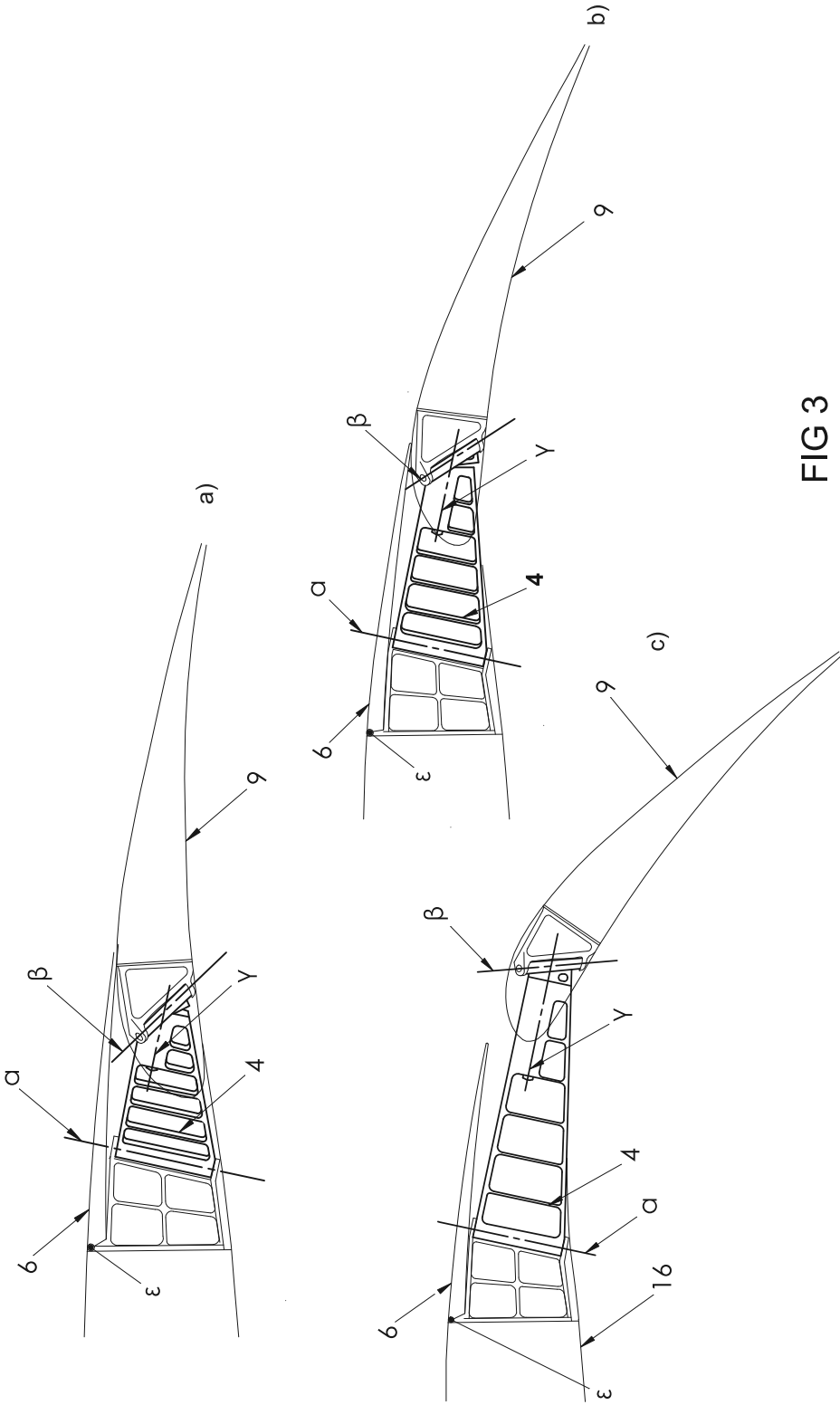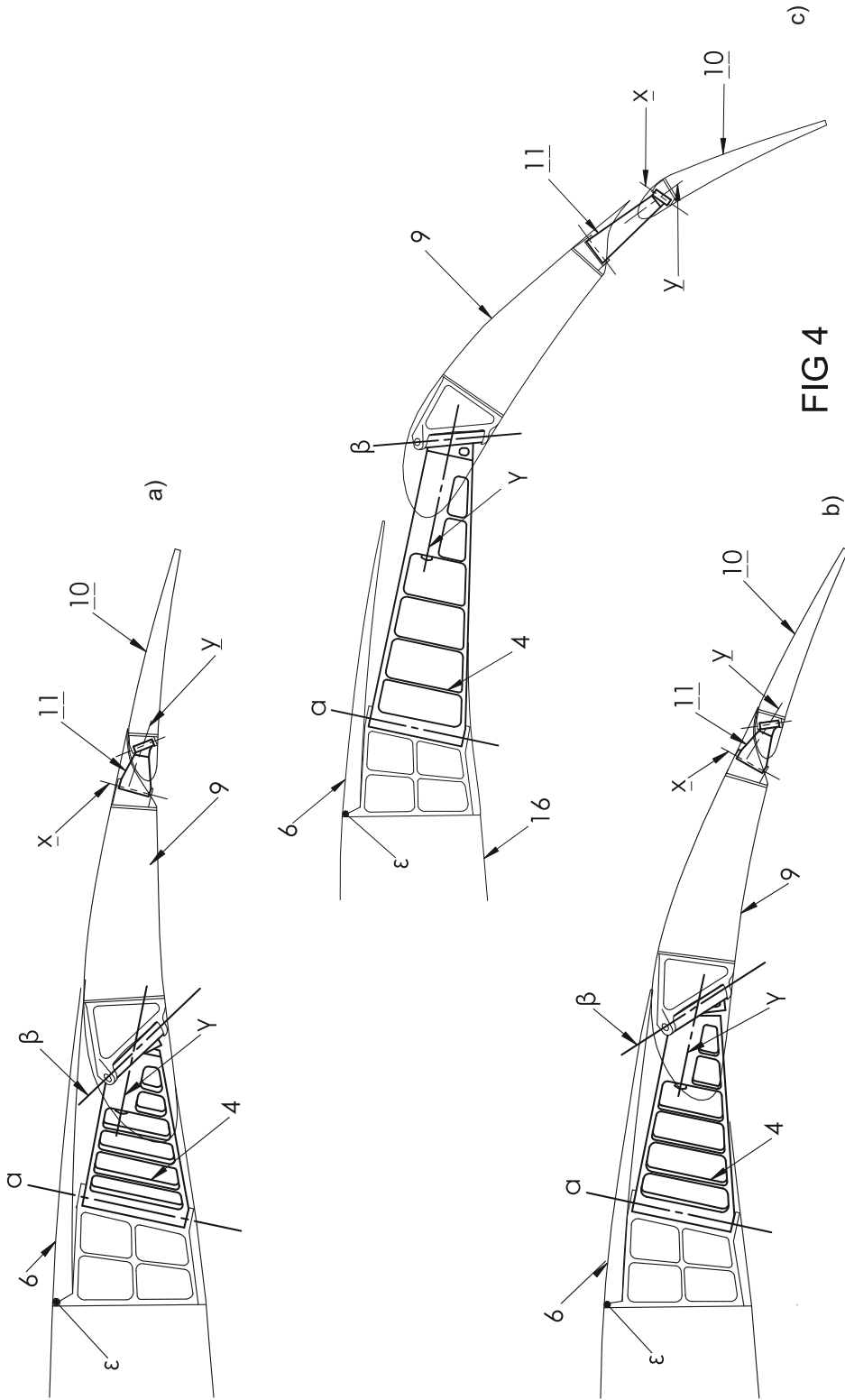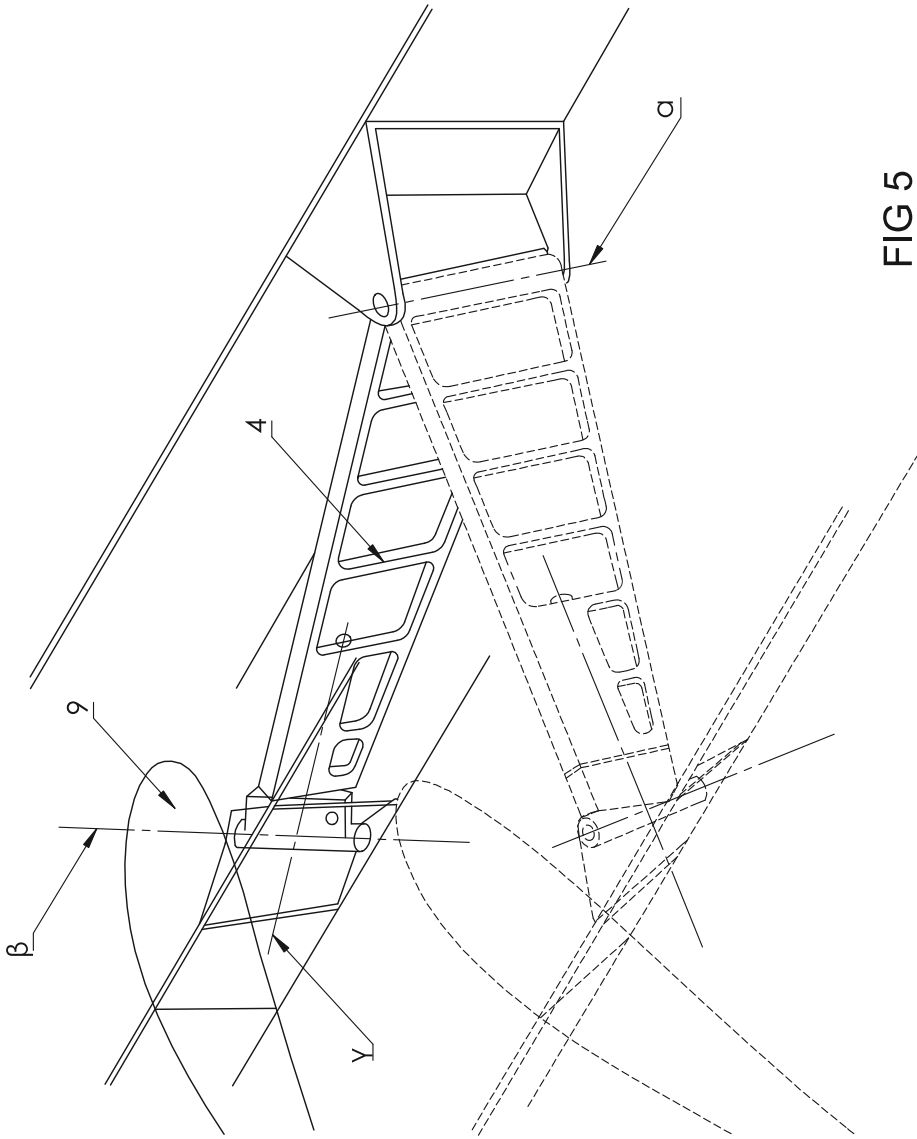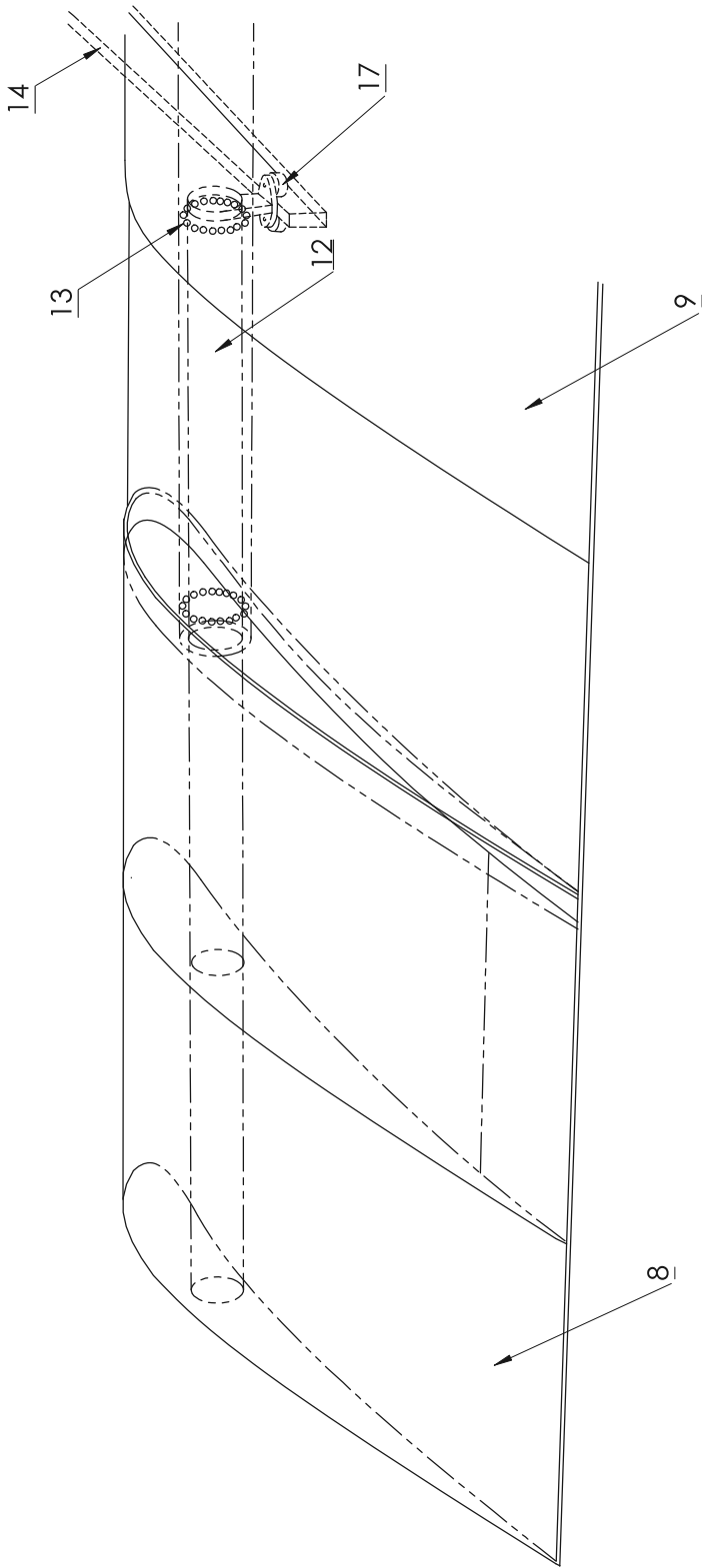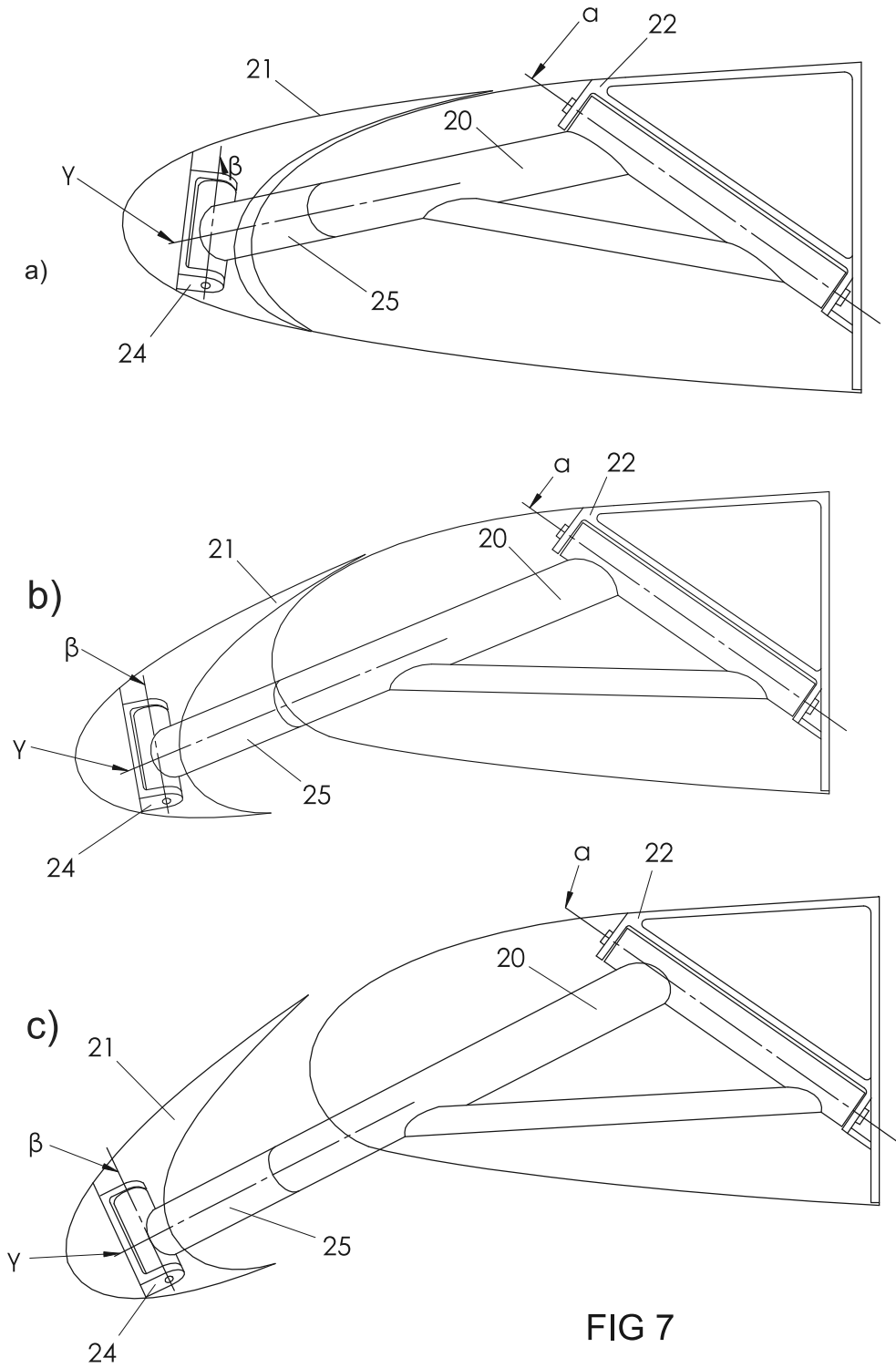
FIG 9

FIG 10

Curriculum vitae

Personal data

Name: Peep Lauk

Date of birth: 02.08.1966

Place of birth: Elva, Estonia

Citizenship: Estonian

Contact data

E-mail: peep.lauk@eava.ee

Education

2014–2019 Tallinn University of Technology, PhD.

1984–1989 Estonian University of Life Sciences, equalized with MSc

1981–1984 Põlva High School

Language competence

Estonian – native language

English – intermediate

Russian – intermediate

Professional employment

1989–1994 Estonian Agrobiocentre, Junior Scientist

1994–2001 NPK Väetis OÜ, CEO

2001–2009 Fertile-Invest OÜ, CEO

2009–…   Novaviking OÜ, CEO

2013–…   Estonian Aviation Academy, Researcher

Supervised dissertations

Siim Heering, MSc, 2015. Development and optimization of unmanned aerial vehicle systems. Tallinn University of Technology

Marek Tamm, 2018. Strength analysis of the swivel beam trailing edge flap system for commercial aircraft, Estonian Aviation Academy

Timo Korv, 2018. Modular lithium-ion battery assembly for electric aircraft, Estonian Aviation Academy

Participation in scientific projects

2.1.3 Influence of miniflaps on aerodynamic characteristics of aircraft, 2014–2020, Peep Lauk, Estonian Aviation Academy, Development Department

Scientific work

- Lauk, P.; Seegel, K.-E.; Tähemaa, T. (2017). Impact of variable geometry miniflaps on sailplane flight characteristics. Aviation, 21 (4), 119–125.10.3846/16487788.2017.1415228.
- Lauk, P.; Rebassa, J. H.; Kartushinsky, A.; Krupensky, I.; Tisler, S.; Tähemaa, T.; Polonskye, A. (2016). Assemblage of turbulent jet flows through static particulate media. Proceedings of the Estonian Academy of Sciences, 65 (3), 284–296.10.3176/proc.2016.3.05.
- Lauk, Peep; Unt, Karl-Eerik (2015). Influence of miniflaps on sailplane flight characteristics. Aviation, 19 (3), 105–111.10.3846/16487788.2015.1104793.
- Lauk, P.; Seegel, K.-E.; Tähemaa, T. (2018). The Influence of Variable Geometrical Modifications of the Trailing Edge of Supercritical Airfoil on the Characteristics of Aerodynamics. International Journal of Mechanical, Aerospace, Industrial, Mechatronic and Manufacturing Engineering, 12 (4), 261–266.

- Lauk, P.; Seegel, K-E.; Kartušinski, A.; Tisler, S.; Hussainov, M.; Polonsky, A.; Scheglov, I.; Rudi, Ü. (2016). Two-fluid RANS-RSTM-PDF model for turbulent particulate flows. In: R. López-Ruiz (Ed.). Numerical Simulation (340–363). InTech - Open Access Publisher .10.5772/63338.
- Lauk, Peep; Unt, Karl-Eerik. (2014). Miniflap influence on sailplane flight characteristics. Research and Education in Aircraft Design 2014. Ed. Jonas Stankūnas. Vilnius, Lithuania: Antanas Gustaitis Aviation Institute of Vilnius Gediminas Technical University.
- Lauk, Peep; Jakimenko, Jaanus; Vanker, Signe (2016). Projektõpe aine "Ülikerge purilennuki ehitamine" näitel. Õppemetoodiline konverents. Konverentsi teesid: Ennast juhtiv õppija; Kaitseväe Ühendatud õppeasutused, 20.10.2016. Toim. Svetlana Ganina; Andres Saumets. Tartu: Kaitseväe Ühendatud Õppeasutused, 34–36.
- Lauk, P; Tähemaa, T.; Seegel, K-E. (2018). Advanced trailing edge flap design for commercial aircraft, Toulouse, AEGATS´18 Confrence, France / 23 – 25 October 2018.

Elulookirjeldus

Isikuandmed
Nimi: Peep Lauk
Sünniaeg: 02.08.1966
Sünnikoht: Elva, Eesti
Kodakondsus: Eesti

Kontaktandmed
E-post: peep.lauk@eava.ee

Hariduskäik
2014–2019 Tallinna Tehnikaülikool, PhD
1984–1989 Eesti Põllumajanduse Akadeemia, võrdsustatud magistriõppega
1981–1984 Põlva Keskkool, keskharidus

Keelteoskus
Eesti keel – emakeel
Inglise keel – kesktase
Vene keel – kesktase

Teenistuskäik
1989–1994 Eesti Agrobiokeskus, nooremteadur
1994–2001 NPK Väetis OÜ, juhataja
2001–2009 Fertile-Invest OÜ, juhataja
2009–…   Novaviking OÜ, juhataja
2013–…   Eesti Lennuakadeemia, lektor, arendussetsialist

Juhendatud väitekirjad
Siim Heering, MSc, 2015. Mehitamata õhusõiduki süsteemide arendus
ning optimeerimine, Tallinna Tehnikaülikool
Marek Tamm, 2018. Kommertslennukitele mõeldud pöördkonsoolidel
põhineva tagatiiva lahenduse tugevusanalüüs, Eesti Lennuakadeemia
Timo Korv, 2018. Modulaarne liitiumioon akukomplekt elektritoitel
õhusõidukile, Eesti Lennuakadeemia

Osalemine teadusprojektides
2.1.3 Miniklappide mõju lennukite aerodünaamilistele omadustele,
Peep Lauk, 2014–2020, Eesti Lennuakadeemia, Arendusosakond

Teadustöö
- Lauk, P.; Seegel, K.-E.; Tähemaa, T. (2017). Impact of variable geometry miniflaps on sailplane flight characteristics. Aviation, 21 (4), 119−125.10.3846/16487788.2017.1415228.
- Lauk, P.; Rebassa, J. H.; Kartushinsky, A.; Krupensky, I.; Tisler, S.; Tähemaa, T.; Polonskye, A. (2016). Assemblage of turbulent jet flows through static particulate media. Proceedings of the Estonian Academy of Sciences, 65 (3), 284−296.10.3176/proc.2016.3.05.
- Lauk, Peep; Unt, Karl-Eerik (2015). Influence of miniflaps on sailplane flight characteristics. Aviation, 19 (3), 105−111.10.3846/16487788.2015.1104

- Lauk, P.; Seegel, K.-E.; Tähemaa, T. (2018). The Influence of Variable Geometrical Modifications of the Trailing Edge of Supercritical Airfoil on the Characteristics of Aerodynamics. International Journal of Mechanical, Aerospace, Industrial, Mechatronic and Manufacturing Engineering, 12 (4), 261–266.
- Lauk, P.; Seegel, K-E.; Kartušinski, A.; Tisler, S.; Hussainov, M.; Polonsky, A.; Scheglov, I.; Rudi, Ü. (2016). Two-fluid RANS-RSTM-PDF model for turbulent particulate flows. In: R. López-Ruiz (Ed.). Numerical Simulation (340–363). InTech - Open Access Publisher .10.5772/63338.
- Lauk, Peep; Unt, Karl-Eerik. (2014). Miniflap influence on sailplane flight characteristics. Research and Education in Aircraft Design 2014. Ed. Jonas Stankūnas. Vilnius, Lithuania: Antanas Gustaitis Aviation Institute of Vilnius Gediminas Technical University.
- Lauk, Peep; Jakimenko, Jaanus; Vanker, Signe (2016). Projektõpe aine "Ülikerge purilennuki ehitamine" näitel. Õppemetoodiline konverents. Konverentsi teesid: Ennast juhtiv õppija; Kaitseväe Ühendatud õppeasutused, 20.10.2016. Toim. Svetlana Ganina; Andres Saumets. Tartu: Kaitseväe Ühendatud Õppeasutused, 34–36.
- Lauk, P; Tähemaa, T.; Seegel, K-E. (2018). Advanced trailing edge flap design for commercial aircraft, Toulouse, AEGATS´18 Confrence, France / 23 – 25 october 2018.